

**Improving Stochastic Simulation-based Optimization for Selecting
Construction Method of Precast Box Girder Bridges**

Mohammed Mawlana

**A Thesis in
The Department
of
Building, Civil, and Environmental Engineering**

**Presented in Partial Fulfillment of the Requirements
For the Degree of
Doctor of Philosophy (Building Engineering) at
Concordia University
Montreal, Quebec, Canada**

July, 2015

© Mohammed Mawlana, 2015

CONCORDIA UNIVERSITY

School of Graduate Studies

This is to certify that the thesis prepared

By: Mohammed Mawlana

Entitled: **Improving Stochastic Simulation-based Optimization for Selecting Construction Method of Precast Box Girder Bridges**

and submitted in partial fulfillment of the requirements for the degree of

DOCTOR OF PHILOSOPHY (Building Engineering)

complies with the regulations of the University and meets the accepted standards with respect to originality and quality.

Signed by the final Examining Committee:

<u>Dr. Gerard J. Gouw</u>	Chair
<u>Dr. Simaan AbouRizk</u>	External Examiner
<u>Dr. Javad Dargahi</u>	External to Program
<u>Dr. Osama Moselhi</u>	Examiner
<u>Dr. Tarek Zayed</u>	Examiner
<u>Dr. Amin Hammad</u>	Supervisor

Approved by Dr. Mohammed Zaheeruddin
Chair of Department

July 07, 2015

Dr. Amir Asif

Dean of Faculty

ABSTRACT

Improving Stochastic Simulation-based Optimization for Selecting Construction Method of Precast Box Girder Bridges

Mohammed Mawlana, Ph.D.

Concordia University, 2015

A large amount of reconstruction work is expected on existing highways due to the fact that highway infrastructures in North America are approaching or have surpassed their service life. The literature of construction engineering and management suggest that urban highway construction projects often overrun in budget and time. Bridges are crucial elements of urban highways, therefore, efficient planning of the construction of bridges is deemed necessary. Bridge construction operations are characterized as equipment-intensive, repetitive, have cyclic nature and involve high uncertainties. Without selecting the best construction method and the optimum number of equipment and crews, projects will take longer and cost more than necessary. The main objectives of this research are to: (1) develop a quantitative method that is capable of obtaining near optimum construction scenarios for bridge construction projects; and (2) obtain these optimum scenarios with an accurate estimate of their objective functions, a high confidence in their optimality and within a short period of time.

The ability of stochastic simulation-based optimization to find near optimum solutions is affected mainly by: (1) the number of candidate solutions generated by the optimization algorithm; and (2) the number of simulation replications required for each candidate solution to achieve a desirable statistical estimate. As a result, a compromise between the accuracy of the estimate of the performance measure index of a candidate solution and the optimality of that candidate solution must be made. Moreover, comparing the performance of different candidate solutions based on the mean values is not accurate because the means of the two objectives (i.e., cost and time) are not always the means of the joint distribution of the two objectives. Finally, the resulting near optimum solutions are not necessarily achievable.

In order to achieve the abovementioned objectives, the following research developments were made: (1) a stochastic simulation-based multi-objective optimization model; (2) a method for incorporating variance reduction techniques into the proposed model; (3) a method to execute the proposed model in parallel computing environment on a single multi-core processor; and (4) a method to apply joint probability to the outcome of the proposed model. The proposed methods showed an average of 84% reduction in the computation time and an average of 18% improvement in the hypervolume indicator over the traditional method when variance reduction techniques are used. Combining variance reduction computing with parallel computing resulted in a time saving of 90%. The use of the joint probability method showed an improvement over the traditional method in the accuracy of selecting the project duration (D) and cost (C) combination that satisfies a certain joint probability. For simulation models with high correlation between the outputs, ΔD and ΔC are not as large as in simulation models with moderate or low correlation, which indicates the existence of a negative relationship between correlation and ΔD and ΔC . In addition, the existence of high correlation permits the reduction of the number of simulation replications required to get a sound estimation of a project, which also indicates the existence of a negative relationship between correlation and the number of replications required.

ACKNOWLEDGEMENTS

I gratefully acknowledge the earnest support and patience of my supervisor Dr. Amin Hammad during the course of my research. I would, also, like to thank the member of my committee, Dr. Simaan M. AbouRizk, Dr. Javad Dargahi, Dr. Osama Moselhi, and Dr. Tarek Zayed for their valuable inputs and precious time.

I would like to acknowledge the support of Bentley Inc. for providing the Darwin Optimization Framework. Furthermore, the help and support provided by Dr. Zheng Yi Wu is highly appreciated. In addition, I would like to thank Dr. Julio C. Martinez and Dr. Photios G. Ioannou for providing the simulation software STROBOSCOPE. Moreover, the discussion with Ministry of Transport of Quebec, Mr. Adel Zaki from SNC-Lavalin, Dr. Ghislain Dionne and Mr. Emre Yildiz from CIMA+, Mr. Claude Énault from Guay Inc. are greatly appreciated.

I would like to express sincere gratitude to my friends Naseem Ibrahim and Faridaddin Vahdatikhaki for their intellectual discussions, and constructive and valuable comments. In addition, I would like to thank my friend Elias Mohama for explaining some programming concepts which helped in implementing the proposed methods.

Last but most certainly not least, I am grateful and will always be indebted to my parents for their unconditional love, affection, patience, and encouragements.

Table of Contents

Table of Figures	x
List of Tables	xiii
List of Abbreviations	xv
1. Chapter 1: Introduction	1
1.1 General Background.....	1
1.2 Problem Statement	2
1.3 Research Objectives	6
1.4 Research Significance	7
1.5 Thesis Organization.....	8
2 Chapter 2: Literature Review	10
2.1 Introduction	10
2.2 Selecting a Bridge Construction Method	10
2.2.1 Bridge Construction Methods	10
2.2.2 Method Selection	20
2.3 Construction Simulation.....	22
2.3.1 Simulation in Construction	22
2.3.2 Bridge Construction Methods Simulation	24
2.4 Optimization.....	25
2.4.1 Multi-objective Optimization.....	26
2.4.2 Genetic Algorithms	28
2.5 Stochastic Simulation-based Optimization	30
2.5.1 Optimizing Construction Methods.....	32
2.5.2 Limitations of Traditional Simulation-based Optimization.....	33
2.6 Stochastic Dominance	33
2.6.1 Variance Reduction Techniques	35
2.7 Required Computation Time	37
2.7.1 Parallel Computing of Genetic Algorithms	38
2.8 Correlation of Objective Functions	39
2.8.1 Joint Probability of Bivariate Discrete Random Variables.....	40

2.9	Summary	42
3	Chapter 3: Overview of Proposed Methodology	43
3.1	Introduction	43
3.2	Developing Stochastic Simulation-based Multi-objective Optimization Model	43
3.3	Solving the problem of stochastic dominance and reducing the number of simulation replications Using Variance Reduction Techniques	45
3.4	Reducing the Computation Time to Solve the Optimization Problem Using Parallel Computing on a Single Multi-core Processor	45
3.5	Applying Joint Probability for Evaluating the Duration and Cost of Stochastic Simulation Models	45
3.6	Summary	46
4	Chapter 4: Stochastic Simulation-based Multi-objective Optimization Model.....	47
4.1	Introduction	47
4.2	Proposed Model.....	47
4.3	Modeling the Decision Variables.....	48
4.4	Optimization Objectives.....	50
4.4.1	Minimizing the Project's Total Duration	50
4.4.2	Minimizing the Project's Total Cost.....	51
4.5	Optimization Constraints.....	54
4.6	Simulation Models of the Construction Methods	54
4.6.1	Span-by-span Precast Full Span Erection Using Launching Gantry	55
4.6.2	Span-by-span Precast Segmental Erection Using Launching Gantry.....	56
4.6.3	Span-by-span Precast Segmental Erection Using Falsework Support.....	56
4.6.4	Span-by-span Precast Segmental Erection Using Under-Slung Girder	57
4.7	Integration of Simulation and Optimization.....	62
4.8	Model Implementation	64
4.9	Case Study.....	65
4.10	Summary and Conclusions.....	75
5	Chapter 5: Solving the Problem of Stochastic Dominance And Reducing the Number of Simulation Replications Using Variance Reduction Techniques	76
5.1	Introduction	76
5.2	Synchronization of Random Numbers	77

5.2.1	Synchronization of CRN Technique Using Same Streams.....	80
5.2.2	Synchronization of CRN Technique Using New Streams.....	84
5.2.3	Synchronization of AV Technique and CM Using Same streams and New Streams	85
5.3	Comparing the Candidate Solutions.....	88
5.4	Comparing and Selecting the Best VRT	89
5.5	Method Implementation	92
5.6	Case Studies	93
5.6.1	Case Study A.....	93
5.6.2	Case Study B.....	103
5.7	Summary and Conclusions.....	113
6	Chapter 6: Reducing the Computation Time to Solve the Optimization Problem using Parallel Computing on a Single Multi-core Processor	115
6.1	Introduction	115
6.2	Proposed Method.....	116
6.3	Method Implementation	119
6.4	Case Studies	121
6.4.1	Case Study A.....	122
6.4.2	Case Study B.....	125
6.4.3	Case Study C.....	126
6.5	Summary and Conclusions.....	127
7	Chapter 7: Joint Probability for Evaluating the Duration and Cost of Stochastic Simulation Models	128
7.1	Introduction	128
7.2	Proposed Method.....	128
7.3	Applying Joint Probability to Pareto Solutions.....	130
7.3.1	Constructing Joint Probability Mass Function.....	130
7.3.2	Constructing Marginal and Conditional Cumulative Probability Functions	139
7.4	Generating Joint Probabilistic Pareto Fronts.....	141
7.5	Analyzing the Selected Solution	143
7.5.1	Estimating Duration and Cost Joint Contingency.....	143
7.5.2	Generating a Schedule to Meet a Specific Probability	146

7.6	Method Implementation	148
7.6.1	Applying the Joint Probability	148
7.6.2	Generating a Schedule with a Specified Probability.....	151
7.7	Case Studies	151
7.7.1	Case study A: Cyclic Project	153
7.7.2	Case Study B: Non-repetitive Project.....	155
7.7.3	Case study C: Repetitive project.....	158
7.7.4	Cast Study D: Joint Probabilistic Pareto Front	159
7.8	Summary and Conclusions.....	160
8	Chapter 8: Conclusions and Future Work.....	166
8.1	Summary and Conclusions of the Research Work.....	166
8.2	Research Contributions	168
8.3	Limitations and Recommendations for Future Work.....	169
	References	171
9	Appendix A: Tasks Durations Used in the Simulation Models.....	188
10	Appendix B: Cost Data Used in the Simulation Models.....	190

Table of Figures

Figure 2-1 Schematic Drawing of Precast Full Span Launching Method	13
Figure 2-2 Precast Full Span Concrete Box Girder Loaded on a Trolley	14
Figure 2-3 Operation of a Launching Gantry	14
Figure 2-4 Launching Gantry Picking-up the Precast Span	14
Figure 2-5 Launching Gantry Places the Precast Span on the Pier Cap	14
Figure 2-6 Schematic of Short Line Match Casting System.....	15
Figure 2-7 Schematic Drawings of Segmental Span-by-span Construction Method	18
Figure 2-8 Classification of Optimization Problems	25
Figure 2-9 Pareto Front.....	27
Figure 2-10 Flowchart of Fast Messy Genetic Algorithm	29
Figure 2-11 Integration of Optimization Engine and Simulation	30
Figure 2-12 Simulation-based Optimization Methods.....	31
Figure 2-13 Deterministic Versus Stochastic Simulation.....	31
Figure 2-14 Master-slave Parallel GA Framework.....	38
Figure 3-1 Overview of the Proposed Methodology	43
Figure 4-1 Stochastic Simulation-based Multi-objective Model	47
Figure 4-2 Simulation Model of Full Span Bridge Construction Using Launching Gantry.....	57
Figure 4-3 Simulation Model of Span-by-span Segmental Bridge Construction Using Launching Gantry	58
Figure 4-4 Simulation Model of Span-by-span Segmental Bridge Construction Using Falsework Support.....	59
Figure 4-5 Simulation Model of Span-by-span Segmental Bridge Construction Using Under-slung Girder	60
Figure 4-6 Integration between Discrete Event Simulation and Fast Messy Genetic Algorithm.	62
Figure 4-7 Algorithm for Non-dominated Sorting of Pareto Fronts.....	63
Figure 4-8 Implementation of Stochastic Simulation-based Optimization Model	64
Figure 4-9 All the Generated Candidate Solutions in the First Run.....	68
Figure 4-10 Improvement of Pareto Solutions over the Generations	68
Figure 4-11 Scatter Plot of the Project Duration and Cost Combinations for Solutions 10 and 11	71

Figure 4-12 Project Duration Distribution of Solutions 10 and 11.....	71
Figure 4-13 Project Cost Distribution of Solutions 10 and 11.....	72
Figure 4-14 Pareto Fronts Generated in the First and Second Run	72
Figure 5-1 Algorithm for Incorporating CRN and CRN _{ns} Techniques.....	77
Figure 5-2 Algorithm for Incorporating (a) AV and CM, and (b) AV _{ns} and CM _{ns} Techniques...	78
Figure 5-3 Schematic of Stream Spacing for CRN Technique.....	82
Figure 5-4 Procedure for Comparing and Selecting the Best VRT	88
Figure 5-5 Case Study A: Correlation between Pilot Study Solutions (Project Duration and cost) Using CRN and CRN _{ns} Techniques, and Traditional Method	95
Figure 5-6 Case Study A: Correlation between Pilot Study Solutions (Project Duration and cost) Using AV and AV _{ns} Techniques, and Traditional Approach.....	98
Figure 5-7 Case Study A: Correlation between Pilot Study Solutions (Project Duration and cost) Using CM and CM _{ns} Techniques, and Traditional Method	100
Figure 5-8 Case Study A: Pareto Fronts Generated After Evaluating 100,000 Candidate Solutions	101
Figure 5-9 Case Study A: Pareto Fronts Generated after 6.93 Hours.....	102
Figure 5-10 Case Study B: Correlation between Pilot Study Solutions (Project Duration and cost) Using CRN and CRN _{ns} Techniques, and Traditional Method.....	105
Figure 5-11 Case Study B: Correlation between Pilot Study Solutions (Project Duration and cost) Using AV and AV _{ns} Techniques, and Traditional Method.....	107
Figure 5-12 Case Study B: Correlation between Pilot Study Solutions (Project Duration and cost) Using CM and CM _{ns} Techniques, and Traditional Method.....	109
Figure 5-13 Case Study B: Pareto Fronts with the Tradeoff between Project Duration and Cost	111
Figure 5-14 Case Study B: Pareto Fronts Generated after 8.38 Hours.....	112
Figure 6-1 Simulation Execution Time Versus the Number of Replications	115
Figure 6-2 Parallel Simulation-based Optimization Method	117
Figure 6-3 Algorithm for Distributing the Population Among the Cores.....	118
Figure 6-4 Defining STROBOSCOPE as an Object.....	119
Figure 6-5 Directing the Candidate Solutions Towards their Corresponding Core.....	120
Figure 6-6 Architecture of Intel i7 Quad-core Processor.....	121

Figure 6-7 Required Time to Solve the Optimization Problem for Case Study A	122
Figure 6-8 Required Time to Solve the Optimization Problem for Case Study B.	124
Figure 7-1 Proposed Method of Joint Probability.....	128
Figure 7-2 Flowchart of Constructing the Joint, Marginal, and Conditional Probability Functions	132
Figure 7-3 Algorithms for Applying Joint Probability	133
Figure 7-4 Examples of Joint Probability Mass Functions.....	136
Figure 7-5 Examples of Marginal Frequency Histograms.....	139
Figure 7-6 Flowchart for Finding the Best Combination.....	143
Figure 7-7 Flowchart for Estimating Duration and Cost Joint Contingency	144
Figure 7-8 Flowchart for Selecting Best Seed Number	146
Figure 7-9 Implementation Summary of Proposed Methodology	148
Figure 7-10 Flowchart of Joint Probability Implementation	149
Figure 7-11 Flowchart of Generating Schedule.....	151
Figure 7-12 Scatter Plot of Project Duration and Cost Combinations for Case Study A	152
Figure 7-13 Schedule Network for Case Study B.....	155
Figure 7-14 Scatter Plot of Project Duration and Cost Combinations for Case Study B	156
Figure 7-15 Scatter Plot of Project Duration and Cost Combinations for Case Study C	158
Figure 7-16 Pareto Fronts Generated Using Traditional Method.....	161
Figure 7-17 Pareto Fronts Generated Using 50% Joint Cumulative Probability.....	162
Figure 7-18 Pareto Fronts Generated Using 75% Joint Cumulative Probability.....	162
Figure 7-19 Pareto Fronts Generated Using 95% Joint Cumulative Probability.....	163
Figure 7-20 Probabilistic Pareto Fronts for 50%, 75%, and 95% Joint Cumulative Probability	163

List of Tables

Table 2-1 STROBOSCOPE Elements Used to Build Up the Simulation Models	24
Table 4-1 Overtime Policies Used in this Research.....	48
Table 4-2 Tasks Durations Used in the Simulation Model.....	66
Table 4-3 Quantitative Decisions Variables Used in the Optimization.....	66
Table 4-4 fmGA Configuration Used in the Case Study	67
Table 4-5 Details of the Pareto Set of Solutions for the First Run	69
Table 4-6 Details of the Pareto Set of Solutions for the Second Run.....	73
Table 5-1 Types of Synchronization Required for Different VRTs	76
Table 5-2 Synchronization of Different VRTs for Tasks A and B Using the Same Streams Approach.....	81
Table 5-3 Synchronization of Different VRTs for Tasks A and B Using the New Streams Approach.....	86
Table 5-4 Case Study A: Pilot Study Statistical Results of Using Traditional Method, and CRN and CRN _{ns} Techniques	94
Table 5-5 Case Study A: Pilot Study Statistical Results of Using Traditional Method, and AV and AV _{ns} Techniques	97
Table 5-6 Case Study A: Pilot Study Statistical Results of Using Traditional Method, and CM and CM _{ns} Techniques.....	99
Table 5-7 Case Study A: Results of the Simulation-based Optimization Experiments.....	101
Table 5-8 Case Study B: Pilot Study Statistical Results of Using Traditional Method, and CRN and CRN _{ns} Techniques.....	104
Table 5-9 Case Study B: Pilot Study Statistical Results of Using Traditional Method, and AV and AV _{ns} Techniques.....	106
Table 5-10 Case Study B: Pilot Study Statistical Results of Using Traditional Method, and CM and CM _{ns} Techniques.....	108
Table 5-11 Case Study B: Results of the Simulation-based Optimization Experiments	111
Table 6-1 Achieved Speedup, Efficiency, and Time Saving for Case Study A	123
Table 6-2 Achieved Speedup, Efficiency, and Time Saving for Case Study B	125
Table 6-3 Achieved Speedup and Efficiency for Case Study C	126
Table 7-1 Example of Contingency Table	135

Table 7-2 Probability Information of the Four Combinations	141
Table 7-3 Summary of Performance Metrics for Case studies A, B, and C	152
Table 7-4 Project Duration and Cost of Different Cumulative Probabilities for Case Study A.	153
Table 7-5 Different Number of Simulation Replications for Case Study A.....	154
Table 7-6 Project Information for Case Study B	155
Table 7-7 Project Duration and Cost of Different Cumulative Probabilities of Case Study B ..	156
Table 7-8 Different Number of Simulation Replications for Case Study B.....	157
Table 7-9 Analysis of Schedule Generation for Case Study B.....	160
Table 7-10 Project Duration and Cost of Different Cumulative Probabilities of Case Study C	161
Table 7-11 Different Number of Simulation Replications for Case Study C.....	161
Table A-1 Deterministic Tasks Durations for Precast Full Span Erection Using Launching Gantry	188
Table A-2 Tasks Durations for Precast Segmental Erection Using Launching Gantry.....	188
Table A-3 Tasks Durations for Precast Segmental Erection Using Falsework Support.....	189
Table A-4 Tasks Durations for Precast Segmental Erection Using Under-slung Girder	189

List of Abbreviations

ABC	Accelerated Bridge Construction
AEC	Architecture, Engineering and Construction
AHB	Analytic Hierarchy Process
ARN	Arbitrary Random Number
AV	Antithetic Variates
CM	Combined Method
CRN	Common Random Number
fmGA	fast messy Genetic Algorithm
GAs	Genetic Algorithms
NCC	Number of Casting Crews
NDT	Number of Delivery Trucks
NIM	Number of Inner Molds
NOM	Number of Outer Molds
NPC	Number of Preparation Crews
NRC	Number of Rebar Cage Molds
NSC ₁	Number of Stressing Crews
NSC ₂	Number of Steel Crews
OP	Overtime Policy
PCI	Probabilistically Complete Initialization
PYD	Precast Yard Distance
PYS	Precast Yard Storage Capacity
RN	Random Number
RRN	Required Random Number
ST	Storage Time (hr)
VBA	Visual Basic for Applications
VRT	Variance reduction Techniques

CHAPTER 1: INTRODUCTION

1.1 General Background

Highway infrastructures in North America are approaching or have surpassed their service life; as a result, an intensive amount of reconstruction work is expected on existing highways. Such activities affect drivers, highway workers, business and other community functions (Jeannotte and Chandra, 2005; Mahoney et al., 2007). Current practices in the construction industry suggest that urban highway construction projects often overrun in budget and time due to the high cost of equipment and materials, change orders of work, meteorological and environmental factors, potential conflicts with stakeholders, economical and social activities, and a large number of unpredictable factors (Dawood and Shah, 2007; Hannon, 2007).

The construction of urban highways differs from other construction projects because of (Saag, 1999): (1) the huge cost involved in urban highways construction, which requires different and innovative financing techniques; (2) the magnitude of the work to be undertaken often requires organizational modifications at the transportation agency level; (3) the partial closure or disruption of travel on these important traffic routes has a daily effect on drivers and the community as a whole; (4) the need to ensure travel continuity through or around the construction zone; (5) the need for communication with, and involvement of, the public spans all phases of project development; and (6) the combination of construction under traffic and heavy traffic volumes results in situations with the potential for unsafe conditions unless anticipated beforehand.

Urban highways comprise roads, tunnels and bridges. Bridges are crucial elements of urban highways because they are used to span over obstacles. Several transportation agencies have shifted to Accelerated Bridge Construction (ABC) as an alternative to conventional construction methods. This recent shift was driven by the need to minimize traffic impacts caused by extended onsite construction activities. ABC refers to reducing the onsite construction time of bridges by using innovative planning, design, materials and construction methods (Federal Highway Administration, 2013). ABC has proven to have essential benefits over conventional construction methods. These benefits can be noticed in the improved safety during construction, the higher quality and durability of the bridge, as well as in the reduction of onsite construction

time, traffic impacts, social costs and environmental impacts. The use of precast concrete bridges is considered one of the popular ABC approaches.

Bridge construction projects are characterized as equipment-intensive, repetitive, have cyclic nature and involve high uncertainties. Consequently, it is essential for the success of these projects to select proper equipment for each operation (Lee, 2003). In general, the goals behind selecting a fleet of equipment are: increase work safety, minimize cost, reduce equipment idle time, and maximize productivity. The fact that operation's cycles have many components, which vary in their values, makes the analysis of productivity very difficult (Wright, 1996; El-Moslmani, 2002). The uncertainties associated with bridge construction operations are a result of: (1) the different job conditions, for example equipment breakdown, and inclement weather, under which those operations are performed (Marzouk et al., 2006); (2) the use of a construction method for the first time or lack of experience with the used construction method; and (3) the spatio-temporal environment that may have potential conflicts.

1.2 Problem Statement

The construction method is one of the main factors that impact the cost, productivity, and efficiency of construction projects (Thomas et al., 1990). As a result, selecting the appropriate construction method is crucial for the success of the project. The selection of the method for constructing a bridge is a complex decision-making problem. During the planning phase of a precast concrete bridge construction project, planners have to make several decisions related to: (1) the construction method; (2) the location and settings of the casting yard; (3) the transportation of the precast concrete elements; (4) the number of resources; and (5) the overtime policy. Every set of these decisions is referred to as construction scenario. The terms construction scenario and candidate solutions are used interchangeably throughout the thesis. Each of these decisions impacts substantially the conflicting objectives of construction projects, which are minimizing the project's total duration and minimizing the project's total cost. In addition, evaluating the impact of each construction scenario on meeting the project objectives is not a straightforward process. Without selecting the optimum construction scenario, projects will take longer and cost more than necessary. Therefore, a new decision-making model is needed to support planners in performing this challenging planning task. This model should be capable of: (1) selecting the optimum construction scenario that will simultaneously optimize the conflicting

objectives of minimizing the project's total duration and cost; (2) considering the decision variables that have an impact on the project objectives such as the construction method, the overtime policy, and the settings of the casting yard; and (3) meeting the project constraints such as the number of available resources, project deadline or budget. The complexity and the uncertainty of construction operations, and the limited knowledge of the behavior of the operations under different construction scenarios make it impossible to describe such operations using a closed form formula. Therefore, discrete event simulation can be used to model the complexity of the construction operations while the uncertainty can be modeled by incorporating stochastic durations and costs into the model. In order to find the optimum scenario, an enumeration and evaluation of all possible combinations can be carried out, which is not feasible for large problems. Therefore, simulation must be integrated with an optimization algorithm in order to optimize the construction operations.

The efficiency of the stochastic simulation-based optimization is affected mainly by: (1) the number of candidate solutions generated by the optimization algorithm; and (2) the number of simulation replications required for each candidate solution to achieve a desirable statistical estimate. As the search space and/or the number of simulation replications increase, the computation requirements increase to a prohibitive level. As a result, a compromise between the accuracy of the estimate of a candidate solution and the optimality of that solution must be made (Cheng and Lee, 2011). The accuracy of the estimate of a candidate solution refers to how close that estimate is to the true mean of a performance measure index. The optimality of a candidate solution refers to the quality of the candidate solution (i.e., how close the candidate solution is to the optimum solution). Obtaining inaccurate estimates of the means of the performance measure indices may lead to a well-known problem called stochastic dominance. State of the art indicates that this type of problem occurs when an inferior candidate solution is perceived as an optimum solution due to an error in the estimate of the mean of the objective functions. In addition, the current state of art does not produce consistent optimum solutions every time the optimization is run. It is desirable to obtain an accurate estimate of the mean of the performance measure index with the least number of replications possible. By doing so, the problem of stochastic dominance will be solved and the computation requirements will be reduced. Several researchers have proposed methods, known as Variance Reduction Techniques (VRTs), to reduce the required number of simulation replications while maintaining a good estimate of the performance measure

index (Kleijnen 1975; Schruben and Margolin 1978; Bratley et al. 1987; L'Ecuyer 1994). Reducing the number of simulation replications will significantly reduce the computation time and efforts needed to solve the simulation-based optimization problem. To the knowledge of the author, however, these techniques have never been used in the context of simulation-based optimization. As a result, these techniques are not readily available to be used in this context. In addition, the effectiveness of the simulation-based optimization method incorporating VRTs is not studied. Therefore, there is a need for a method that will incorporate VRTs into the simulation-based optimization model.

Furthermore, it has been reported repeatedly that the use of metaheuristic optimization methods, such as Genetic Algorithms, for optimizing large-scale construction projects requires long computation time (Feng et al. 2000; Li and Love 1997; Li et al. 1999; Hegazy and Petzold 2003; Kandil and El-Rayes 2006). Using stochastic simulation adds another dimension to the complexity of the optimization problem, and as a result, it increases the required computation time. Several researches have proposed the use of parallel computing in order to reduce the required computation time to solve the optimization problem (Kandil and El-Rayes, 2006; Kandil et al., 2010; Yang et al., 2012; Salimi et al., 2014). By reducing the time required to optimize a problem, a larger area of the search space can be covered within the same period of time. As a result, the confidence in the optimality of the optimum solutions will increase.

While the simulation-based optimization is an effective approach that can be best used at the planning phase to determine the optimum construction method and resource configuration, there is very little guarantee that the generated plans remain optimal through the execution phase. This is due to all the uncertainties that face the project execution. These uncertainties can be due to: (1) the conditions under which the project is performed; (2) the scope of the project; or (3) the available resources. Therefore, re-planning and re-allocation of resources might be necessary when a deviation from the initial plan is detected. Therefore, it is important to obtain the new optimum solutions in a timely manner. Although the use of parallel computing reduces the required computation time, it requires the use of a cluster of computers, which often comes with a high price tag. To overcome this problem, this research takes advantage of the advancement in multi-core processors. A method for implementing parallel computing on a single multi-core processor is proposed in this research to reduce the computation time.

Another problem with simulation-based optimization is that a candidate solution is evaluated in terms of the mean value of each objective function separately. The focus is usually on quantifying the impact of uncertainty on the project schedule (Lu 2003; Zhang et al. 2008; Al-Bataineh et al. 2013; Nguyen et al. 2013). This approach provides insight on the probability of completing the project within a specific duration. In multi-performance measure indices problems (Zhang et al. 2006; Hassan and Gruber 2008; Marzouk et al. 2009; Lee et al. 2010; Mawlana and Hammad 2013), the performance measure indices of a model is represented by the duration and cost values as a pair. However, these values are found by explicitly averaging the durations and costs of simulation replications without regard to their simultaneous occurrence. In addition, when comparing the performance measure indices of the model under different probabilities of occurrence, each performance measure index is assessed separately. The traditional method does not provide any information on the probability of the project cost given a specific project duration, and vice versa. Without this information, the decision maker cannot quantify the impact of selecting a project duration meeting a probability of occurrence of the project cost, and vice versa. That is, the correlation between the duration and cost is not examined and the impact each performance measure index has on the other performance measure index is ignored. Due to the fact that there is a correlation between the project duration and cost, the analysis of the model performance measure indices must consider the simultaneous occurrence of the project duration and cost through the use of joint probability (Feng et al. 2000; Yang 2011). The traditional method is valid only if a perfect correlation between the project duration and cost exists, and the marginal and joint distributions follow a normal distribution. However, this is not always the case for construction projects. In addition, a specific pair of performance measure indices selected based on the traditional method is not necessarily achievable. The results of simulation replications may not generate a replication that has the same pair of performance measure indices. The achievable performance measure indices' values for that model could be higher or lower than the values of the performance measures indices pair. Even if a specific performance measures indices pair is generated by the simulation replications, there is no method available for tracing this pair in order to generate the schedule of that pair. Therefore, there is a need for an analytical method to overcome these shortcomings.

1.3 Research Objectives

The main aim of this research is to develop and integrate new models for planning and scheduling of precast box girder bridge construction projects. The objectives of this research along with the addressed research questions are:

Objective 1:

To develop a stochastic simulation-based multi-objective optimization model for the construction of precast concrete box girder bridges that is capable of (1) finding near optimum construction scenarios; and (2) simultaneously minimizing the project's total duration and cost.

Research Questions:

(1) What are the decision variables that should be considered? (2) How can the project duration and cost be formulated and estimated? (3) How to integrate the optimization algorithm with simulation? (4) What precast box girder bridge construction method should be used? (5) What is the optimum number of resources to be used? and (6) How this selection is affected by overtime policy and the settings of the casting yard?

Objective 2:

To develop a new method to: (1) increase the quality of the optimum solutions; (2) increase the confidence in the optimality of the optimum solutions; and (3) reduce the computation time required for performing a stochastic simulation-based multi-objective optimization by incorporating VRTs.

Research Questions:

(1) How VRTs can be applied in the context of simulation-based optimization methods? (2) How to compare the optimum solutions? (3) How to compare and evaluate different VRTs? (4) What is the impact of these techniques on the quality of optimum solutions? (5) What is the impact of these techniques on the optimality of the optimum solutions? and (6) What is the time saving that can be achieved using these techniques?

Objective 3:

To propose a method to reduce the computation time required for performing a stochastic simulation-based multi-objective optimization by performing parallel computing on a single multi-core processor.

Research Questions:

(1) How parallel computing can be implemented using existing optimization and simulation tools? (2) How the simultaneous multithreading technology impacts the computation time? What is the time saving that can be achieved by this implementation? (3) What is the optimum number of cores to be used? and (4) How does the time saving achieved using the proposed tools compare to the use of another tools?

Objective 4:

To develop a method to reduce project risk and provide the decision makers with more accurate and useful information to plan and manage their projects using the joint probability.

Research Questions:

(1) How the joint probability can be applied to the output of the optimization process? (2) How to calculate the conditional probability of the project cost given a specific project duration, and vice versa? (3) How to find the best project duration and cost that meet a specific joint probability? (4) How to estimate the project schedule and cost joint contingency using the joint probability? and (5) How to generate a schedule representing a specific joint probability?

1.4 Research Significance

The current research aims to support and enhance decision-making in construction projects and to aid planners to select a near optimum construction scenario and therefore minimize the project total duration and cost. Applying this framework is expected to have a noteworthy impact on: (1) selecting the best construction method in terms of duration and cost; (2) selecting the number of resources, overtime policy, and casing yard setting to be used to increase productivity and meet project objectives; (3) reducing the computation time required to optimize construction operations; (4) increasing the confidence in the quality and optimality of the optimum solutions; (5) reducing project risk; and (6) providing the decision makers with more accurate and useful

information to plan and manage their projects. Thus, this research will provide significant benefits to contractors and construction management firms.

1.5 Thesis Organization

This research will be presented as follows:

Chapter 2: Literature Review: This chapter presents a review of the literature on selecting bridge construction method, construction simulation, optimization, and stochastic simulation-based optimization. In addition, a comprehensive literature review is given about the research related to the selection and optimization of bridge construction methods. The aim of this review is to identify the research gaps that need to be addressed in this research.

Chapter 3: Overview of Proposed Methodology: This chapter presents an overview of the proposed methodology of a stochastic simulation-based multi-objective optimization model for the planning and scheduling of precast box girder bridge construction projects

Chapter 4: Stochastic Simulation-based Multi-objective Optimization Model: This chapter presents a stochastic simulation-based optimization model for planning, scheduling and optimizing precast box girder bridge construction operations. The aim of the model is to select a near-optimum construction scenario that satisfies predefined objectives.

Chapter 5: Solving the Problem of Stochastic Dominance And Reducing the Number of Simulation Replications Using Variance Reduction Techniques: This chapter presents a method to incorporate VRTs into the stochastic simulation-based optimization model.

Chapter 6: Reducing the Computation Time to Solve the Optimization Problem using Parallel Computing on a Single Multi-core Processor: This chapter presents a method for implementing the simulation-based optimization model in a parallel computing environment on a single multi-core processor.

Chapter 7: Joint Probability for Evaluating the Duration and Cost of Stochastic Simulation Models: This chapter presents a new joint probability method that is going to be applied to sub-populations' Pareto fronts generated by the stochastic simulation-based optimization model.

Chapter 8: Conclusions and Future Work: This chapter summarizes the work and concludes with the findings of this thesis. In addition, it highlights the contributions and lists the limitations of the developed models. Finally, it suggests some recommendations for future work.

CHAPTER 2: LITERATURE REVIEW

2.1 Introduction

This chapter presents a review of the literature on selecting bridge construction method, construction simulation, optimization, stochastic simulation-based optimization. In addition, a comprehensive literature review is given about the research related to the selection and optimization of bridge construction methods. The aim of this review is to identify the research gaps that need to be addressed in this research. The limitations of the traditional simulation-based optimization are defined. In addition, it reviews what other researches proposed to overcome these limitations. Finally, the topics that are used in this research to overcome these limitations are reviewed.

2.2 Selecting a Bridge Construction Method

2.2.1 Bridge Construction Methods

In this research, the focus is on the construction of concrete box girder bridges using the following construction methods: (1) precast full-span erection using launching gantry; (3) precast segmental span erection using launching gantry; (4) precast segmental span erection using false-work; and (4) precast segmental span erection using under-slung girder. Therefore, these construction methods are reviewed below.

Precast Full Span Concrete Box Girder Construction

This construction method is well suited for bridges that span over obstacles, have minimal horizontal radius, and are comprised of similar span lengths. The advantages of this construction method are: (1) achieving high quality of concrete spans due to manufacturing in a casting yard; (2) reducing construction time and cost (Pan et al., 2008); (3) minimizing disruption to the existing traffic network; (4) reducing the need for scaffolding work (Benaim, 2008); (5) achieving very high rate of production; and (6) improving safety because of the reduced on site activities (VSL International Ltd., 2013). However, this method requires high level of technology, has high equipment cost, needs large areas for casting and storing, and is not suitable when the access is difficult (Hewson, 2003). This construction method has been applied to

several projects around the globe such as Taiwan High Speed Rail, Seven Mile Bridge, Singapore MRT (VSL International Ltd., 2013), Saudi Arabia-Bahrain Causeway, and Vasco da Gama Bridge (Hewson, 2003). The span length is typically between 30 m and 55 m and weighs between 600 tons and 1500 tons (NRS Bridge Construction Equipment , 2008). However, the span length may be over 100 m and weigh thousands of tones. The width of the span ranges from 5 m to more than 12 m, which makes this construction method applicable for both light-rail systems and highway bridges. The bridge can be either constructed as simply supported or as continuous spans. The precast full span is placed on the bearings in the case of simply supported. On the other hand, in the case of the continuous setting, neighboring spans are joined together using tensioning rods and in-situ concrete stitch (Hewson, 2003).

The construction of a precast full span concrete box girder bridge is done in two phases: (1) the fabrication of a full span length of a concrete box girder at the casting yard; and (2) the erection of the full span using various techniques onsite. In the first phase, the process starts by erecting the reinforcement and stressing ducts of the bottom slab and the webs. Then an inner mold is installed where the top slab reinforcement and stressing ducts erection takes place. At this stage all the reinforcement work is completed and a rebar cage is ready to be casted. The rebar cage is then put into an outer mold where the casting takes place. Next, the inner mold is removed when the full span reaches a sufficient strength. At this point, the first stage of pre-stressing is performed and the full span is transported to the storage area to complete curing and be stored. When the full span reaches a sufficient strength, the second stage of pre-stressing takes place (VSL International Ltd., 2013). In the second phase, the full span precast box girders are transported to the construction site by trailers, trolleys or barges. The selection of the transportation method depends on the distance between the casting yard and the construction site, the erection equipment used, the size of the span, and the terrain and bridge site access.

This method is used for bridges comprising single box girder where a launching gantry is used to erect the precast full span box girders as shown in Figure 2-1. The girders are loaded to a trolley (Figure 2-2) which travels along the completed section of the bridge to reach to the location of the span that will be launched as shown in Figure 2-3(a). Next, the launching gantry picks up the precast girder (Figure 2-3(b), Figure 2-4) and places it on the pier cap (Figure 2-5). Finally, the

launching gantry repositions to the new launching location as shown in Figure 2-3(c) (Rajagopalan, 2006; Benaim, 2008; Rosignoli, 2010; VSL International Ltd., 2013).

Precast Segmental Concrete Box Girder Construction

This construction method has been widely used in the past for the construction of both rail and highway bridges. The concept behind this method is that each span is casted in short segments, transported into the construction site and finally joining the segments together. In general, the construction methods under this category share the following advantages: (1) achieving high quality through factory production of the segments; (2) achieving high construction productivity rate (Podolny and Muller, 1982); (3) minimizing the disruption to construction site; and (4) being suitable for tight curves and complex geometry (Hewson, 2012). However, this method requires a high level of technology, has high equipment cost, and needs large areas for casting and storing (Hewson, 2003). The span length is typically between 40 m and 150 m with segment length of 3.5 m to 8 m and weighing up to 90 tons. The segment length is chosen based on the available handling equipment and transportation network. The width of the span ranges from 6 m to 16 m which makes this construction method applicable for both light-rail systems and highway bridges (Hewson, 2003).

As in the case of precast full span box girder bridges, the construction of a precast segmental concrete box girder bridge is done in two phases: (1) the casting of the segments of a concrete box girder bridge at the casting yard; and (2) the erection of these segments using various techniques onsite. There are two main techniques for casting the segments which are the short line and the long line methods. These two methods are based on the match-cast principle where new segments are cast against the previously cast segment so that the faces of the segments fits perfectly (Sauvageot, 1999), i.e., the segments are cast so that their relative erecting position is the same as their relative casting position (Barker, 1980).

Most match-cast segmental bridges use the short line method since it can be used for any shape of deck alignment (Benaim, 2008). Therefore, this research will focus on this method. Figure 2-6 shows a schematic drawing of the short line match casting method. In the short line method, segments are cast in the same stationary form and against the previously cast segment. The previously cast segment is then moved to the storage and the newly cast segment is cast against.

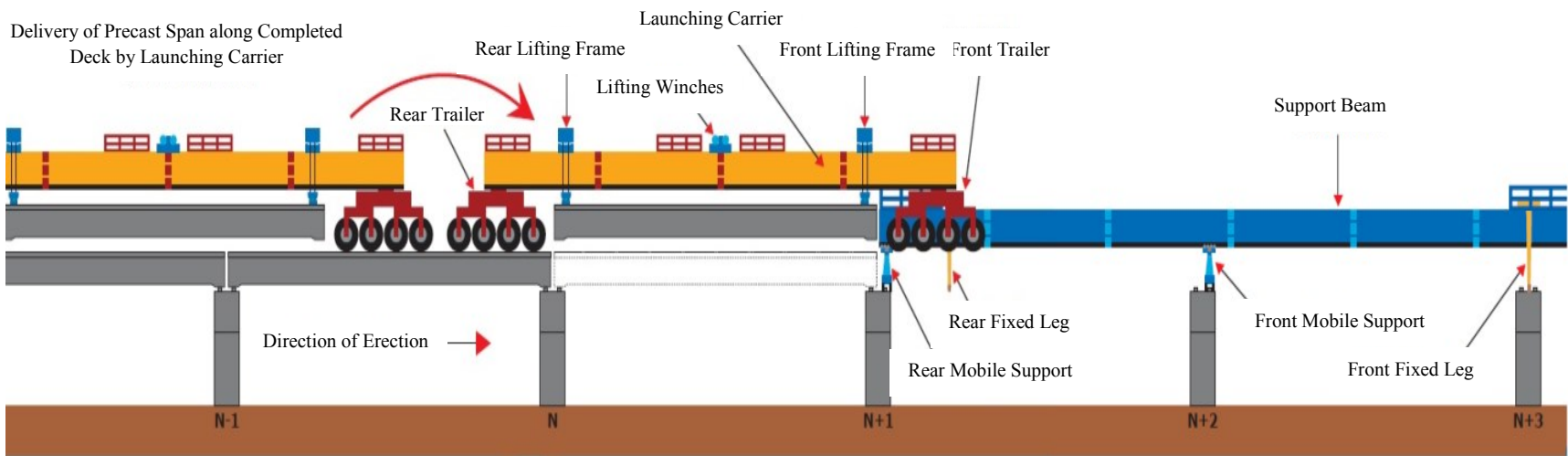


Figure 2-1 Schematic Drawing of Precast Full Span Launching Method (VSL International Ltd., 2013)



Figure 2-2 Precast Full Span Concrete Box Girder Loaded on a Trolley (Colossal Transport Solutions, 2011)

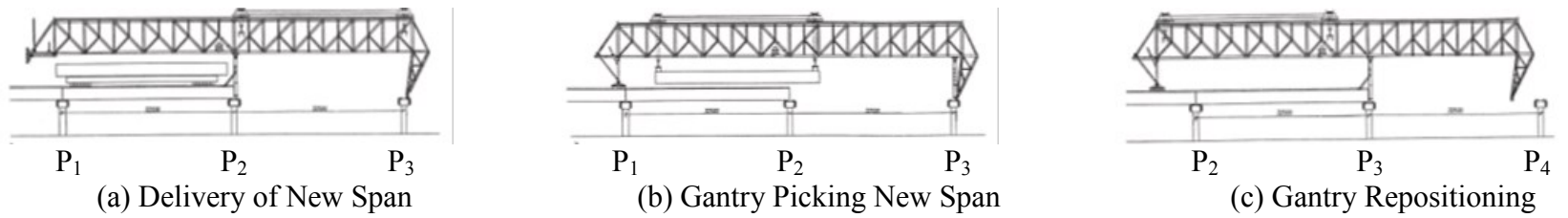


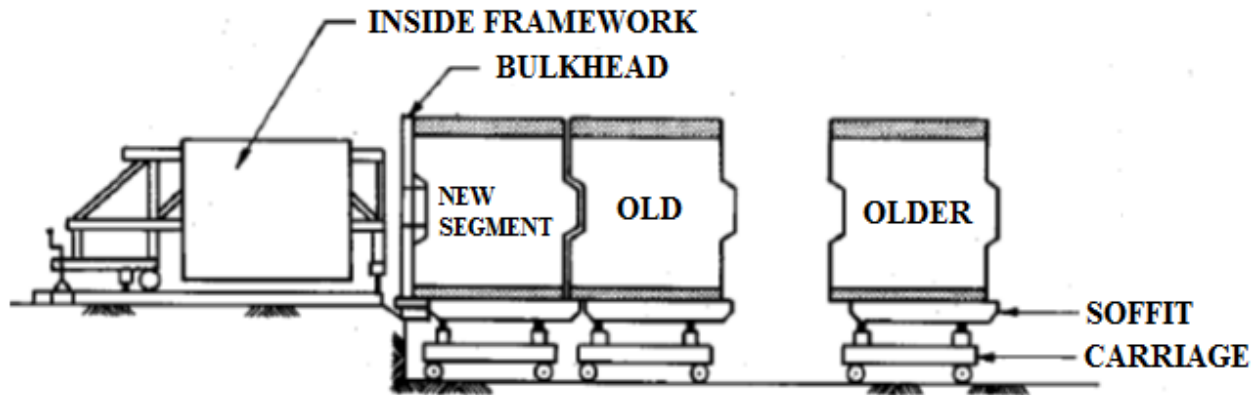
Figure 2-3 Operation of a Launching Gantry (Benaim, 2008)



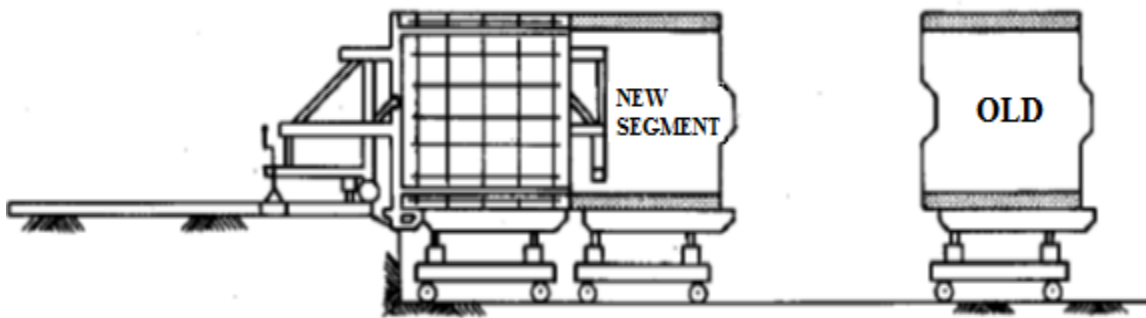
Figure 2-4 Launching Gantry Picking-up the Precast Span (Continental Engineering Corporation, 2006)



Figure 2-5 Launching Gantry Places the Precast Span on the Pier Cap (Struktur DF International, 2011)



(a) Older Segment is Moved to Storage



(b) New Segment is Moved to Cast Against

Figure 2-6 Schematic of Short Line Match Casting System (Barker, 1980)

In the second phase, the segmental precast box girders are transported to the construction site by trailers, trolleys or barges. The selection of the transportation method depends on the distance between the casting yard and the construction site, the erection equipment used, the size of the span, and the terrain and bridge site access. The erection methods of segmental box girder bridges can be grouped into four categories: (1) span-by-span construction, (2) balanced cantilever construction, (3) progressive placement construction, and (4) incremental launching (Podolny and Muller, 1982). This research focuses on the construction methods that belong to the first category where segments are delivered to the construction site and joined together to form the bridge spans. There are three basic methods for treating the joints between the segments: (1) cast in situ joints, where the segments are joined with reinforced concrete or mortar (Mondorf, 2006); (2) glued joints, where the segments are joined together using a bonding agent such as epoxy or cementitious product which is applied to the contact areas of the segments (Liebenberg, 1992); and (3) dry joints where the segments are joined without the use of any bonding material. The last two methods require the use of key-ways which are obtained by

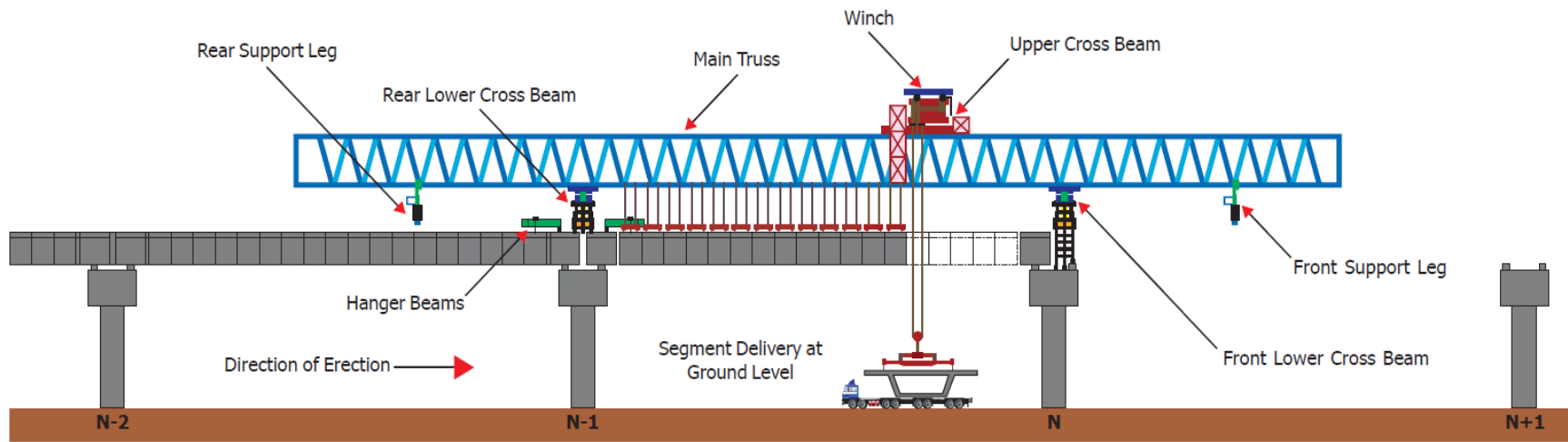
match-casting (Mondorf, 2006). This research focuses on the use of glued joints since it can accommodate minor damages in the faces of the segments, facilitate connecting the segments, and provide a waterproof seal (Benaim, 2008).

The span-by-span erection method starts at one end and progresses towards the other end. Using this method, the segments of each span are positioned, aligned, and post-tensioned to form the final span. Three erection techniques are considered for the construction of precast segmental concrete box girder bridges in a span-by-span setting using (a) launching gantry, (b) falsework support, and (c) under-slung girder.

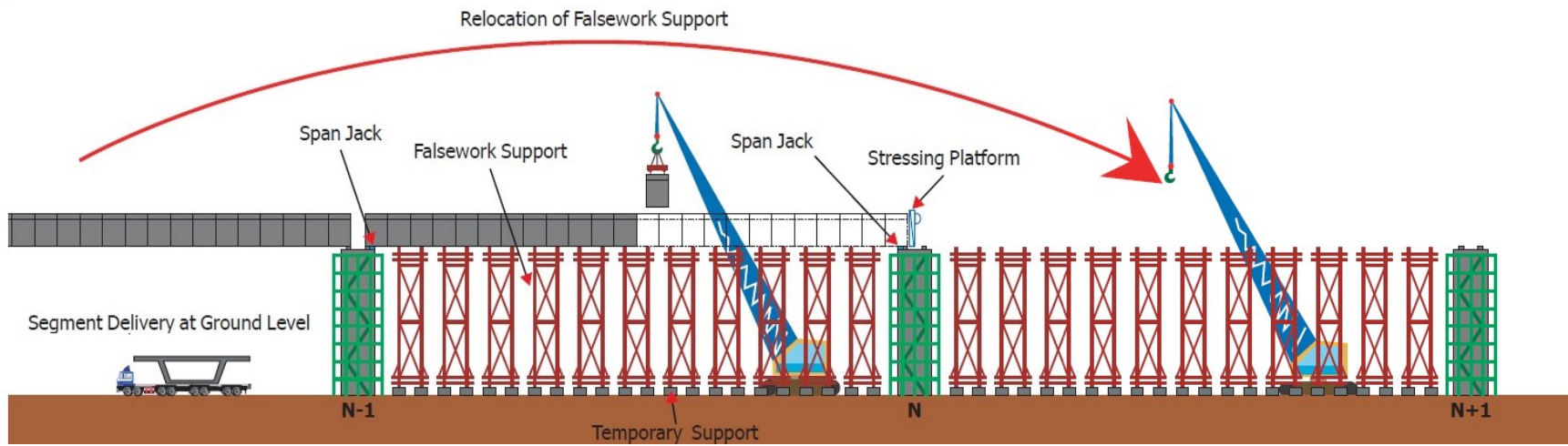
(a) Span-by-span precast segmental erection using launching gantry (Figure 2-7(a)) has been used extensively in the past on highway and light-rail projects such as Deep Bay link, Metro de Santiago, Bandra Worli Bridge, Pusan Bridge, and Penny's Bay bridge (VSL International Ltd., 2013). Gantries are limited to erecting the deck in a sequential manner and are delayed if problems occur at any pier or in any span.

(b) Span-by-span precast segmental erection using falsework support (Figure 2-7(b)) has been used extensively in the past on highway and light-rail projects such as Deep Bay Link, Penny's Bay, West Link, East Rail (VSL International Ltd., 2013). Full height falsework support is used in this erection technique; therefore, a conventional scaffold support or heavy shoring can be used depending on the effective height of the structure and the imposed loading of the falsework system (VSL International Ltd., 2013). In this method, segments are delivered one by one by trailers on the ground and placed on the falsework using cranes. Once an entire span is erected, the segments are jacked, aligned, joined and post-tensioned (Gerwick, 1993). The advantages of using the falsework system are: (1) the falsework erection and dismantling do not require highly skilled labor; (2) it is adjustable to complex and variable geometry of the superstructure; (3) the falsework sections are limited in size and easily transportable (Liebenberg, 1992); (4) the construction work can proceed on multiple spans; and (5) the crew size can be fully optimized to ensure work continuity (VSL International Ltd., 2013). However, the use of this method comes with some disadvantages such as the system is cumbersome and slow; strong foundation conditions might be required (Liebenberg, 1992); and good access is required for the delivery of the segments and crane maneuvering (Hewson, 2012).

(c) Span-by-span precast segmental erection using under-slung girder (Figure 2-7(c)) has been used extensively in the past on highway and light-rail projects such as West Rail, Windsor Flood Plane, Gautrain Viaducts (VSL International Ltd., 2013), Extension, Mancunian Way, and Long Key Bridge (Mondorf, 2006). Under-slung girders are usually steel structures that have the length of one to two spans. The under-slung girder is supported directly on the piers or on pier brackets independent of the conditions of the ground below the bridge. This erection technique combines features of the two above-mentioned techniques. Some under-slung girders can launch themselves automatically to the next span after completing the erection of the previous span as in the launching gantry technique. In addition, segments are placed on the girder by using cranes as in the falsework support technique (Mondorf, 2006). The advantages of this erection technique are: (1) the equipment required is not overly heavy; (2) the span length may vary stepwise within a certain range (Mondorf, 2006).

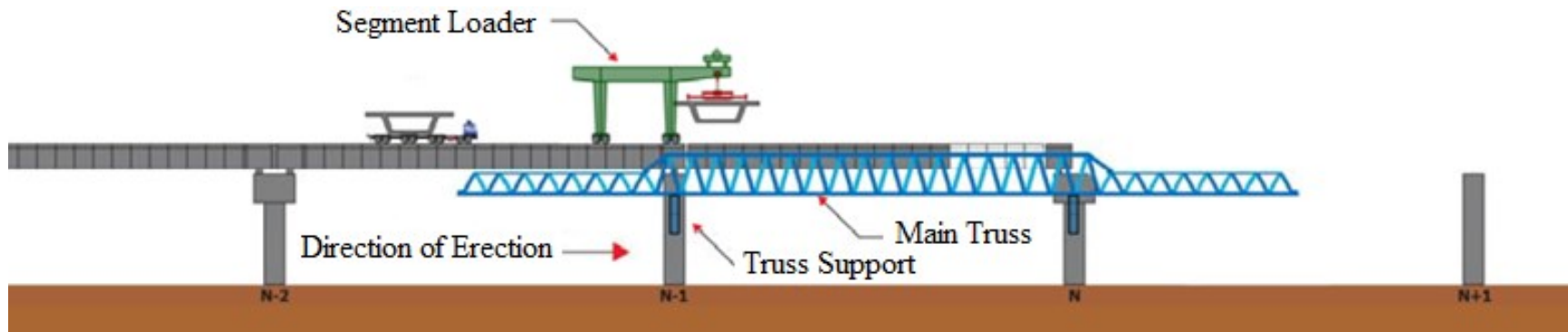


(a) Using Launching Gantry



(b) Using False-work

Figure 2-7 Schematic Drawings of Segmental Span-by-span Construction Method (VSL International Ltd., 2013)



(c) Using Under-slung Girder

Figure 2-7 (continued) Schematic Drawings of Segmental Span-by-span Construction Method (VSL International Ltd., 2013)

2.2.2 Method Selection

The selection of the construction method for constructing a bridge is a complex decision-making problem that includes many decisions. In addition, having multiple project objectives to be achieved adds to the complexity of the problem. Few researchers have worked on the selection of the bridge construction method. Murtaza et al. (1993) developed an expert system to analyze the use of modular construction for a power plant project. Tabai et al. (1998) developed a construction method selection support system for the construction of concrete slabs in building. Soetanto et al. (2006) developed a multi-criteria framework for selecting the structural frame. Chen et al. (2010) developed a decision support tool that aids planners in selecting the construction method of concreting (cast in-situ versus precast) different building elements. For bridges and elevated highways construction method selection, only two works have been found in the literature and they are presented below.

Youssef et al. (2005) developed an intelligent decision-support system to evaluate the alternative construction methods of concrete bridge superstructures in Egypt. The system is supposed to aid professionals during the planning stage of a project. This system compares the following construction methods: stationary formwork, advancing shoring system, incremental launching, launching girder, and cast in-situ balanced cantilever. The system uses Analytic Hierarchy Process (AHP) to evaluate and recommend one of the above construction methods for a given situation. The main criteria used to evaluate alternatives are cost, duration, bridge physical characteristics, characteristics of the construction method, and the surrounding environment. These criteria were identified through 13 interviews with industry professionals. Furthermore, 31 questionnaires were conducted to rank the importance of each criterion. The system proposes the applicable construction methods based on the bridge physical characteristics and the surrounding environment information provided by the user. A database of rules of thumb, which are used to identify the applicable alternatives, was created by conducting five structured interviews with industry experts. The user of the system enters the weight of each criterion and sub-criterion. Furthermore, the user has to fill the cost information related to each feasible construction method. Finally, the relative weights are divided by the cost for each alternative where the alternative with the highest resulting value is the best construction method for that project.

Pan (2008) proposed a fuzzy AHP model to overcome the incapability of traditional AHP to transform an expert preference into an exact number. The proposed method was applied to the problem of selecting the suitable bridge superstructure construction method. The important criteria and their relationship to the decision problem were developed as per the suggestions of bridge professionals. The main criteria used in this model are quality, cost, safety, duration, and shape of bridge. Questionnaires were used to obtain a pairwise comparison by using linguistic terms for each criterion. Three pre-selected construction methods were used in the comparison: precast full span launching method, cast in-situ advancing shoring method, and cast in-situ balanced cantilever method. The suitable construction method is cast in-situ advancing shoring method according to the study regardless of the characteristics or surrounding of the bridge. In addition, the quality and safety of the construction method are found to be the two most important criteria, while the bridge shape is found to be the least important criterion. In order to use this system, the user should define the hierarchy of the decision problem, and the pairwise comparison judgments. Thus, a high level of expertise in bridge construction is required to use the proposed system.

Despite the notable contributions of the abovementioned researches, they have the following shortcomings, individually or collectively: (1) they are subjective since they were based on qualitative analysis; (2) they are restricted by the region where the surveys used to build those models were conducted; (3) they ignore the characteristics and constraints of each bridge construction project and each construction method; (4) they require a high level of expertise; (5) they do not take the availability of resources into consideration; and (6) they do not optimize the selected construction method.

However, the complexity and the uncertainty of construction operations, and the limited knowledge of the behavior of the operations under different combinations of resources make it impossible to describe such operations using a closed form formula. Therefore, discrete event simulation can be used to model the complexity of the construction operations while the uncertainty can be modeled by incorporating stochastic durations and/or costs into a discrete event simulation model.

2.3 Construction Simulation

2.3.1 Simulation in Construction

Simulation is a powerful tool that can be used to mimic the behavior of real-world systems over time (Law and Kelton, 1991). Simulation can determine the output of a system based on the variations in the input to a system (Halpin and Riggs, 1992). Simulation has been used in many fields such as supply chain (He et al. 2014), transportation (Frantzeskakis and Frantzeskakis 2006), fluid dynamics (Vernay et al. 2014), design optimization (Wang et al. 2014), power systems (Degeilh and Gross 2015), and biology (Székely Jr. and Burrage 2014). Construction simulation is a well matured research area. Several construction simulation methods and tools have been proposed and developed such as CYCLONE (Halpin, 1977), RESQUE (Chang, 1986), COOPS (Liu, 1991), CIPROS (Odeh, 1992), STROBOSCOPE (Martínez, 1996), and SIMPHONY (Hajjar and AbouRizk, 1999), to name a few.

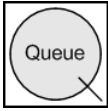
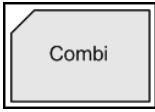
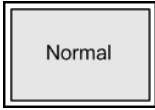

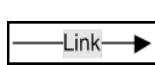
The construction processes that have a repetitive and cyclic nature can be planned and analyzed using simulation (Touran, 1990). Simulation in construction has been used for planning and resource allocation (AbouRizk et al. 1992), comparing the outcome of alternative construction methods (Oloufa 1993), analyzing earthmoving operations (McCahill and Bernold 1993; Marzouk and Moselhi 2003) and bridge construction operations (Huang et al., 1994; Abraham and Halpin, 1998; Reddy et al., 1999; López and Halpin, 2000; Hong and Hastak, 2007; Marzouk et al., 2007; Marzouk et al., 2008; Pan et al., 2008; Said et al. 2009; Ailland et al., 2010; Mawlana et al., 2012; Mawlana and Hammad, 2015).

This research uses STROBOSCOPE to develop the simulation models. STROBOSCOPE, an acronym for STate- and ResOurce-Based Simulation of COnstruction ProcEsses, is a general-purpose discrete-event simulation system. STROBOSCOPE uses the activity-scanning paradigm which is well suited for modeling construction processes that have a cyclic nature. STROBOSCOPE is capable of dynamically accessing the state of the simulation and the properties of the resources involved in an operation. The number of resources waiting in a queue; the total number of instances of each task; and the first time or the last time a particular activity started are all examples of the state of the simulation. The properties of resources refer to the specific characteristics of each resource such as the cost, capacity, or weight. Moreover,

STROBOSCOPE can accommodate deterministic and stochastic modeling of construction operations. This allows for extensive sensitivity analysis to be carried out, which in turn reduces the risk associated with the project. STROBOSCOPE is used because it: (1) is user friendly; (2) has built-in functions and stream management tool that allow for the implementation of any variance reduction technique; (3) can be controlled using many programming languages; and (4) is well documented.

Stroboscope models are based on a network of interconnected modeling elements (as shown in Table 2-1). In addition, a series of programming statements are used to give the elements a unique behavior and to control the simulation. The modeling elements consist of nodes and links. Links are used to connect the network nodes and indicate the direction and type of resources that flow through them. Every link represents the flow of one type of resources only, which can be a single resource (e.g. empty truck) or combined resources (e.g. truck loaded with soil). The node at the tail of the link is the predecessor and the node at the head is the successor. There are two types of nodes in STROBOSCOPE which are *queues* and *activities*. *Queues* are nodes that hold that resources when they are either stored there or waiting to be used. Each *queue* is associated with a particular resource type. On the other hand, *activities* are nodes that represent tasks in which the resources are productive. Resources engaged in an activity stay tied for the duration of the activity. There are three types of *activities* in STROBOSCOPE which are the *normal*, the *combi*, and the *consolidator*. The *normal* and the *combi* activities differ in two aspects. The first is the way the activities may start and the second is the way they acquire the resources they need. *Combi* activities represent tasks that must meet certain conditions in order for them to start. Most of the time, these conditions are related to the availability of resources in the *queues* preceding that *combi*. That is, *combi* activities withdraw the required resources from the preceding *queues*. Therefore, *combi* activities can only be preceded by *queues* because inactive resources reside only in *queues*. *Normal* activities, on the other hand, represent tasks that start immediately after other tasks end. Moreover, they acquire the required resources from the preceding task that has just finished. *Consolidators* are used to accumulate resources or to block resources flow until certain conditions are met. After these conditions are met, all resources are released and sent to the desired nodes.

Table 2-1 STROBOSCOPE Elements Used to Build Up the Simulation Models (Martínez, 1996)

Symbol	Description
	Queues hold resources that are idle. Each Queue is associated with a particular resource type.
	Combi activities represent tasks that start when certain conditions are met.
	Normal activities represent tasks that start immediately after other tasks end.
	Consolidators are activities that start and finish their instances depending exclusively on the resources they receive.
	Links connect network nodes and indicate the direction and type of resources that flow through them.

2.3.2 Bridge Construction Methods Simulation

Simulation has been used to study the performance of bridge construction methods, for example, the construction of the deck of a cable-stayed bridge using balanced cantilever method (Huang et al., 1994), the construction of concrete box girder bridge deck using cast-in place on false-work and stepping formwork (Marzouk et al., 2006), incremental launching method (Marzouk et al., 2007), lifting for precast balanced cantilever bridges (Marzouk et al., 2008), cantilever carriage for cast in place balanced cantilever bridges (Said et al., 2009), and the construction of precast concrete box girder using the full-span launching gantry method (Pan et al., 2008; Mawlana et al., 2012). However, the previous work did not optimize the construction method of bridges. In addition, simulation can only evaluate the performance measure index of an operation for a given scenario. In order to find the optimum scenario, an enumeration and evaluation of all possible combinations must be carried out, which is not feasible for large problems. Therefore, simulation must be integrated with an optimization technique in order to optimize the bridge construction methods.

2.4 Optimization

Optimization can be defined as the process of finding one or more solutions that satisfy all constraints while minimizing (or maximizing) one or more specified objectives (Branke et al., 2008). An optimization problem can be expressed as follows:

Minimize (or Maximize) an objective

Subject to a set of constraints

As shown in Figure 2-8, optimization can be mainly classified based on the number of the objective functions, the uncertainty in the decision variables or objective functions' values, and the type of the optimization problem. The optimization problem is called a single optimization problem or multi-objective optimization problem if it has a single objective or multiple objectives, respectively. The optimization is considered deterministic when the value of the objective function for a set of decision variables can be estimated with certainty. On the other hand, stochastic optimization occurs when the value of the objective function for a set of decision variables cannot be estimated with certainty.

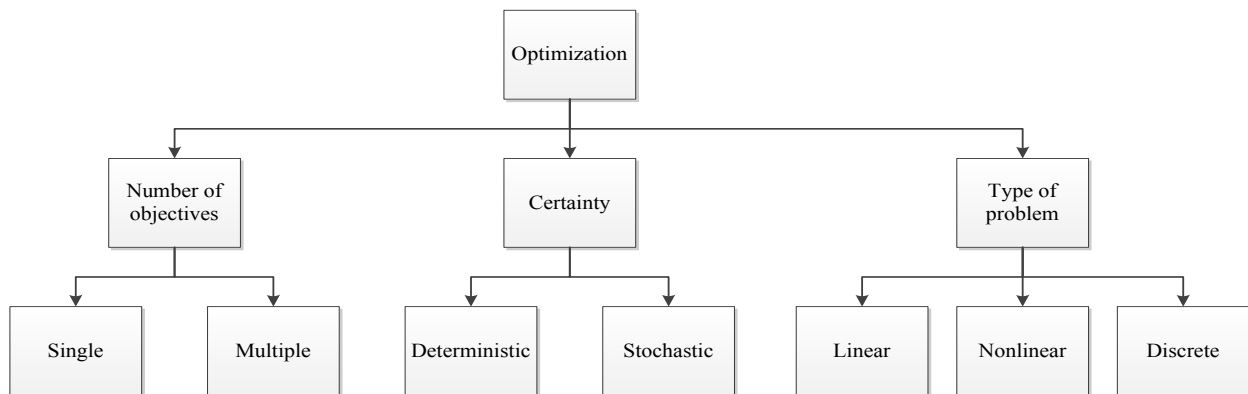


Figure 2-8 Classification of Optimization Problems

The form of the equations that represent the objective functions and the decision variables describes the type of the optimization problem. These equations can be linear, nonlinear, or discrete (Diwekar, 2008). Linear optimization (mainly called linear programming) is the optimization of the problems that have linear objective functions and constraints, and scalar and continuous decision variables. Nonlinear optimization (mainly called nonlinear programming) is

the optimization of the problems that have nonlinear objective functions and constraints, or either of them. Moreover, these problems must have scalar and continuous decision variables. Discrete optimization is the optimization of the problems that have discrete decision variables. Discrete optimization can be categorized into integer programming, mixed integer linear programming, and mixed integer nonlinear programming problems. The integer programming problem involves scalar and integer decision variables. However, the objective functions and constraints can be either linear or nonlinear. Mixed integer refers to the combination of integers and continuous decision variables. Mixed integer linear programming problems have linear objective functions and constraints while mixed integer nonlinear programming problem have nonlinear objective functions and/or constraints.

2.4.1 Multi-objective Optimization

The problems that require the consideration of multiple objectives simultaneously are called multi-objective optimization problems. Cohon (1978) describes a multi-objective optimization as the process of finding a range of efficient solutions or a preferred solution to a problem using a set of procedures. Mathematical functions are used to formulate the objective functions and constraints as a set of decision variables. Consequently, a general definition of multi-objective optimization problem can be formally written as follows (Nakayama et al., 2009).

$$\text{Minimize (or Maximize) } f(\mathbf{x}) = \{f_1(\mathbf{x}), f_2(\mathbf{x}), \dots, f_m(\mathbf{x})\} \quad \text{Equation 2-1}$$

$$\text{Subject to } \begin{aligned} h_i(\mathbf{x}) &= 0 \\ g_j(\mathbf{x}) &\geq 0 \end{aligned}$$

Where x is the vector of decision variables, $f(\mathbf{x})$ is the set of objectives to be minimized, $f_1(\mathbf{x})$ is the function of the first objective, $g(\mathbf{x})$ and $h(\mathbf{x})$ are the functions of the sets of inequality and equality constraints.

The objectives in a multi-objective optimization problem can be totally conflicting, non-conflicting, or partially conflicting (Goh and Tan, 2009). The complexity of multi-objective optimization problems rises from the existence of multiple, conflicting objectives with a large, complex search space (Jimenez, 2007). Most real-world problems have partially conflicting objectives where finding a single optimum solution that satisfies all the objectives is not possible. There are two main approaches to solve a multi-objective optimization problem:

(1) combining the multiple objective functions into a single objective function; or (2) obtaining a set of non-dominated optimum solutions (Jimenez, 2007). Consequently, the preferable outcome of a multi-objective optimization problem is a set of non-dominated optimum solutions which represent the potential tradeoff among the objectives as shown in Figure 2-9. In other words, moving from one solution to another means that an objective is being traded for another. Tradeoff refers to the improvement of one objective by worsening the other objective. Each solution in this set is called a Pareto solution or non-dominated solution which can be defined as a solution that no improvement can be done to one objective without worsening the other objective. The set of optimum solutions is called the Pareto set or the non-dominated set and the graphical representation of Pareto set in the objective function space is called the Pareto front as shown in Figure 2-9. The points in the figure represent some of the feasible solutions. Points *A*, *B*, *C*, *D* are example of the non-dominated solutions which form the Pareto front.

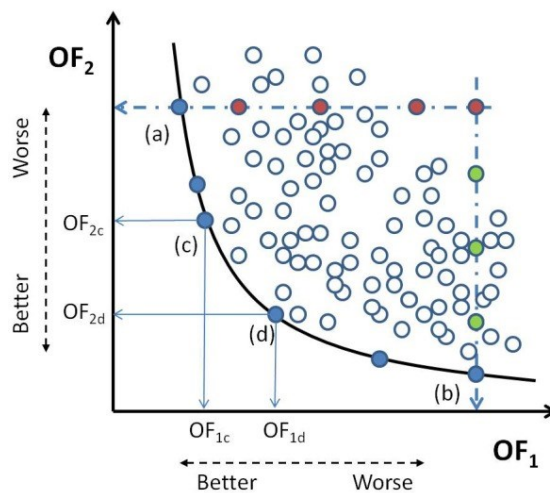


Figure 2-9 Pareto Front (Pozo et al., 2012)

The tradeoff analysis between time and cost is one of the most important aspects of construction engineering and management (Feng et al., 2000). In this tradeoff, the decision maker can select the solution that has the best compromise in term of time and cost. A tradeoff exists because reducing the project duration requires the use of extra resources which in turn will increase the project direct cost. Thus, this intricate relation between project duration and cost promotes opportunities to find the project setting or resource allocation plan that will optimize the project duration and cost.

There are two main approaches to solve this tradeoff problem which are mathematical programming and metaheuristic search methods. Mathematical programming methods, such as linear programming and integer programming, express the objective functions and constraints of an optimization problem using closed form formula. Although these methods have been applied to solve the tradeoff problem, they have some limitations such as: (1) formulating the constraints and the objective functions is time consuming and prone to errors (Liu et al., 1995); (2) some approaches do not provide the optimum solution (Feng et al., 2000); (3) the inability to handle more than one objective (Zheng et al., 2005; Reddy and Kumar, 2007); and (4) being inefficient for solving large complex problems (Adeli and Karim, 1997; Senouci and El-Rayes, 2009). Metaheuristic methods can be classified into population-based methods, such as Ant Colony Optimization and Genetic Algorithms (GAs), and trajectory methods, such as Simulated Annealing and Tabu Search. Simulated annealing and Tabu search sometimes can be stuck at a local optimum solution and requires a large computation time (Jimenez, 2007).

2.4.2 Genetic Algorithms

GAs are considered to be one of the standard methods for solving multi-objective optimization problems (Liao et al., 2011). They are capable of getting an approximation of the Pareto front in a single optimization run (Jimenez, 2007). This is achieved by searching the different parts of the solution landscape in a parallel way (Yu and Gen, 2010). GAs guarantee to identify the optimum tradeoffs and do not tend to be stuck at a local optimum like other metaheuristic methods (Abraham et al., 2005). In addition, GAs are very practical because of the following reasons: (1) they can be applied to multi-objective optimization problems regardless of the problem representation (Deb, 2001), (2) they are insensitive to the shape of the Pareto-front (Goh and Tan, 2009), and (3) they are easy to implement, and could be implemented in a parallel environment (Abraham et al., 2005). The simple GA is a set-based stochastic search algorithm that was developed by Holland (1975) based on the natural evolution theory. Since the development of the simple GA, several researchers have introduced several improvements to it. Among these is the fast messy Genetic Algorithm (fmGA) (Goldberg et al., 1993). The fmGA has proven to be effective in optimizing decision making in construction operations (Feng and Wu, 2006; Cheng and Wu, 2009). This research uses the fmGA to solve the optimization problem of selecting the bridge construction scenario.

Fast Messy Genetic Algorithm

The fast messy Genetic Algorithm (fmGA) was developed to overcome some of the problems faced while using the simple GA and the messy Genetic Algorithm. The fmGA operates by iterating within two loops which are the outer and inner loops. This process is summarized in Figure 2-10. The fmGA starts from the outer loop by random initialization of the competitive template. Each outer loop, which is called an *era*, performs an inner loop. The inner loop consists of three phases namely the *initialization*, the *primordial*, and the *juxtapositional* phases. The *initialization* phase starts by generating an initial population of size N using the probabilistically complete initialization (PCI) technique. Each generated solution is evaluated to measure its fitness. The *primordial* phase uses thresholding selection and building block filtering to increase the proportion of the better solutions by filtering out the worse solutions. All filtered solutions are evaluated at this phase. This process is repeated until the *primordial* termination criterion is met. Finally, the *juxtapositional* phase applies thresholding selection, and two operations namely cut and splice, and mutation. All generated solutions are evaluated in this phase. This process is repeated until the *juxtapositional* termination criterion is met. The template of the new *era* is set to the best solution found at the end of the *juxtapositional* phase. The outer loop stops when the termination criterion is met.

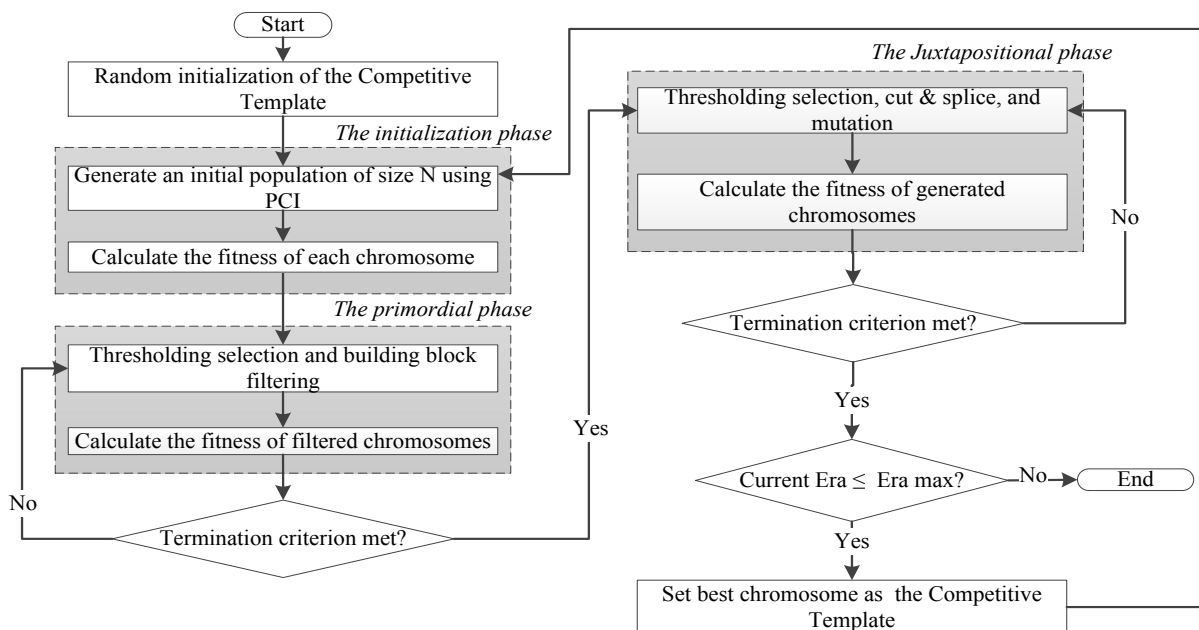


Figure 2-10 Flowchart of Fast Messy Genetic Algorithm

2.5 Stochastic Simulation-based Optimization

As mentioned in *Section 2.3.2*, simulation must be coupled with optimization in order to optimize the bridge construction operations. Simulation-based optimization can be defined as the process of using a heuristic algorithm to guide the simulation analysis without the need to perform an exhaustive analysis of all the possible combinations of input variables (Carson and Maria, 1997). The purpose of simulation-based optimization is to find the configuration of decision variables that will optimize the objective function of the model. Figure 2-11 shows a schematic of the integration of simulation and optimization. The process starts by generating candidate solutions by the optimization engine. These solutions are then sent to the simulation engine to be evaluated. Finally, the performance measure index of each solution is reported back to the optimization engine.

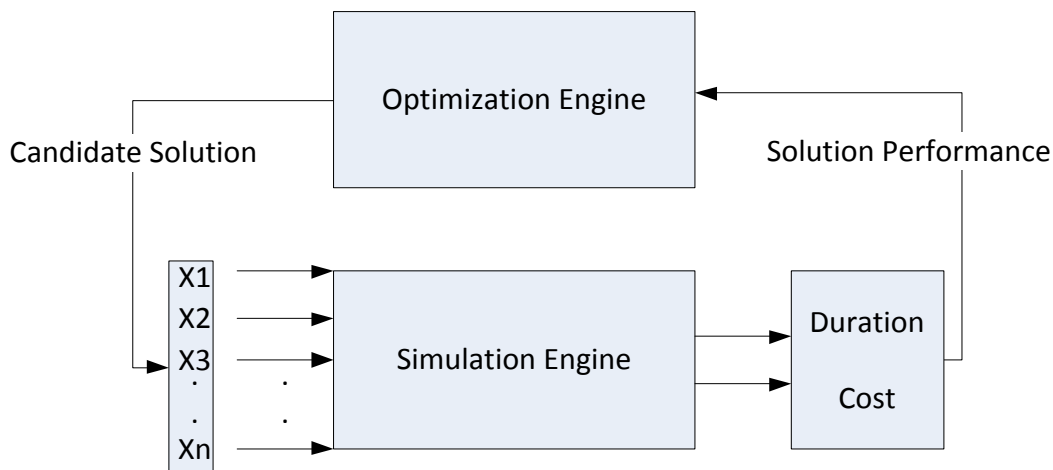


Figure 2-11 Integration of Optimization Engine and Simulation

Several optimization approaches (Figure 2-12) have been used in simulation-based optimization mainly random search, gradient-based procedures, ranking and selection, metaheuristic algorithms, response surface methodology, and stochastic approximation (Carson and Maria, 1997; Fu et al., 2008; Keskin et al., 2010). Selecting the optimization approach depends on the objective functions and the values of the decision variables. Random search and metaheuristic algorithms are appropriate for problems with non-differentiable objective functions, decision variables with discrete values, and large number of alternatives (Barton and Meckesheimer, 2006). Combinations of simulation with metaheuristic optimization methods such as Particle

Swarm (Zhang et al., 2006; Yang et al., 2012), Genetic Algorithm (Alberto et al., 2002; Hegazy and Kassab, 2003; Mawlana and Hammad, 2013; Alanjari et al., 2014), Ant Colony (Marzouk et al., 2009), Belief networks (McCabe, 1998), and Tabu Search (Glover et al., 1996) have been used to find near-optimum solutions.

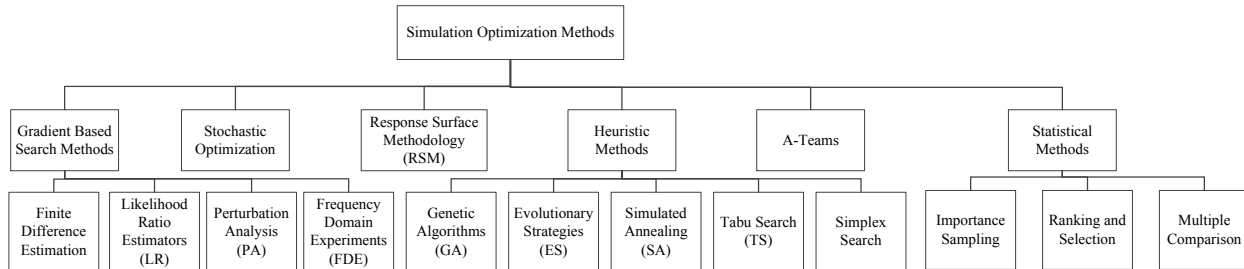
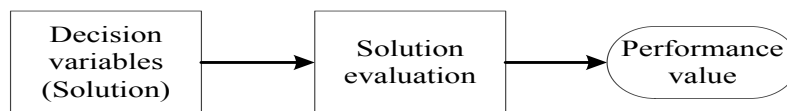
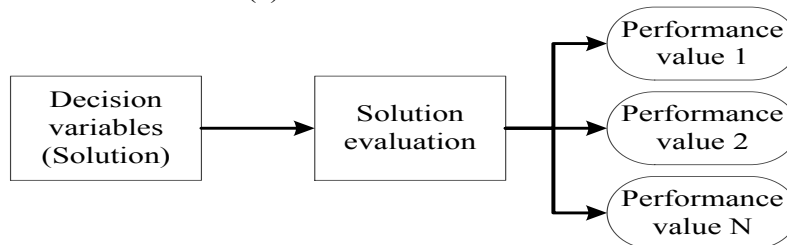


Figure 2-12 Simulation-based Optimization Methods (Carson and Maria, 1997)

Simulation-based optimization can be either deterministic or stochastic. Deterministic simulation-based optimization refers to the process of finding the configuration of the decision variables that optimizes a problem through the use of deterministic simulation to evaluate the performance measure index of candidate solutions. On the other hand, stochastic simulation-based optimization uses stochastic simulation to evaluate the performance measure index of candidate solutions. A deterministic simulation returns the same value of performance measure index for a specific configuration of decision variables whenever that configuration is evaluated as shown in Figure 2-13(a). Whereas a stochastic simulation returns a different value performance measure index every time a specific configuration of decision variables is evaluated as shown in Figure 2-13(b).



(a) Deterministic Simulation



(b) Stochastic Simulation

Figure 2-13 Deterministic Versus Stochastic Simulation

2.5.1 Optimizing Construction Methods

Optimization of construction operations has been studied in the literature in different application areas such as concrete plant operations (Cao et al. 2004), concrete placing (Hegazy and Kassab, 2003), and earthwork operations (Marzouk and Moselhi, 2004). However, very little research has been done with regard to the optimization of construction methods of bridges.

Marzouk et al. (2009) presented a stochastic simulation-based optimization framework for optimizing the operations of constructing bridge decks using the launching girder system. The bridge deck construction using launching girder system contains two main processes: (1) beams fabrication, and (2) beams erection. The first process includes reinforcement installation, beam casting, curing, storing and transporting of the concrete beams to the construction site. On the other hand, the second process includes the erection of the concrete beams, the installation of the formwork, reinforcement, and casting of the deck of the bridge. This framework consists of three modules which interact in a cyclic manner: optimization, simulation, and reporting modules. The optimization module uses ant colony optimization and it searches for the near-optimum solution by minimizing the time and cost of construction. This framework accounts for seven decision variables: location of casting yard, time lag, number of casting forms, number of preparation platform, curing method, number of yard reinforcement crews, and number of stressing crews. Two multi-objective approaches are used to transform the multiple objectives into a single objective: function-transformation and modified distance approaches. The simulation module is used for estimating the total duration and cost of bridge deck construction. STROBOSCOPE was used to build the simulation model that represents the two main processes of this system. The tasks durations are expressed using probability distributions to take into account any uncertainties. The total duration of the construction operation is measured from the start of the first beam fabrication to the prestressing of the last span precast beams. This duration is obtained directly from running the simulation while the total cost of the operation is calculated based on the durations of the casting and erection operations, which are obtained from the simulation.

Nassar et al. (2011) introduced a simulation-based optimization framework to solve the time-cost tradeoff problem of constructing a bridge deck using the advanced shoring method. The main concept of this method is that the formwork used for the casting the bridge deck is done on stepping erection girders. These girders are supported on the piers and they advance after casting

the span to the following span. The in-situ concreteing is carried out in two stages. The first stage consists of fixing the steel reinforcement and casting the bottom slab and webs. The second stage consists of fixing the steel reinforcement and casting of the top slab. Particle swarm optimization was used to solve this multi-objective problem while STROBOSCOPE was used to model the construction operations of this construction method. The objective function was defined as the product of the cost and the simulation time of the construction operation.

2.5.2 Limitations of Traditional Simulation-based Optimization

Despite the advantages that can be achieved by using simulation-based optimization, it still has a few limitations. Three limitations are identified, as was explained in Section 1.2, which are: (1) the stochasticity of the objective functions could result in an inaccurate estimate of the objective functions, which leads to the problem of stochastic dominance; (2) the need to perform N replications to obtain an estimate of the objective functions, which is time consuming; and (3) the correlation of the objective functions is ignored.

2.6 Stochastic Dominance

The use of stochastic simulation to evaluate the candidate solutions may cause an uncertainty in the estimate of the objective functions. This uncertainty will impact the performance of the optimization algorithm because it can mislead the optimization process by selecting a solution that is dominated by another solution. In other words, inferior solutions can be perceived as non-dominated solutions and vice versa. Consequently, the optimization algorithm may not provide the decision makers with the optimum solutions. This problem is known as stochastic dominance (Goh and Tan 2009). That is, the dominance relationship between the candidate solutions is not fixed. This problem occurs when the distributions of the candidate solutions overlap.

One of the basic approaches to overcome this limitation is to use explicit averaging. Explicit averaging is done by calculating the average of a number of simulation replications (N) for each candidate solution (a configuration of decision variables) using the simulation engine (Feng et al., 2000; Cheng and Lee, 2011). The purpose of these replications is to capture the uncertainty and to obtain a good confidence level in the estimate of a solution's performance measure index. A stochastic simulation optimization problem can be described as (Cheng and Lee, 2011):

$$\min_{\theta \in \Theta} \langle J_1(\theta), \dots, J_H(\theta) \rangle \quad \text{Equation 2-2}$$

$$\bar{J}_l(\theta) = E[L_l(\theta, \omega)] \quad \text{Equation 2-3}$$

Where $J_H(\theta)$ is the H -th objective function, θ is a vector of all the decision variables, Θ is the search space of the problem, ω is a simulation replication with a certain uncertainty, $L_l(\theta, \omega)$ is the performance measure index of the l -th objective function calculated with uncertainty using simulation, E is an expectation of the performance measure index.

Based on the objective function, $L_l(\theta, \omega)$ can represent the cost, the duration, or the cycle time of an operation. Since one simulation replication is not representative of a stochastic simulation model, several replications must be made to obtain a sound estimate of $E[L_l(\theta, \omega)]$. The sample mean is the standard approach to estimate $E[L_l(\theta, \omega)]$ as shown in Equation 2-4 (Cheng and Lee, 2011).

$$\bar{J}_l(\theta) = \frac{1}{N} \sum_{j=1}^N L_l(\theta, \omega_j) \quad \text{Equation 2-4}$$

where N is the number of replications, \bar{J}_l is the mean value of the l -th objective function, ω_j is the j -th simulation replication.

To overcome this limitation, this research proposes using VRTs. The following sub-section describes the most widely used VRTs, which are Common Random Numbers (CRN) and Antithetic Variates (AV) (Kleijnen 1975; Schruben and Margolin 1978; Wilson, 1983).

2.6.1 Variance Reduction Techniques

VRTs were developed to reduce the variance of a performance measure index of a simulation model without increasing the number of simulation replications (James, 1985). Thus, they result in reducing the computation efforts needed by reducing the required number of simulation replication. This can be done, as explained in the following subsections, by inducing positive correlation between the simulation replications or a negative correlation between the simulation replications in a pair. In the field of construction engineering and management, there exists few works where VRTs were used. CRN was used to compare alternative resource configurations of earthmoving operations (AbouRizk et al., 1990) and to compare two construction methods for rock tunneling (Ioannou and Martinez, 1995).

Common Random Numbers

CRN is used to compare the performance measure index of a simulation model across different candidate solutions. In the context of this research, the different candidate solutions are the resource combinations generated by the optimization algorithm. The concept of CRN is that the decision maker wants to compare the performance measure index of the different candidate solutions under the same uncertainty conditions so that any improvement in the performance measure index is solely due to the change in the resource combination. In other words, every stochastic task instance's duration in a candidate solution will have the same probability as its counterpart in another candidate solution. For instance, all the candidate solutions will have the same duration of the first instance of task A . This is done by controlling the random numbers used to generate the random variates (i.e., durations) for each stochastic task and reusing them across the different candidate solutions (Kleijnen 1975; Schruben and Margolin 1978; Asmussen and Glynn 2007). By doing so, a positive correlation is induced between the different candidate solutions. Traditionally, two candidate solutions are compared relatively to each other using Equation 2-5 (Kleijnen, 1974).

$$\bar{Z}(N) = \frac{\sum_{n=1}^N (X_{1n} - X_{2n})}{N} \quad \text{Equation 2-5}$$

Where $\bar{Z}(N)$ is the average difference between the output of two candidate solutions, N is the number of replications performed, and X_{1n} and X_{2n} are the performance measure index of the n -th replication of candidate solutions 1 and 2, respectively. In order to check if the CRN technique is actually working, the variance of the difference ($S_z^2(N)$) should be less than the summation of the variances of candidate solution 1 ($S_1^2(N)$) and candidate solution 2 ($S_2^2(N)$) over the same number of replications as shown in Equation 2-6 (Law 2007).

$$S_z^2(N) < S_1^2(N) + S_2^2(N) \quad \text{Equation 2-6}$$

In addition, Equation 2-7, which indicates the existence of a positive correlation between the two candidate solutions, must hold true.

$$\rho(X_{1n}, X_{2n}) > 0 \quad \text{Equation 2-7}$$

Antithetic Variates

AV is used to obtain the performance measure index of a single candidate solution of the simulation model. The concept of AV is that the simulation replications are run in pairs where the second replication (antithetic) in a pair uses complementary random numbers to the ones used in the first replication (standard). In other words, each replication in a pair has the exact opposite probability of the other replication in the same pair. For instance, if the first instance of task A in the standard replication of a pair has an optimistic duration, then the first instance of the same task in the antithetic replication of the pair will have a pessimistic duration. The reasoning behind this concept is that getting a performance measure index estimate on each side of the mean will give a closer estimate to the mean than having both performance measure index estimates on one side of the mean. AV is realized by controlling the random numbers used to generate the random variates for each stochastic task in the standard replication and then subtracting the used random numbers from one and using them in the antithetic replication in the same order they were used in the standard replication. This technique will induce a negative correlation between the replications in a pair (Bratley et al. 1987; L'Ecuyer 1994). The average performance measure index of a candidate solution can be found using Equation 2-8 (Emshoff and Sisson, 1970).

$$\bar{X}(N/2) = \frac{\sum_{p=1}^{N/2} (X'_p + X''_p)}{N} \quad \text{Equation 2-8}$$

Where $\bar{X}(N/2)$ is the average performance measure index of a simulation model over $N/2$ pairs, N is the number of replications performed, and X'_p and X''_p are the performance measure index of the standard and antithetic replications of the p -th pair, respectively. In order to check if the AV technique is actually working, the variance of the average performance measure index obtained when pairs are run using AV should be less than the variance of the average performance measure index obtained when pairs are run independently. In addition, Equation 2-9 which indicates the existence of a negative correlation between the two replications in a pair must hold true.

$$\rho(X'_p, X''_p) < 0 \quad \text{Equation 2-9}$$

2.7 Required Computation Time

To reduce the required computation time, two approaches have been proposed which are: (1) increasing the computation power; and (2) reducing the number of required replications. Several researches implemented simulation-based optimization using parallel computing in order to reduce the computation time required to solve the optimization problem (Heidelberger, 1988; Schruben, 1992; Yucesan et al., 1995; Lagana et al., 2006 to name some). In these implementations, the number of simulation replications is fixed for all the candidate solutions. Salimi et al. (2015) reported a huge improvement when parallel computing was used to optimize a precast full span bridge construction using launching gantry. However, deterministic simulation was used which only requires one simulation replication per candidate solution. In addition, a cluster of 64 cores was used to solve the optimization problem. This amount of computation power comes with a high price tag and it is not always accessible by planners, which makes the use of the parallel computing impractical.

On the other hand, several different approaches to reduce the number of simulation replications have been proposed. The main difference is how to allocate the computation efforts among the candidate solutions. In these approaches, the number of replications for each solution is not fixed. Rinott (1978) proposed a two-stage indifference-zone procedure. Using this procedure, all candidate solutions are run for a fixed number of replications in the first stage. In the second stage, additional simulation replications are added for each candidate solution based on the sample variances obtained in the first stage. Chen et al. (1996) and Chen et al. (1997) applied the same concept but the number of additional simulation replications was based on the sample means and sample variances of the candidate solutions obtained in the first stage. Despite the fact that the proposed approaches do reduce the number of simulation replications, and as a result, the total computation time, they still require a large number of replications for some of the candidate solutions.

To overcome this limitation, this research proposes combining VRTs and parallel computing to reduce the number of required replications required and the required computation time simultaneously. The following section describes briefly the concept of parallel computing.

2.7.1 Parallel Computing of Genetic Algorithms

Parallel computing is all about distributing the amount of work to be done among several processors and executing the work simultaneously in order to reduce the computation time (Cantú-Paz, 1997). To perform parallel computing, one can use a computer with a multi-core or multi-processors or a group of computers connected together (Barney, 2013). However, most parallel computing implementations of GAs have been on a cluster of computers (74.6%) or Massive Parallel Processors (21.4%) (Munawar et al., 2008).

Enormous research has been done to execute GAs in parallel environments. The execution of GAs in parallel environments can be classified into four categories which are: (1) global single-population master-slave, (2) multiple-population coarse-grained, (3) single-population fine-grained, and (4) hierarchical (Munawar et al., 2008). This research focuses on using global single-population master-slave paradigm.

In the global single population master-slave paradigm, one core, which is called the master, generates the initial population and subsequent populations by performing the GA operations at the end of each generation. Each population is then subdivided and distributed to the other processors, which are called slaves. Once each slave evaluates their portion of the population, their performance measure index values are reported back to the master. This process is repeated until the termination criterion is met (Cantú-Paz, 1997). This paradigm is illustrated in Figure 2-14.

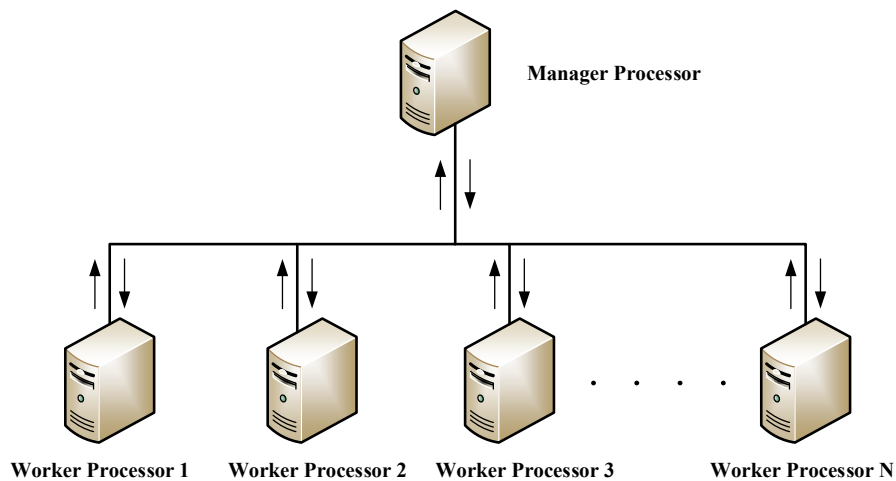


Figure 2-14 Master-slave Parallel GA Framework (Kandil & El-Rayes, 2006)

In the field of the construction engineering and management, a couple of works can be found related to the use of parallel computing for simulation-based optimization model. Yang et al. (2012) proposed integrating Particle Swarm optimization algorithm with Monte-Carlo simulation to plan bridge maintenance. The model was implemented in a parallel computing framework on a cluster of computers. Salimi (2014) proposed using Non-dominated Sorting Genetic Algorithm with discrete event simulation to optimize bridge construction operations. The model was implemented in a parallel computing framework on a server and a cluster of computers.

2.8 Correlation of Objective Functions

Due to the fact that there is a correlation between the project duration and cost, the analysis of the model performance measure indices must consider the simultaneous occurrence of the project duration and cost through the use of the joint probability (Feng et al. 2000; Yang 2011). The joint probability has been used in several applications such as integrated cost-schedule risk analysis (Hulett 2011a; Hulett 2011b; Covert 2013), flood frequency analysis (Kao and Chang 2012), system reliability analysis of flexible pavements (Dilip et al. 2013), estimating extreme sea levels (Liu et al. 2010), and failure analysis of a series structural system (Zhao et al. 2007). Examining the literature, one can notice that no research has focused on the correlation of the objective functions in simulation-based optimization. To overcome this limitation, this research proposes applying the joint probability to the objective functions obtained from stochastic simulation. The next sub-section explains briefly the theory of joint probability of bivariate discrete random numbers.

2.8.1 Joint Probability of Bivariate Discrete Random Variables

When a stochastic experiment is performed, the outcomes of this experiment are: (1) the solution space which represents all the possible outcomes of the experiment; and (2) the probability assigned to each outcome of that experiment. Each outcome can have one or more performance measure indices values. The stochastic experiment outcome is called univariate random variable, bivariate random variables, or multivariate random variables, which reflects a single performance measure index value, two performance measure indices values, or more than two performance measure indices values, respectively. For example, the duration and cost of a project alternative are considered bivariate random variables in a time-cost tradeoff problem.

There are two main types of random variables: discrete random variables and continuous random variables. A discrete random variable is the variable that can take a finite or a countable number of values, while a continuous random variable can take any value in an interval (Anderson et al., 2012). The method of calculating the probability of an outcome of an experiment depends on the number of random variables. For the purpose of this research, finding the joint probability of bivariate discrete random variables is the main interest. However, the concept can be extended to include multivariate random variables.

The probability of more than one random variable to occur simultaneously is called joint probability. The joint range is the set of all pairs of (real number) values that the bivariate (X, Y) can take and is represented by $\mathfrak{R}_{X,Y}$ (Forbes et al. 2011). In this research, however, random variables that assume natural number values $\mathbb{N}_{X,Y}$ are of interest because: (1) it is more practical to have the duration of a project rounded to the nearest day and the cost of a project rounded to the nearest round number; (2) it reduces the computation time required to perform the joint probability calculations; and (3) it improves the performance and the outcome of an optimization algorithm, when integrated with simulation, by ignoring the small improvements of the objectives' values. Mathematically speaking, if X and Y are discrete random variates, then the joint probability mass function of X and Y is (Evans and Rosenthal 2010):

$$f(x, y) = P(X = x \cap Y = y), \text{ for } (x, y) \in \mathbb{N}_{X,Y} \quad \text{Equation 2-10}$$

The joint probability statement (Equation 2-11) represents the probability that the value of the univariate X is less than or equal to x and the value of the univariate Y is less than or equal to y , simultaneously.

$$f(x, y) = P[X \leq x \cap Y \leq y] \quad \text{Equation 2-11}$$

The domain of the joint probability is the set of all probability values (α) that a probability statement can take and is denoted by $\mathfrak{R}_{x,y}^\alpha$ where $\alpha \in [0,1]$. The joint cumulative distribution function, Equation 2-12, maps the values of the random variates (X, Y) from the joint range $\mathbb{N}_{X,Y}$ into the joint probability domain $\mathfrak{R}_{x,y}^\alpha$. This function is equal to one when x and y reach their maximum values.

$$f(x, y) = P[X \leq x \cap Y \leq y] = \alpha, \forall (x, y) \in \mathbb{N}_{X,Y}, \alpha \in \mathfrak{R}_{x,y}^\alpha \quad \text{Equation 2-12}$$

Marginal distributions represent the probabilities of the values of one variable in the bivariate regardless of the value of the other variable in the bivariate. The marginal probability function for discrete variate of X is calculated for each x value by adding the joint probability function associated with the bivariate values $(x, y) \in \mathbb{N}_{X,Y}$ having fixed x as shown in Equation 2-13. The marginal probability function of Y is given by Equation 2-14 (Forbes et al. 2011):

$$f(x) = \sum_{y \in \mathbb{N}_Y} f(x, y) \quad \text{Equation 2-13}$$

$$f(y) = \sum_{x \in \mathbb{N}_X} f(x, y) \quad \text{Equation 2-14}$$

Conditional distributions are used to calculate the probability of the value of one element in the bivariate given the value of the other variate. The conditional probability function of X given that $Y = y$ is calculated by dividing the joint probability function by the marginal probability function of Y for fixed $Y = y$ for all $(x, y) \in \mathbb{N}_{X,Y}$ as shown in Equation 2-15. The conditional probability function of Y given that $X = x$ is given by Equation 2-16 (Forbes et al. 2011):

$$f(x|y) = \frac{P[X = x, Y = y]}{P[Y = y]} = \frac{f(x, y)}{f(y)} \quad \text{Equation 2-15}$$

$$f(y|x) = \frac{P[X = x, Y = y]}{P[X = x]} = \frac{f(x, y)}{f(x)} \quad \text{Equation 2-16}$$

2.9 Summary

This chapter presented a review of the literature on selecting bridge construction method, construction simulation, optimization, and stochastic simulation-based optimization. In addition, a comprehensive literature review is given about the research related to the selection and optimization of bridge construction methods. This review highlighted the gaps and shortcomings of the existing research in the field of bridge construction planning and scheduling and the related methods for overcoming these shortcomings.

CHAPTER 3: OVERVIEW OF PROPOSED METHODOLOGY

3.1 Introduction

This chapter presents an overview of the proposed methodology of a stochastic simulation-based multi-objective optimization model for the planning and scheduling of precast box girder bridge construction projects. Figure 3-1 shows the overview of the proposed methodology. The core of this methodology consists of a stochastic simulation-based multi-objective optimization model that is used to find the near-optimum construction scenario. This research consists of four main components that are necessary to realize the proposed methodology: (1) developing a stochastic simulation-based multi-objective optimization model; (2) solving the problem of stochastic dominance and reducing the number of simulation replications using variance reduction techniques; (3) reducing the computation time to solve the optimization problem using parallel computing on a single multi-core processor; and (4) applying joint probability for evaluating the duration and cost of stochastic simulation models.

3.2 Developing Stochastic Simulation-based Multi-objective Optimization Model

The objectives of this component are to develop a stochastic simulation-based multi-objective optimization model for the construction of precast concrete box girder bridges that is capable of (1) finding near optimum construction scenarios; and (2) simultaneously minimizing the project's total duration and cost. This component is presented in *Chapter 4* and is subdivided into the following tasks:

- (a) Describing the proposed model.
- (b) Identifying and modeling the decision variables related for each construction method.
- (c) Formulating the objective functions that are used to estimate construction cost and duration.
- (d) Defining the optimization constraints.
- (e) Developing the simulation models of the selected construction methods.
- (f) Designing the integration between the optimization algorithm and the simulation models.
- (g) Implementing the proposed model.
- (h) Demonstrating the effectiveness of the proposed model.

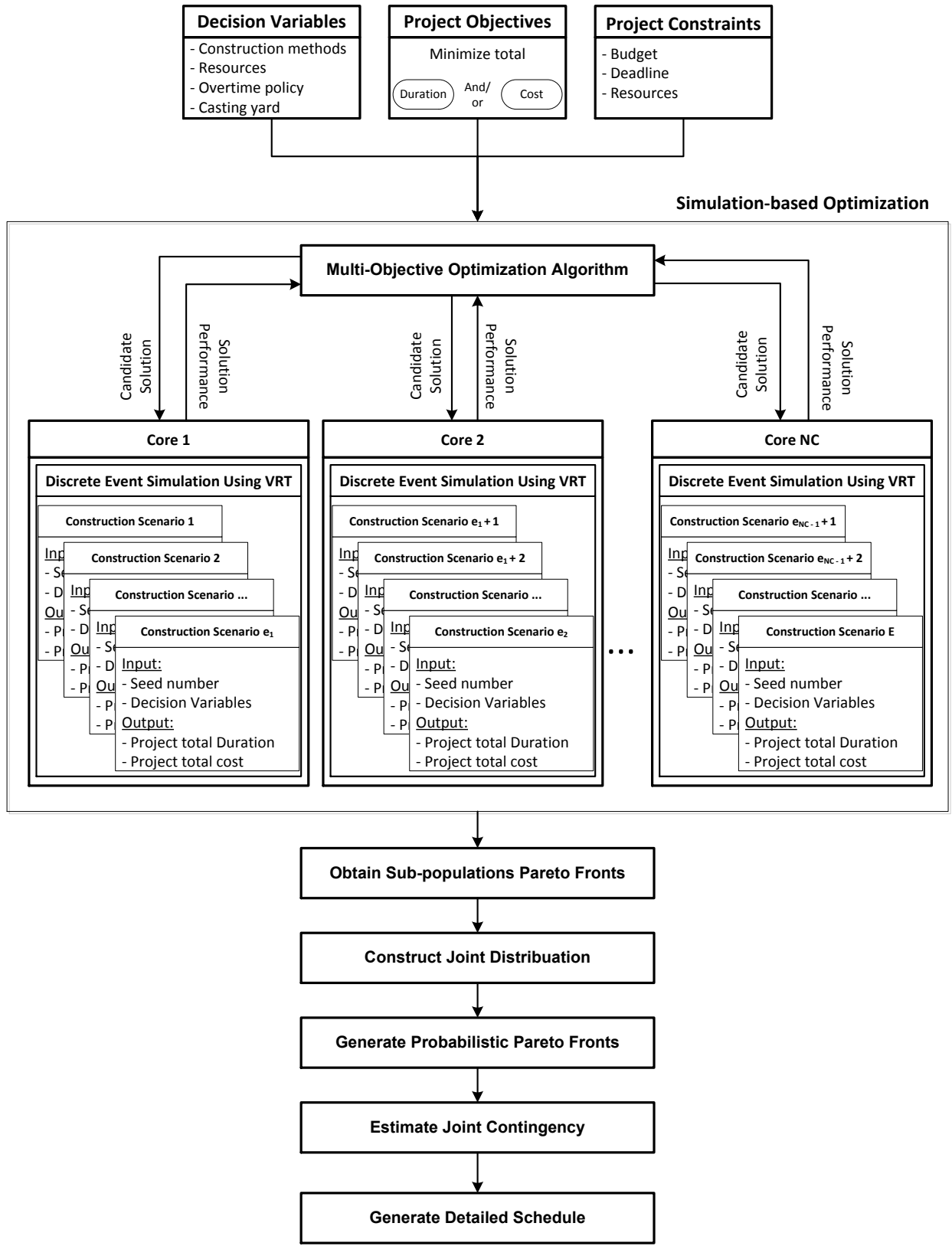


Figure 3-1 Overview of the Proposed Methodology

3.3 Solving the problem of stochastic dominance and reducing the number of simulation replications Using Variance Reduction Techniques

The objectives of this component are to develop a new method to: (1) increase the quality of the optimum solutions; (2) increase the confidence in the optimality of the optimum solutions; and (3) reduce the computation time required for performing a stochastic simulation-based multi-objective optimization by incorporating VRTs. This component is presented in *Chapter 5* and is subdivided into the following tasks:

- (a) Identifying and modeling the required synchronization.
- (b) Formulating a method to compare the performance measure indices of the candidate solutions.
- (c) Developing a method to compare and select the best VRT.
- (d) Implementing the proposed method.
- (e) Demonstrating the effectiveness of the proposed method.

3.4 Reducing the Computation Time to Solve the Optimization Problem Using Parallel Computing on a Single Multi-core Processor

The objective of this component is to propose a method to reduce the computation time required for performing a stochastic simulation-based multi-objective optimization by performing parallel computing on a single multi-core processor. This component is presented in *Chapter 6* and is subdivided into the following tasks:

- (a) Describing the proposed method.
- (b) Implementing the method.
- (c) Demonstrating the effectiveness of the proposed method

3.5 Applying Joint Probability for Evaluating the Duration and Cost of Stochastic Simulation Models

The objective of this component is to develop a method to reduce project risk and provide the decision makers with more accurate and useful information to plan and manage their projects

using joint probability. This component is presented in *Chapter 7* and is subdivided into the following tasks:

- (a) Describing the proposed method.
- (b) Introducing a method to apply joint probability to Pareto solutions.
- (c) Proposing the concept of joint probabilistic Pareto fronts.
- (d) Developing a method to analyze the selected solution.
- (e) Implementing the proposed method.
- (f) Demonstrating the effectiveness of the proposed method.

3.6 Summary

This chapter presented an overview of the proposed methodology of a stochastic simulation-based multi-objective optimization model for the planning and scheduling of precast box girder bridge construction projects. This research consists of four main components that are necessary to realize the proposed methodology: (1) developing a stochastic simulation-based multi-objective optimization model; (2) solving the problem of stochastic dominance and reducing the number of simulation replications using variance reduction techniques; (3) reducing the computation time to solve the optimization problem using parallel computing on a single multi-core processor; and (4) applying joint probability for evaluating the duration and cost of stochastic simulation models. The steps needed to achieve each component were presented.

CHAPTER 4: STOCHASTIC SIMULATION-BASED MULTI-OBJECTIVE OPTIMIZATION MODEL

4.1 Introduction

This chapter presents a stochastic simulation-based multi-objective optimization model for planning, scheduling, and optimizing precast box girder bridge construction projects. This model can be used by contractors to enhance and improve the current practice of decision making in bridge construction projects. The aim of the model is to select a near-optimum construction scenario that simultaneously minimizes the project duration and cost. The construction scenario in this context consists of two main elements. The first element is the construction method that is used to construct a bridge. The second element is the decision variables that have an impact on the duration and cost of the project. In this research four construction methods are considered which are: (1) precast full-span erection using launching gantry; (2) precast segmental span erection using launching gantry; (3) precast segmental span erection using false-work; and (4) precast segmental span erection using under-slung girder. It is assumed that the decision-maker will shortlist the feasible construction methods for the project. It should be noted that this model can be extended to include other bridge construction methods. The rest of this chapter: (1) describes the proposed model; (2) identifies and models the decision variables related for each construction method; (3) formulates the objective functions that are used to estimate construction cost and duration; (4) defines the optimization constraints; (5) develops the simulation models of the selected construction methods; (6) design the integration between the optimization algorithm and simulation; (7) implements the model; and (8) demonstrates the effectiveness of the proposed model.

4.2 Proposed Model

The proposed stochastic simulation-based optimization model is presented in Figure 4-1. The main objective of the model is to select a set of near-optimum construction scenarios that minimizes the total project duration and total project cost. This model is used to select the near-optimum construction scenarios based on quantitative analysis rather than qualitative analysis as mentioned earlier in *Section 2.2.2*. FmGA is used to search the space of the decision variables

and generate the candidate solutions based on the combinations of the decision variables (e.g., number of stressing crews, number of equipment, etc.). Discrete event simulation is used to estimate the values of the objective functions (i.e., duration and cost) for each candidate solution which are then used by fmGA to guide its search for near-optimum solutions. The output of the proposed model is a set of Pareto fronts, which is the preferable outcome of a multi-objective optimization problem. These Pareto solutions are non-dominated optimum solutions which represent the potential tradeoff among the project objectives for each construction method.

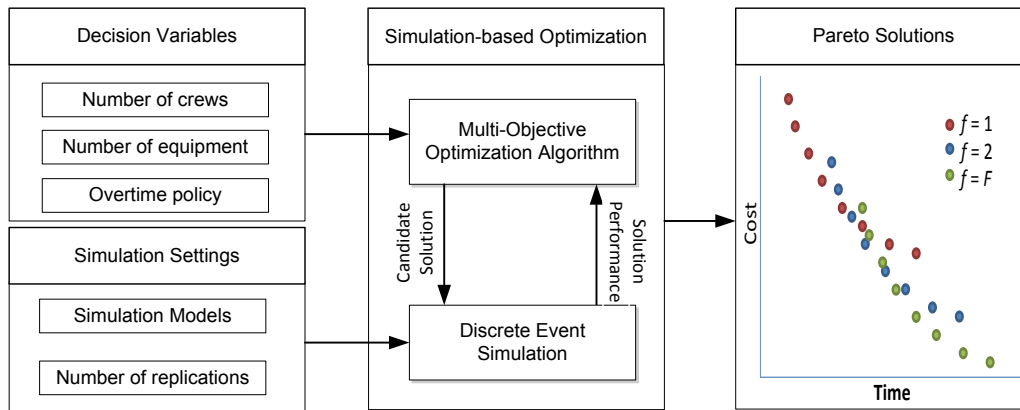


Figure 4-1 Stochastic Simulation-based Multi-objective Model

4.3 Modeling the Decision Variables

As explained earlier, a construction scenario consists of the construction method that is used to construct a bridge and the decision variables that have an impact on the duration and cost of the project. In order to select the optimum bridge construction scenario, several decision variables that have an impact on the project duration and/or cost are identified. These decision variables can be classified into qualitative and quantitative variables.

Qualitative variables are the ones that represent a choice of carrying out a task such as the construction method, the curing method, and the overtime policy. Each of abovementioned construction methods uses a different set of equipment which has an impact on the mobilization cost and direct cost of equipment. In addition, these methods have different production rates that impact the project’s total duration, and as a result, the indirect cost of the project. Two curing methods are considered, namely, regular curing and accelerated curing. Both of these curing

methods have an impact on the duration of the project. Moreover, the accelerated curing method has an impact on the project's total cost. Finally, 15 overtime policies are used in this research as shown in Table 4-1. Each policy has a different number of working hours per day and different number of working days per week. The impact of working overtime on productivity is based on the average loss of productivity over a four week period (RSMeans Engineering Department, 2011). The cost adjustment factor represents the increase in cost due to working overtime based on doubling the regular wage (RSMeans Engineering Department, 2011). These adjustments are used to calculate the tasks' durations and costs based on the selected overtime policy.

Table 4-1 Overtime Policies Used in this Research

Policy	Working Hours per Day	Working Days per Week	Productivity Adjustment Factor (%)	Cost Adjustment Factor (%)
1	8	5	100.00	100.00
2	9	5	103.90	111.10
3	10	5	109.60	120.00
4	11	5	123.10	127.30
5	12	5	131.10	133.30
6	8	6	103.90	116.70
7	9	6	108.10	125.90
8	10	6	114.30	133.30
9	11	6	126.90	139.40
10	12	6	135.60	144.40
11	8	7	112.70	128.60
12	9	7	119.40	136.50
13	10	7	127.00	142.90
14	11	7	137.90	148.10
15	12	7	145.50	152.40

On the other hand, quantitative variables are the ones that can be given a numerical value. The quantitative decision variables are: (1) the number of delivery trucks, (2) the distance from the casting yard to the construction site, (3) the number of rebar cage molds, (4) the number of casting molds, (5) the number of different types of crews, (6) the number of equipment, (7) the yard storage capacity, and (8) the storage time of the precast element. Each of these variables has a direct impact on the project's total duration and/or total cost. Each set of the qualitative and quantitative decision variables represents a candidate solution to the optimization problem.

4.4 Optimization Objectives

This model aims to support decision makers in searching and finding near-optimum precast box girder bridge construction scenarios that (1) minimize the project's total duration; and/or (2) minimize the project's total cost. Therefore, the objective function of this model can be single objective (i.e. duration or cost), or multi-objective (i.e. duration and cost). The following subsections further discuss these two objectives.

4.4.1 Minimizing the Project's Total Duration

The total duration of the bridge construction operations is estimated by the discrete event simulation models. The total project duration is equal to the total time needed to perform the construction operations from the casting operation to the erection operation. The project's duration in working days can be calculated by dividing the total simulation time (expressed in hours) by the number of working hours per day as shown in Equation 4-1.

$$PDWD = \frac{TST}{WHD \times 60} \quad \text{Equation 4-1}$$

where,

$PDWD$ = project's duration in working days

TST = total simulation time in minutes

WHD = working hours per day

The above equation calculates the total number of days required to finish the project. However, it is more beneficial to calculate the project's duration in calendar days as shown in Equation 4-2.

$$PDCD = PDWD + \left\lfloor \frac{PDWD}{WDW} \right\rfloor \times (7 - WDW) \quad \text{Equation 4-2}$$

where,

$PDCD$ = project's duration in calendar days

WDW = working days per week

$\lfloor \rfloor$ represents the floor of a real number

4.4.2 Minimizing the Project's Total Cost

The total cost of the project consists of two main elements as shown in Equation 4-3. Those elements are the indirect and direct costs.

$$PTC = PIC + PDC \quad \text{Equation 4-3}$$

where,

PTC = project's total cost

PIC = project's indirect cost

PDC = project's direct cost

The indirect cost of the project is a function of the project's total duration and is calculated by multiplying the duration of the project by the contractor's daily indirect cost in addition to the mobilization cost as shown in Equation 4-4.

$$PIC = (PDWD \times DIC) + PMC \quad \text{Equation 4-4}$$

where,

DIC = contractor's daily indirect cost

PMC = project's mobilization and demobilization costs

The mobilization cost includes the equipment and crew mobilization costs. The equipment mobilization cost includes the mobilization cost of each equipment from the contractor's storage to the construction site and the demobilization cost of that equipment from the construction site to the contractor's storage as shown in Equation 4-5. It is assumed that the mobilization total cost is the same as the demobilization total cost; therefore, a factor of 2 is used in Equation 4-5 and Equation 4-6.

$$PEMC = 2 \times \sum_{a=1}^A Equip_a \times MCE_a \quad \text{Equation 4-5}$$

where,

$PEMC$ = project's equipment mobilization and demobilization costs

A = number of equipment types utilized in the project

$Equip_a$ = number of equipment of type (a) utilized in the project

MCE_a = mobilization cost of an equipment of type (a)

Similarly, the crew mobilization cost is calculated using Equation 4-6.

$$PCMC = 2 \times \sum_{b=1}^B Crew_b \times MCC_b \quad \text{Equation 4-6}$$

where,

$PCMC$ = project's crew mobilization and demobilization costs

B = number of crew types utilized in the project

$Crew_b$ = number of crews of type (b) utilized in the project

MCC_b = mobilization cost of a crew of type (b)

The project's direct cost includes the direct cost of equipment, crews, casting yard land, and the curing of concrete segments as shown in Equation 4-7.

$$PDC = DCE + DCC + DCCY + DCU \quad \text{Equation 4-7}$$

where,

DCE = direct cost of equipment

DCC = direct cost of crews

$DCCY$ = direct cost of the land used to set up the casting yard

DCU = direct cost of curing of concrete segments

The direct cost of equipment is the summation of the cost of all the equipment assigned to the project as shown in Equation 4-8. The cost for each equipment type is calculated by multiplying the hourly cost of the equipment by the number of equipment used by the total number of hours that equipment type is assigned to the project.

$$DCE = \sum_{a=1}^A HCE_a \times Equip_a \times THE_a \quad \text{Equation 4-8}$$

where,

HCE_a = hourly cost of an equipment of type (a)

THE_a = total number of hours equipment of type (a) is assigned to the project

The direct cost of crews is calculated in a similar manner to that of the equipment as shown in Equation 4-9. However, the direct cost of crews is adjusted by a factor based on the overtime policy used in the project.

$$DCC = \sum_{b=1}^B HCC_b \times Crew_b \times THC_b \times CAF \quad \text{Equation 4-9}$$

where,

HCC_b = hourly cost of a crew of type (b)

THC_b = total number of hours crew of type (b) is assigned to the project

CAF = cost adjustment factor

The direct cost of the land used to set up the casting yard is calculated by multiplying the capacity of the casting yard by the cost per space per day of usage as shown in Equation 4-10.

$$DCCY = PYS \times CCD \times STH \quad \text{Equation 4-10}$$

where,

PYS = precast yard storage capacity

CCD = storage capacity cost per hour

STH = storage total time used in hours

Finally, the direct cost of curing is calculated by multiplying the number of precast segments by the cost of the selected curing method as shown in Equation 4-11.

$$DCU = NPS \times CMC \quad \text{Equation 4-11}$$

where,

NPS = number of precast segments

CMC = curing method cost

4.5 Optimization Constraints

The optimization model takes into consideration two types of constraints when generating and evaluating the candidate solutions: (1) decision variables constraints; and (2) objective functions constraints. The decision variables constraints specify the maximum available or allowable value for each of the quantitative decision variables mentioned above. The objective functions constraints can be specified to ensure that the project's total duration of any construction scenario does not exceed a certain deadline and/or the project's total cost of any construction scenario does not exceed a certain budget as shown in Equation 4-11 and Equation 4-12, respectively.

$$PDCD_e \leq PDCD_{max} \quad \forall e = 1, 2, \dots, E \quad \text{Equation 4-12}$$

$$PTC_e \leq PTC_{max} \quad \forall e = 1, 2, \dots, E \quad \text{Equation 4-13}$$

where,

$PDCD_e$ = project's total duration in calendar days of construction scenario e

$PDCD_{max}$ = maximum allowable project's total duration in calendar days

PTC_e = project's total cost of construction scenario e

PTC_{max} = maximum allowable project's total cost

4.6 Simulation Models of the Construction Methods

Discrete event simulation is used to develop the simulation models for the casting and erecting operations of the bridges. Each simulation model will represent a template for a single construction method. The purpose of using simulation is to find the project's total duration and total cost based on the set of the qualitative and quantitative decision variables (e.g., construction method, number of crews, number of equipment, etc.). Therefore, the simulation templates are modeled in a generic format to allow for an automated interaction between the optimization algorithm and the simulation as will be explained in detail in *Section 4.7*.

The rest of this section presents the following simulation models and explains their flow of work: (1) precast full-span erection using launching gantry; (2) precast segmental span erection using

launching gantry; (3) precast segmental span erection using false-work; and (4) precast segmental span erection using under-slung girder. The developed simulation models focus on the construction of the superstructure element of the bridge and it is assumed that the spans are simply supported. The bridge construction operations considered in this research can be classified into: (1) casting of segments/spans; (2) transportation of segments/spans to the construction site; and (3) erection of the precast segments/spans. The modeling elements used in developing the models are described in Table 2-1. Verification and validation of the simulation models are done by tracing the different entities in the simulation model to assure that the logic of the models are correct and they are running as expected (Sargent 2010).

4.6.1 Span-by-span Precast Full Span Erection Using Launching Gantry

The quantitative decisions that are specific to this construction method (in addition to those explained in *Section 4.3*) are: the number of inner molds, the number of outer molds, and the number of stressing crews. The developed simulation model of bridge construction using precast full span launching method is shown in Figure 4-2. The simulation starts by initializing the queues that hold the resources needed for the construction operations. The steel crew starts placing the steel reinforcement and the tendons' ducts for the bottom slab and the webs of the full precast span using a rebar mold. Then, an inner mold is loaded to the finished rebar cage. Afterwards, the steel crew places the steel reinforcement for the top slab. Next, the finished rebar cage is placed in an outer mold. Then, the casting crew casts the span. At this point, the cast span undergoes the curing process. Afterwards, the inner mold is removed and the first stage of post-tensioning is performed by the pre-stressing crew. The span is then moved to the storage area where the second post-tensioning stage takes place. Next, a trailer is loaded with a precast concrete box girder span. Then, the trailer travels to the access point of the bridge construction site. When the launching gantry is ready, the onsite crane will unload the precast span and load it to a trolley. After being unloaded, the trailer returns to the precast yard to be loaded again. The trolley travels to the point where the span will be launched. When the trolley reaches the desired location, the launching gantry repositions to the new span's location. Then, the launching gantry picks up the span from the trolley. Afterwards, the trolley returns to be loaded again. At the same time, the launching gantry erects the new span at its location. Then, the permanent bearings are grouted. Finally, the load of the span is transferred from the temporary bearings to the permanent

bearings. The resources used in grouting the permanent bearings and transferring the loads from the temporary bearings to the permanent bearings are modeled implicitly.

4.6.2 Span-by-span Precast Segmental Erection Using Launching Gantry

The developed simulation model of bridge construction using precast segmental erection using launching gantry method is shown in Figure 4-3. The simulation starts by initializing the queues that hold the resources needed for the construction operations. The steel crew places the steel reinforcement and the tendons' ducts for the segment using a rebar mold. Next, the finished rebar cage is placed in a casting mold. Then, the casting crew casts the segment. At this point, the casted segment undergoes the curing process. Afterwards, the mold is removed and the segment is then moved to the storage area. Next, a trailer is loaded with a precast concrete box girder segment. Then, the trailer travels to the bridge construction site. When the launching gantry is ready, it picks up the segment from the trailer and places it at its final location. After being unloaded, the trailer returns to the precast yard to be loaded again.

The launching gantry will keep placing segments until it acquires all the segments required to form one span. Then, these segments are aligned and glued. Next, the external post-tensioning rods are installed and stressed. Finally, the launching gantry repositions to a new span's location and repeats the process. The resources used in aligning, gluing, and stressing the segments are modeled implicitly.

4.6.3 Span-by-span Precast Segmental Erection Using Falsework Support

The developed simulation model of bridge construction using precast segmental erection using launching gantry method is shown in Figure 4-4. The casting and transportation operations of this construction method follow the same steps as explained in *Section 4.6.2*. Once the trailer reaches the construction site and the site crane is ready, the crane picks up the segment from the trailer and places it at its final location on the falsework. After being unloaded, the trailer returns to the precast yard to be loaded again. The site crane will keep placing segments until it acquires all the segments required to form one span. Then, these segments are aligned and glued. Next, the external post-tensioning rods are installed and stressed. Afterwards, the load of the span is transferred to the permanent bearings. Finally, the site crane repositions the falsework to the new

span's location and repeats the process. As in the previous model, the resources used in aligning, gluing, and stressing the segments are modeled implicitly.

4.6.4 Span-by-span Precast Segmental Erection Using Under-Slung Girder

The developed simulation model of bridge construction using precast segmental erection using under-slung girder method is shown in Figure 4-5. The casting, transportation, and erection operations of this construction method follow the same steps as explained in *Section 4.6.2*. The only difference is that the trailer will travel over the completed spans of the bridge to deliver the segments. Therefore, only one trailer is allowed to travel over the bridge. This is controlled by the queue *Space_Available* as shown in Figure 4-5.

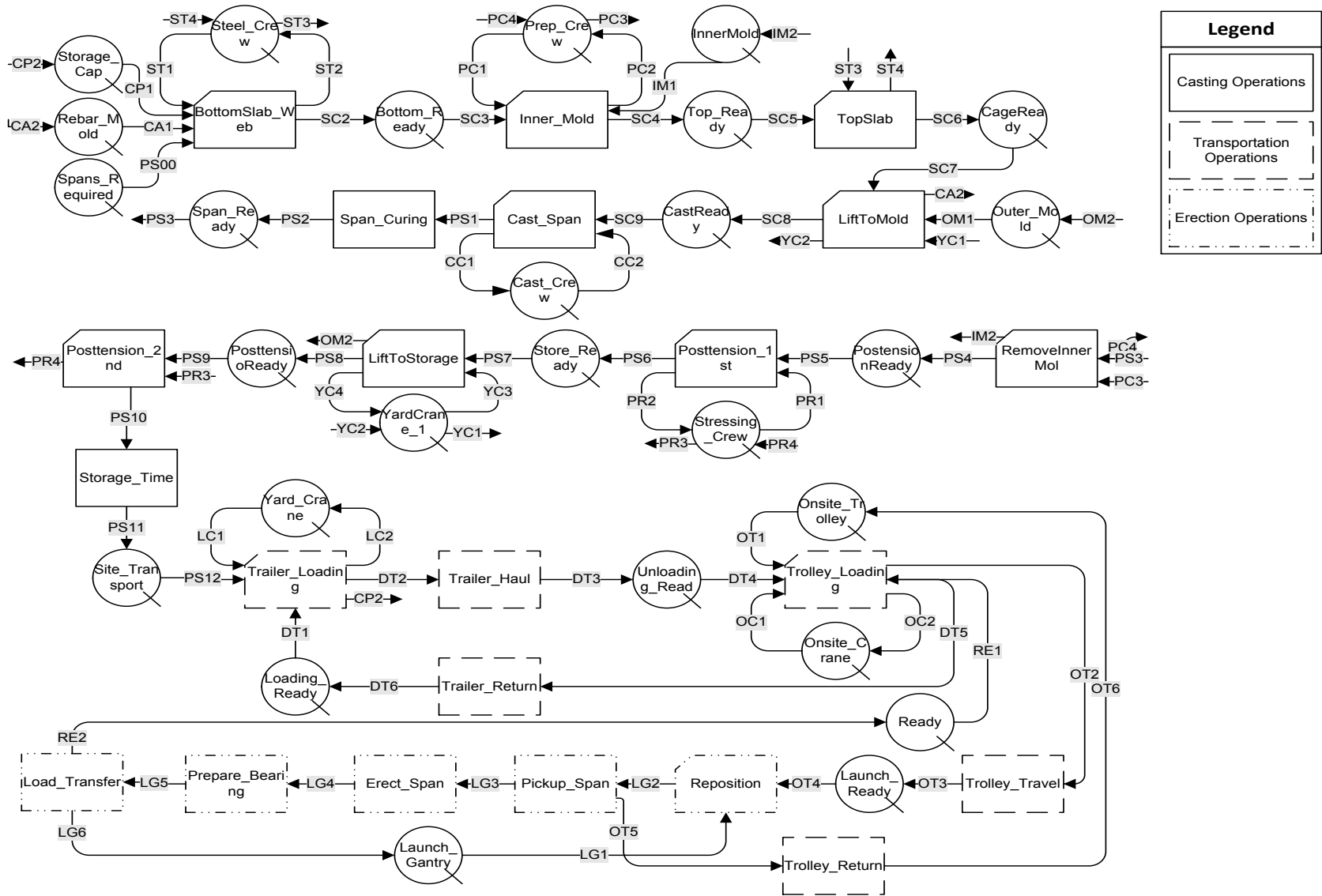


Figure 4-2 Simulation Model of Full Span Bridge Construction Using Launching Gantry

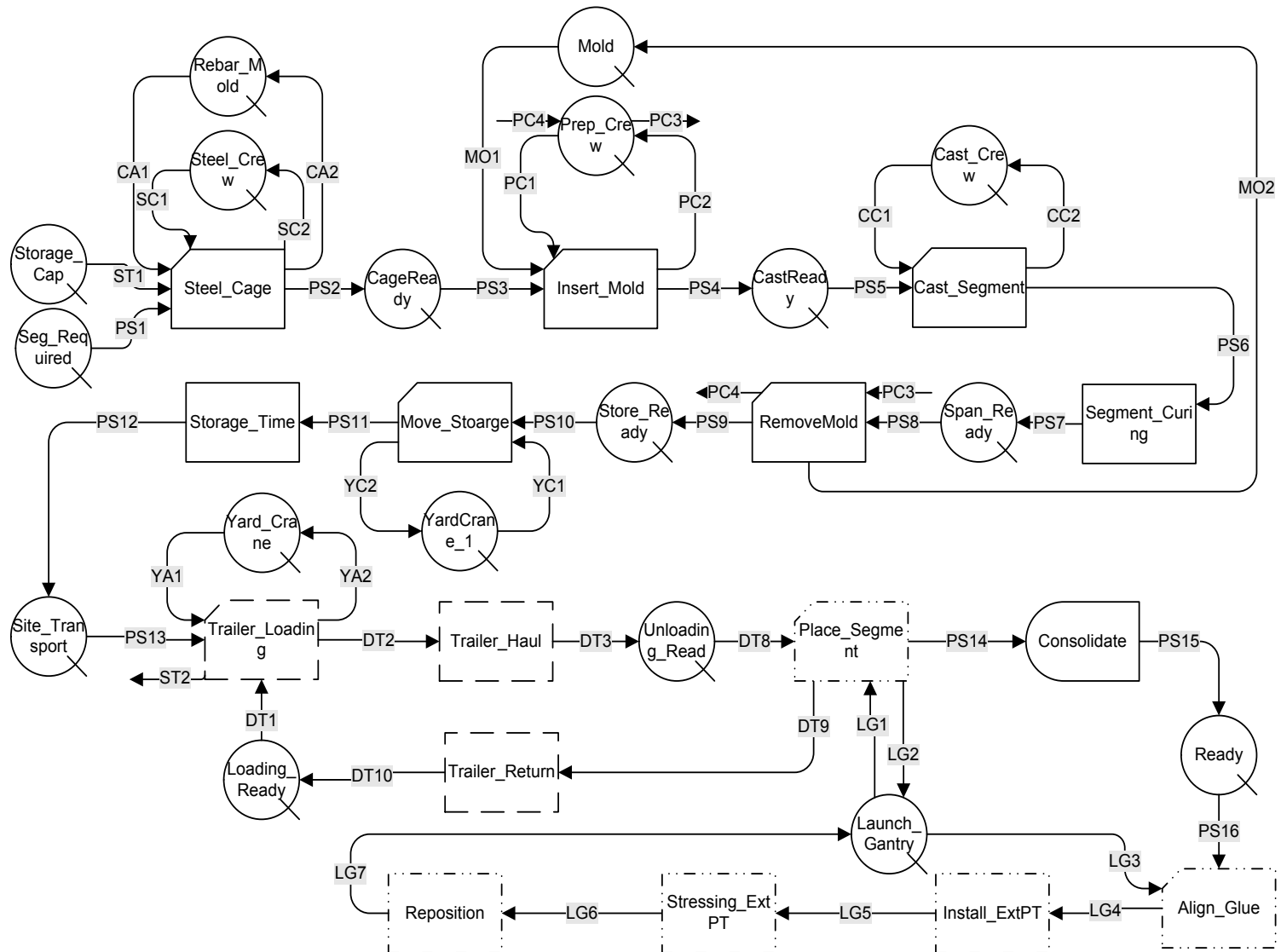


Figure 4-3 Simulation Model of Span-by-span Segmental Bridge Construction Using Launching Gantry

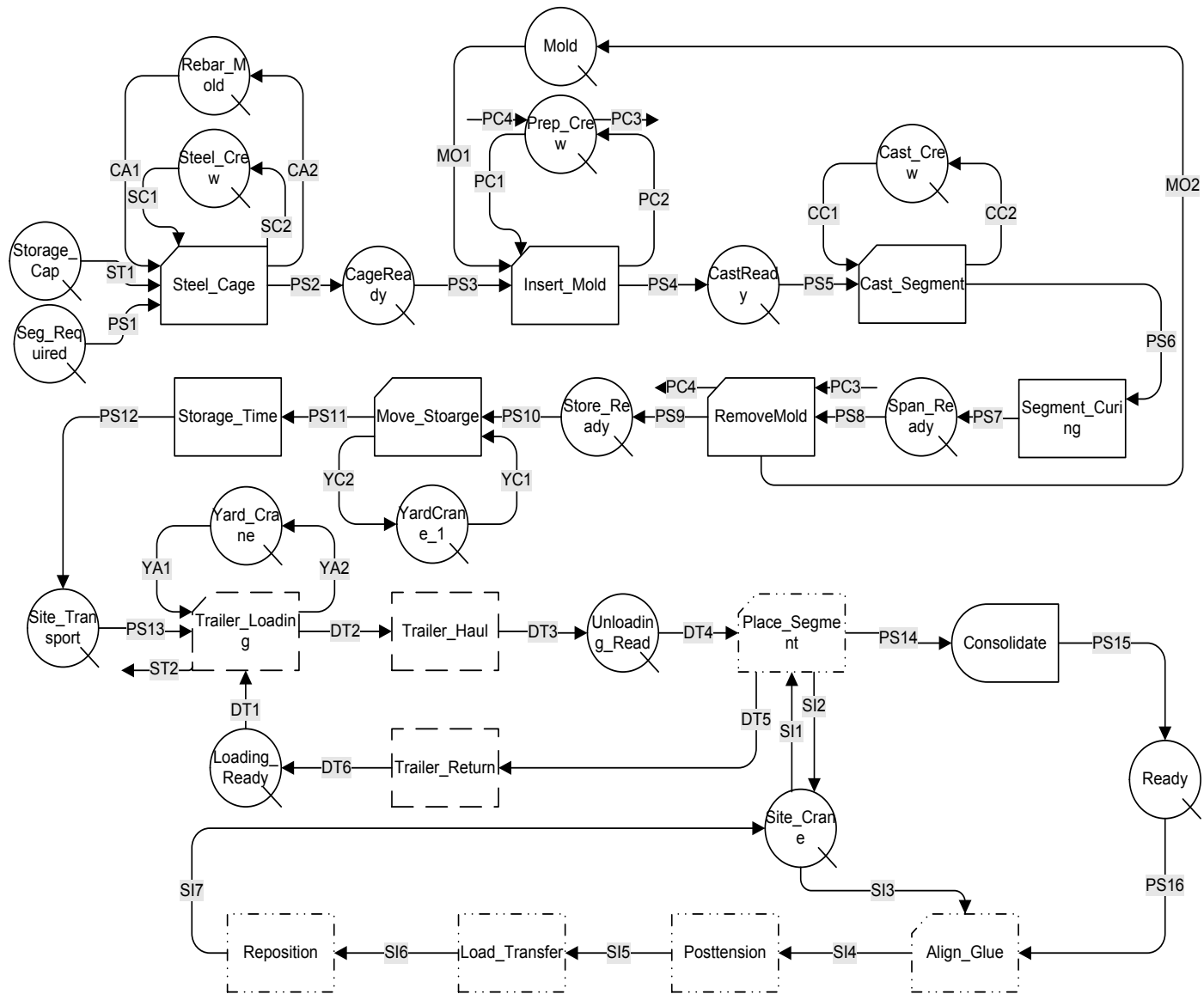


Figure 4-4 Simulation Model of Span-by-span Segmental Bridge Construction Using Falsework Support

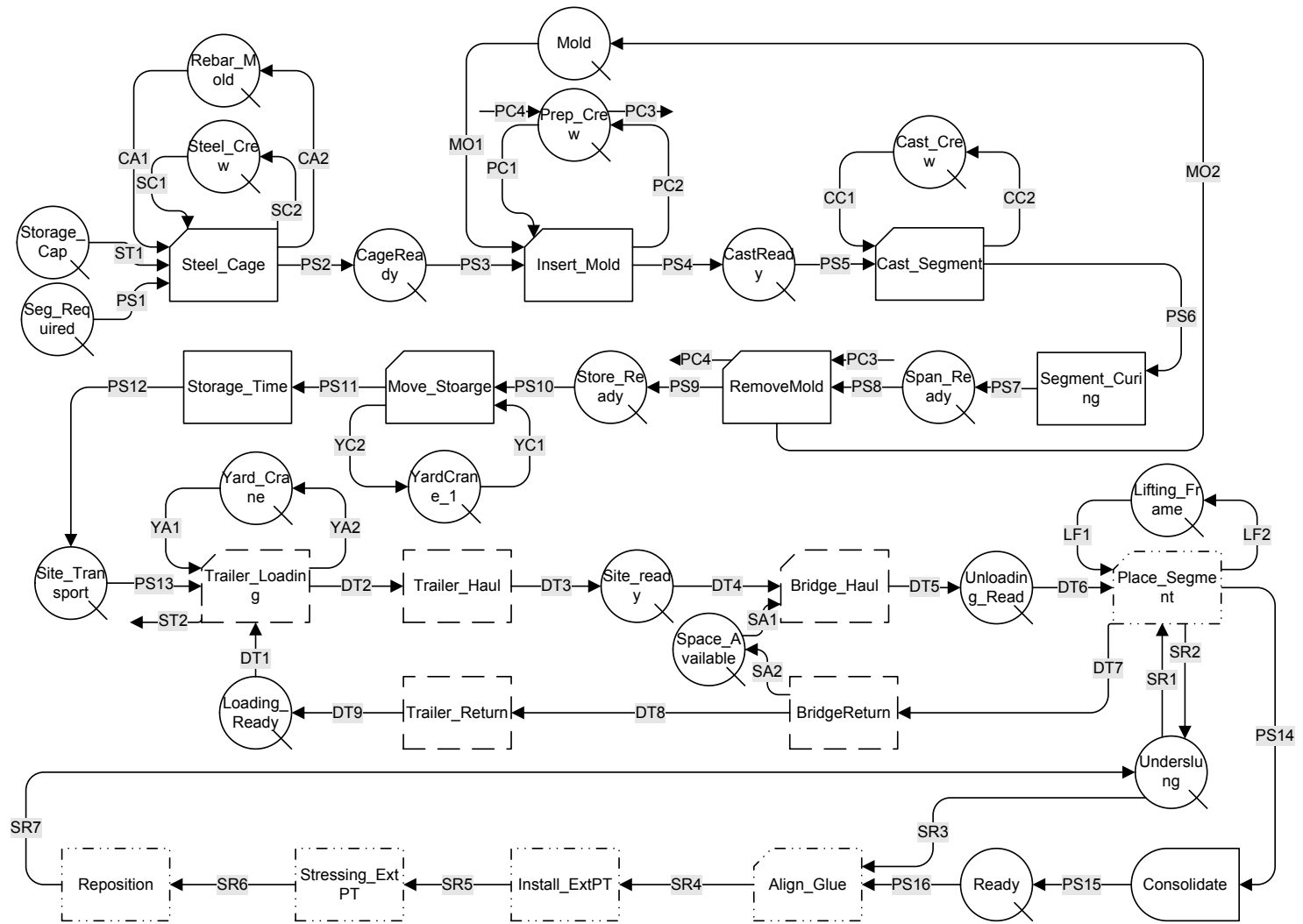


Figure 4-5 Simulation Model of Span-by-span Segmental Bridge Construction Using Under-slung Girder

4.7 Integration of Simulation and Optimization

The simulation is integrated with the optimization algorithm to evaluate the generated candidate solutions as shown in Figure 4-6. Two cycles were added to the fmGA which are: (1) the sub-population cycle where each sub-population represents a specific construction method; and (2) the simulation cycles where the values of the objective functions of candidate solutions are calculated. The fmGA (explained in *Section 2.4.2*) starts by generating F sub-populations where each sub-population (f) represents a specific construction method. Therefore, the number of sub-populations is equal to the number of applicable construction methods. Each sub-population goes through the steps of the fmGA as shown in Figure 4-6. Each sub-population consists of number of eras (G) where each *era* (g) consists of the three phases of the Inner Loop of the fmGA. At the beginning of the first era ($g = 1$), a competitive template is randomly initialized. Afterwards, an initial population of size E using the PCI technique is generated in the *initialization phase*. The fitness evaluation of the candidate solutions using simulation is referred to as the *simulation cycle* in Figure 4-6. Each candidate solution (e) encapsulates the decision variables of the construction scenario. The process of the *simulation cycle* starts by selecting the simulation template corresponding to the construction method f . Then the simulation template is modified based on the value of the decision variables of each candidate solution. The values of the objective functions of each candidate solution are reported back to fmGA. After all the solutions have been evaluated, thresholding selection and building block filtering in the *primordial phase* take place. All filtered solutions go through the *simulation cycle* to be evaluated. After the termination of this phase, thresholding selection, cut and splice, and mutation are applied in the *juxtapositional phase*. The template of the new *era* is set to the best candidate solution found at the end of the *juxtapositional phase*. The sub-population is terminated when the maximum number of *eras* is reached. This process is repeated for all the other sub-populations.

The optimization process will terminate once the maximum number of sub-populations is reached. The set of optimum solutions that were accepted by fmGA for each sub-population is presented as Pareto fronts. Figure 4-7 shows the algorithm for performing non-dominated sorting for the set of Pareto fronts. Every construction scenario in the set is compared to all others. A construction scenario is considered non-dominated when there exist no other construction scenario that can improve one objective function without worsening the other objective function.

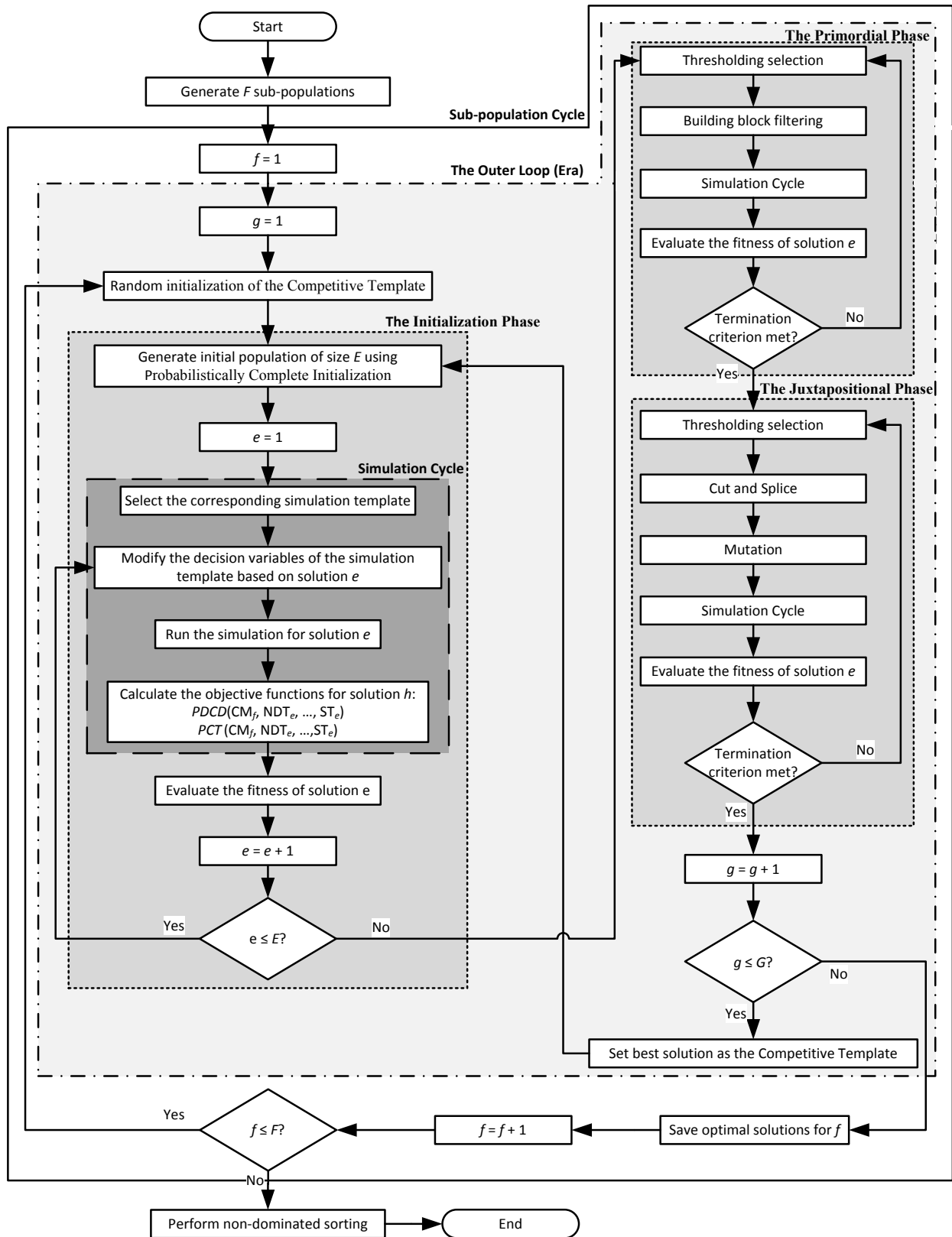


Figure 4-6 Integration between Discrete Event Simulation and Fast Messy Genetic Algorithm

Since scenarios are represented by combinations of the project's total duration and total cost, the combination $(PDCD_i, PTC_i)$ is considered a dominated scenario if: (1) it has an equal or higher duration and higher cost of all the other combinations $(PDCD_j, PTC_j)$; or (2) it has a higher duration and an equal or higher cost of all the other combinations. Otherwise, the combination $(PDCD_i, PTC_i)$ is a non-dominated construction scenario. These Pareto fronts are further analyzed as will be described in *Chapter 7*. All non-dominated construction scenarios present the final Pareto front.

```

FOR EACH  $(PDCD_i, PTC_i) \in Set$ 
     $S_{nd} = \emptyset$  Set of non-dominated construction scenarios
     $(PDCD_i, PTC_i) \in S_{nd}$ 
    FOR EACH other  $(PDCD_j, PTC_j) \in Set$ 
        IF  $(PDCD_j \leq PDCD_i \text{ and } PTC_j < PTC_i)$  or  $(PDCD_j < PDCD_i \text{ and } PTC_j \leq$ 
 $PTC_i)$  THEN
            Remove  $(PDCD_i, PTC_i)$  from  $S_{nd}$ 

```

Figure 4-7 Algorithm for Non-dominated Sorting of Pareto Fronts

4.8 Model Implementation

The simulation models of the construction methods are implemented in STROBOSCOPE. On the other hand, Darwin optimization framework (Wu, et al., 2012), which utilizes an fmGA, is used to solve the optimization problem. The implementation of the integration between these two tools (Figure 4-8) was done in Microsoft Visual C# (Microsoft Corporation, 2015a). STROBOSCOPE was embedded in Darwin optimization framework to evaluate each candidate solution generated by the optimization through simulation. The process starts by determining the minimum, maximum, and increment values for each decision variables. The values of the decision variables are represented by variables (e.g. x1, x2, etc.) in the source code of the simulation model. Next, the optimization tool generates the candidate solutions. The developed code extracts the values of the decision variables, opens the simulation source code, and replaces the variables (x1, x2, etc.) with the extracted values. Then, it starts the simulation tool and creates a new model with the modified source code. Next, it runs the simulation for N

replications and extracts the average project duration and cost at the end of the simulation. Finally, the code exports the project duration and cost to the optimization tool and ends the simulation model. The process is repeated for all the candidate solutions generated by the optimization tool.

At the end each sub-population, a text file with the Pareto solutions is created. Microsoft Excel (Microsoft Corporation 2015b) is used to extract the project’s total duration and cost of Pareto solutions via Visual Basic for Applications (VBA) (Microsoft Corporation 2015c). Finally, the developed code performs non-dominated sorting across all the sub-populations and presents the final Pareto front.

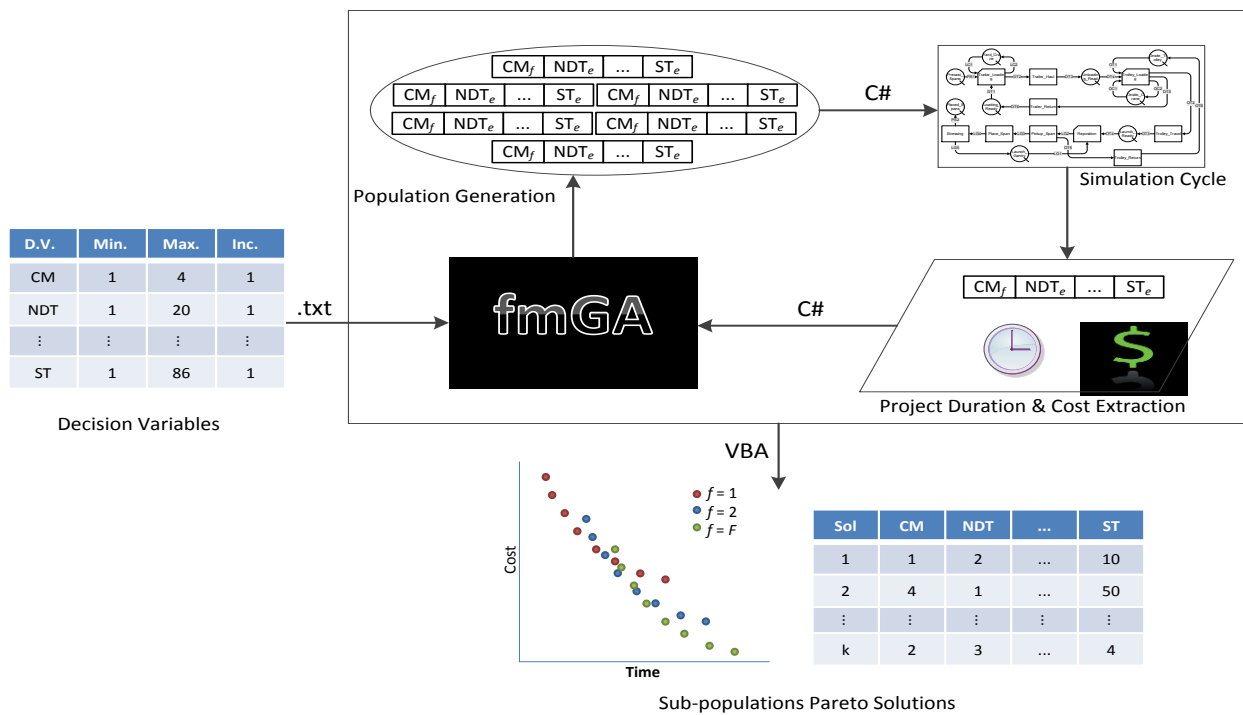


Figure 4-8 Implementation of Stochastic Simulation-based Optimization Model

4.9 Case Study

A case study is presented here to demonstrate the effectiveness of the developed stochastic simulation-based multi-objective model. The model is used to search for a near-optimum construction scenario that minimizes project total cost and duration without any constraints regarding the deadline or the budget. The case study consists of constructing a precast full span

box girder bridge using launching gantry method. The bridge consists of 35 spans with identical spans of length 25 m.

Table 4-2 shows the durations of the tasks used in this simulation model for this case study. The durations of the casting operation tasks were adapted from (Marzouk et al., 2007), and it is assumed that the tasks' durations are linearly related to the length of the span. The durations of the launching process tasks are adapted from (VSL International Ltd., 2013) by adding a range of $\pm 50\%$ in order to have a distribution for the durations. Most of the tasks' durations are represented by a distribution to model the uncertainty associated with this construction method. In this case study, it is assumed that there are two curing methods namely regular and accelerated. The *Span_Curing* task has a duration of 600 or 1200 minutes for accelerated and regular curing method, respectively. Traveling tasks, such as *Trailer Haul*, are represented as functions of distance and speed as shown in Equation 4-14. The cost data used in the simulation model is presented in *Appendix B*.

$$TD = \frac{DIS}{\min[HRSL, LEMS]} + DF \quad \text{Equation 4-14}$$

where,

TD = transportation duration in hours

DIS = distance from the casting yard to the construction site or from the access of the construction site to the launching location in km

HRSL = haul or return speed limit in km/hr

LEMS = loaded or empty max speed in km/hr

DF = delay function expressed as a uniform distribution

This case study was run twice to compare the consistency of the optimum solutions. Table 4-3 summarizes the quantitative decision variables considered in this example along with their minimum, maximum, and increment values. Table 4-4 shows the suggested range for each parameter of the fmGA provided by the tool. In addition, it shows the configuration used in this example. This optimization is run for 100,000 candidate solutions through two eras where each era consists of 500 generations and each generation has a population of 100. The mean values of the objective functions of each solution were found after 100 simulation replications.

Table 4-2 Durations of the Tasks Used in the Simulation Model

Task	Duration (minutes)	Task	Duration (minutes)
BottomSlab_Web	Triangular [640, 961, 1280] *	Trailer_Haul	F (Distance, Speed)
Inner_Mold	Triangular [120, 300, 480] *	Trolley_Loading	Triangular[30, 60, 90] **
TopSlab	Triangular [660, 984, 1300] *	Trailer_Return	F (Distance, Speed)
LiftToMold	Triangular[23, 45, 68]	Trolley_Travel	F (Distance, Speed)
Cast_Span	Triangular [520, 771, 1020] *	Reposition	Triangular[120, 240, 360] **
Span_Curing	(600 or 1200) *	Pickup_Span	Triangular[30, 60, 90]**
RemoveInnerMol	Triangular [90, 255, 420] *	Trolley_Return	F (Distance, Speed)
Posttension_1 st	Triangular [120, 300, 480] *	Erect_Span	Triangular[120, 240, 360] **
LiftToStorage	Triangular [30, 60, 90] **	Trolley_Return	F (Distance, Speed)
Posttension_2 nd	Triangular [120, 300, 480] *	Prepare_Bearing	Triangular[120, 240, 360] **
Trailer_Loading	Triangular[30, 60, 90] **	Load_Transfer	Triangular[30, 60, 90] **
* Adapted from (Marzouk et al., 2007)			
** Adapted from (VSL International Ltd., 2013)			

This example was run on an Intel Core i7, Quad-core processor, 3.4 GHz computer with 16 GB Random Access Memory (RAM) running 64-bit Windows 7 operating system and it took almost 7 hours to reach the specified number of trials. The computation time was for only one construction method and a small fraction of the search space. The computation time will increase rapidly if more than one construction method is used or a larger area of the search space is considered.

Table 4-3 Quantitative Decisions Variables Used in the Optimization

Decision Variable	Minimum	Maximum	Increment
Number of delivery trucks (NDT)	1	20	1
Precast yard distance (km) (PYD)	10	100	10
Number of rebar cage molds (NRC)	1	20	1
Number of inner molds (NIM)	1	20	1
Number of outer molds (NOM)	1	20	1
Number of preparation crews (NPC)	1	20	1
Number of stressing crews (NSC ₁)	1	20	1
Number of steel crews (NSC ₂)	1	20	1
Number of casting crews (NCC)	1	20	1
Precast yard storage capacity (PYS)	1	50	5
Storage time (hr) (ST)	1	84	1

Table 4-4 fmGA Configuration Used in the Case Study

Parameter	Suggested Range	Used Value
Cut rate	0.01 to 0.05	0.017
Splice rate	0.8 to 1.0	0.6
Mutation rate	0.001 to 0.03	0.015
Population size	50 to 100	100
Generations per era	500 to 1,000	500
Number of eras		2
Maximum trials	10,000 to Huge	100,000
Size of search space		6.4512×10^{15}

Figure 4-9 shows all the generated candidate solutions for the first run. Figure 4-10 shows the improvement of the Pareto solutions over several generations. The model was able to generate a set of solutions where each solution represents a construction scenario. Table 4-5 presents the values of the decision variables and the objective functions for the first run of the Pareto front. The Pareto front solutions provide non-dominated tradeoff between minimizing the project duration and minimizing the construction cost. A tradeoff exists because reducing the project duration requires the use of extra resources, which in turn will increase the project cost. The solution representation shows the values of the decision variables. Each decision variable has an abbreviation as shown in Table 4-3. For example, *PYD* represents the distance from the precast yard to the access point of the construction site. In *Solution 4*, for example, the distance is 100 km and this solution requires the use of accelerated curing method and overtime policy 13 which is 10 hours per day and 7 days per week as shown in Table 4-5. *Solution 1* requires 72 calendar days and \$3.17 million to finish the construction compared to 107 calendar days and \$1.57 million as required by *Solution 13*. *Solution 1* reduces the project duration by more than 32% compared to *Solution 13* but it will cost almost 2 times more. *Solution 1* represents the shortest project duration and the most expensive project alternative. It also represents the highest transportation agency expenditure and the shortest duration of public inconvenience or traffic interruption. On the other extreme, *Solution 13* represents the longest project duration and the cheapest alternative. Between these two extremes, there are other feasible solutions from which the decision maker can select the construction scenario. For example, *Solution 7* requires 83 days and \$2.05 million to finish the project.

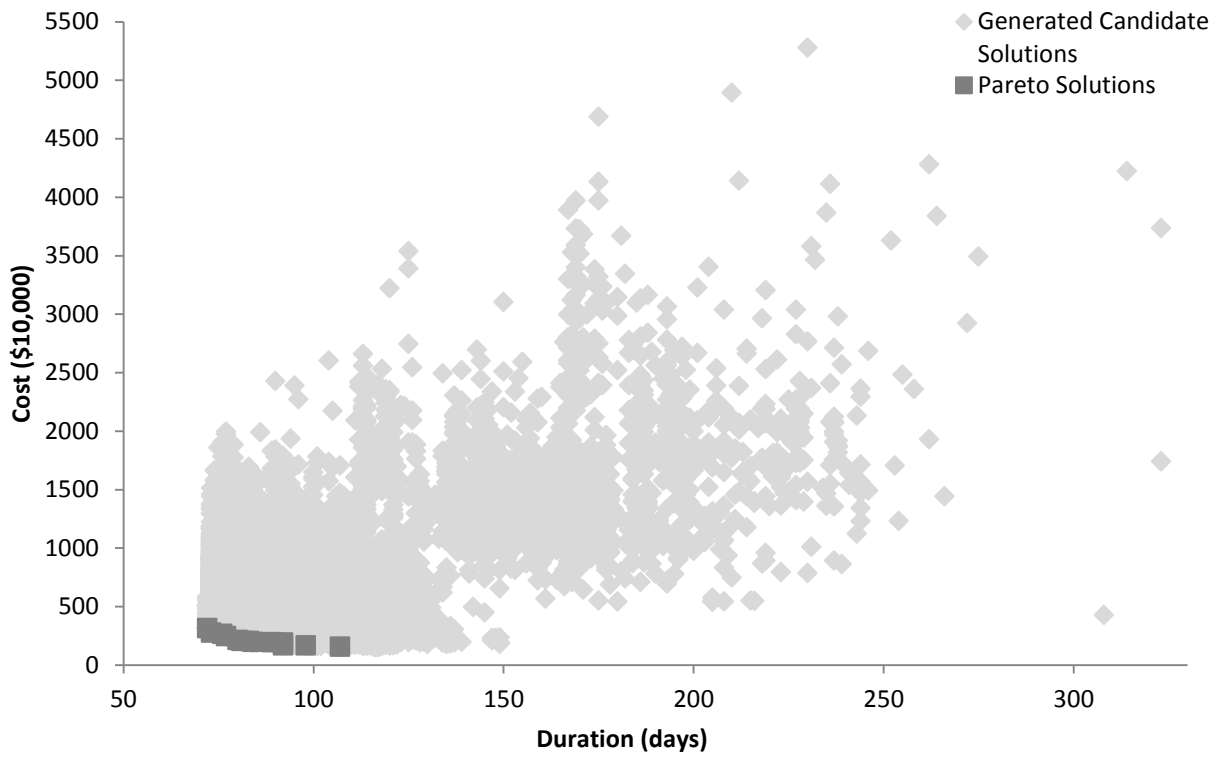


Figure 4-9 All the Generated Candidate Solutions in the First Run

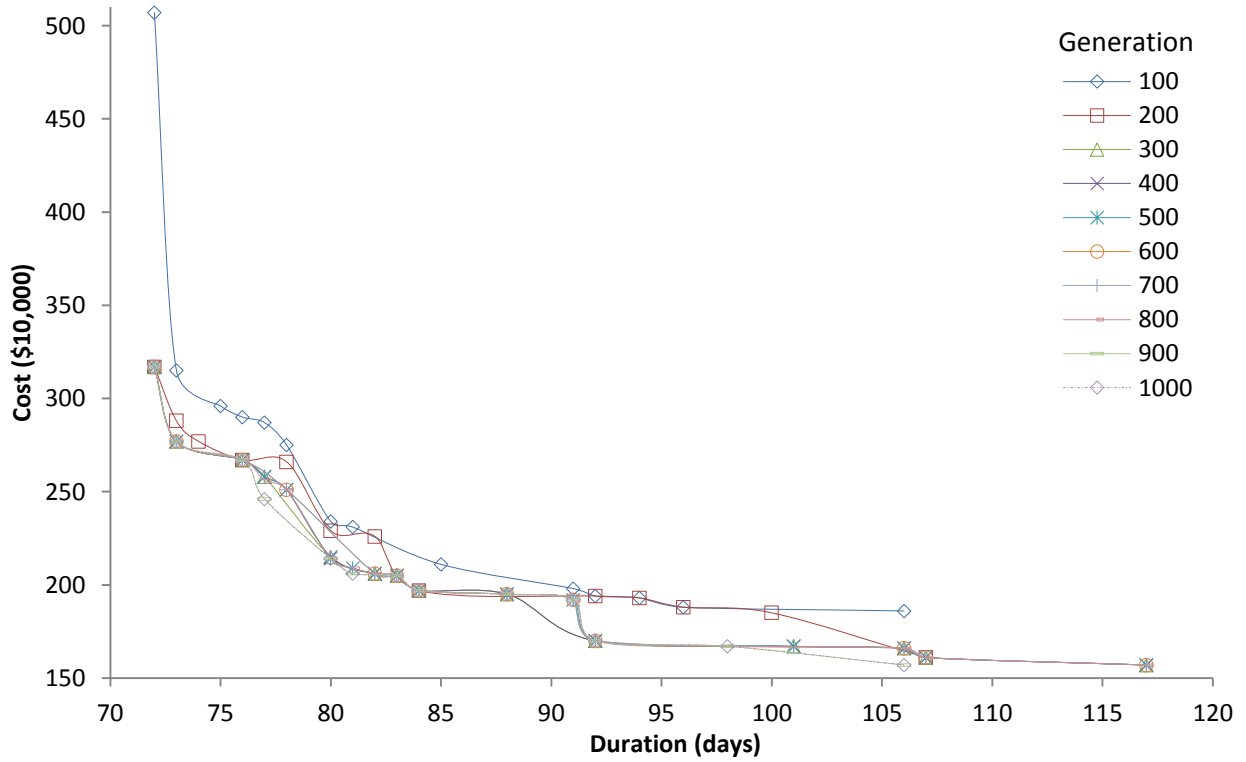


Figure 4-10 Improvement of Pareto Solutions over the Generations

Table 4-5 Details of the Pareto Set of Solutions for the First Run

Sol	NDT	PYD	NRC	NIM	NOM	NPC	NSC ₁	NSC ₂	NCC	Curing Method	Overtime Policy	PYS	ST (hours)	Duration (days)	Cost (\$10,000)
1	3	40	16	20	18	6	4	15	6	Accelerated	15	35	1	72	317
2	1	60	13	20	20	3	3	11	5	Accelerated	15	40	3	73	277
3	2	20	14	20	20	4	2	9	5	Accelerated	14	50	4	76	266
4	1	100	20	20	18	5	7	12	6	Accelerated	13	50	6	77	247
5	1	100	14	20	19	3	4	11	9	Accelerated	8	40	1	80	214
6	1	100	17	20	19	3	3	10	5	Accelerated	12	45	6	81	207
7	1	90	13	20	20	4	2	11	5	Accelerated	8	50	3	83	205
8	2	50	13	20	20	4	3	11	7	Accelerated	7	50	1	84	197
9	1	10	16	16	20	6	2	9	5	Accelerated	7	40	28	89	195
10	1	100	13	20	20	3	3	10	6	Accelerated	6	50	3	92	169
11	1	100	13	16	20	4	10	11	5	Accelerated	6	40	3	92	193
12	1	90	9	20	19	2	3	7	4	Accelerated	2	50	3	98	167
13	1	100	18	20	20	7	4	12	5	Accelerated	1	50	6	107	157

However, as shown in Table 4-5, *Solutions 10 and 11* have the same project duration but different project cost. Based on these values, *Solution 10* dominates *Solution 11* since it has a lower costly construction. However, since stochastic simulation is used, the values of the objective functions, which are represented by the mean, can change every time that same candidate solution is evaluated. By examining the log of the optimization, it has been found that the *Solutions 10 and 11* have other pair values of (92, 170) and (91, 192), respectively for the duration and cost of the project. Based on these values, the two solutions are non-dominated. This problem impacts the quality of the optimum solutions generated by the optimization algorithm. This problem occurs when the distribution of the project's total duration or cost for a candidate solution overlap with another candidate solution. Figure 4-11 shows the scatter plot of project duration and cost combinations for *Solutions 10 and 11* after 1,000 simulation replications. It can be noticed that *Solutions 10 and 11* have almost the same project's duration for many of the replications. This is also evident in Figure 4-12 and Figure 4-13 which show the project's total duration and total cost distributions for the two solutions, respectively. Another shortcoming of the traditional stochastic simulation-based multi-objective optimization is that the optimum solutions generated at the end of the optimization process will differ every time the optimization is performed. Table 4-6 shows the optimum solutions in the second run for the same example above with the same exact settings. It can be noticed from the two tables that none of the solutions are repeated in the two runs. Figure 4-14 shows the two Pareto fronts from the two runs.

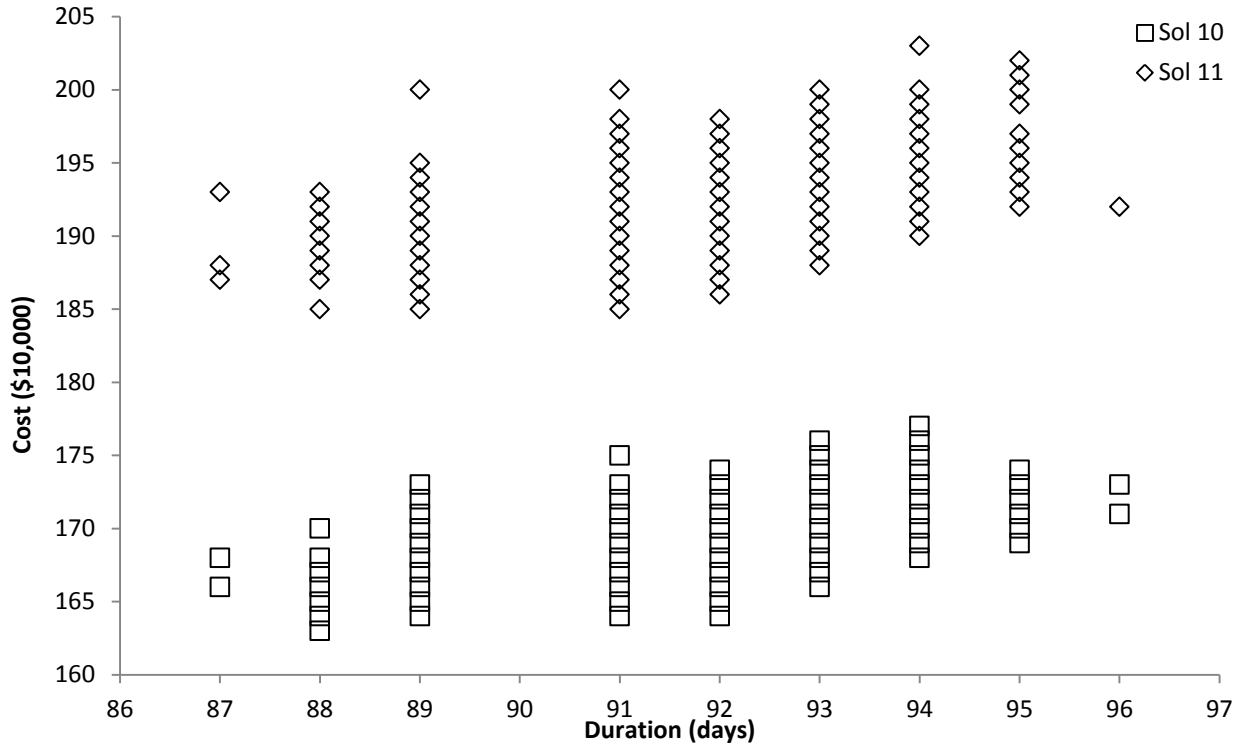


Figure 4-11 Scatter Plot of the Project Duration and Cost Combinations for Solutions 10 and 11

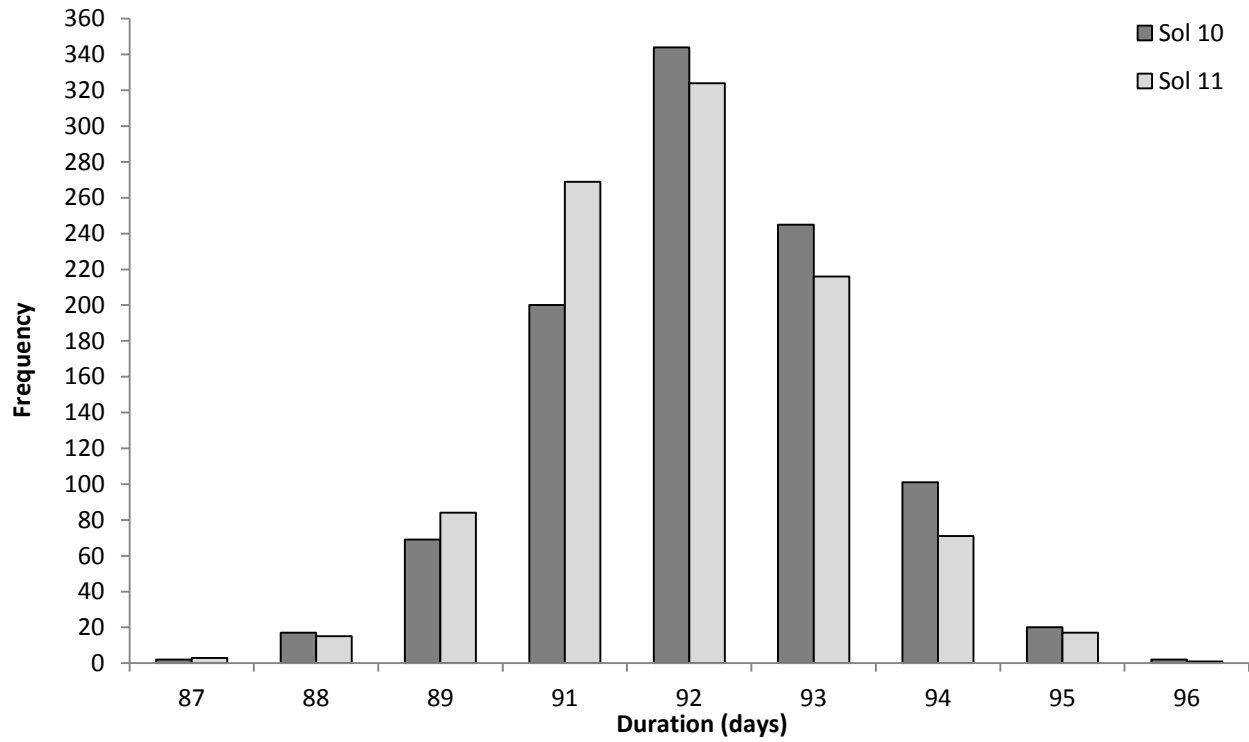


Figure 4-12 Project Duration Distribution of Solutions 10 and 11

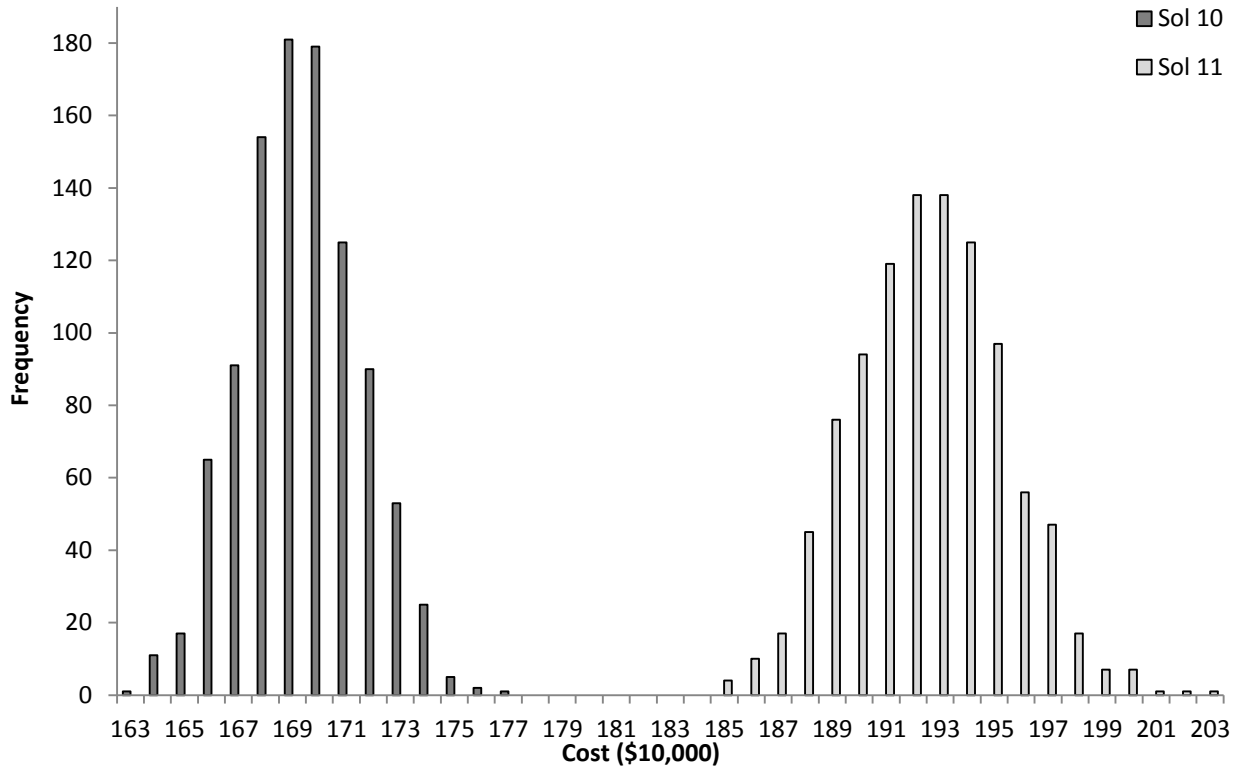


Figure 4-13 Project Cost Distribution of Solutions 10 and 11

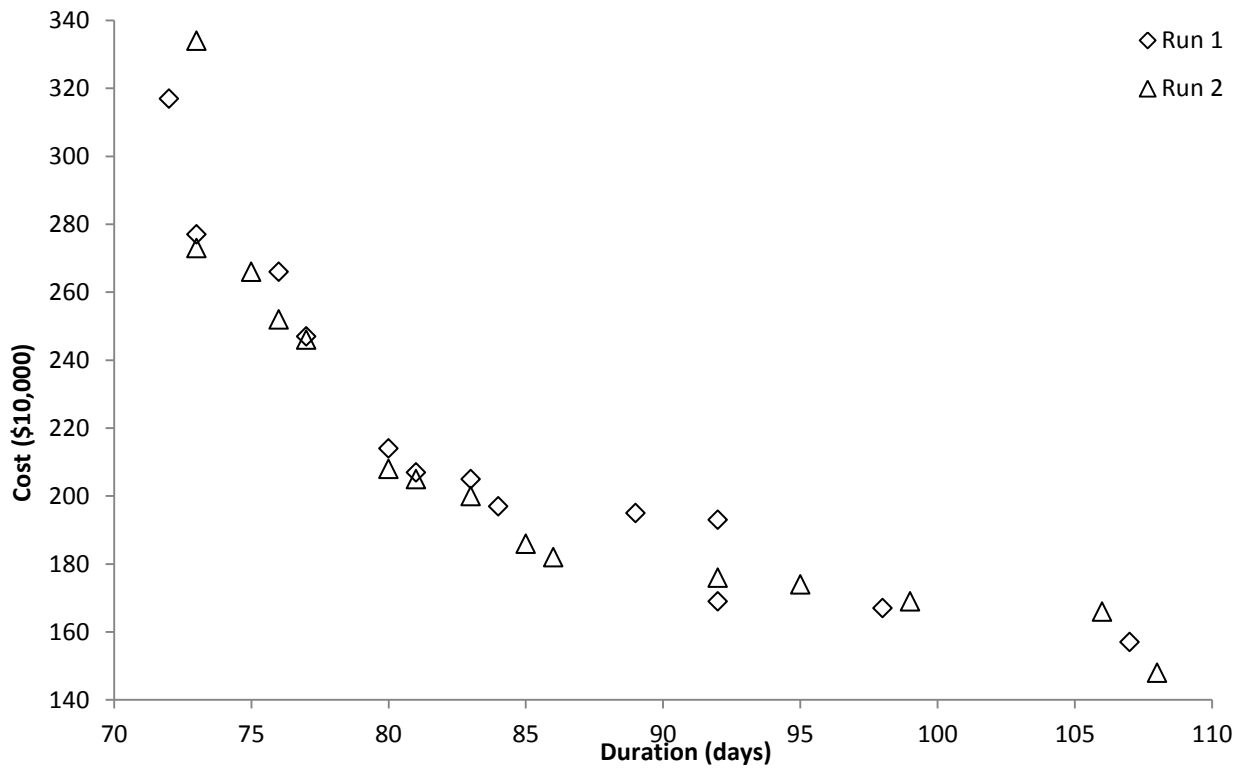


Figure 4-14 Pareto Fronts Generated in the First and Second Run

Table 4-6 Details of the Pareto Set of Solutions for the Second Run

Sol	NDT	PYD	NRC	NIM	NOM	NPC	NSC ₁	NSC ₂	NCC	Curing Method	Overtime Policy	PYS	ST (hours)	Duration (days)	Cost (\$10,000)
1	1	30	14	15	20	3	2	9	5	Accelerated	15	40	1	73	273
2	2	90	13	15	20	6	4	15	5	Accelerated	15	40	1	73	334
3	1	100	14	20	20	5	4	11	5	Accelerated	14	40	1	75	266
4	2	100	13	16	19	5	4	11	5	Accelerated	13	40	1	76	252
5	1	10	15	16	20	6	3	11	5	Accelerated	13	40	3	77	246
6	1	100	14	20	20	3	2	9	5	Accelerated	12	35	1	80	208
7	1	100	13	16	20	4	3	9	6	Accelerated	8	50	9	81	205
8	1	30	16	20	20	4	3	10	4	Accelerated	8	50	24	83	200
9	1	100	13	20	20	4	4	10	5	Accelerated	7	40	7	85	186
10	1	100	20	20	20	3	4	9	5	Accelerated	7	40	1	86	182
11	2	40	13	20	20	3	4	11	5	Accelerated	6	50	1	92	176
12	1	100	20	20	17	2	3	10	4	Regular	6	50	8	95	174
13	1	100	10	20	17	2	3	10	3	Accelerated	2	45	2	99	169
14	1	100	18	20	17	5	3	17	4	Accelerated	1	50	8	106	166
15	1	20	20	20	20	3	4	9	5	Accelerated	1	40	2	108	148

4.10 Summary and Conclusions

This chapter presented the proposed stochastic simulation-based multi-objective optimization model dedicated for planning bridge construction operations. The aim of the model is to select a near-optimum construction scenario that satisfies predefined objectives. This model is used to select the near-optimum construction scenarios based on quantitative analysis rather than qualitative analysis. The construction scenario in this context consists of two main elements. The first element is the construction method that is used to construct a bridge. The second element is the decision variables that have an impact on the duration and cost of the project. Two cycles were added to the fmGA which are: (1) the sub-population cycle where each sub-population represents a specific construction method; and (2) the simulation cycle where the values of the objective functions of candidate solutions are calculated. This chapter: (1) identified and modeled the decision variables related for each construction method; (2) formulated the objective functions that are used to estimate construction cost and duration; (3) defined the optimization constraints; (4) developed the simulation models of the selected construction methods; (5) designed the integration between the optimization algorithm and simulation; (6) implemented the model; (7) demonstrated the effectiveness of the proposed model.

As demonstrated in the case study, the proposed model was able to generate a set of solutions where each solution represents a construction scenario. However, it has been demonstrated that applying methods that exist in the current state of the art is inefficient in dealing with the problem of stochastic dominance. As a result, inferior candidate solutions may be presented among the optimum solutions. In addition, the traditional method does not produce consistent optimum solutions every time the optimization is run. Moreover, the traditional method required almost 7 hours to evaluate 100,000 candidate solutions for a single construction method. As a result, the computation time required will increase as the number of construction methods considered increases. To overcome these problems, VRTs are incorporated in the proposed stochastic simulation-based multi-objective model to examine their efficiency as will be explained in *Chapter 5*.

CHAPTER 5: SOLVING THE PROBLEM OF STOCHASTIC DOMINANCE AND REDUCING THE NUMBER OF SIMULATION REPLICATIONS USING VARIANCE REDUCTION TECHNIQUES

5.1 Introduction

This chapter presents a method to incorporate VRTs into the stochastic simulation-based optimization model presented in *Chapter 3*. The main objectives of using VRTs within the proposed model are: (1) increasing the quality of the optimum solutions; (2) increasing the confidence in the optimality of the optimum solutions; and (3) reducing the computation time required for performing the stochastic simulation-based multi-objective optimization. Applying this new method would solve the problem of stochastic dominance as discussed in *Sections 2.6* and *4.9* and as a result, the quality of the optimum solutions is increased. In addition, this new method would allow project planners to optimize construction operations faster by reducing the number of simulation replications required to obtain a good estimate of the candidate solutions, which will make the use of stochastic simulation-based optimization more appealing. The saved time can be used to cover a larger area of the search space, which results in increasing the confidence in the optimality of the optimum solutions. Although VRTs have been used in simulation studies in the past, they are used here in a novel way to improve the performance of the optimization process.

Three VRTs are studied in this research, which are CRN, AV, and a hybrid method that combines CRN and AV, which is referred to as the Combined Method (CM) in the rest of the thesis. The idea of using more than one VRT simultaneously is not new. However, very few researches studied the CM technique (Kleijnen, 1975; Schruben and Margolin 1978; Tew and Wilson, 1994). As mentioned in *Section 2.6.1*, CRN is used to compare several candidate solutions while AV is used for a single candidate solution. It is appealing to combine these two techniques in simulation-based optimization where CRN will be used to compare the different candidate solutions generated by the optimization algorithm while AV will be used in estimating the performance measure indices of each candidate solution. In this case, the average difference between two candidate solutions can be estimated using Equation 5-1.

$$\bar{Z}(N/2) = \frac{\sum_{p=1}^{N/2} [(X'_{1p} + X''_{1p})/2 - (X'_{2p} + X''_{2p})/2]}{N/2} \quad \text{Equation 5-1}$$

It is important to mention that the statistical results obtained using VRTs cannot be used to derive any statistical information of the optimum candidate solution. Therefore, a number of replications must be performed for the near optimum solutions at the end of the optimization process in order to obtain sound statistical information of these solutions. The incorporation of VRTs in simulation-based multi-objective optimization model is done in three steps: synchronization of random numbers, comparing the candidate solutions, and comparing and selecting the best VRT. Consequently, the rest of this chapter aims to: (1) identify and model the required synchronization; (2) formulate a method to compare the performance measure indices of the candidate solutions; (3) develop a method to compare and select the best VRT; (4) implement the proposed method; and (5) demonstrate the effectiveness of the proposed method.

5.2 Synchronization of Random Numbers

An important criterion for the success of the incorporation of VRTs is the synchronization of the random numbers. The synchronization is done up to four levels depending on the type of the VRT used as shown in Table 5-1. CRN has three levels of synchronization, which are between the stochastic tasks, between the replications, and between the candidate solutions. AV has also three levels of synchronization, which are between the stochastic tasks, between the replications in a pair, and between the pairs. On the other hand, the CM has four levels of synchronization, which are between the stochastic tasks, between the replications in a pair, between the pairs, and between the candidate solutions.

Table 5-1 Types of Synchronization Required for Different VRTs

Synchronization Between	CRN	AV	CM
Tasks	x	x	x
Replications/Pairs	x	x	x
Replications in a pair		x	x
Candidate solutions	x		x

Random numbers for each task in each replication can be generated from the *same streams* used in the previous replication or from *new streams*. To differentiate between the two approaches, the

first approach is referred to by the name of the technique (i.e., CRN, AV, and CM) while the second approach is referred to by “ns” subscripted next to the name of the technique (i.e., CRN_{ns}, AV_{ns}, and CM_{ns}). The first and the second approaches are described in detail in *Sections 5.2.1* and *5.2.2*, respectively.

Figure 5-1 and Figure 5-2 show the algorithms for incorporating the VRTs into simulation-based optimization. The process starts by generating (L) generations where each generation has a population of size (E) by the optimization algorithm. Each candidate solution (e) is then evaluated using simulation where it will be run for several replications. In each replication, at least one instance of each task (o) is created. Finally, the performance measure indices of each candidate solution is returned back to the optimization algorithm. However, for the clarity of the explanation, the synchronization process will be explained in the following sections starting from the tasks, then the replications, and finally the candidate solutions.

<pre> 1 // Repeat for all generations 2 FOR $l = 1$ TO L 3 // Repeat for all solutions in the population 4 FOR $e = 1$ TO E 5 $ARN = \text{Constant}$ 6 // Repeat for all replications 7 FOR $n = 1$ TO N 8 IF $n = 1$ 9 Space streams using ARN and RRN_{max} 10 ELSE 11 // Repeat for all tasks 12 FOR $o = 1$ TO O 13 Continue from last S_oRN 14 END FOR 15 END IF 16 Simulate the model 17 Collect D_{en} and C_{en} 18 END FOR 19 Calculate $\overline{D_e}$ and $\overline{C_e}$ 20 END FOR 21 Sort candidate solutions 22 END FOR </pre>	<pre> 1 // Repeat for all generations 2 FOR $l = 1$ TO L 3 // Repeat for all solutions in the population 4 FOR $e = 1$ TO E 5 $ARN = \text{Constant}$ 6 // Repeat for all replications 7 FOR $n = 1$ TO N 8 IF $n = 1$ 9 Space streams using ARN and RRN_{max} 10 ELSE 11 Space streams using RN and RRN_{max} 12 END IF 13 Simulate the model 14 Collect D_{en} and C_{en} 15 Assign $RN = S_{[(n \times o) + 1]}RN_l$ 16 END FOR 17 Calculate $\overline{D_e}$ and $\overline{C_e}$ 18 END FOR 19 Sort candidate solutions 20 END FOR </pre>
---	---

(a) Using same streams

(b) Using new streams

Figure 5-1 Algorithm for Incorporating CRN and CRN_{ns} Techniques

```

1 // Repeat for all generations
2 FOR  $l = 1$  TO  $L$ 
3 // Repeat for all solutions in the population
4 FOR  $e = 1$  TO  $E$ 
5    $ARN = \text{Variable} *$ 
6 // Repeat for all pairs
7   FOR  $p = 1$  TO  $N/2$ 
8 // Standard replication
9   IF  $p = 1$ 
10    Space streams using  $ARN$  and  $RRN_{max}$ 
11  ELSE
12 // Repeat for all tasks
13    FOR  $o = 1$  TO  $O$ 
14    Use saved  $S_oRN$ 
15    END FOR
16  END IF
17  Simulate the model
18  Collect  $D'_{mp}$  and  $C'_{mp}$ 
19 // Antithetic replication
20  IF  $p = 1$ 
21    Space streams using  $ARN$ 
22  ELSE
23 // Repeat for all tasks
24    FOR  $o = 1$  TO  $O$ 
25    Use saved  $S_oRN$ 
26    END FOR
27  END IF
28  Simulate the model using
29  Collect  $D''_{ep}$  and  $C''_{ep}$ 
30  Calculate  $\overline{D_{ep}}$  and  $\overline{C_{ep}}$ 
31 // Repeat for all tasks
32  FOR  $o = 1$  TO  $O$ 
33  Save last  $S_oRN$  used
34  END FOR
35 END FOR
36 Calculate  $\overline{D_e}$  and  $\overline{C_e}$ 
37 END FOR
38 Sort candidate solutions
39 END FOR

```

* For the CM technique, $ARN = \text{Constant}$

(a) Using same streams

```

1 // Repeat for all generations
2 FOR  $l = 1$  TO  $L$ 
3 // Repeat for all solutions in the population
4 FOR  $e = 1$  TO  $E$ 
5    $ARN = \text{Variable} *$ 
6 // Repeat for all pairs
7   FOR  $p = 1$  TO  $N/2$ 
8 // Standard replication
9   IF  $p = 1$ 
10    Space streams using  $ARN$  and  $RRN_{max}$ 
11  ELSE
12    Space streams using  $RN$  and  $RRN_{max}$ 
13  END IF
14  Simulate the model
15  Collect  $D'_{mp}$  and  $C'_{mp}$ 
16 // Antithetic replication
17  IF  $p = 1$ 
18    Space streams using  $ARN$  and  $RRN_{max}$ 
19  ELSE
20    Space streams using  $RN$  and  $RRN_{max}$ 
21  END IF
22  Simulate the model
23  Collect  $D''_{ep}$  and  $C''_{ep}$ 
24  Calculate  $\overline{D_{ep}}$  and  $\overline{C_{ep}}$ 
25  Assign  $RN = S_{[(n \times O) + 1]}RN_l$ 
26  END FOR
27  Calculate  $\overline{D_e}$  and  $\overline{C_e}$ 
28 END FOR
29 Sort candidate solutions
30 END FOR

```

* For the CM technique, $ARN = \text{Constant}$

(b) Using new streams

Figure 5-2 Algorithm for Incorporating (a) AV and CM, and (b) AV_{ns} and CM_{ns} Techniques

5.2.1 Synchronization of CRN Technique Using Same Streams

5.2.1.1 Synchronization Between Stochastic Tasks

In this research, VRTs are applied for every stochastic task in the simulation model. In order to ensure proper synchronization between the stochastic tasks, each stochastic task is assigned an independent stream from which random numbers can be generated. The length of a stream for a certain task should be enough to generate the required number of random numbers without overlapping with other streams. This is necessary to keep the statistical independence of the stochastic tasks in the simulation model. The random numbers used for each task cannot be used for another task. Using the same random numbers for more than one task will create a dependency between these tasks that must be avoided.

In a simulation model, the lengths of streams can be of equal size or variable sizes. In most cases, equal size streams are sufficient and they are always faster than variable size streams. For the purpose of this research, streams with equal lengths are used. Regardless of the approach used, it is crucial to determine the number of required random numbers (*RRN*) for each task in order to determine the minimum required length of the streams. The task with the maximum *RRN* is used as the basis for determining the length of the streams. Equation 5-2 can be used to determine the maximum *RRN* for a VRT using the same streams approach.

$$\arg \max_o RRN_o = Inst_o \times RNU_o \times N \quad \forall o = 1, 2, \dots, O \quad \text{Equation 5-2}$$

where,

RRN_o = required random numbers for the stochastic task o

$Inst_o$ = total number of instances that will be created of task o in a replication

RNU_o = number of random numbers used to produce a random variate for task o

RNU depends on the type of the distribution function used to model the uncertainty of the task. Martinez (1996) lists the *RNU* for different distribution functions. For example, assuming a simulation model has two tasks, *A* and *B*, that are modeled using triangular distribution (*RNU* = 1) and is replicated four times, and assuming that task *A* has two instances and task *B* has one instance, this will result in *RRN* equal to eight and four for tasks *A* and *B*, respectively. The streams are then spaced based on the maximum *RRN* starting from an Arbitrary Random Number

(ARN). The ARN , which is generated randomly by the optimization algorithm, is used as the starting value for the first stream.

Table 5-2(a) shows examples of synchronization of CRN for the two tasks A and B . The term S_1RN_1 , for example, reads as random number 1 (RN_1) generated from stream 1 (S_1). By examining columns (3) and (4) of this table, it can be noticed that all the random numbers for tasks A and B in the first replication ($n = 1$) are generated from S_1 and S_2 , respectively. In addition, it can be noticed that none of the RNs are used more than once in the same replication.

5.2.1.2 Synchronization Between Replications

As explained above, for the independence of stochastic tasks, the synchronization between the replications is necessary to keep the independence between the different replications. The random numbers used for each task in a replication cannot be used in another replication to avoid creating a dependency between these replications. Figure 5-3(a) shows the schematic of stream spacing for the CRN technique. S_1 and S_2 have a stream of length eight (i.e., a maximum of eight RNs can be generated from each stream). In this approach, random numbers for each task, in the subsequent replication, are generated from the same stream assigned to that task. Therefore, the random numbers generated for the subsequent replication must start from the next random number after the last random number generated in the previous replication. Columns (3) and (4) of Table 5-2(a) demonstrate this approach where the second replication starts from S_1RN_3 and S_2RN_2 for tasks A and B , respectively. S_1RN_3 and S_2RN_2 are the next random numbers after the last random numbers used for task A (S_1RN_2) and task B (S_2RN_1) in the first replication.

Figure 5-1(a) shows the algorithm for incorporating the CRN technique. The synchronization between the replications is represented in lines 7 to 18. The first replication uses the ARN and the maximum RRN to assign a stream for each stochastic task. The simulation is performed by generating random numbers for each task o from the assigned stream (S_oRN). For subsequent replications, each task will continue from the last S_oRN used.

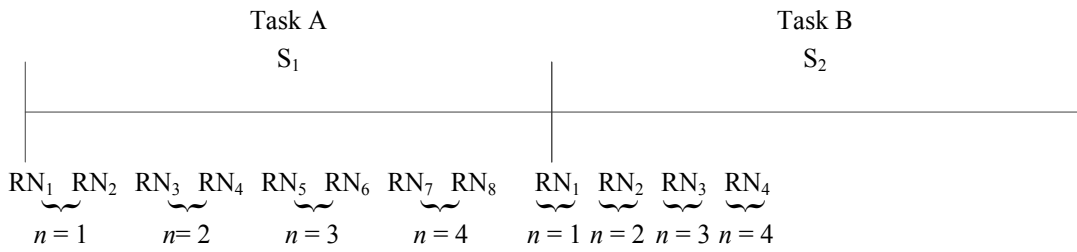
Table 5-2 Synchronization of Different VRTs for Tasks A and B Using the Same Streams Approach

(a) CRN

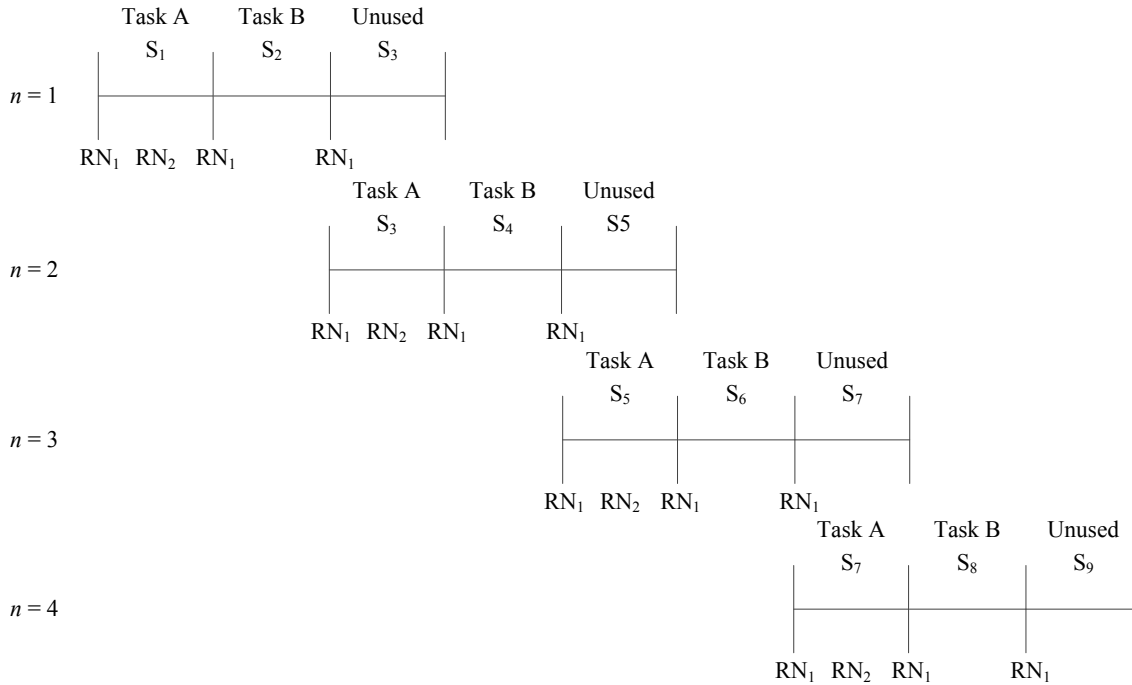
		CRN			
		Solution 1		Solution 2	
(1)	(2)	(3)	(4)	(5)	(6)
n	$Inst$	Task A	Task B	Task A	Task B
1	1	S_1RN_1	S_2RN_1	S_1RN_1	S_2RN_1
	2	S_1RN_2		S_1RN_2	
2	1	S_1RN_3	S_2RN_2	S_1RN_3	S_2RN_2
	2	S_1RN_4		S_1RN_4	
3	1	S_1RN_5	S_2RN_3	S_1RN_5	S_2RN_3
	2	S_1RN_6		S_1RN_6	
4	1	S_1RN_7	S_2RN_4	S_1RN_7	S_2RN_4
	2	S_1RN_8		S_1RN_8	

(b) AV and CM

			AV				CM			
			Solution 1		Solution 2		Solution 1		Solution 2	
(1)	(2)	(3)	(4)	(5)	(6)	(7)	(8)	(9)	(10)	(11)
p	n	$Inst$	Task A	Task B	Task A	Task B	Task A	Task B	Task A	Task B
1	1	1	S_1RN_1	S_2RN_1	S_1RN_1'	S_2RN_1'	S_1RN_1	S_2RN_1	S_1RN_1	S_2RN_1
		2	S_1RN_2		S_1RN_2'		S_1RN_2		S_1RN_2	
	2	1	$1 - S_1RN_1$	$1 - S_2RN_1$	$1 - S_1RN_1'$	$1 - S_2RN_1'$	$1 - S_1RN_1$	$1 - S_2RN_1$	$1 - S_1RN_1$	$1 - S_2RN_1$
		2	$1 - S_1RN_2$		$1 - S_1RN_2'$		$1 - S_1RN_2$		$1 - S_1RN_2$	
2	3	1	S_1RN_3	S_2RN_2	S_1RN_3'	S_2RN_2'	S_1RN_3	S_2RN_2	S_1RN_3	S_2RN_2
		2	S_1RN_4		S_1RN_4'		S_1RN_4		S_1RN_4	
	4	1	$1 - S_1RN_3$	$1 - S_2RN_2$	$1 - S_1RN_3'$	$1 - S_2RN_2'$	$1 - S_1RN_3$	$1 - S_2RN_2$	$1 - S_1RN_3$	$1 - S_2RN_2$
		2	$1 - S_1RN_4$		$1 - S_1RN_4'$		$1 - S_1RN_4$		$1 - S_1RN_4$	



(a) Using same streams



(b) Using new streams

Figure 5-3 Schematic of Stream Spacing for CRN Technique

5.2.1.3 Synchronization Between Candidate Solutions

To ensure proper synchronization and dependency between the candidate solutions, the ARN must be controlled by using the same ARN for all the candidate solutions. As mentioned earlier, ARN is used to space the streams from which the random numbers are generated. This synchronization is represented in line 5 in Figure 5-1(a). For each candidate solution (e) in a population of size (E) of generation (I) generated by the optimization algorithm, the same ARN is used (i.e., $ARN = \text{constant}$). This synchronization can be seen in columns (3) to (6) of Table 5-2(a). It can be noticed that the two candidate solutions use the same streams and random numbers of tasks A and B for all the instances and replications when CRN technique is used.

5.2.2 Synchronization of CRN Technique Using New Streams

5.2.2.1 Synchronization Between Stochastic Tasks

This synchronization is done in a similar manner as explained in *Section 5.2.1.1* with the only difference in the maximum *RRN*. If random numbers are generated from a new stream in each replication, then Equation 5-3 can be used to determine the maximum *RRN* for a VRT.

$$\arg \max_o RRN_o = Inst_o \times RNU_o \quad \forall o = 1, 2, \dots, O \quad \text{Equation 5-3}$$

Using this approach, the *RRN* values for tasks *A* and *B* are two and one, respectively.

5.2.2.2 Synchronization Between Replications

As explained earlier, the new streams approach generates random numbers in the subsequent replication for each task from a new stream. That is, tasks are assigned new streams by spacing the streams in the subsequent replications based on the first random number generated from an additional stream that will be created in advance but will not be used by any task in the current replication.

Figure 5-3(b) shows the schematic of stream spacing for the CRN_{ns} technique. For example, in the first replication, three streams of length 2 (the maximum *RRN*) are being spaced. S_1 and S_2 will be used by tasks *A* and *B*, respectively. On the other hand, S_3 has not being used by any task and S_3RN_1 is the first random number in S_3 . In the second replication, S_3RN_1 will be used to space three new streams and so forth.

Table 5-3(a) shows similar examples to those shown in Table 5-2(a) when CRN_{ns} is used. As can be seen in columns (3) and (4), the random numbers for tasks *A* and *B* are generated from a different stream in each replication (i.e., $S_1, S_3, S_5,$ and S_7 for task *A*) and (i.e., $S_2, S_4, S_6,$ and S_8 for task *B*). It can be noticed that no one stream has been used for both tasks, which is necessary to maintain the independency between tasks as mentioned earlier.

Figure 5-1(b) shows the algorithm for incorporating the CRN_{ns} technique. This synchronization is represented in lines 7 to 16 of Figure 5-1(b). The first replication uses the generated *ARN* and the maximum *RRN* to assign a stream for each stochastic task. The simulation is performed by generating random numbers for each task *o* from the assigned stream $S_{[o + O \times (n-1)]}$. At the end of

each replication, RN will be assigned RN_1 from the unused stream ($S_{[(n \times O) + 1]}$) generated at the beginning of the replication.

5.2.2.3 Synchronization Between Candidate Solutions

This synchronization is done in a similar manner as explained in *Section 5.2.1.3*. This synchronization is represented in line 5 in Figure 5-1(b) and can be seen in columns (3) to (6) of Table 5-3(a).

5.2.3 Synchronization of AV Technique and CM Using Same streams and New Streams

5.2.3.1 Synchronization Between Stochastic Tasks

When AV or CM is used, the term N in Equation 5-2 represents the number of pairs instead of the number of replications. The number of pairs will equal $N/2$ since each pair has two replications. The synchronization between stochastic tasks is done in a similar manner for the same streams and the new streams approaches as explained in *Sections 5.2.1.1* and *5.2.2.1*. This synchronization is can be seen in columns (4) and (5), and (8) and (9) of Table 5-2(b) for AV and CM, respectively; and in columns (4) and (5), and (8) and (9) of Table 5-3(b) for AV_{ns} and CM_{ns} , respectively.

5.2.3.2 Synchronization Between Pairs

The synchronization between pairs is done in a similar manner for the same streams and the new streams approaches as explained in *Sections 5.2.1.2* and *5.2.2.2*. As explained above for the independence of replications, the synchronization between the pairs is necessary to keep the independence between the different pairs. Figure 5-2(a) shows the algorithm for incorporating the AV and the CM. Random numbers for subsequent pairs, in the same streams approach, are generated from the same stream assigned to each task as represented in lines 7 to 35 of Figure 5-2(a). This synchronization is can be seen in columns (4), (5), (8) and (9) of Table 5-2(b) where the second pair starts from S_1RN_3 and S_2RN_2 for tasks A and B , respectively.

Figure 5-2(b) shows the algorithm for incorporating the AV_{ns} and the CM_{ns} . In this case, random numbers for subsequent pairs are generated from the new streams as represented in lines 7 to 26 of Figure 5-2(b). The first pair uses the generated ARN and the maximum RRN to assign a stream

for each stochastic task. The simulation is performed by generating random numbers for each task o from the assigned stream $S_{[o + o \times (p-1)]}$. At the end of each pair, RN will be assigned RN_I from the unused stream ($S_{[(p \times o) + 1]}$) generated at the beginning of the pair. This synchronization can be seen in columns (4), (5), (8) and (9) of Table 5-3(b) where the second pair starts from S_3RN_I and S_4RN_I for tasks A and B , respectively. It can be noticed from Table 5-2(b) and Table 5-3(b) that there is no one random number from any stream that has been used more than once, which is necessary to maintain the independency between the pairs as mentioned earlier.

5.2.3.3 Synchronization Between Replications in a Pair

This synchronization is necessary when AV and the CM techniques are used. To synchronize the two replications in a pair, they must use complementary RN . This synchronization is exhibited in columns (4) to (11) of Table 5-2(b) and Table 5-3(b). For example in column (4), the first instance of task A in the standard replication of the first pair uses the random number S_1RN_I and the same instance of the same task uses the random number $I - S_1RN_I$ in the antithetic replication of the first pair. In order to synchronize the replications in a pair, the complementary random number used for the standard replication must be used in the antithetic replication of the same pair as shown in lines 9 to 16 and 20 to 27 in Figure 5-2(a) and lines 9 to 13 and 17 to 21 in Figure 5-2(b).

5.2.3.4 Synchronization Between Candidate Solutions

A key difference between CM and AV is that there exists no synchronization between the different candidate solutions when AV is used. In other words, each solution experience different uncertainty conditions under AV. This synchronization is represented in line 5 in Figure 5-2(a) and (b), and can be seen in columns (4) to (11) of Table 5-2(b) and Table 5-3(b). It can be noticed that the two candidate solutions use the same streams and random numbers of tasks A and B for all the instances, replications, and pairs when CM technique is used. It can be noticed that ARN is fixed when synchronization is required between the candidate solutions and variable otherwise.

Table 5-3 Synchronization of Different VRTs for Tasks A and B Using the New Streams Approach

(a) CRN

		CRN			
		Solution 1		Solution 2	
(1)	(2)	(3)	(4)	(5)	(6)
n	<i>Inst</i>	Task A	Task B	Task A	Task B
1	1	S_1RN_1	S_2RN_1	S_1RN_1	S_2RN_1
	2	S_1RN_2		S_1RN_2	
2	1	S_3RN_1	S_4RN_1	S_3RN_1	S_4RN_1
	2	S_3RN_2		S_3RN_2	
3	1	S_5RN_1	S_6RN_1	S_5RN_1	S_6RN_1
	2	S_5RN_2		S_5RN_2	
4	1	S_7RN_1	S_8RN_1	S_7RN_1	S_8RN_1
	2	S_7RN_2		S_7RN_2	

(b) AV and CM

			AV				CM			
			Solution 1		Solution 2		Solution 1		Solution 2	
(1)	(2)	(3)	(4)	(5)	(6)	(7)	(8)	(9)	(10)	(11)
p	n	<i>Inst</i>	Task A	Task B	Task A	Task B	Task A	Task B	Task A	Task B
1	1	1	S_1RN_1	S_2RN_1	S_1RN_1'	S_2RN_1'	S_1RN_1	S_2RN_1	S_1RN_1	S_2RN_1
		2	S_1RN_2		S_1RN_2'		S_1RN_2		S_1RN_2	
	2	1	$1 - S_1RN_1$	$1 - S_2RN_1$	$1 - S_1RN_1'$	$1 - S_2RN_1'$	$1 - S_1RN_1$	$1 - S_2RN_1$	$1 - S_1RN_1$	$1 - S_2RN_1$
		2	$1 - S_1RN_2$		$1 - S_1RN_2'$		$1 - S_1RN_2$		$1 - S_1RN_2$	
2	3	1	S_3RN_1	S_4RN_1	S_3RN_1'	S_4RN_1'	S_3RN_1	S_4RN_1	S_3RN_1	S_4RN_1
		2	S_3RN_2		S_3RN_2'		S_3RN_2		S_3RN_2	
	4	1	$1 - S_3RN_1$	$1 - S_4RN_1$	$1 - S_3RN_1'$	$1 - S_4RN_1'$	$1 - S_3RN_1$	$1 - S_4RN_1$	$1 - S_3RN_1$	$1 - S_4RN_1$
		2	$1 - S_3RN_2$		$1 - S_3RN_2'$		$1 - S_3RN_2$		$1 - S_3RN_2$	

5.3 Comparing the Candidate Solutions

In order to use CRN in simulation-based optimization, the performance measure indices of each candidate solution should be compared pairwise. Knowing that the optimization would run for a large number of candidate solutions, performing pairwise comparison would dramatically increase the number of trails. For example, if the optimization is run for 1,000 candidate solutions, the total number of pairwise comparisons would be 499,500, which can be found using the pairwise comparisons formula $(q \times (q - 1)/2)$ where q is the number of candidate solutions (Bible et al., 2011). Using pairwise comparisons in the optimization will defeat one of the purposes of using CRN (i.e., reduce the computation time). Therefore, the pairwise comparisons shown in Equation 2-5 should be rewritten as the following for the project duration:

$$\bar{Z}(N) = \frac{\sum_{n=1}^N (D_{1n} - D_{2n})}{N} = \frac{\sum_{n=1}^N D_{1n}}{N} - \frac{\sum_{n=1}^N D_{2n}}{N} \quad \text{Equation 5-4}$$

In order to choose between the two candidate solutions, the sign of $\bar{Z}(N)$ should be examined. If $\bar{Z}(N)$ is negative, then the average duration of candidate solution 2 is greater than the average duration of candidate solution 1, and therefore, candidate solution 1 is better than candidate solution 2, and vice versa. This is equivalent to saying that $\bar{D}_1 < \bar{D}_2$ which is more practical when comparing a large number of candidate solutions as in the case of simulation-based optimization problems.

In multi-objective optimization problems, the performance of a simulation model consists of two or more measure indices, e.g., the total project duration and cost. Traditionally, CRN is used to compare two candidate solutions based on a single performance measure index. To compare more than one performance measure index, the notation of solution domination is used. A candidate solution is considered non-dominant when there is no other candidate solution that can improve one performance measure index without worsening the other performance measure index. Candidate solutions are represented by combinations of average duration and average cost (\bar{D}_e, \bar{C}_e) that are calculated as represented in lines 19, 17, 36, and 27 in Figure 5-1(a), Figure 5-1(b), Figure 5-2(a), and Figure 5-2(b), respectively. One candidate solution is better than another if Equation 5-5 holds true.

$$(\bar{D}_e \leq \bar{D}_{m \neq e} \text{ and } \bar{C}_e < \bar{C}_{m \neq e}) \text{ or } (\bar{D}_e < \bar{D}_{m \neq e} \text{ and } \bar{C}_e \leq \bar{C}_{m \neq e}) \quad \forall e, m = 1, 2, \dots, E \quad \text{Equation 5-5}$$

That is, candidate solution e has an equal or lower duration and lower cost than candidate solution m or candidate solution e has a lower duration and an equal or lower cost than candidate solution m .

5.4 Comparing and Selecting the Best VRT

The procedure used to compare and select the best VRT is presented in Figure 5-4. VRTs may not necessarily reduce the variance of the simulation model under study, and therefore, a pilot study should be done in order to measure the improvements that can be achieved using these techniques (Law, 2007). In order to select the best technique, performance metrics should be clearly identified. The main purpose of using VRT is to reduce the variance of a performance measure index obtained as an output from a simulation model. Therefore, the variance of the performance measure indices is the first metric to be used to compare the VRTs. This metric has been used in previous research to compare the performance of the VRTs (Kleijnen, 1975; Schruben and Margolin 1978). Equation 5-6, Equation 5-7, and Equation 5-8 are used to calculate the variance of the CRN technique, the AV technique and the CM technique, respectively.

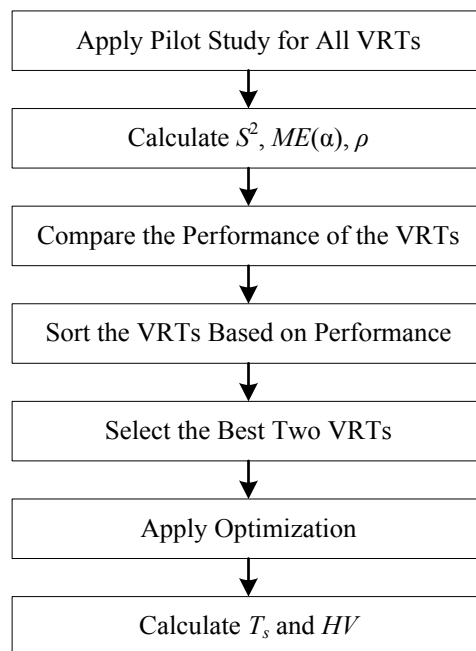


Figure 5-4 Procedure for Comparing and Selecting the Best VRT

$$S_z^2(N) = \frac{\sum_{n=1}^N [Z_n - \bar{Z}(N)]^2}{N - 1} \quad \text{Equation 5-6}$$

where,

$$Z_n = X_{1n} - X_{2n}$$

$$S_x^2(N/2) = \frac{\sum_{p=1}^{N/2} [X_p - \bar{X}(N/2)]^2}{\frac{N}{2} - 1} \quad \text{Equation 5-7}$$

where,

$$X_p = \frac{X'_p + X''_p}{2}$$

$$S_p^2(N/2) = \frac{\sum_{p=1}^{N/2} [Z_p - \bar{Z}(N/2)]^2}{\frac{N}{2} - 1} \quad \text{Equation 5-8}$$

where,

$$Z_p = \frac{X'_{1p} + X''_{1p}}{2} - \frac{X'_{2p} + X''_{2p}}{2}$$

Another performance metric that is considered is the margin of error ($ME(\alpha)$), also known as half-length of confidence interval, of the performance measure index of the simulation model. This can be calculated for each technique using Equation 5-9 (Mendenhall et al, 2008).

$$ME(\alpha) = z \sqrt{\frac{S_z^2(N)}{N}} \quad \text{Equation 5-9}$$

where,

z = critical z score of the normal distribution representing α confidence level

The correlation is calculated to examine the impact of the applied VRT. The correlation between the different candidate solutions, between the pairs within each candidate solution, and between the pairs across different candidate solutions can be calculated using Equation 5-10, Equation 5-11, and Equation 5-12, respectively.

$$\rho(X_{1n}, X_{2n}) = \frac{\sum_{n=1}^N [X_{1n} - \bar{X}_1(N)][X_{2n} - \bar{X}_2(N)]}{(N-1)\sqrt{S_1^2(N)S_2^2(N)}} \quad \text{Equation 5-10}$$

$$\rho(X'_p, X''_p) = \frac{\sum_{p=1}^{N/2} [X'_p - \bar{X}'(N/2)][X''_p - \bar{X}''(N/2)]}{(N/2-1)\sqrt{S'^2(N/2)S''^2(N/2)}} \quad \text{Equation 5-11}$$

$$\rho(X_{1p}, X_{2p}) = \frac{\sum_{p=1}^{N/2} [X_{1p} - \bar{X}_1(N/2)][X_{2p} - \bar{X}_2(N/2)]}{(N/2-1)\sqrt{S_1^2(N/2)S_2^2(N/2)}} \quad \text{Equation 5-12}$$

$ME(\alpha)$ can also be used to approximately estimate the required number of replications (N_{ME}) using the traditional method to achieve similar margin of error as shown in Equation 5-13 (Law, 2007).

$$N_{ME} = \frac{S^2(N) N}{S_z^2(N)} \quad \text{Equation 5-13}$$

To measure the improvements in the performance of proposed stochastic simulation-based multi-objective optimization methods, two metrics are identified, which are the time saving and the hypervolume indicator. The time saving measures the reduction in the computing time of the optimization process that was achieved by the proposed method and can be calculated using Equation 5-14.

$$T_s = \frac{T_T - T_{VRT}}{T_T} \times 100 \quad \text{Equation 5-14}$$

where,

T_s = time savings

T_T = time required to solve the optimization problem using the traditional method

T_{VRT} = time required to solve the optimization problem using VRT

The hypervolume indicator is the most common measure used to compare the performance of multi-objective evolutionary algorithms (Zitzler et al., 2007). This indicator measures the area of the search space that is dominated by the Pareto front obtained using evolutionary algorithms (Zitzler et al., 2003). The Pareto front with the largest hypervolume indicator is better than the other Pareto fronts since it takes into account the optimality and the diversity of the front

(Bradstreet, 2011). After estimating the hypervolume indicator, the percentage difference between the traditional method and the proposed method is calculated using Equation 5-15.

$$\Delta HV = \frac{HV_T - HV_P}{HV_T} \times 100 \quad \text{Equation 5-15}$$

Where,

ΔHV = percentage difference in hypervolume indicator

HV_T = hypervolume indicator using the traditional method

HV_p = hypervolume indicator VRT

5.5 Method Implementation

The algorithms in Figure 5-1 and Figure 5-2 are implemented in STROBOSCOPE. STROBOSCOPE is used because it has built-in functions and stream management tool that allow for the implementation of any VRT. Assigning different streams for each stochastic task can be done by using the built-in distribution functions, such as sTriangular and sNormal, which allows the modeller to specify the stream from which to retrieve the random numbers. Spacing the streams can be done by using the built-in SEEDALL statement:

SEEDALL *IntFrom1to2147483646* [*SeparationInHundredThousands*]

Where *IntFrom1to2147483646* is an arbitrary integer seed number set by the user between 1 and 21,474,483,646. *SeparationInHundredThousands* represents the separation between streams in hundred thousands. For example, if *SeparationInHundredThousands* is set to 1, then 100,000 random numbers can be used from each stream before it overlaps with the next stream. The *SeparationInHundredThousands* can be calculated by taking the ceiling of the maximum required random numbers (as calculated by Equation 5-2 or Equation 5-3) of all the stochastic tasks in a model divided by 100,000 as shown in Equation 5-16.

$$\textit{SeparationInHundredThousands} = \left\lceil \frac{\textit{Maximum RRN}}{100,000} \right\rceil \quad \text{Equation 5-16}$$

To find the last used seed number in a stream, the built-in `sSeed[Stream]` function is used where *Stream* is the stream assigned to a task. This seed number is used later on to point the stream to that specific random number in the subsequent replications using the built-in SEEDN statement:

```
SEEDN Stream IntFrom1to2147483646
```

5.6 Case Studies

Two case studies are used to demonstrate the effectiveness of the proposed method. Case Study A is about the construction of a precast full span box girder bridge using launching method. Case Study B is about the construction of a precast segmental box girder bridge using launching gantry method. The bridge, for both case studies, consists of 35 spans with identical spans of length 25 m. For Case Study B, each span consists of 9 segments. Table 4-2 shows the tasks durations used in Case Study A, while Table A-1 shows the tasks durations used for Case Study B. The cost data used in the simulation models of both case studies are presented in *Appendix B*.

5.6.1 Case Study A

5.6.1.1 Pilot Study to Compare VRTs

To select the best VRT, a pilot study was made to compare the performance of the three techniques and their *new streams* versions. The comparison was done over Solutions 9, 10, and 11 from Table 4-5. The purpose of choosing these three solutions is to show how the problem of stochastic dominance, which was demonstrated in *Section 4.9*, can be dealt with. Nine different configurations, which are CRN, AV, CM, CRN_{ns}, AV_{ns}, CM_{ns}, and their corresponding traditional method, are compared across these solutions. The statistical results of traditional method, CRN, and CRN_{ns} for 10 replications are presented in Table 5-4. It can be noticed that using the CRN and the CRN_{ns} has reduced the variance on average by 79% and 67%, respectively, compared with the traditional method. In addition, the margin of error is reduced on average by 57% and 43%, respectively compared with the traditional method. The average induced correlations across the three solutions are 0.88 and 0.72, respectively.

Figure 5-5 shows the correlation between the pilot study solutions using CRN, CRN_{ns} and traditional method. It can be noticed from Figures 5-5(a), (b), (c), and (d) that the outcome of each replication for the three solutions moves in the same direction (i.e. synchronized) which

results in high positive correlation. On the other hand, the traditional method does not have this synchronization as shown in Figure 5-5(e) and (f). To achieve similar margins of error to CRN and CRN_{ns}, the traditional method should perform on average 76 and 66 replications, respectively. From these results, it can be concluded that the use of CRN and CRN_{ns} achieved the desirable variance reduction.

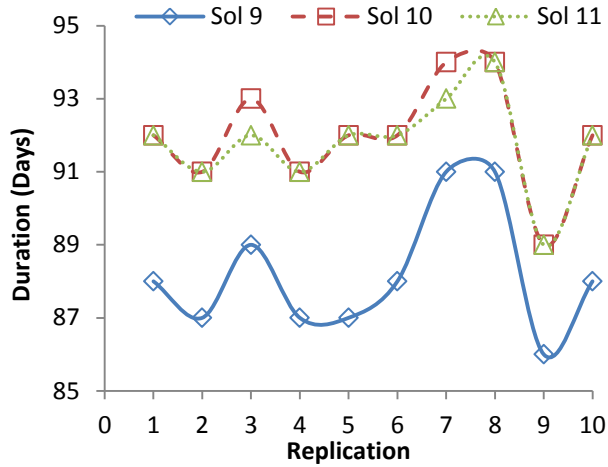
Table 5-5 presents the statistical results of using traditional method, AV, and AV_{ns} for 5 pairs of the three solutions (i.e., 10 replications). From these results, it can be noticed that using the AV failed to reduce the variance for *Solution 11*. On the other hand, AV_{ns} failed in inducing a negative correlation between the replications in the pairs for *Solution 9*.

Figure 5-6 shows the correlation between the solutions using AV, AV_{ns}, and traditional method. The ideal condition for the AV technique to work effectively would be when the replications in a pair are at an equal distance from the mean in opposite directions. This can be noticed in Figure 5-6 (c) and (d) for *Solution 10* and that is why this solution has a high negative correlation (i.e., -0.92 for project duration and -0.83 for project cost).

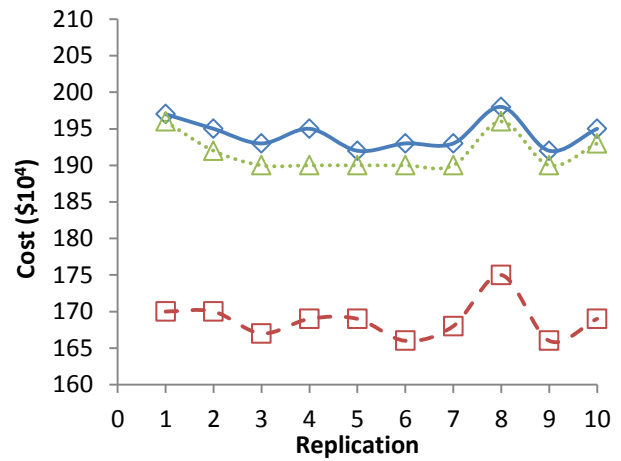
The statistical results of using the traditional method, CM, and CM_{ns} for 5 pairs are presented in Table 5-6. Using the CM and the CM_{ns} techniques has reduced the variance on average by 92% and 89%, respectively compared with the traditional method. In addition, the margin of error is reduced by 72% and 68%, respectively compared with the traditional method. The average induced correlation across the three solutions is 0.29 and 0.37, respectively. Figure 5-7 shows the correlation between the solutions using CM, CM_{ns}, and the traditional method. It can be noticed from Figure 5-7(a), (b), (c), and (d) that the outcome of each replication for the three solutions does not move in the same direction (i.e. synchronized) in all the pairs which results in low positive correlation. On the other hand, the traditional method does not have this synchronization as shown in Figure 5-7(e) and (f). To achieve similar margins of error to CM and CM_{ns}, the traditional method should perform on average 78 and 57 replications, respectively. From these results, it can be concluded that the CM and CM_{ns} achieved the desirable variance reduction.

Table 5-4 Case Study A: Pilot Study Statistical Results of Using Traditional Method, and CRN and CRN_{ns} Techniques

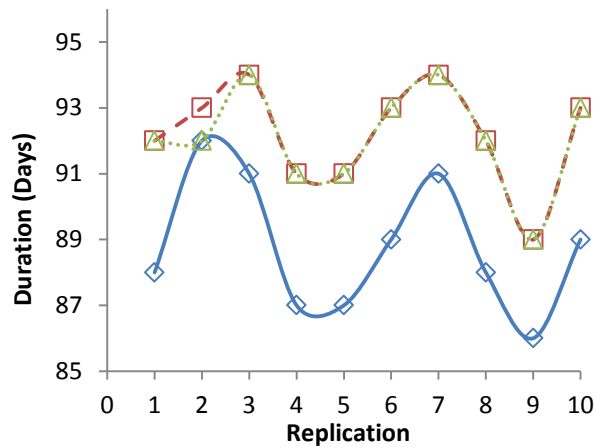
	Traditional						CRN							CRN _{ns}						
	Sol 9-10		Sol 9-11		Sol 10-11		Sol 9-10		Sol 9-11		Sol 10-11		Avg.	Sol 9-10		Sol 9-11		Sol 10-11		Avg.
	Dur. (days)	Cost (\$10 ⁴)	Dur. (days)	Cost (\$10 ⁴)	Dur. (days)	Cost (\$10 ⁴)	Dur. (days)	Cost (\$10 ⁴)	Dur. (days)	Cost (\$10 ⁴)	Dur. (days)	Cost (\$10 ⁴)		Dur. (days)	Cost (\$10 ⁴)	Dur. (days)	Cost (\$10 ⁴)	Dur. (days)	Cost (\$10 ⁴)	
$S_p^2(10)$	4.32	10.84	6.10	6.32	2.44	4.68	0.40	2.04	0.71	1.16	0.18	2.84		0.93	5.21	1.57	1.88	0.10	3.33	
$\Delta S_p^2(10)$							91%	81%	88%	82%	93%	39%	79%	78%	52%	74%	70%	96%	29%	67%
$ME(90\%)$	1.08	1.71	1.28	1.31	0.81	1.12	0.33	0.74	0.44	0.56	0.22	0.88		0.50	1.19	0.65	0.71	0.16	0.95	
ΔME							70%	57%	66%	57%	73%	22%	57%	54%	31%	49%	46%	80%	16%	46%
$\rho(X_{1n}, X_{2n})$	0.20	-0.39	0.15	0.08	0.64	0.42	0.93	0.84	0.87	0.91	0.96	0.78	0.88	0.88	0.31	0.78	0.78	0.98	0.62	0.72
N_{ME}							108	53	86	55	138	16	76	46	21	39	34	244	14	66



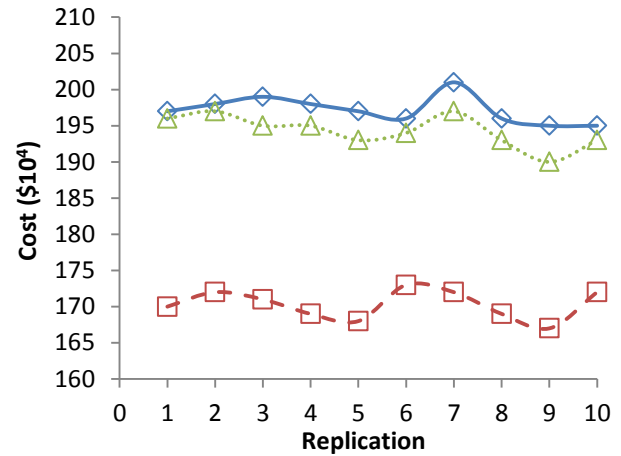
(a) Project Duration Using CRN



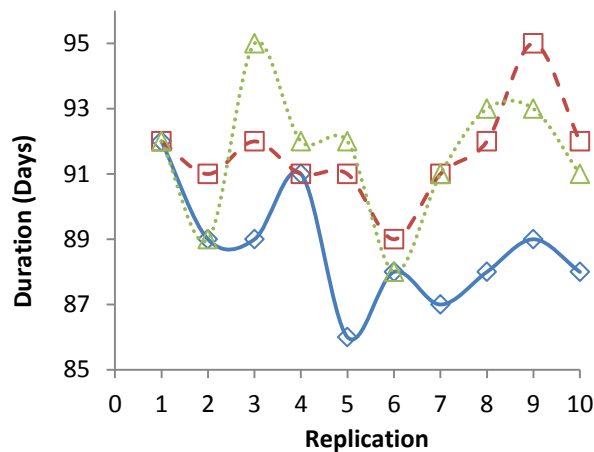
(b) Project Cost Using CRN



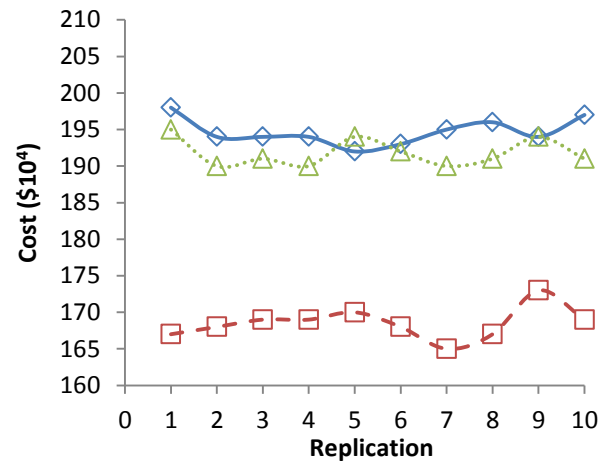
(c) Project Duration Using CRN_{ns}



(d) Project Cost Using CRN_{ns}



(e) Project Duration Using Traditional Method



(f) Project Cost Using Traditional Method

Figure 5-5 Case Study A: Correlation between Pilot Study Solutions (Project Duration and cost) Using CRN and CRN_{ns} Techniques, and Traditional Method

The problem of stochastic dominance, which was highlighted in *Section 4.9*, can be better understood and visualized by examining *Solution 10* and *11* in Figure 5-5(a), (b), (e), and (f). In Figure 5-5(b) and (f), *Solution 10* has a lower cost than *Solution 11* for all the replications. In other words, *Solution 10* always dominates *Solution 11*. On the other hand, in Figure 5-5(a) and (e), the two solutions overlap at different replications. From Figure 5-5(e), *Solution 10* has lower duration than *Solution 11* in 4 replications out of 10. In other words, there is a 40% probability of eliminating *Solution 11* from the set of optimum solutions because in 40% of the replication it is dominated by *Solution 10*. The same conclusion can be found by comparing Figure 5-7(a), (b), (e), and (f). By using CRN/CRN_{ns} and the CM/CM_{ns}, this probability is reduced to 0%. That is, *Solution 10* will not dominate *Solution 11* as a result to an error in estimating the solution mean duration which is caused by stochastic simulation.

CRN/CRN_{ns} and the CM/CM_{ns} techniques have increased the efficiency of the simulation by reducing the variance of the total project duration and cost of the three solutions. To this end, any of the four configurations (CRN, CRN_{ns}, CM, CM_{ns}) can be selected to be used in the optimization process. For the purpose of this example, the four configurations are used in the optimization to study their impact on the optimality of the optimum solutions.

5.6.1.2 Using the Selected VRTs in Simulation-based Optimization

The proposed method was used to optimize the bridge construction example presented in *Section 4.9*. Using the VRTs permitted the reduction of the number of simulation replications from 100 to 10 replications. At the end of the optimization each Pareto solution was run for 100 simulation replication to obtain accurate statistical information as mention in *Section 5.1*. Figure 5-8 shows the Pareto fronts of CRN/CRN_{ns}, CM/CM_{ns}, and the traditional method generated after evaluating 100,000 candidate solutions. Examining the Pareto fronts, it can be noticed that the four techniques and the traditional method were able to generate close Pareto fronts. Table 5-7 summarizes the results of this study. The first experiment, which was run for 100,000 candidate solutions, shows that the four techniques have higher hypervolume indicator than the traditional method with an average 18% improvement. This experiment was run on the same machine used in *Section 4.9*. It took 6.93 hours to finish the optimization using the traditional method as shown in Table 5-7. On the other hand, it took about 1 hour using the VRTs, which results in an average time saving of 81% over the traditional method.

Table 5-5 Case Study A: Pilot Study Statistical Results of Using Traditional Method, and AV and AV_{ns} Techniques

	Traditional						AV							AV _{ns}						
	Sol 9		Sol 10		Sol 11		Sol 9		Sol 10		Sol 13		Avg.	Sol 9		Sol 10		Sol 11		Avg.
	Dur. (days)	Cost (\$10 ⁴)	Dur. (days)	Cost (\$10 ⁴)	Dur. (days)	Cost (\$10 ⁴)	Dur. (days)	Cost (\$10 ⁴)	Dur. (days)	Cost (\$10 ⁴)	Dur. (days)	Cost (\$10 ⁴)		Dur. (days)	Cost (\$10 ⁴)	Dur. (days)	Cost (\$10 ⁴)	Dur. (days)	Cost (\$10 ⁴)	
$S_p^2(5)$	2.33	2.08	1.55	3.50	1.93	1.45	0.38	0.38	0.05	0.33	0.05	1.93		0.80	1.08	0.08	0.58	0.20	0.93	
$\Delta S_p^2(5)$							84%	82%	97%	91%	97%	-33%	70%	66%	48%	95%	84%	90%	36%	70%
$ME(90\%)$	1.12	1.06	0.92	1.38	1.02	0.89	0.45	0.45	0.16	0.42	0.16	1.02		0.66	0.76	0.20	0.56	0.33	0.71	
ΔME							60%	57%	82%	70%	84%	-15%	56%	41%	28%	78%	59%	68%	20%	49%
$\rho(X_{1p}, X_{2p})$	0.38	0.11	0.50	0.81	0.17	0.11	-0.86	-0.93	-1.00	-0.93	-0.96	-0.86	-0.92	-0.38	0.13	-0.93	-0.94	-0.95	-0.70	-0.63
N_{ME}							31	28	155	54	193	4	77	15	10	103	30	48	8	36

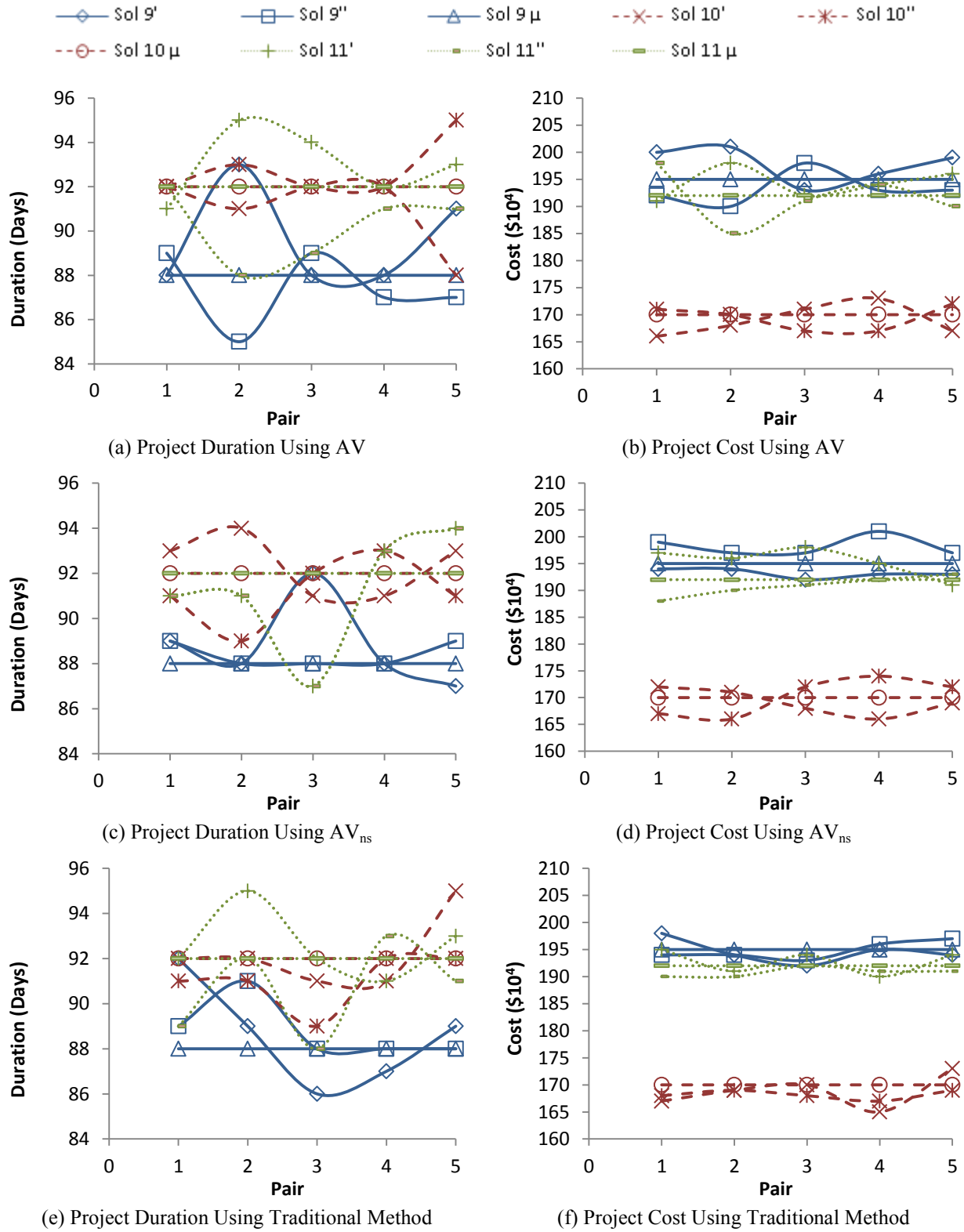
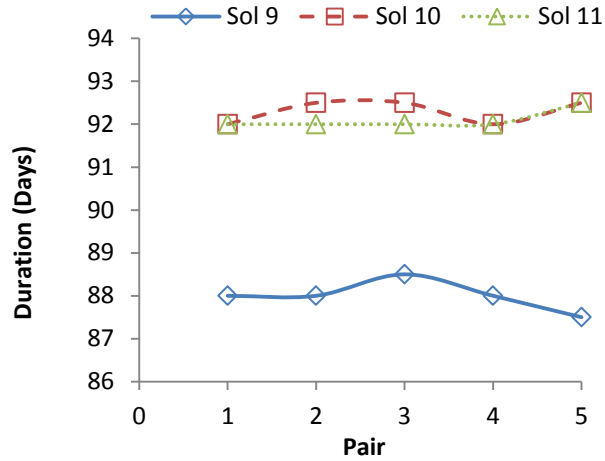


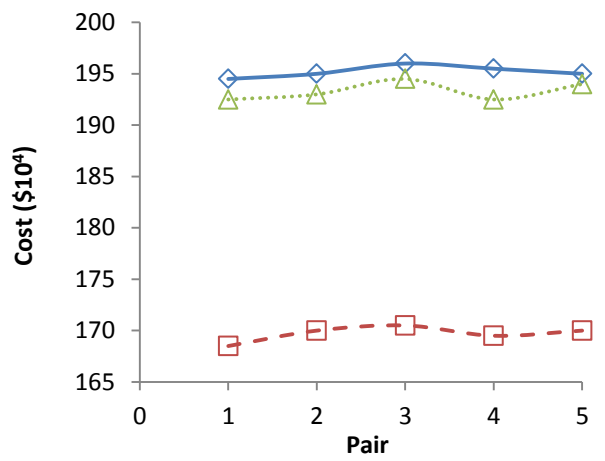
Figure 5-6 Case Study A: Correlation between Pilot Study Solutions (Project Duration and cost) Using AV and AV_{ns} Techniques, and Traditional Approach

Table 5-6 Case Study A: Pilot Study Statistical Results of Using Traditional Method, and CM and CM_{ns} Techniques

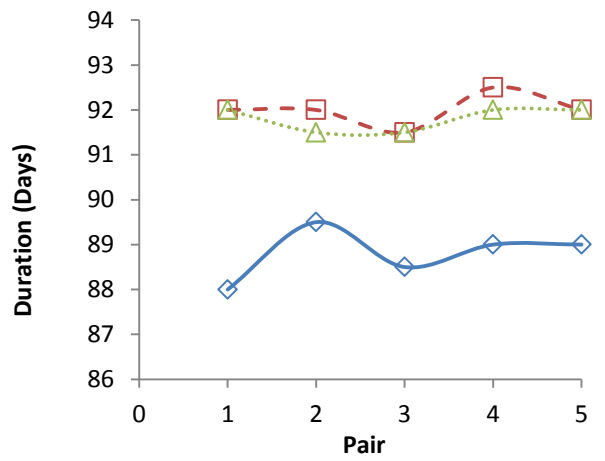
	Traditional						CM							CM _{ns}						
	Sol 9-10		Sol 9-11		Sol 10-11		Sol 9-10		Sol 9-11		Sol 10-11		Avg.	Sol 9-10		Sol 9-11		Sol 10-11		Avg.
	Dur. (days)	Cost (\$10 ⁴)	Dur. (days)	Cost (\$10 ⁴)	Dur. (days)	Cost (\$10 ⁴)	Dur. (days)	Cost (\$10 ⁴)	Dur. (days)	Cost (\$10 ⁴)	Dur. (days)	Cost (\$10 ⁴)		Dur. (days)	Cost (\$10 ⁴)	Dur. (days)	Cost (\$10 ⁴)	Dur. (days)	Cost (\$10 ⁴)	
$S_p^2(5)$	2.80	6.95	2.93	4.18	1.88	2.83	0.20	0.25	0.30	0.55	0.08	0.30		0.32	0.58	0.50	0.57	0.08	0.30	
$\Delta S_p^2(5)$							93%	96%	90%	87%	96%	89%	92%	88%	92%	83%	86%	96%	89%	89%
$ME(90\%)$	1.23	1.94	1.26	1.50	1.01	1.24	0.33	0.37	0.40	0.55	0.20	0.40		0.42	0.56	0.52	0.56	0.20	0.40	
ΔME							73%	81%	68%	64%	80%	67%	72%	66%	71%	59%	63%	80%	67%	68%
$\rho(X_{1p}, X_{2p})$	0.28	-0.26	0.31	-0.19	0.46	0.47	0.00	0.75	-0.79	0.58	0.41	0.80	0.29	0.31	0.55	-0.32	0.55	0.65	0.46	0.37
N_{ME}							70	139	49	38	125	47	78	43	60	29	36	125	47	57



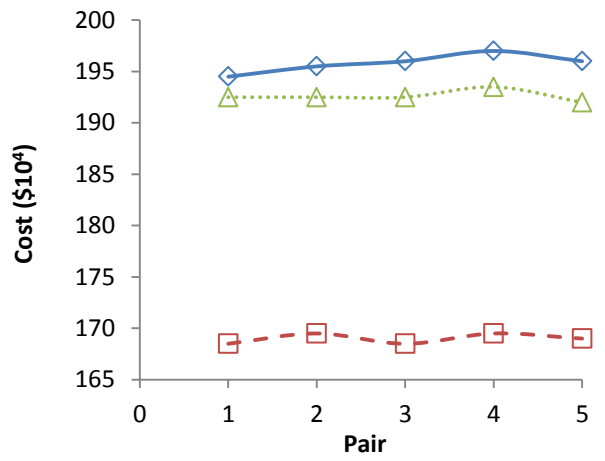
(a) Project Duration Using CM



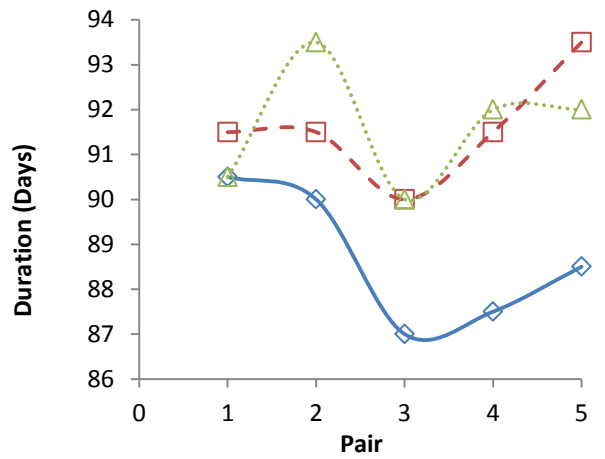
(b) Project Cost Using CM



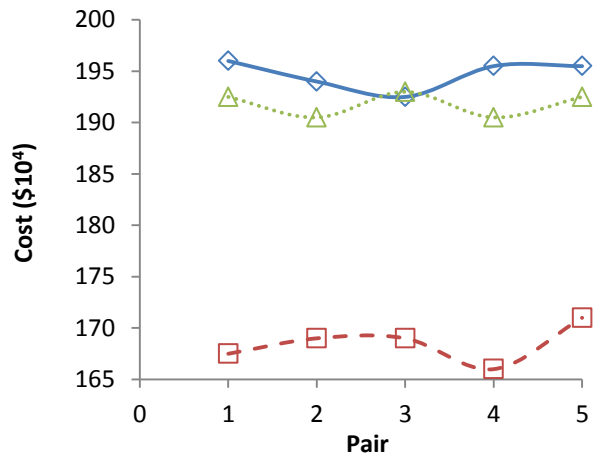
(c) Project Duration Using CM_{ns}



(d) Project Cost Using CM_{ns}



(e) Project Duration Using Traditional Method



(f) Project Cost Using Traditional Method

Figure 5-7 Case Study A: Correlation between Pilot Study Solutions (Project Duration and cost) Using CM and CM_{ns} Techniques, and Traditional Method

Table 5-7 Case Study A: Results of the Simulation-based Optimization Experiments

Method		N	p	$NOCS$	HV	ΔHV	CT (hours)	T_s
1 st Experiment	Traditional	100	N/A	100,000	7,597	N/A	6.93	N/A
	CRN	10	N/A	100,000	7,838	16%	1.37	80%
	CRN _{ns}	10	N/A	100,000	8,038	18%	1.27	82%
	CM	N/A	5	100,000	8,162	20%	1.33	81%
	CM _{ns}	N/A	5	100,000	7,943	17%	1.28	82%
2 nd Experiment	CRN	10	N/A	484,210	8,022	18%	6.93	0%
	CRN _{ns}	10	N/A	515,871	8,051	19%	6.93	0%
	CM	N/A	5	505,471	8,155	20%	6.93	0%
	CM _{ns}	N/A	5	531,571	8,037	18%	6.93	0%

$NOCS$ = Number of optimization candidate solutions; HV = Hypervolume indicator; CT = Computation time; N/A = Not applicable

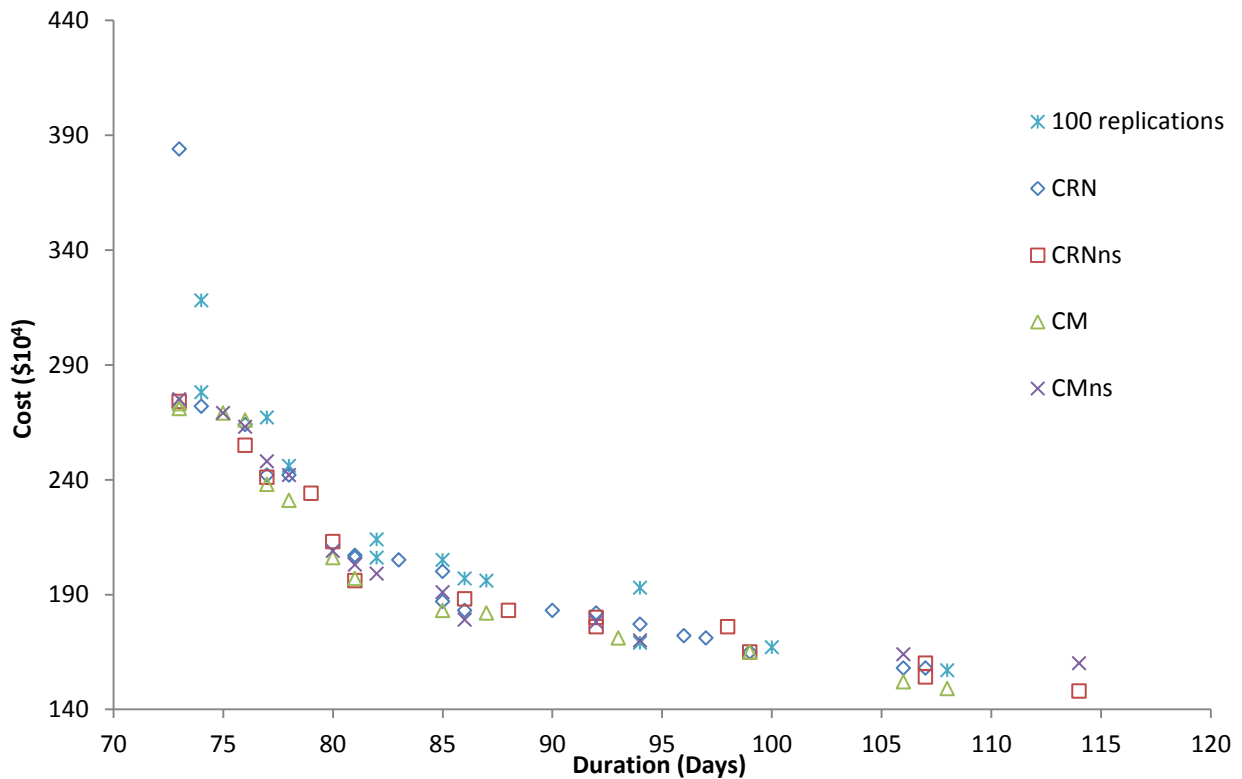


Figure 5-8 Case Study A: Pareto Fronts Generated After Evaluating 100,000 Candidate Solutions

Figure 5-9 shows the Pareto fronts of CRN/CRN_{ns}, CM/CM_{ns}, and the traditional method generated after 6.93 hours. The second experiment, which was run for the same duration it took the traditional method in the first experiment (i.e., 6.93 hours), shows that the four techniques evaluated four times more candidate solutions than the traditional method. In addition, the second experiment resulted in an average of 19% improvement in the hypervolume indicator over the traditional method.

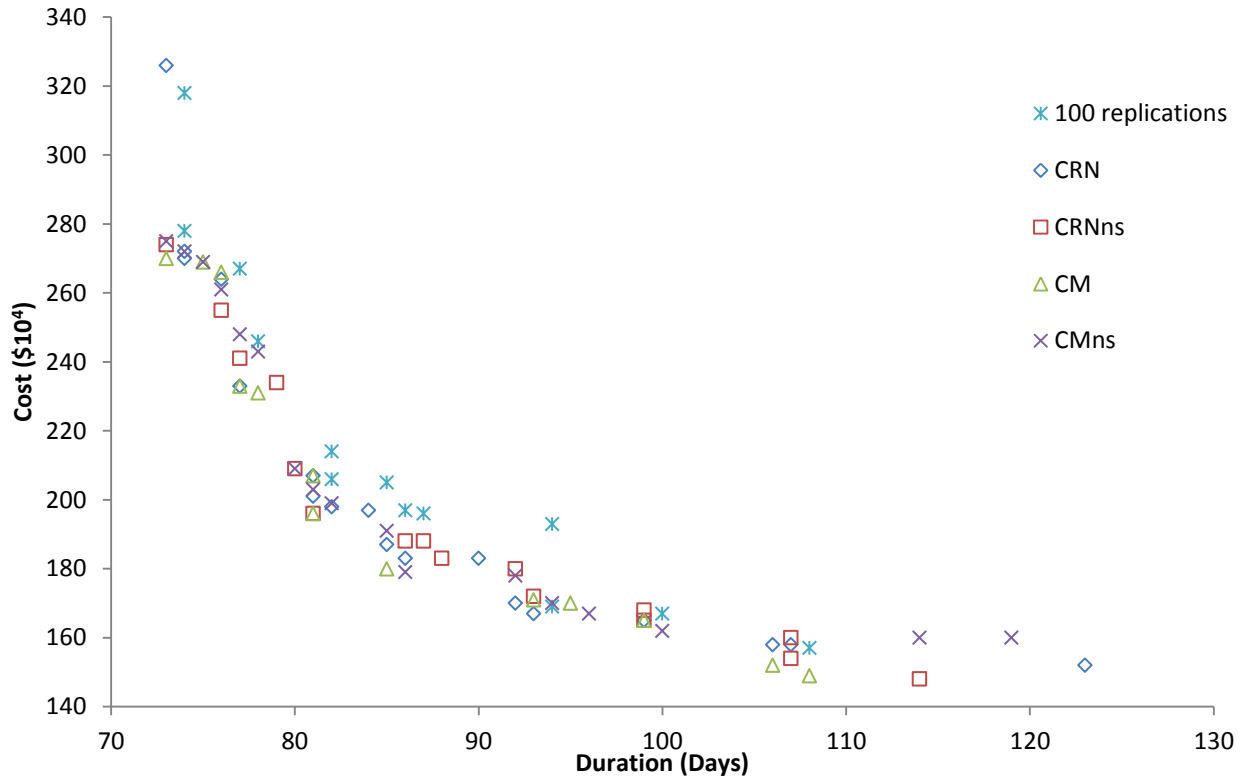


Figure 5-9 Case Study A: Pareto Fronts Generated after 6.93 Hours

5.6.2 Case Study B

5.6.2.1 Pilot Study to Compare VRTs

Similar to Case Study A above, the comparison was done over three candidate solutions with nine different configurations. The statistical results of traditional method, and CRN and CRN_{ns} techniques for 10 replications are presented in Table 5-8. It can be noticed that using the CRN and the CRN_{ns} has reduced the variance on average by 92% and 89%, respectively, compared with the traditional method. In addition, the margin of error is reduced on average by 73% and

70%, respectively, compared with the traditional method. The average induced correlations across the three candidate solutions are 0.97 and 0.98, respectively.

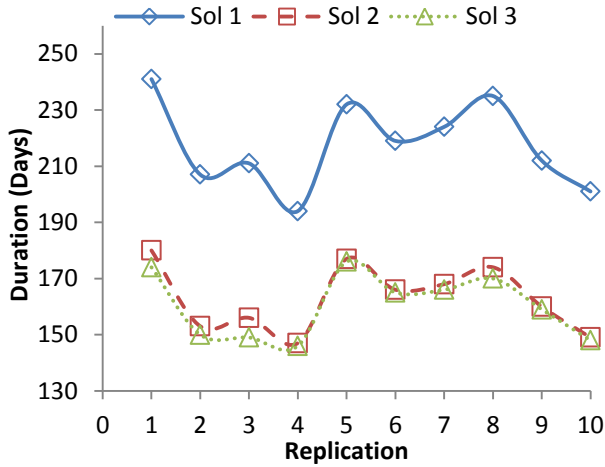
Figure 5-10 shows the correlation between the pilot study solutions using CRN, CRN_{ns} and traditional method. It can be noticed from Figure 5-10(a), (b), (c), and (d) that the outcome of each replication for the three solutions moves in the same direction (i.e. synchronized) which results in high positive correlation. On the other hand, the traditional method does not have this synchronization as shown in Figure 5-10(e) and (f). To achieve similar margins of error to CRN and CRN_{ns}, the traditional method should perform on average 220 and 202 replications, respectively. From these results, it can be concluded that the use of CRN and CRN_{ns} achieved the desirable variance reduction.

Table 5-9 presents the statistical results of using traditional method, and AV and AV_{ns} techniques for 5 pairs of the candidate solutions (i.e., 10 replications). From these results, it can be noticed that using the AV and the AV_{ns} failed in inducing a negative correlation between the replications in a pair for the candidate solutions 1 and 2. Figure 5-11 shows the correlation between the solutions using AV and AV_{ns}, and the traditional method. The ideal condition for the AV technique to work effectively would be when the replications in a pair are at an equal distance from the mean in opposite directions. This can be noticed in Figure 5-11(c) and (d) for solution 2 and that is why this solution has a high negative correlation (i.e., -0.92 for project duration and -0.83 for project cost).

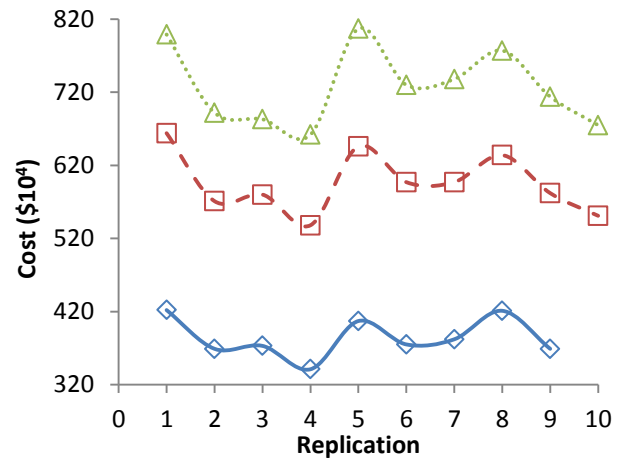
The statistical results of using the traditional method, and CM and CM_{ns} techniques for 5 pairs are presented in Table 5-10. Using the CM and the CM_{ns} techniques has reduced the variance on average by 92% and 93%, respectively compared with the traditional method. In addition, the margin of error is reduced by 74% and 77%, respectively compared with the traditional method. The average induced correlation across the three candidate solutions is 0.97 and 0.98, respectively. Figure 5-12 shows the correlation between the solutions using CM, CM_{ns}, and the traditional method.

Table 5-8 Case Study B: Pilot Study Statistical Results of Using Traditional Method, and CRN and CRNns Techniques

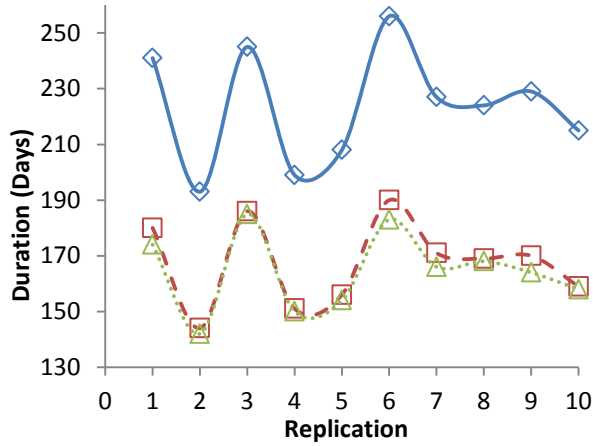
	Traditional						CRN							CRN _{ns}						
	Sol 1-2		Sol 1-3		Sol 2-3		Sol 1-2		Sol 1-3		Sol 2-3		Avg.	Sol 1-2		Sol 1-3		Sol 2-3		Avg.
	Dur. (days)	Cost (\$10 ⁴)	Dur. (days)	Cost (\$10 ⁴)	Dur. (days)	Cost (\$10 ⁴)	Dur. (days)	Cost (\$10 ⁴)	Dur. (days)	Cost (\$10 ⁴)	Dur. (days)	Cost (\$10 ⁴)		Dur. (days)	Cost (\$10 ⁴)	Dur. (days)	Cost (\$10 ⁴)	Dur. (days)	Cost (\$10 ⁴)	
$S_p^2(10)$	294	1929	505	4662	347	4588	17	253	34	809	5	238		30	416	55	729	6	130	
$\Delta S_p^2(10)$							94%	87%	93%	83%	99%	95%	92%	90%	78%	89%	84%	98%	97%	89%
$E(90\%)$	8.9	22.9	11.7	35.5	9.7	35.2	2.2	8.3	3.1	14.8	1.18	8.0		2.9	10.6	3.9	14.1	1.3	5.9	
ΔE							76%	64%	74%	58%	88%	77%	73%	68%	54%	67%	60%	87%	83%	70%
$\rho(X_{1p}, X_{2p})$	0.06	0.09	-0.77	-0.71	-0.20	-0.14	0.99	0.97	0.95	0.94	0.98	0.97	0.97	0.99	0.99	0.97	0.96	0.99	0.98	0.98
N_E							167	76	146	58	678	193	220	97	46	91	64	562	351	202



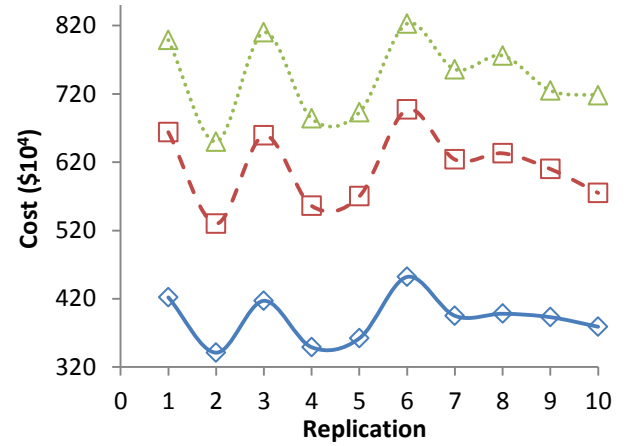
(a) Project Duration Using CRN



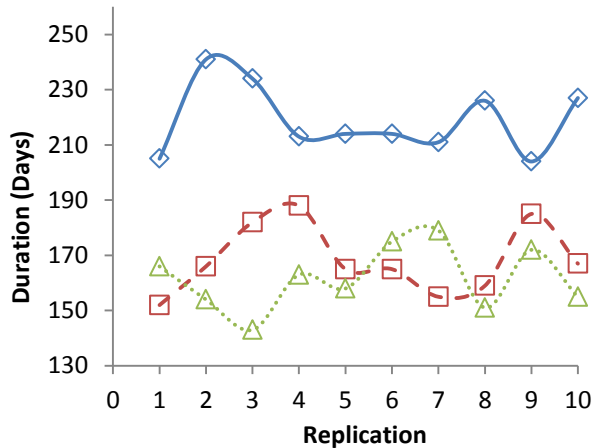
(b) Project Cost Using CRN



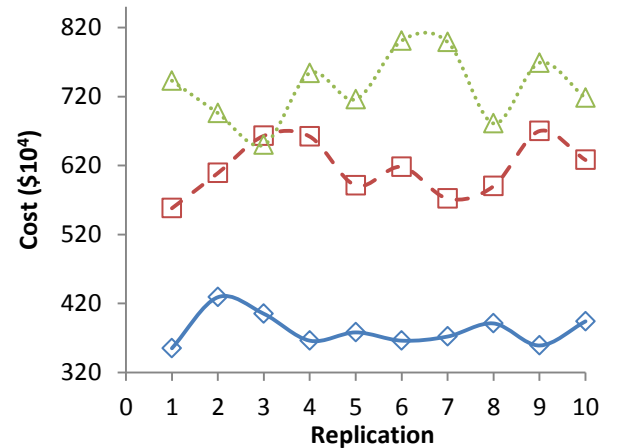
(c) Project Duration Using CRN_{ns}



(d) Project Cost Using CRN_{ns}



(e) Project Duration Using Traditional Method

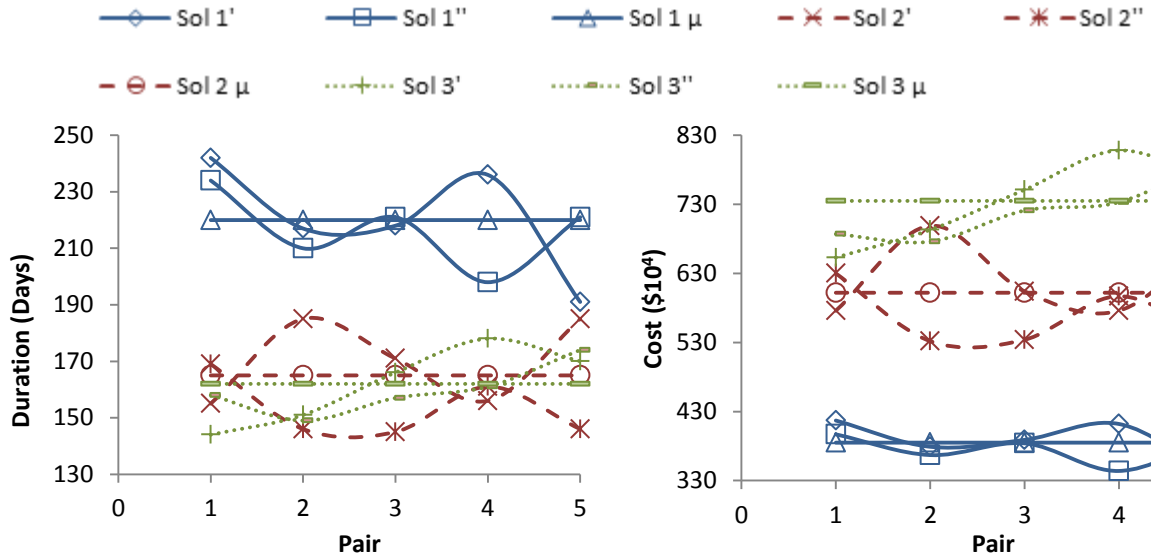


(f) Project Cost Using Traditional Method

Figure 5-10 Case Study B: Correlation between Pilot Study Solutions (Project Duration and cost) Using CRN and CRN_{ns} Techniques, and Traditional Method

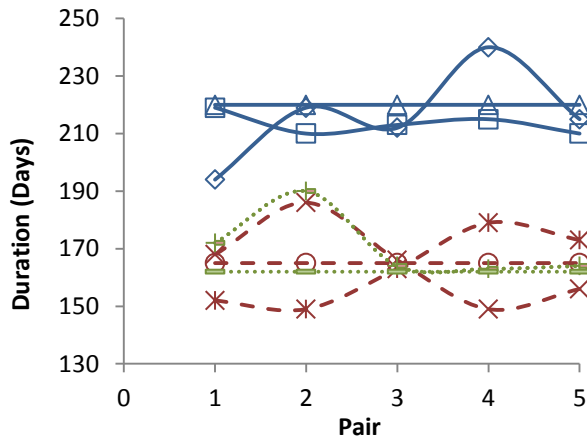
Table 5-9 Case Study B: Pilot Study Statistical Results of Using Traditional Method, and AV and AVns Techniques

	Traditional						AV							AV _{ns}						
	Sol 1		Sol 2		Sol 3		Sol 1		Sol 2		Sol 3		Avg.	Sol 1		Sol 2		Sol 3		Avg.
	Dur. (days)	Cost (\$10 ⁴)	Dur. (days)	Cost (\$10 ⁴)	Dur. (days)	Cost (\$10 ⁴)	Dur. (days)	Cost (\$10 ⁴)	Dur. (days)	Cost (\$10 ⁴)	Dur. (days)	Cost (\$10 ⁴)		Dur. (days)	Cost (\$10 ⁴)	Dur. (days)	Cost (\$10 ⁴)	Dur. (days)	Cost (\$10 ⁴)	
$S_p^2(5)$	39	121	101	1307	53	1222	141	258	13	348	104	2432		60	250	7	226	47	1271	
$\Delta S_p^2(5)$							-259%	-113%	87%	73%	-96%	-99%	-68%	-53%	-106%	93%	83%	12%	-4%	4%
$E(90\%)$	4.6	8.1	7.4	26.6	5.3	25.7	8.7	11.8	2.7	13.7	7.5	36.3		5.7	11.6	2.0	11.1	5.0	26.2	
ΔE							-89%	-46%	64%	48%	-40%	-41%	-17%	-24%	-44%	73%	58%	6%	-2%	11%
$\rho(X_{1p}, X_{2p})$	-0.12	-0.18	0.33	0.31	0.08	0.01	-0.03	-0.32	-0.88	-0.77	0.54	0.66	-0.13	-0.36	0.47	-0.92	-0.83	0.01	0.20	-0.24
N_E							1	2	38	19	3	3	11	3	2	70	29	6	5	19

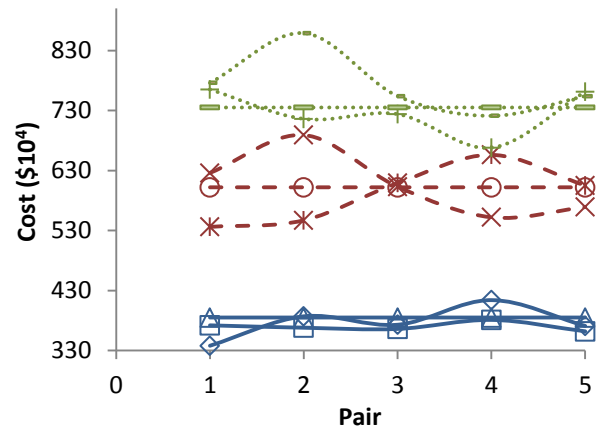


(a) Project Duration Using AV

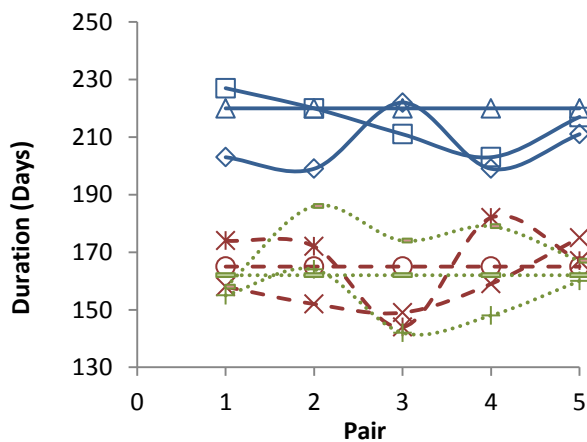
(b) Project Cost Using AV



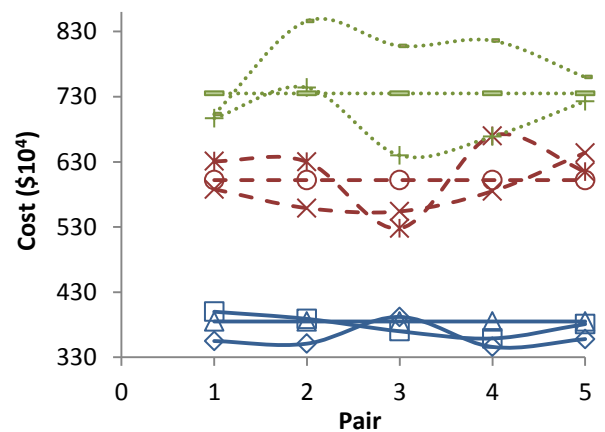
(c) Project Duration Using AV_{ns}



(d) Project Cost Using AV_{ns}



(e) Project Duration Using Traditional Method

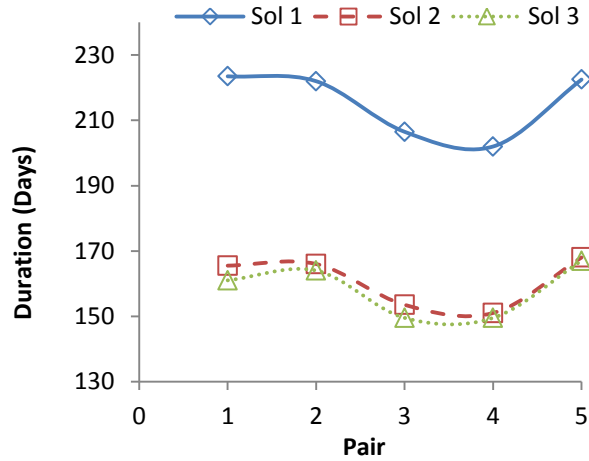


(f) Project Cost Using Traditional Method

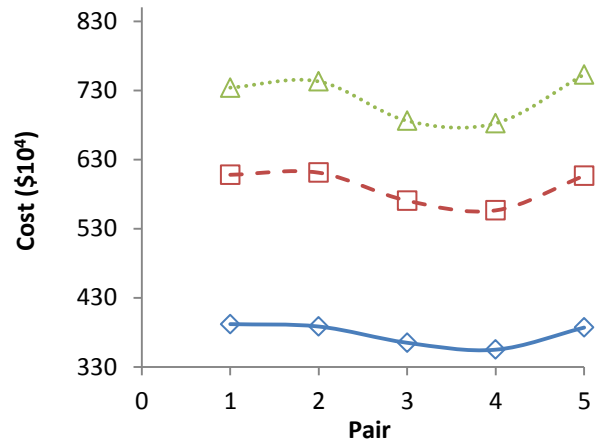
Figure 5-11 Case Study B: Correlation between Pilot Study Solutions (Project Duration and cost) Using AV and AV_{ns} Techniques, and Traditional Method

Table 5-10 Case Study B: Pilot Study Statistical Results of Using Traditional Method, and CM and CMns Techniques

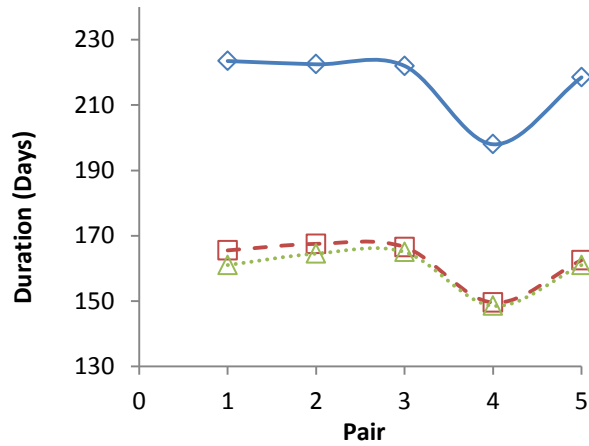
	Traditional						CM							CM _{ns}						
	Sol 1-2		Sol 1-3		Sol 2-3		Sol 1-2		Sol 1-3		Sol 2-3		Avg.	Sol 1-2		Sol 1-3		Sol 2-3		Avg.
	Dur. (days)	Cost (\$10 ⁴)	Dur. (days)	Cost (\$10 ⁴)	Dur. (days)	Cost (\$10 ⁴)	Dur. (days)	Cost (\$10 ⁴)	Dur. (days)	Cost (\$10 ⁴)	Dur. (days)	Cost (\$10 ⁴)		Dur. (days)	Cost (\$10 ⁴)	Dur. (days)	Cost (\$10 ⁴)	Dur. (days)	Cost (\$10 ⁴)	
$S_p^2(5)$	204	1965	130	1603	124	2342	7	83	13	346	2	129		13	86	22	153	2	23	
$\Delta S_p^2(5)$							96%	96%	90%	78%	98%	94%	92%	94%	96%	83%	90%	98%	99%	93%
$E(90\%)$	10.5	32.6	8.4	29.5	8.2	35.6	2.0	6.7	2.7	13.7	1.1	8.3		2.6	6.8	3.4	9.1	1.1	3.5	
ΔE							81%	80%	68%	54%	86%	77%	74%	75%	79%	59%	69%	87%	90%	77%
$\rho(X_{1p}, X_{2p})$	-0.51	-0.68	-0.41	-0.34	0.20	0.07	0.99	0.99	0.94	0.94	0.98	0.96	0.97	0.99	0.98	0.96	0.96	0.98	0.99	0.98
N_E							141	119	48	23	256	91	113	79	115	30	52	299	516	182



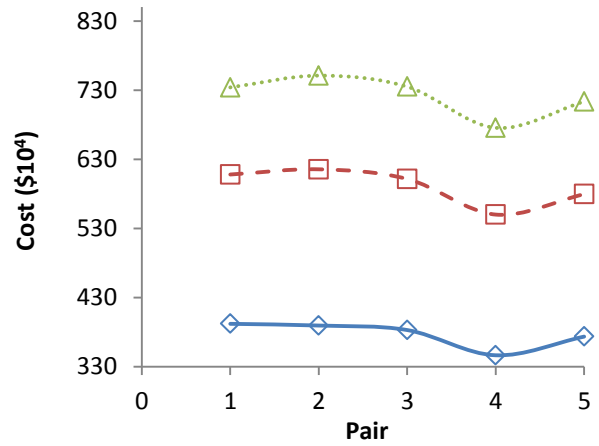
(a) Project Duration Using CM



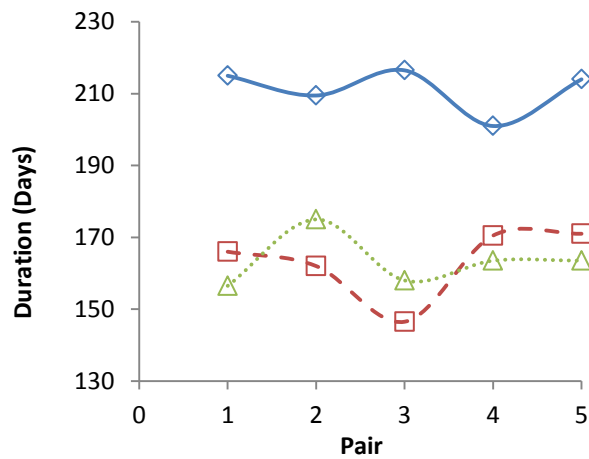
(b) Project Cost Using CM



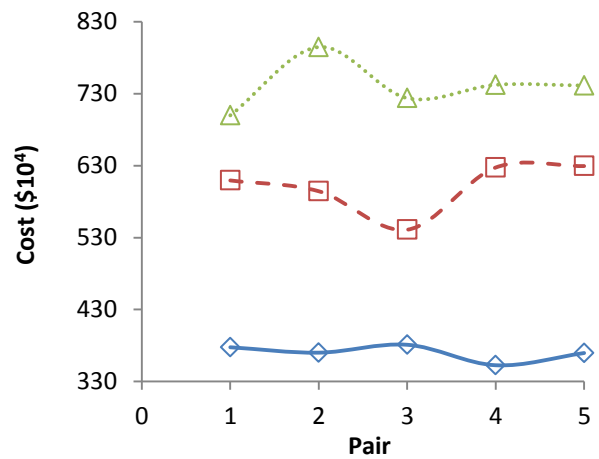
(c) Project Duration Using CM_{ns}



(d) Project Cost Using CM_{ns}



(e) Project Duration Using Traditional Method



(f) Project Cost Using Traditional Method

Figure 5-12 Case Study B: Correlation between Pilot Study Solutions (Project Duration and cost) Using CM and CM_{ns} Techniques, and Traditional Method

It can be noticed from Figure 5-12(a), (b), (c), and (d) that the outcome of each replication for the three solutions moves in the same direction (i.e. synchronized) which results in high positive correlation. On the other hand, the traditional method does not have this synchronization as shown in Figure 5-12(e) and (f). To achieve similar margins of error to CM and CM_{ns} , the traditional method should perform on average 113 and 182 replications, respectively. From these results, it can be concluded that the CM and CM_{ns} achieved the desirable variance reduction.

CRN/ CRN_{ns} and the CM/ CM_{ns} techniques have increased the efficiency of the simulation by reducing the variance of the total project duration and cost of the three candidate solutions. To this end, any of the four configurations (CRN, CRN_{ns} , CM, CM_{ns}) can be selected to be used in the optimization process. For the purpose of this paper, the four configurations are used in the optimization to study their impact on the quality of the optimum solutions.

5.6.2.2 Using the Selected VRTs in Simulation-based Optimization

The proposed method was used to optimize the bridge construction and was able to generate a set of optimal solutions where each solution represents a project setting. As in Case Study A, using the VRTs permitted the reduction of the number of the simulation replications from 100 to 10 replications per candidate solution. At the end of the optimization each Pareto solution was run for 100 simulation replication to obtain accurate statistical information as mention in *Section 5.1*. Figure 5-13 shows the Pareto front solutions that provided non-dominated tradeoff between minimizing the project duration and minimizing the project cost. Examining the Pareto fronts, it can be noticed that the four techniques and the traditional method were able to generate very close Pareto fronts. Table 5-11 summarizes the results of this study. The first experiment, which was run for 50,000 candidate solutions, shows that the four techniques have almost similar hypervolume indicator as the traditional method. This experiment was run on the same machine used in *Section 4.9*. It took 8.38 hours to finish the optimization using the traditional method as shown in Table 5-11. On the other hand, it took about 1 hour using the VRTs, which results in an average time saving of 87%. Figure 5-14 shows the Pareto fronts of CRN/ CRN_{ns} , CM/ CM_{ns} , and the traditional method generated after 8.38 hours. The second experiment, which was run for the same duration it took the traditional method in the first experiment (i.e., 8.38 hours), shows that the four techniques resulted in an average of 6% improvement in the hypervolume indicator over the traditional method.

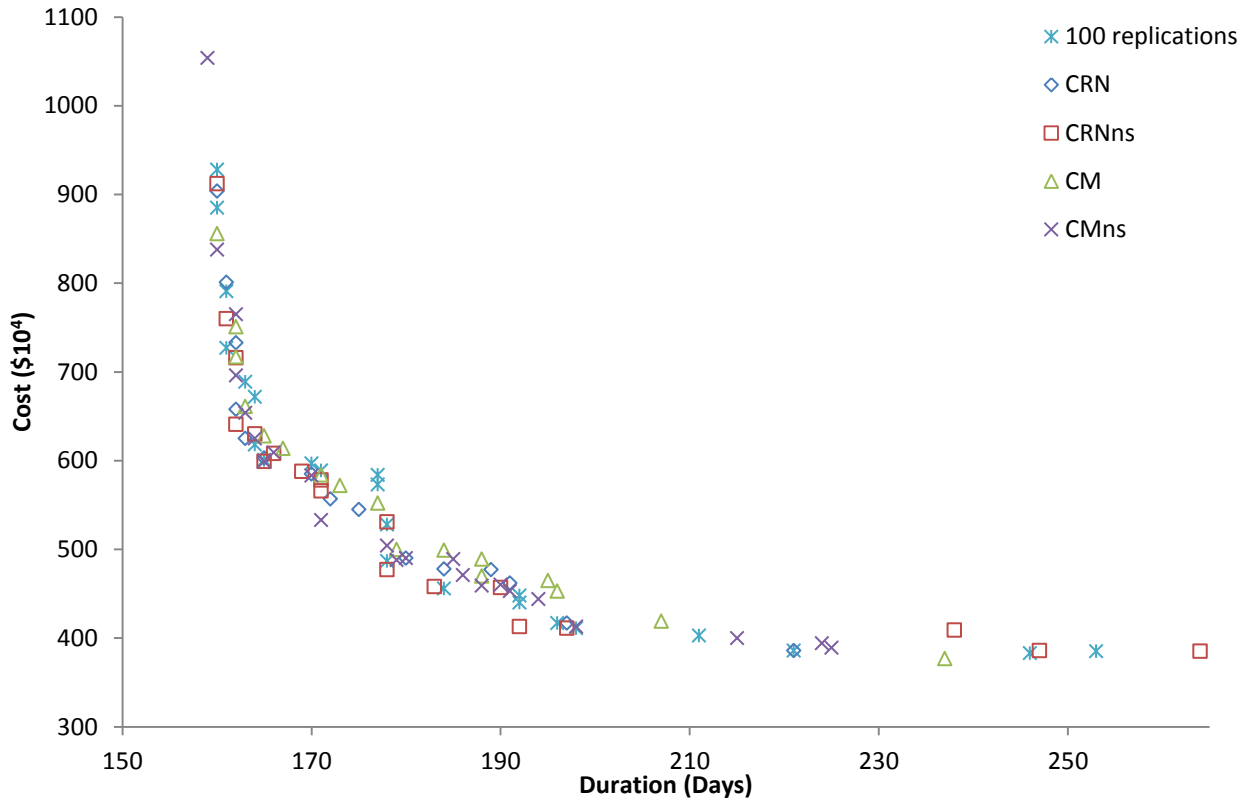


Figure 5-13 Case Study B: Pareto Fronts with the Tradeoff between Project Duration and Cost

Table 5-11 Case Study B: Results of the Simulation-based Optimization Experiments

	Method	N	p	$NOCS$	HV	ΔHV	CT (hours)	T_s
1 st Experiment	Traditional	100	N/A	50,000	55,031	N/A	8.38	N/A
	CRN	10	N/A	50,000	54,737	-1%	1.05	87%
	CRN _{ns}	10	N/A	50,000	54,764	-1%	1.07	87%
	CM	N/A	5	50,000	53,417	-3%	1.10	87%
	CM _{ns}	N/A	5	50,000	54,986	0%	1.04	87%
2 nd Experiment	CRN	10	N/A	352,057	57,929	5%	8.38	0%
	CRN _{ns}	10	N/A	358,008	58,407	6%	8.38	0%
	CM	N/A	5	364,108	58,095	5%	8.38	0%
	CM _{ns}	N/A	5	369,608	58,425	6%	8.38	0%

$NOCS$ = Number of optimization candidate solutions; HV = Hypervolume indicator; CT = Computation time; N/A = Not applicable

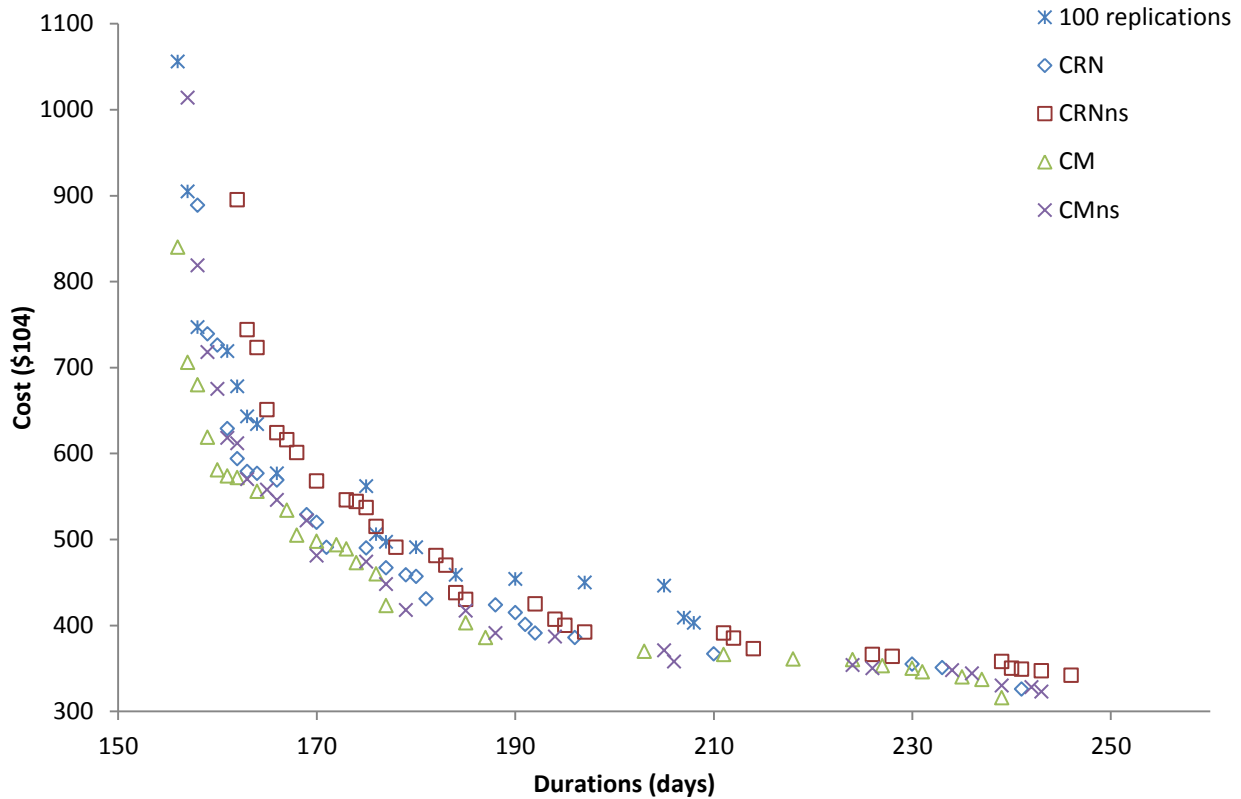


Figure 5-14 Case Study B: Pareto Fronts Generated after 8.38 Hours

5.7 Summary and Conclusions

This chapter presented a new method that incorporates VRTs into stochastic simulation-based multi-objective optimization. Although VRTs have been used in simulation studies in the past, they are used here in a novel way to improve the performance of the optimization process. The proposed method considered three VRTs, which are CRN, AV and the CM techniques. For each VRT, two approaches for managing the streams were explained, namely, the same streams and the new streams. This chapter: (1) identified and modeled the required synchronization; (2) formulated a method to compare the performance measure indices of the candidate solutions; (3) developed a method to compare and select the best VRT; (4) implemented the proposed method; and (5) demonstrated the effectiveness of the proposed method.

Using explicit averaging (traditional method) may not always solve the problem of stochastic dominance. As a result, inferior candidate solutions may be presented among the optimum solutions. In addition, the traditional method does not produce consistent optimum solutions

every time the optimization is run. Moreover, the traditional method requires a large computation effort to optimize multiple construction methods. To overcome these problems, VRTs are incorporated in the proposed stochastic simulation-based multi-objective model to examine their efficiency.

The proposed method allowed reducing the number of the simulation replications from 100 to 10 replications per candidate solution. At the end of the optimization each Pareto solution was run for 100 simulation replication to obtain accurate statistical information as mention in *Section 5.1*. The proposed method showed an average of 81% reduction in the computation time and an average of 18% improvement in the hypervolume indicator over the traditional method in Case Study A. On the other hand, in Case Study B, the method showed an 87% reduction in the computation time compared with the traditional method while maintaining a high quality of the optimal solutions. Using the time saved in Case Study B, an average of 6% improvement in the hypervolume indicator over the traditional method can be achieved. In both case studies, the CRN, CRN_{ns}, CM, and CM_{ns} techniques were founded to be effective in reducing the variance of the project duration and cost. Although AV did not show good results in the pilot studies, this should not necessarily be the case for other simulation models. In addition, AV would have similar time savings if it succeeds in inducing negative correlation between the replications in pairs. One limitation of the use of VRTs is that a pilot study is always required since there is no one VRT that is guaranteed to work for all simulation models.

CHAPTER 6: REDUCING THE COMPUTATION TIME TO SOLVE THE OPTIMIZATION PROBLEM USING PARALLEL COMPUTING ON A SINGLE MULTI-CORE PROCESSOR

6.1 Introduction

This chapter presents a method for implementing the simulation-based optimization model in a parallel computing environment on a single multi-core processor. The use of parallel computing is not new in simulation or optimization; however, it is interesting to study the behavior of running simulation-based optimization on a single system with multicore architecture. In addition, it is of interest to examine the impact of multithreading on the performance of simulation-based optimization. The use of stochastic discrete event simulation to evaluate the objective functions adds another dimension to the complexity of the optimization problem, and as a result, it increases the required computation time. The computation time, for a simple simulation mode, will increase almost in a linearly manner as the number of replications performed is increased as shown in Figure 6-1. Although the time is very small per solution, evaluating 100,000 solutions, which is usually a small fraction of the search space of an optimization problem, will take around 7 hours as was mentioned in *Section 4.9*. The main objective of this method is to reduce the computation time required by traditional simulation-based optimization models using the manager/worker paradigm, which was described in *Section 2.7.1*. The time saving achieved by this method can be used to increase the confidence in the optimality of the optimum solutions. This increase can be achieved by increasing the number of evaluated candidate solutions which results in covering a larger portion of the search space of the optimization problem. In addition, this is the first time, to the best knowledge of the author, that stochastic discrete event simulation-based optimization has been proposed using parallel computing on a single multi-core processor. The rest of this chapter: (1) describes the proposed method; (2) implements the method and demonstrates its effectiveness.

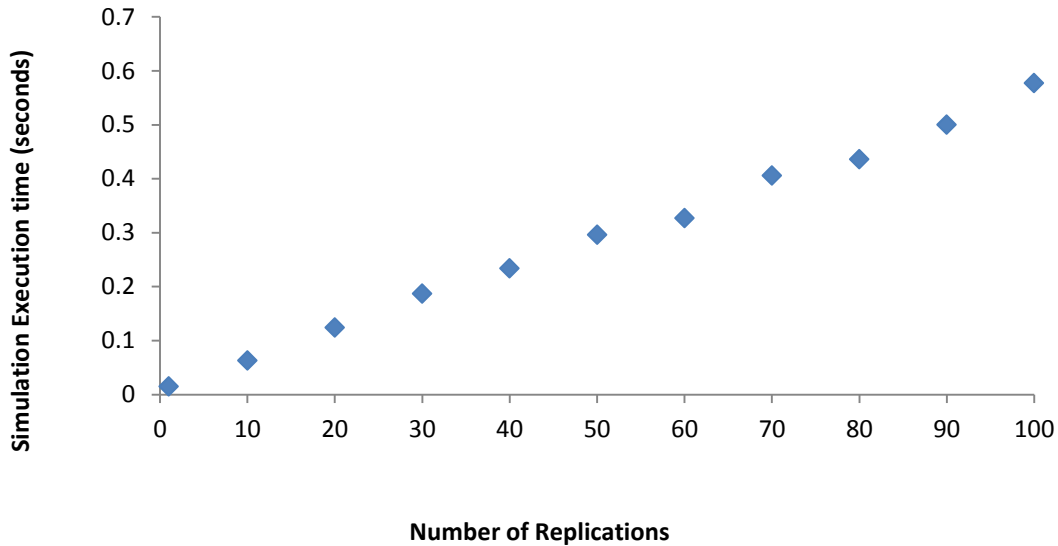


Figure 6-1 Simulation Execution Time Versus the Number of Replications

6.2 Proposed Method

The proposed parallel simulation-based optimization method (Figure 6-2) can be used by decision makers to improve the efficiency of the current practice of decision-making in construction projects. The process starts by generating an initial population of size E by the master core (core 1) as shown in line 2 in Figure 6-3. Then, the master core subdivides the population among the number of slave cores assigned to the optimization process as shown in lines 4 to 18 in Figure 6-3. Core 1 acts as a master during the generation and the fitness evaluation of the population. During the evaluation process, the master core could become a slave core if the optimization algorithm is set to perform the execution on: (1) one core, or (2) a number of cores that is larger than the total number of available cores. For example, in a computer with four cores, the master core will become a slave core if the optimization is set to perform the execution on 5 cores or higher. Each slave core, thereafter, evaluates the performance measure indices of the assigned candidate solutions using discrete event simulation. Once all the slaves evaluate all the generated candidate solutions, the master core evaluates the fitness of the population. If the termination criterion is met, the optimization process ends and the Pareto solutions are presented. Otherwise, the master core will sort the current population and generate a new population by performing cut-splice and mutation. The new population will go through the same steps again.

Two metrics are used to measure the performance of parallel computing. The speedup measures the amount of time saved by executing the program in parallel (Cantú-Paz 2000). It is calculated by dividing the required time to solve the optimization problem using sequential computing (traditional method) by the required time to solve the optimization problem using parallel computing as shown in Equation 6-1. The required time is measured from the beginning of the simulation-based optimization to its termination.

$$SU = \frac{T_{seq}}{T_{par}} \quad \text{Equation 6-1}$$

where,

SU = achieved speedup

T_{seq} = required time sequential computing

T_{par} = required time using parallel computing

The second metric considered is the efficiency of executing the program in parallel. In other words, it measures the portion of the processor power used to solve the optimization problem. The other portion of the processor power is typically consumed by synchronization and communication overhead (Fox et al. 1988). This metric is calculated by dividing the achieved speedup by the number of cores used as shown in Equation 6-2.

$$EF = \frac{SU}{NC} \quad \text{Equation 6-2}$$

Where,

EF = efficiency of executing the program in parallel

NC = number of cores used

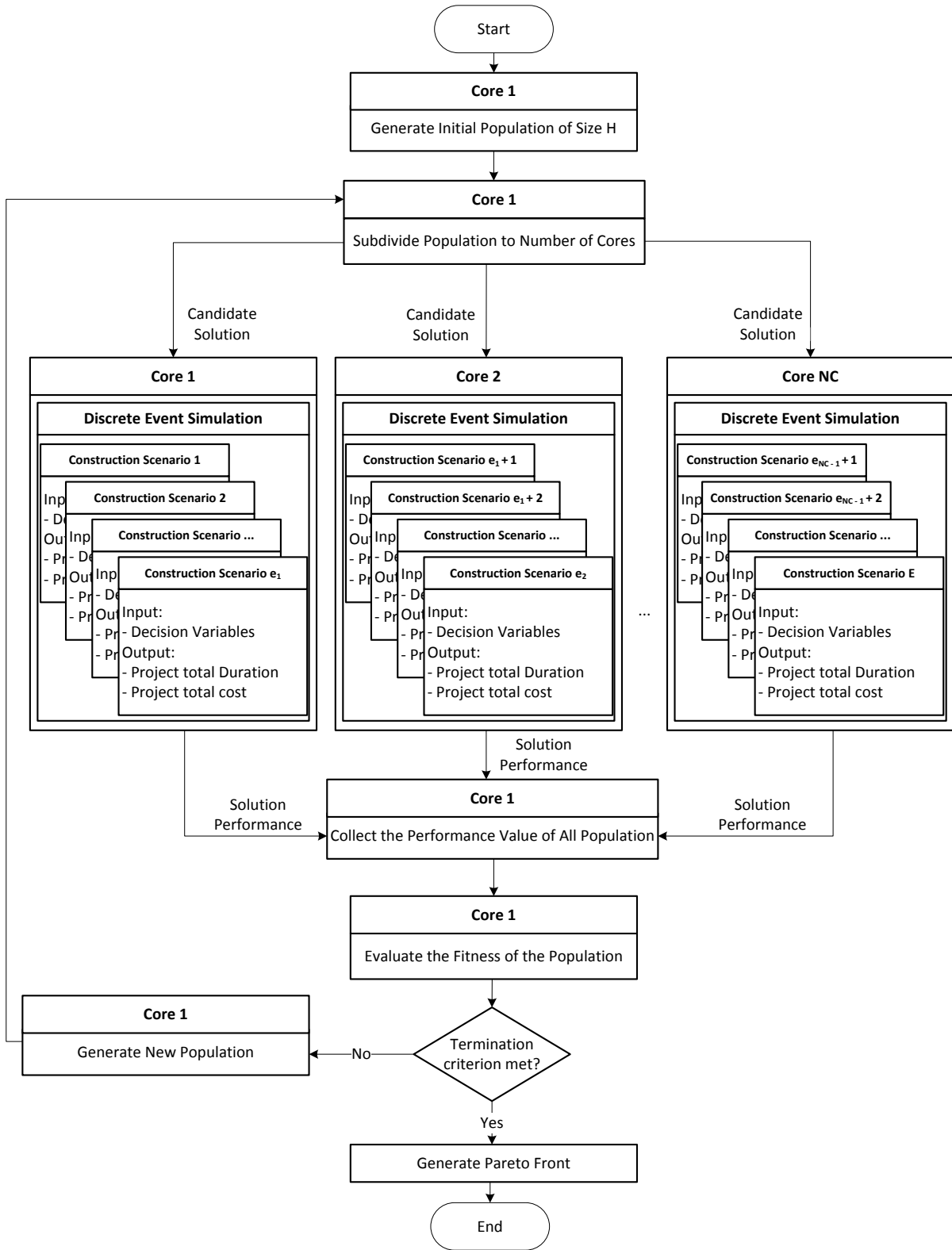


Figure 6-2 Parallel Simulation-based Optimization Method

```

1 // Repeat for all generations
2 FOR  $l = 1$  TO  $L$ 
3 // Repeat for all solutions in the population
4 FOR  $e = 1$  TO  $E$ 
5 IF rank = 1
6     Evaluate  $e$  using Core 1
7     RETURN  $\overline{D}_e$  and  $\overline{C}_e$ 
8 ELSE IF rank = 2
9     Evaluate  $e$  using Core 2
10    RETURN  $\overline{D}_e$  and  $\overline{C}_e$ 
11 ELSE IF rank = 3
12    Evaluate  $e$  using Core 3
13    RETURN  $\overline{D}_e$  and  $\overline{C}_e$ 
14 ELSE IF rank = 4
15    Evaluate  $e$  using Core 4
16    RETURN  $\overline{D}_e$  and  $\overline{C}_e$ 
17 END IF
18 END FOR
19 END FOR

```

Figure 6-3 Algorithm for Distributing the Population Among the Cores

6.3 Method Implementation

Darwin optimization framework, which is equipped with parallel computing capabilities, is used to implement the parallel computing of the proposed method. In order to enable the integration between the optimization framework and STROBOSCOPE, the latter is defined as an object as shown in Figure 6-4. In other words, STROBOSCOPE was embedded in Darwin optimization framework to evaluate each candidate solution generated by the optimization through simulation. The first two lines define STROBOSCOPE as an object called StropApp. The third line represents the name of the function which will be called to start STROBOSCOPE. Lines 4 and 6 to 8 will try to create an instance of STROBOSCOPE if it is not created yet. Since STROBOSCOPE was not designed to be executed in parallel on a multi-core single processor, several problems were encountered during the implementation. When the optimization framework is run in parallel, it creates multiple instances of the user defined objective function. The number of instances is equal to the number of cores. Since the objective functions defined in this research utilizes STROBOSCOPE, multiple instances of STROBOSCOPE are created at the

same time. Doing so will force STROBSCOPE to crash. In order to overcome this problem, two steps are necessary.

The first step is defining an object for each STROBOSCOPE's instance. For example if the number of the cores is four, four objects of STROBOSCOPE must be defined as shown in Figure 6-4. Each STROBOSCOPE instance has a unique object name. The second step is inserting a delay function between the creations of the instances. This is shown in line 5 of Figure 6-4. The gap between the creations is set to 3,500 milliseconds. This delay period was chosen by trial and error and it is the shortest possible delay period to avoid crashing.

```
1 public static object StroboApp;
2 public static System.Type objDocType;
3 static object GetStrobo() {
4     Try {if (StroboApp == null) {
5         Thread.Sleep(3500);
6         objDocType = System.Type.GetTypeFromProgID("Stroboscope.Document");
7         StroboApp = System.Activator.CreateInstance(objDocType);} }
8     catch (Exception ex) { MessageBox.Show("Program error: " + ex.Message, "Error1");
9         StroboApp = null;}
10 return StroboAp };
```

Figure 6-4 Defining STROBOSCOPE as an Object

To this point, the optimization framework will be able to create multiple instances of STROBOSCOPE without any problem. However, the candidate solutions will only be sent to the first instance since the optimization framework is unaware of other objects. Therefore, the second problem is the synchronization between the optimization framework and STROBOSCOPE. This synchronization is necessary to subdivide and distribute the population to the correct core. In order to overcome this problem, the candidate solutions must be directed to the correct core based on its rank as early described in Figure 6-3. This implementation is shown in Figure 6-5. Similar IF functions are defined for every STROBOSCOPE instance. Line 1 checks the rank of the candidate solution. For example, if the rank is equal to 1, then the optimization framework will call the STROBOSCOPE instance assigned to core 1. Line 2 will pass the decision variables to STROBOSCOPE and return the values of the objective functions.

So far, the parallel computing implementation works without any errors. For each candidate solution, a new STROBOSCOPE instance will be created and the simulation model will run for

that candidate solution. At end of end of the simulation, that STROBOSCOPE instance will be terminated. The process of creating and terminating each STROBOSCOPE instance takes around 4 seconds. By doing so, the simulation-based optimization would take 111 hours just to create and terminate a STROBOSCOPE instance for each of the 100,000 candidate solutions that were evaluated in *Section 4.9*. STROBOSCOPE allows running multiple simulation models in each instance. By taking advantage of that, there is no need to create STROBOSCOPE instance for each candidate solution. A number of STROBOSCOPE instances equal to the number of cores used for the parallel computing are created at the beginning of the optimization process. Each STROBOSCOPE instance is only created once and all the corresponding candidate solutions are evaluated in those instances. This is done by creating a new simulation model for each candidate solution within a STROBOSCOPE instance. Running too many models in one instance will slow down the speed of the simulation and will leads to it crash. STROBOSCOPE will crash approximately after running 1,600 simulation models. In addition, the simulation will start to slow down dramatically after running 200 simulation models. To overcome this problem, each STROBOSCOPE instance will close all the simulation models when they reach 200 models. This implementation is shown in lines 3 to 7 in Figure 6-5. In addition, a delay function of 900 milliseconds is inserted before closing the models to prevent STROBOSCOPE from crashing.

```
1 if(rank == 1) {
2   total = temp.testStroboRun(x1, x2, x3, x4, x5, x6, x7, x8, x9, x10, x11, x12, x13);
3   i = i + 1;
4   if(i == 200) {
5     Thread.Sleep(900);
6     strob.objDocType.InvokeMember("CloseAllOutputs");
7     i = 0;}}
```

Figure 6-5 Directing the Candidate Solutions Towards their Corresponding Core

6.4 Case Studies

To demonstrate the effectiveness of the proposed method, three case studies are considered. Case Study A compares the performance metrics of executing the simulation-based optimization model across three desktop computers. Case Study B compares the performance metrics of executing the model using CRN technique and the traditional method. Case Study C compares

the performance metrics of the used tools with another tool across a desktop computer, a server, and a cluster.

6.4.1 Case Study A

In this case study, the performance metrics of the simulation-based optimization using stochastic simulation is compared across three different desktop computers. The three computers are equipped with Intel Core i7, 3.4 GHz Quad-core processor. Each of these computers is equipped with different RAM size. Computers 1, 2, and 3 have a RAM of 8 GB, 12GB, and 16GB, respectively. The architecture of this processor is shown in Figure 6-6. The processor has four physical cores where each physical core has two hardware threads. These hardware threads are also called logical cores. Each physical core can run execute two threads at the same time, which is known as simultaneous multithreading (Hillar, 2010).

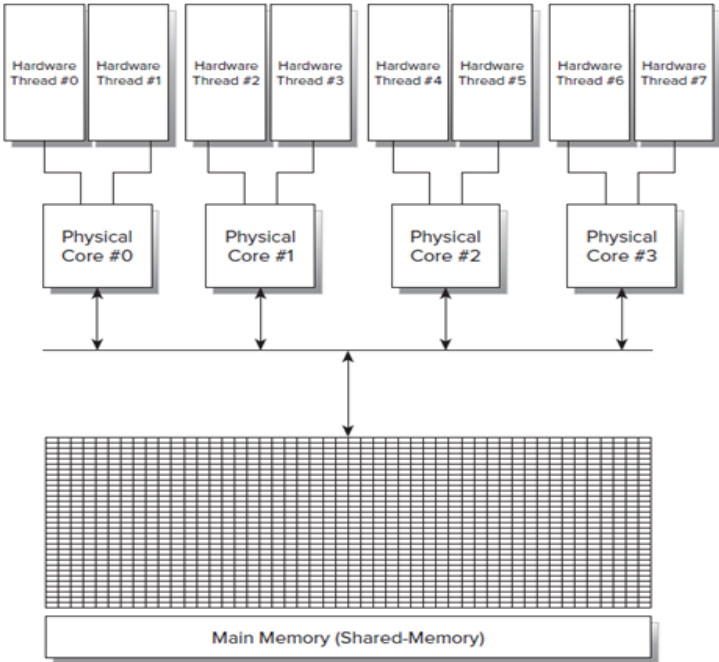


Figure 6-6 Architecture of Intel i7 Quad-core Processor (Hillar, 2010)

The case study consists of constructing a precast full span box girder bridge using launching gantry method. The bridge consists of 35 spans with identical spans of length 25 m. Table 4-2 shows the durations of the tasks used in this simulation model for this case study. The cost data used in the simulation model is presented in *Appendix B*.

The stochastic simulation-based multi-objective model was run for two eras, where each era has 500 generations and each generation has a population size of 100. The model was set to be executed with the number of cores from 1 to 9 cores (including the master). In the case of 9 cores, one of the cores will be used both as a master and a slave as explained in *Section 6.2*. This is done to study the impact of the simultaneous multithreading on the performance metrics of the proposed method. Figure 6-7 shows the required time to solve the optimization problem for this case study. Table 6-1 shows the achieved speedup, efficiency, and the time saving between the three computers. All the computers achieved the highest speedup when 4 cores are used. It can be noticed that the efficiency of the three computers are decreasing as the number of cores is increased. Among the three computers, Computer 3 has the highest speedup and the shortest time required. Using Computer 3 resulted in an average time saving of 24% and 22% over Computers 1 and 2, respectively. On the other hand, Computer 2 achieved an average saving of 3% over Computer 1.

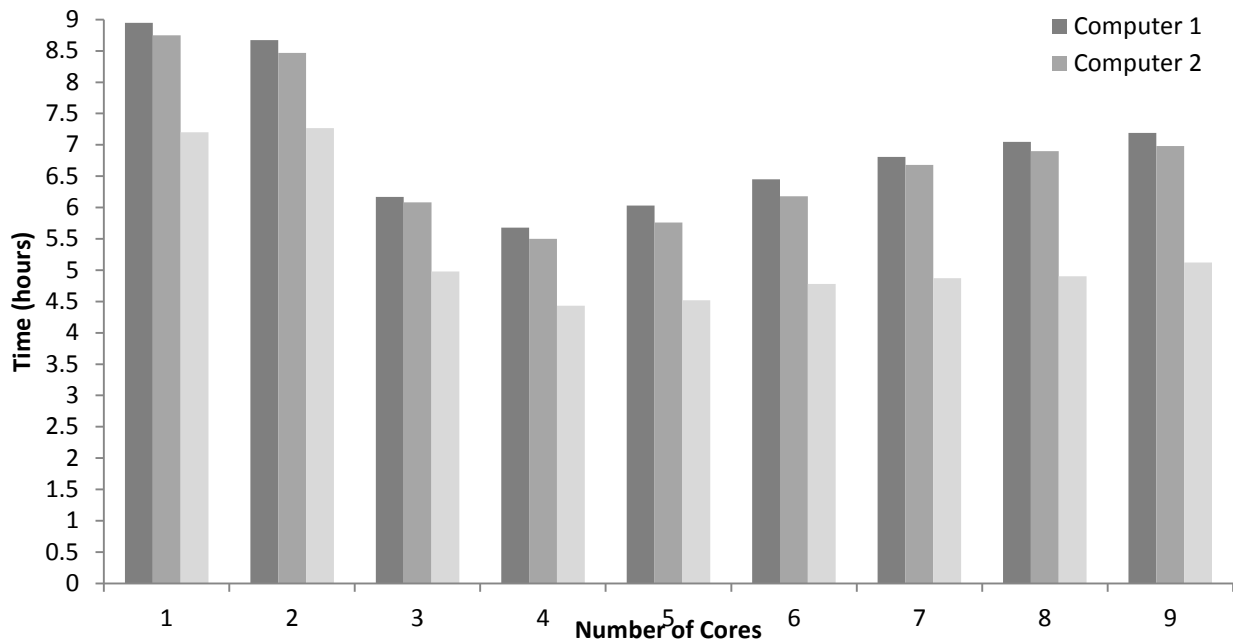


Figure 6-7 Required Time to Solve the Optimization Problem for Case Study A

Table 6-1 Achieved Speedup, Efficiency, and Time Saving for Case Study A

Core	T₁ (h)	T₂ (h)	T₃ (h)	SU₁	SU₂	SU₃	EF₁	EF₂	EF₃	T₁₋₂ (%)	T₁₋₃ (%)	T₂₋₃ (%)
1	8.95	8.75	7.2	1.00	1.00	1.00	1.00	1.00	1.00	2.23	19.55	17.71
2	8.67	8.47	7.27	1.03	1.03	0.99	0.52	0.52	0.50	2.31	16.15	14.17
3	6.17	6.08	4.98	1.45	1.44	1.45	0.48	0.48	0.48	1.46	19.29	18.09
4	5.68	5.5	4.43	1.58	1.59	1.63	0.39	0.40	0.41	3.17	22.01	19.45
5	6.03	5.76	4.52	1.48	1.52	1.59	0.30	0.30	0.32	4.48	25.04	21.53
6	6.45	6.18	4.78	1.39	1.42	1.51	0.23	0.24	0.25	4.19	25.89	22.65
7	6.81	6.68	4.87	1.31	1.31	1.48	0.19	0.19	0.21	1.91	28.49	27.10
8	7.05	6.9	4.9	1.27	1.27	1.47	0.16	0.16	0.18	2.13	30.50	28.99
9	7.19	6.98	5.12	1.24	1.25	1.41	0.14	0.14	0.16	2.92	28.79	26.65

6.4.2 Case Study B

In this case study, the performances metrics of the stochastic simulation-based optimization using CRN and the traditional method are compared. The case study consists of constructing a precast full span box girder bridge using launching gantry method. The bridge consists of 35 spans with identical spans of length 25 m. Table 4-2 shows the durations of the tasks used in this simulation model for this case study. The cost data used in the simulation model is presented in *Appendix B*. The traditional method consists of 100 replications while the CRN technique consists of 10 replications. Similar to Case Study A, The model was set to be executed from 1 to 9 cores and was executed on Computer 3. The stochastic simulation-based multi-objective model was run for two eras, where each era has 500 generations and each generation has a population size of 100.

Figure 6-8 shows the required time to solve the optimization problem for this case study. Table 6-2 shows the achieved speedup, efficiency, and the time saving between the two techniques. Based on these results, the proposed method achieved a maximum speedup of 2 and efficiency of 0.33 when using 6 logical cores for the CRN technique. On the other hand, it achieves a maximum speedup of 1.56 and efficiency of 0.39 when 4 logical cores are used for the traditional method. In addition, the proposed method combined with CRN achieved an average time saving of 83% over the traditional method combined with the proposed method. Moreover, the proposed method combined with CRN (when 6 cores are used) was able to achieve a time saving of 90% over the traditional method (when 1 core is used).

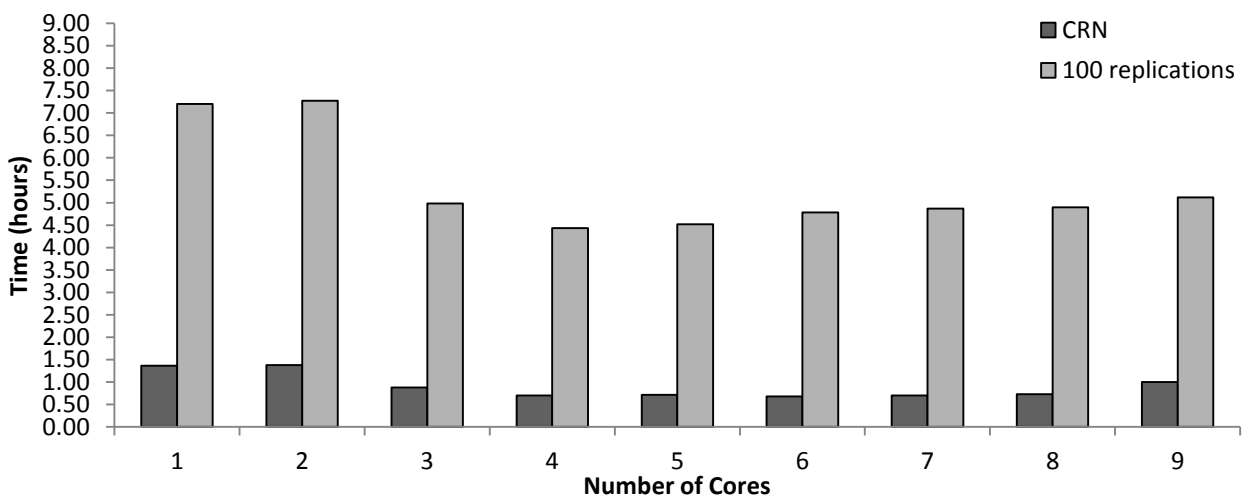


Figure 6-8 Required Time to Solve the Optimization Problem for Case Study B.

Table 6-2 Achieved Speedup, Efficiency, and Time Saving for Case Study B

Core	T_{CRN} (h)	T_T (h)	SU_{CRN}	EF_{CRN}	SU_T	EF_T	T_s (%)
1	1.37	7.2	1.00	1.00	1.00	1.00	81.02%
2	1.38	7.27	0.99	0.49	0.95	0.48	80.97
3	0.88	4.98	1.55	0.52	1.39	0.46	82.26
4	0.70	4.43	1.95	0.49	1.56	0.39	84.20
5	0.72	4.52	1.91	0.38	1.53	0.31	84.14
6	0.68	4.78	2.00	0.33	1.45	0.24	85.70
7	0.70	4.87	1.95	0.28	1.42	0.20	85.63
8	0.73	4.9	1.86	0.23	1.41	0.18	85.03
9	1.00	5.12	1.37	0.15	1.35	0.15	80.47

6.4.3 Case Study C

In this case study, the performance metrics of the tools (i.e., STROBOSCOPE and fmGA) used in this thesis to implement the simulation-based optimization model is compared with another tools that was used in another study to implement the same simulation-based optimization model. The other study done by Salimi (2014) used SimEvents (Mathworks Inc., 2013) module of MATLAB (Mathworks Inc., 2014). Non-dominated Sorting Genetic Algorithm II (NSGA-II) (Deb et al., 2002), which is part of the optimization toolbox within Matlab, was used to solve the optimization problem. Matlab allows a seamless integration between SimEvents and the optimization toolbox. In Salimi’s study, the simulation-based optimization model was executed on a server and a cluster.

The server consists of Intel Xeon E5540, 2.53 GHz triple-based processor with 48 GB RAM. Each processor has four physical cores and they support simultaneous multithreading. On the other hand, the cluster consists of Dual Intel Westmere EP Xeon X5650, 2.66 GHz processor. The cluster consists of 64 physical cores and it supports simultaneous multithreading. The details of the server and cluster study are available in the work of Salimi (2014). The server and cluster were run for 500 generations where each generation has a population of 200.

The simulation-based multi-objective model in this thesis was run for two eras, where each era has 500 generations and each generation has a population of the 100 using Computer 3. Both studies consist of constructing a precast full span box girder bridge using launching gantry method. The bridge consists of 500 spans with identical spans of length 25 m. Table A-1 shows

the durations of the tasks used in this simulation model for this case study. The cost data used in the simulation model is presented in *Appendix B*.

Table 6-3 shows the achieved speedup and efficiency of Computer 3 when deterministic simulation is used. The highest speedup of 2.29 is achieved when 6 and 7 cores are used. However, using 6 cores result in a higher efficiency than 7 cores. The server took 3.33 hours to complete the optimization while the cluster took 0.5 hour. The cluster was successful to reduce the computation time significantly; however, it required the use of 64 cores. The tools used in this thesis were able to outperform Matlab when run on a server and a cluster with a fraction of the number of cores. This is due to the fact that SimEvents reuiques much more time to perform the simulation than STROBOSCOPE.

Table 6-3 Achieved Speedup and Efficiency for Case Study C

	Number of Cores								
	1	2	3	4	5	6	7	8	9
Time (h)	0.65	0.67	0.40	0.37	0.30	0.28	0.28	0.32	0.32
SU	1.00	0.98	1.63	1.77	2.17	2.29	2.29	2.05	2.05
EF	1.00	0.49	0.54	0.44	0.43	0.38	0.33	0.26	0.23

6.5 Summary and Conclusions

This chapter presented a method for implementing the simulation-based optimization model in a parallel computing environment on a single multi-core processor. The method was implemented using the master/slave paradigm. This chapter: (1) described the proposed method; (2) implemented the method and demonstrated the effectiveness.

As demonstrated by the case studies in this chapter, the proposed method was able to achieve substantial time savings. When the proposed method is used by itself, it was able to save 38% of the time required to solve the optimization problem according to Case Study A. In addition, as demonstrated in Case Study B, combining the proposed method with CRN resulted in a time saving of 90%. Finally, Case Study C showed the benefit of using the tools proposed in this thesis over using MATLAB, which is a commercial and popular tool.

CHAPTER 7: JOINT PROBABILITY FOR EVALUATING THE DURATION AND COST OF STOCHASTIC SIMULATION MODELS

7.1 Introduction

This chapter presents a new joint probability method that is applied to sub-populations' Pareto fronts generated by the stochastic simulation-based multi-objective model presented in *Chapter 3*. The main objectives of this method are: (1) to reduce project risk; and (2) to provide the decision makers with more accurate and useful information to plan and manage their projects using joint probability. This method is capable of: (1) calculating the joint probability of the Pareto solutions; and (2) generating Pareto fronts representing a specific joint probability; (3) estimating the duration and cost joint contingency; and (4) generating a schedule to meet a specific joint probability. Applying this method is expected to have a noteworthy impact on reducing project risk and providing the decision makers with more accurate and useful information to plan and manage their projects. The rest of this chapter will: (1) describe the proposed method; (2) introduce a method to apply joint probability to Pareto solutions; (3) propose the concept of joint probabilistic Pareto fronts; (4) develop a method to analyze the selected solution; (5) implement the proposed method and demonstrate its effectiveness.

7.2 Proposed Method

Figure 7-1 shows the proposed method which consists of three main phases. The first phase applies the joint probability to the Pareto solutions obtained through the optimization. The second phase generates the probabilistic Pareto fronts. Finally, the third phase analyzes the solution selected by the decision maker. The proposed method is based on the frequency of an event happening after performing several repetitions of an experiment which is known as the relative frequency. The two most common outputs of the simulation in the field of construction management are the project duration and cost (Zhang et al. 2006; Hassan and Gruber 2008; Marzouk et al. 2009; Lee et al. 2010; Mawlana and Hammad 2013). Therefore, the rest of this chapter is focused on the project duration and cost.

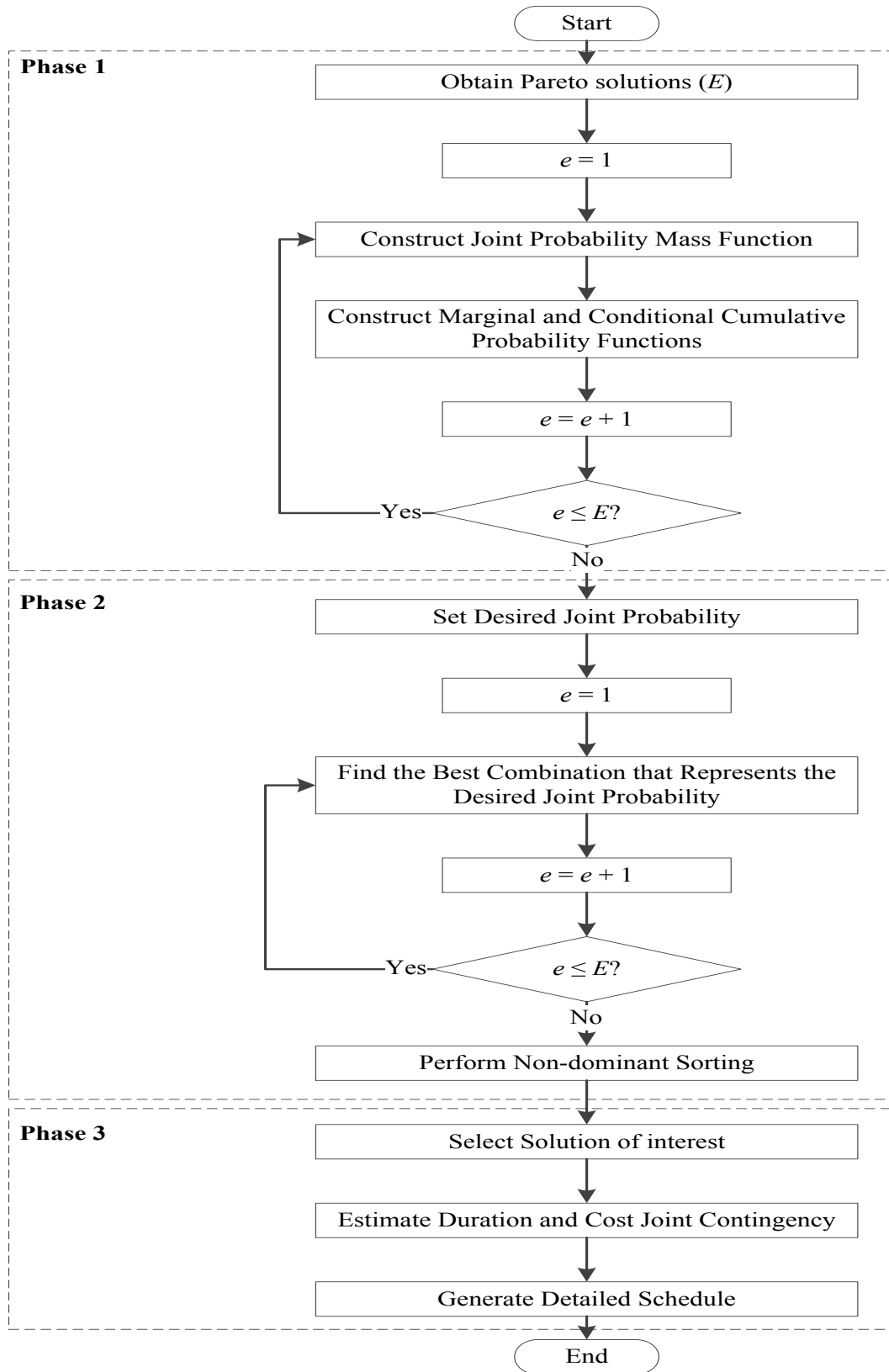


Figure 7-1 Proposed Method of Joint Probability

The advantages of using the proposed method are: (1) it gives a more accurate estimate and more detailed information of the project duration and cost representing a certain confidence level than the current state of art; (2) it is distribution-free because the outputs of the simulation replications are not fitted into a specific statistical distribution; (3) it estimates the project duration and cost joint contingency considering their correlation and impact on each other; and (4) it provides a method to trace the seed numbers resulting in the same project duration and cost.

Using the proposed method, one can answer the following questions: (1) What is the probability of having a project with a duration less than or equal to x and a cost less than or equal to y ? (2) What is the probability of having a project with duration of x or a cost of y ? (3) What are the possible project costs if the project duration is equal to x and vice versa? (4) What are the values the Pareto solutions representing a specified joint probability? (5) What are the time and cost contingencies representing a specific joint confidence level? and (6) What are the durations of the tasks representing a specified joint probability?

7.3 Applying Joint Probability to Pareto Solutions

The first phase starts by obtaining the set of Pareto solutions that are found using the simulation-based optimization model as described in *Chapter 3*. The information of interest at this phase is the values of the decision variables, which represent the construction scenario, for each Pareto solution. These decision variables are used to select the appropriate simulation template and modify the project settings. For each Pareto solution, a joint probability mass function, marginal cumulative probability function, and conditional cumulative probability function are constructed as explained in the sub-sections below.

7.3.1 Constructing Joint Probability Mass Function

Performing N replications of a stochastic simulation model results in N observed project durations and costs of the model. Each replication represents one potential outcome for the project duration and cost. These observations are the basis for constructing the joint probability mass function. A joint probability mass function associates a joint probability with each of the combinations of duration and cost along the duration and cost axes. This mass function can be represented as a joint frequency histogram or as a contingency table. Both representations follow the same steps to be constructed and they result in the same joint probability mass function. The

joint frequency histogram representation provides a better visualization of the mass function than the contingency table. On the other hand, the contingency table representation provides a faster and easier way to calculate the joint probability than the joint frequency histogram.

Figure 7-2 shows the flowchart of constructing the joint probability mass function. First, the observed project's duration and cost should be organized in class intervals. One way to think of class intervals is as the desired resolution of the joint probability distribution. For example, the project duration can be either expressed in days, weeks, months, or even years. That is, the width of the class interval of the project duration can be 1, 7, 30, or 365 days. On the other hand, the project cost can be expressed in hundreds, thousands, or millions of dollars. Different class intervals will result in different joint frequencies and different joint probabilities. Therefore, decision makers have to be very cautious when selecting the class intervals. Based on the selected resolution (width of class interval), Equation 7-1, Equation 7-2, and Equation 7-3 are used to calculate the lowest joint interval, the highest joint interval, and the number of intervals required to contain the observed project's duration and cost, respectively.

$$\text{Lowest Interval (Duration, Cost)} = \left(\left\lfloor \frac{D_{min}}{D_{Res}} \right\rfloor, \left\lfloor \frac{C_{min}}{C_{Res}} \right\rfloor \right) \quad \text{Equation 7-1}$$

$$\text{Highest Interval (Duration, Cost)} = \left(\left\lceil \frac{D_{max}}{D_{Res}} \right\rceil, \left\lceil \frac{C_{max}}{C_{Res}} \right\rceil \right) \quad \text{Equation 7-2}$$

$$\text{Number of Intervals (Duration, Cost)} = (D_{HC} - D_{LC} + 1, C_{HC} - C_{LC} + 1) \quad \text{Equation 7-3}$$

where,

- D_{min} = minimum observed project duration
- D_{max} = maximum observed project duration
- C_{min} = minimum observed project cost
- C_{max} = maximum observed project cost
- D_{res} = selected resolution for the project duration
- C_{res} = selected resolution for the project cost
- D_{HC} = highest duration interval
- D_{LC} = lowest duration interval
- C_{HC} = highest cost interval

C_{LC} = lowest cost interval

For example, if there are 500 observed project's duration and cost from the simulation model with $D_{min} = 65$ days, $D_{max} = 79$ days, $C_{min} = \$38,000$, $C_{max} = \$46,000$, $D_{res} = 1$ day and $C_{res} = \$1000$, then the *Lowest Interval* = (65, 38), the *Highest Interval* = (79, 46), and the *Number of Intervals* = (15, 9). Having this information, the headers of the contingency table are created. The intersection of each cost column and duration row represents one possible duration and cost combination. The maximum number of possible duration and cost combinations is simply the multiplication of the duration *Number of Intervals* (I) by the cost *Number of Intervals* (J). The number of observations reflects the frequency of each duration and cost combination. From the N observed project's durations and costs of the simulation model, the frequency of each combination is calculated using the *Frequency Function* in Figure 7-3. This figure shows the algorithms developed for applying the joint probability related functions and which will be explained throughout the rest of this section.

The calculated frequencies are arranged into the class intervals (d_i, c_j) in Table 7-1 using the *Contingency Table Function* in Figure 7-3. For example, the combination (71, 41) has a frequency of 60. The joint probability of having a project with duration equal to d_i and cost equal to c_j can be calculated using the intersection of two random variables as given by Equation 7-4.

$$\begin{aligned}
 P(D = d_i \cap C = c_j) &= P(D = d_i) \times P(C = c_j | D = d_i) \\
 &= \sum_{j=1}^J f(d_i, c_j) \times \frac{P[D = d_i, C = c_j]}{P[D = d_i]} \\
 &= \frac{\text{total number of replications where } D = d_i}{\text{total number of replications}} \\
 &\quad \times \frac{\text{total number of replications where } D = d_i \text{ and } C = c_j}{\text{total number of replications where } D = d_i} \qquad \text{Equation 7-4} \\
 &= \frac{\text{total number of replications where } D = d_i \text{ and } C = c_j}{\text{total number of replications}}
 \end{aligned}$$

For instance, $P(71, 41) = 0.12$ or 12%. The joint probability for each combination is presented in Table 7-1 between parentheses resulting in the joint probability mass function.

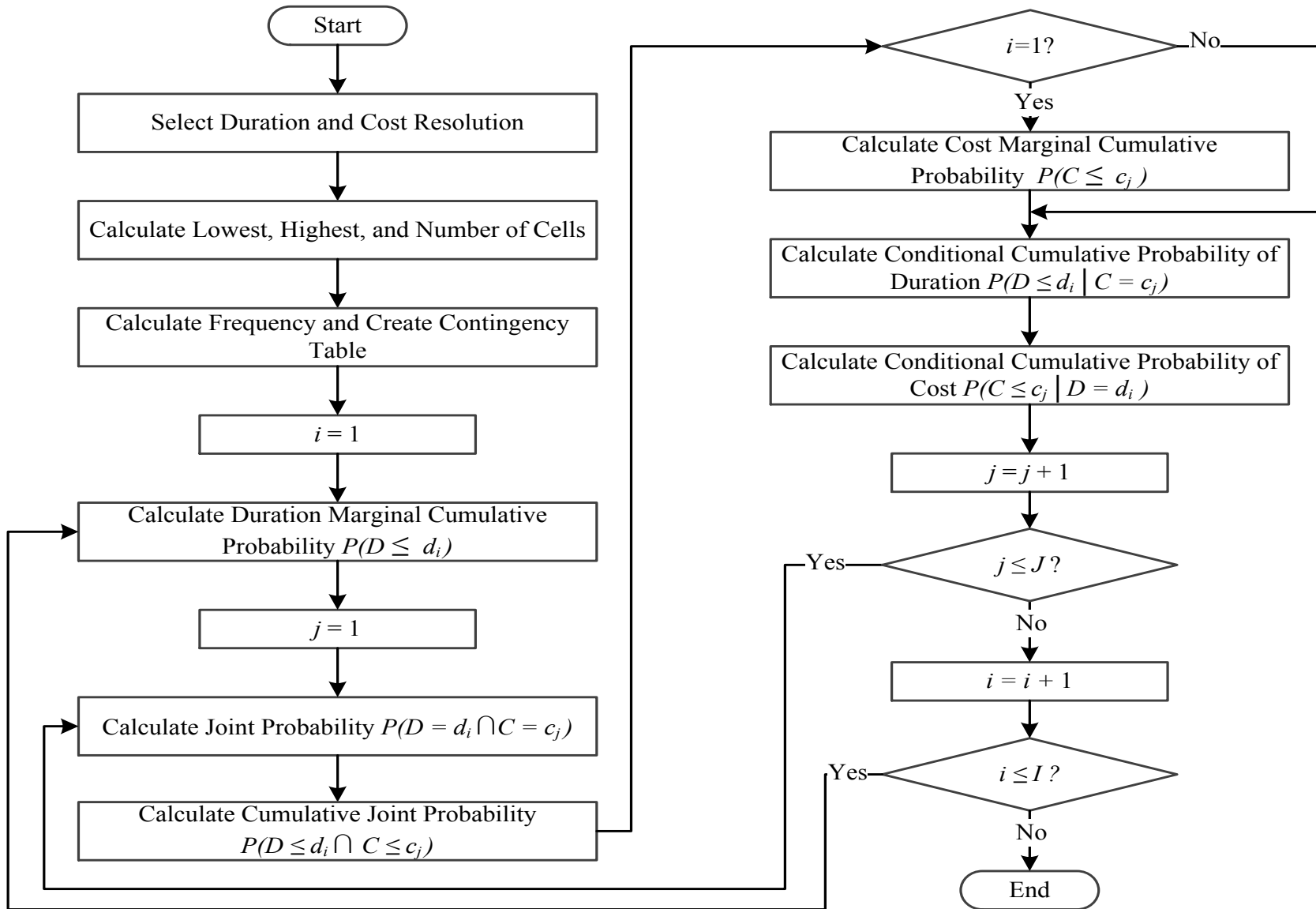


Figure 7-2 Flowchart of Constructing the Joint, Marginal, and Conditional Probability Functions

<p>FUNCTION Main CALL Frequency CALL Contingency Table CALL Joint Probability CALL Duration Marginal Cumulative CALL Cost Marginal Cumulative CALL Duration Conditional Cumulative CALL Cost Conditional Cumulative CALL Find Best Combination End</p>	<p>P_N is an array of the simulation outputs P_M is a copy of P_N T_I is the duration headers in the contingency table T_J is the cost headers in the contingency table P_U is an array that contains unique records of P_N</p>
<p>FUNCTION Frequency FOR each (d_n, c_n) in P_N $Frequency_n = 0$ FOR each (d_m, c_m) in P_M IF $d_n = d_m$ AND $c_n = c_m$ THEN $Frequency_n = Frequency_n + 1$ RETURN $Frequency_n$</p>	<p>FUNCTION Contingency Table FOR each (d_u, c_u) in P_U FOR each duration interval in T_I IF $d_u = d_i$ THEN FOR each cost interval in T_J IF $c_u = c_j$ THEN $Frequency(i, j) = Frequency_u$ RETURN $Frequency(i, j)$</p>
<p>FUNCTION Joint Probability FOR each duration interval in T_I FOR each cost interval in T_J $JointProb(i, j) = Frequency(i, j) / N$ IF $i = 1$ AND $j = 1$ THEN $JointCumProb(i, j) = JointProb(i, j)$ ELSEIF $i = 1$ AND $j > 1$ THEN $JointCum(i, j) = JointCum(i, j-1) + Joint(i, j)$ ELSEIF $i > 1$ AND $j = 1$ THEN $JointCum(i, j) = JointCum(i-1, j) + JointProb(i, j)$ ELSEIF $i > 1$ AND $j > 1$ THEN $JointCum(i, j) = JointCum(i-1, j) + JointCum(i, j-1) - JointCum(i-1, j-1) + JointProb(i, j)$ RETURN $JointProb(i, j)$ and $JointCumProb(i, j)$</p>	<p>FUNCTION Duration Marginal Cumulative FOR each duration interval in T_I FOR each cost interval in T_J $DurMarg_i = DurMarg_i + JointProb(i, j)$ FOR each duration interval in T_I IF $i = 1$ THEN $DurMargCum_i = DurMarg_i$ ELSEIF $i > 1$ THEN $DurMargCum_i = DurMargCum_{i-1} + DurMarg_i$ RETURN $DurMargCum_i$</p>

Figure 7-3 Algorithms for Applying Joint Probability

<p>FUNCTION Cost Marginal Cumulative</p> <p>FOR each cost interval in T_j</p> <p>FOR each duration interval in T_I</p> <p>$CostMarg_j = CostMarg_j + JointProb(i, j)$</p> <p>FOR each cost interval in T_j</p> <p>IF $j=1$ THEN</p> <p>$CostMargCum_j = CostMarg_j$</p> <p>ELSEIF $j > 1$ THEN</p> <p>$CostMargCum_j = CostMargCum_{j-1} + CostMarg_j$</p> <p>RETURN $CostMargCum_j$</p>	<p>FUNCTION Duration Conditional Cumulative</p> <p>FOR each cost interval in T_j</p> <p>FOR each duration interval in T_I</p> <p>$DurCond_{i j} = JointProb(i, j) / CostMarg_j$</p> <p>IF $i = 1$ THEN</p> <p>$DurCondCum_{i j} = DurCond_{i j}$</p> <p>ELSEIF $i > 1$ THEN</p> <p>$DurCondCum_{i j} = DurCondCum_{i-1 j} + DurCond_{i j}$</p> <p>RETURN $DurCondCum_{i j}$</p>
<p>FUNCTION Cost Conditional Cumulative</p> <p>FOR each duration interval in T_I</p> <p>FOR each cost interval in T_j</p> <p>$CostCond_{j i} = JointProb(i, j) / DurMarg_i$</p> <p>IF $j=1$ THEN</p> <p>$CostCondCum_{j i} = CostCond_{j i}$</p> <p>ELSEIF $j > 1$ THEN</p> <p>$CostCondCum_{j i} = CostCondCum_{j-1 i} + CostCond_{j i}$</p> <p>RETURN $CostCondCum_{j i}$</p>	<p>Function Find Best Combination</p> <p>FOR each duration interval in T_I</p> <p>FOR each cost interval in T_j</p> <p>IF $DurCondCum_{i j} \geq 0.5$ AND $CostCondCum_{j i} \geq 0.5$ THEN</p> <p>$Difference(i, j) = Abs(JointCumProb(i, j) - z)$</p> <p>RETURN $Difference(i, j)$</p>

Figure 7-3 (continued) Algorithms for Applying Joint Probability

Figure 7-4(a) shows the joint frequency histogram of the same data of Table 7-1. The sum of the joint probabilities of all the combinations is always equal to 1. The axes of the histogram represent the project duration in days, the project cost in thousands of dollars, and the frequency of each class interval, respectively. The frequency of each combination occurring is represented by the height of the histogram segment that has the duration and cost combination as its base. For example, the base (71, 41) has a height of 60 which indicates that the number of times an observation occurred with the duration of 71 days and cost of \$41,000. This joint probability can be used to select the combination that is more probable if two or more combinations have very close joint cumulative probabilities.

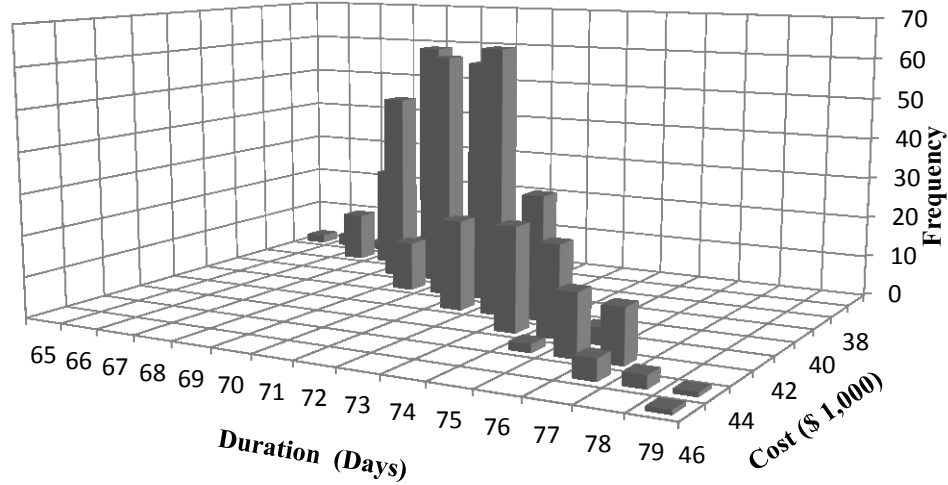
Table 7-1 Example of Contingency Table

$P(d_i, c_j)$			Cost (\$1,000)								$P_D(d_i)$	$P(D \leq d_i)$	
			j = 1	2	3	4	5	6	7	8			J = 9
			38	39	40	41	42	43	44	45			46
Duration (Days)	i = 1	65	2 (0.004)									0.004	0.004
	2	66	3 (0.006)									0.006	0.010
	3	67	2 (0.004)	12 (0.024)								0.028	0.038
	4	68		25 (0.050)								0.050	0.088
	5	69		7 (0.014)	47 (0.940)							0.108	0.196
	6	70			61 (0.122)	12 (0.024)						0.146	0.342
	7	71			2 (0.004)	60 (0.120)						0.124	0.466
	8	72				59 (0.118)	22 (0.044)					0.162	0.628
	9	73				1 (0.002)	64 (0.128)					0.130	0.758
	10	74					30 (0.060)	25 (0.050)				0.11	0.868
	11	75						22 (0.044)	2 (0.004)			0.048	0.916
	12	76						4 (0.008)	15 (0.040)			0.038	0.954
	13	77							13 (0.026)	5 (0.010)		0.036	0.990
	14	78								3 (0.006)		0.006	0.996
	l = 15	79								1 (0.002)	1 (0.002)	0.004	1
$P_C(c_j)$			0.014	0.088	0.220	0.264	0.232	0.102	0.060	0.018	0.002	1	
$P(C \leq c_j)$			0.014	0.102	0.322	0.586	0.818	0.920	0.980	0.998	1		

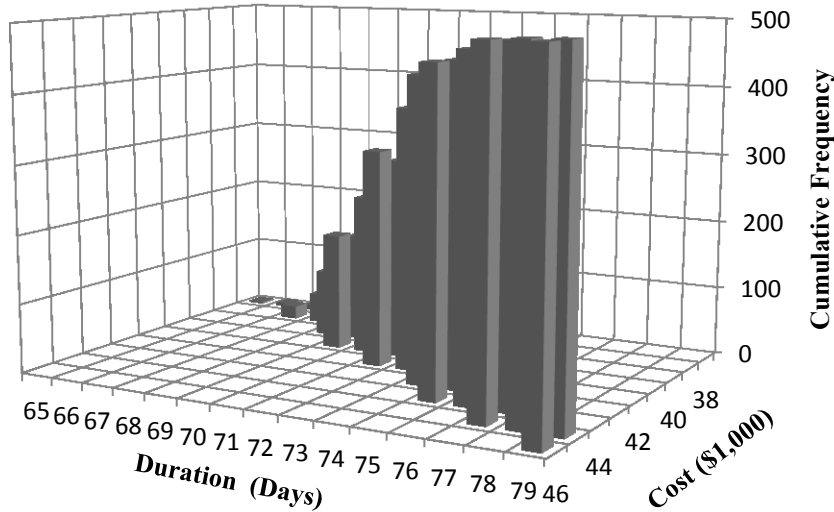
In real life projects, however, decision makers are seldom interested in finding the joint probability of a project duration and cost combination. A more meaningful information is the joint cumulative probability of a project duration and cost combination because it gives an insight on the probability of finishing the project within a specific duration and cost.

The joint cumulative distribution function describes the probability that a project duration and cost combination with a given joint probability mass function has a duration less than or equal to d_i and a cost less than or equal to c_j . The joint cumulative distribution function can be represented by a joint cumulative frequency histogram (Figure 7-4(b)) or a cumulative contingency table that sums the number of observations in all of the cells up to the specified cell. The probability of having a project with a duration less than or equal to d_i and a cost less

than or equal to c_j is calculated using Equation 7-5. The joint probability and joint cumulative probability are calculated for each combination using the *Joint Probability Function* in Figure 7-3



(a) Joint Frequency Histogram



(b) Joint Cumulative Frequency Histogram

Figure 7-4 Examples of Joint Probability Mass Functions

$$P(D \leq d_i \cap C \leq c_j) = \sum_{i=1}^I \sum_{j=1}^J f(d_i, c_j) \times \sum_{j=1}^J \frac{f(d_i, c_j)}{\sum_{j=1}^J f(d_i, c_j)}$$

$$= \frac{\text{total number of replications where } D \leq d_i \text{ and } C \leq c_j}{\text{total number of replications}}$$

Equation 7-5

The probability of the project taking longer than a duration d_i and more than a cost c_j can be calculated using Equation 7-6.

$$P(D > d_i \cap C > c_j) = 1 - P(D \leq d_i \cap C \leq c_j) - P(D > d_i \cap C \leq c_j) - P(D \leq d_i \cap C > c_j) \quad \text{Equation 7-6}$$

For instance, $P(D \leq 71 \cap C \leq 41) = 233/500 = 46.6\%$ and $P(D > 71 \cap C > 41) = 1 - 0.414 - 0 - 0.012 = 53.4\%$.

On the other hand, the possible duration and cost combination (d_i, c_j) that has joint cumulative probability of z can be found by calculating the absolute difference between z and the joint cumulative probability of all the combinations as shown in Equation 7-7.

$$\arg \min_{d,c} h_z(d, c) = |P(D \leq d_i \cap C \leq c_j) - z| \quad \forall (d, c) \in \mathbb{N}_{D,C} \quad \text{Equation 7-7}$$

Decision makers may want to find the probability of completing the project within a specific duration or a specific cost. The probability of having a project with duration less than or equal to d_i or cost less than or equal to c_j can be calculated using Equation 7-8.

$$\begin{aligned} P(D \leq d_i \cup C \leq c_j) &= P(D \leq d_i) + P(C \leq c_j) - P(D \leq d_i \cap C \leq c_j) \\ &= \frac{\text{total number of replications where } D \leq d_i}{\text{total number of replications}} \\ &+ \frac{\text{total number of replications where } C \leq c_j}{\text{total number of replications}} \\ &- \frac{\text{total number of replications where } D \leq d_i \text{ and } C \leq c_j}{\text{total number of replications}} \end{aligned} \quad \text{Equation 7-8}$$

In the field of construction management, the probability of a single performance index is usually used. This probability is called the marginal probability of that performance index when it is the context of joint probability distribution as explained in *Section 7.3.2*.

7.3.2 Constructing Marginal and Conditional Cumulative Probability Functions

The probability of a project duration assuming a value of d_i or less, without regard to the associated project cost, is referred to as the marginal cumulative probability of d_i and is calculated using Equation 7-9. This probability is calculated for each project duration using the *Duration Marginal Cumulative Function* in Figure 7-3.

$$P(D \leq d_i) = \sum_{i=1}^I \sum_{j=1}^J f(d_i, c_j) = \frac{\text{total number of replications where } D \leq d_i}{\text{total number of replications}} \quad \text{Equation 7-9}$$

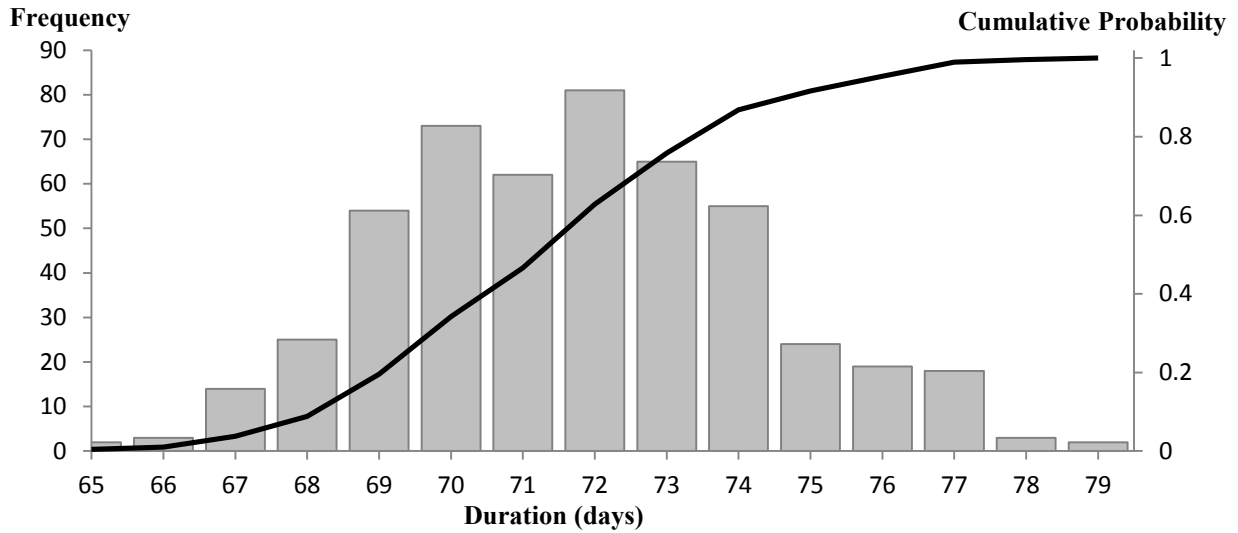
The marginal cumulative probability of the project taking longer than d_i can be found by Equation 7-10.

$$P(D > d_i) = 1 - P(D \leq d_i) \quad \text{Equation 7-10}$$

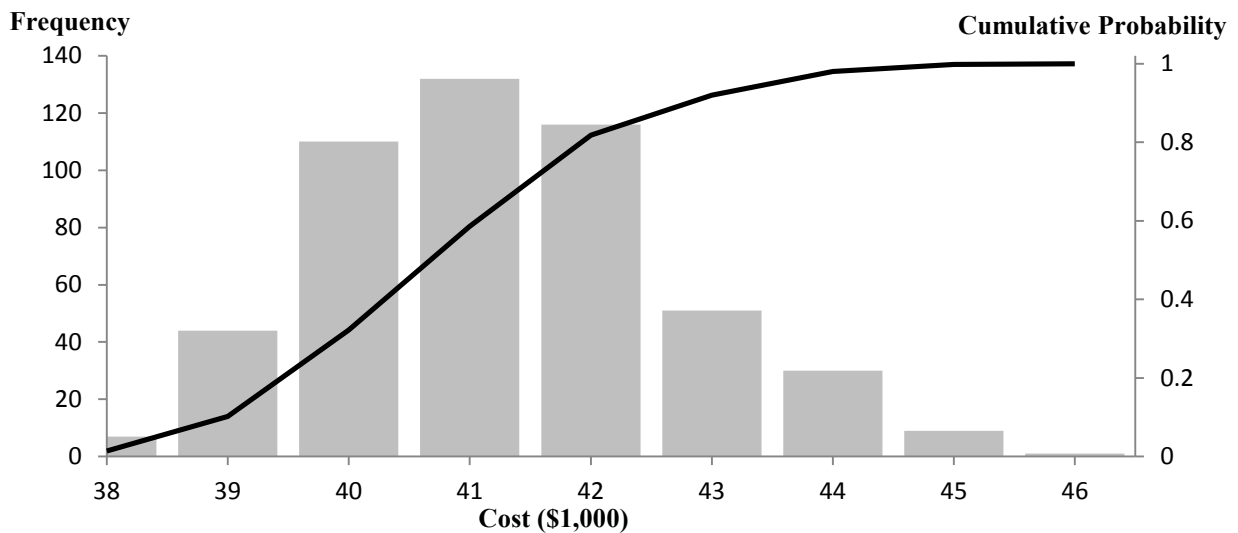
Similar equations to Equation 7-9 and Equation 7-10 and the *Cost Marginal Cumulative Function* (Figure 7-3) are used to find the marginal cumulative probability of the project cost. The marginal probability can be used to analyze each objective separately using the marginal cumulative distribution. The marginal probabilities of project duration and cost are available in the penultimate column and the penultimate row in Table 7-1, respectively. On the other hand, the marginal cumulative probabilities of project duration and project cost are available in the last column and the last row in Table 7-1, respectively. Figure 7-5(a) shows the marginal probability and the marginal cumulative probability of the project duration while Figure 7-5(b) shows the marginal probability and the marginal cumulative probability of the project cost. For instance, $P(D \leq 71) = 233/500 = 46.6\%$, $P(D > 71) = 1 - 0.466 = 53.4\%$, $P(C \leq 41) = 293/500 = 58.6\%$, and $P(C > 41) = 1 - 0.586 = 41.4\%$.

The possible project costs along with their probabilities if the project duration is equal to d_i can be found by filtering out all the joint outcomes of $D = d_i$ and then calculating the conditional probability for every possible cost outcome using Equation 7-11.

$$\begin{aligned} P(C = c_j | D = d_i) &= \frac{P[D = d_i, C = c_j]}{P[D = d_i]} \\ &= \frac{\text{total number of replications where } D = d_i \text{ and } C = c_j}{\text{total number of replications where } D = d_i} \end{aligned} \quad \text{Equation 7-11}$$



(a) Marginal Duration Frequency Histogram



(b) Marginal Cost Frequency Histogram

Figure 7-5 Examples of Marginal Frequency Histograms

The conditional cumulative probability can be used to calculate the probability of having the cost less than or equal to c_j if the project duration is equal to d_i as given by Equation 7-12. The *Cost Conditional Cumulative Function* in Figure 7-3 is used to calculate the conditional probability and conditional cumulative probability for each combination.

$$P(C \leq c_j | D = d_i) = \frac{P[D = d_i, C \leq c_j]}{P[D = d_i]} \quad \text{Equation 7-12}$$

$$= \frac{\text{total number of replications where } D = d_i \text{ and } C \leq c_j}{\text{total number of replications where } D = d_i}$$

Similar equations to Equation 7-11 and Equation 7-12 and the *Duration Conditional Cumulative Function* (Figure 7-3) are used to calculate the possible project durations along with their probabilities if the project cost is equal to c_j . For instance, $P(C \leq 43 | D = 75) = 47/51 = 92.15\%$, $P(D \leq 75 | C = 43) = 22/24 = 91.67\%$. This means that there is 92.15% chance that the project cost will be less than or equal to \$43,000 if the project duration is 75 days. On the other hand, if the project cost is \$43,000, then there is 91.67% chance the project duration will be 75 days. Having a conditional cumulative probability higher than 50% is preferable as shown in *Section 7.4*.

The conditional cumulative probability can be used to analyze the variation of a project cost with respect to a fixed value of the project duration. In addition, it indicates how probable a combination is. Figure 7-2 shows the flowchart of calculating the marginal and conditional cumulative probabilities.

7.4 Generating Joint Probabilistic Pareto Fronts

To generate the joint probabilistic Pareto fronts, a combination of duration and cost is chosen to represent each Pareto solution. The combinations of all Pareto solution are then compared to each other to determine the set of non-dominated combinations as explained in Figure 4-7. The rest of this section describes the developed method for finding the best combination that represents the desired joint probability.

Equation 7-7 describes how to find the duration and cost combination (d_i, c_j) that has the absolute closest joint cumulative probability to the desired z . However, this equation does not give the best combination that represents the desired confidence level. This is due to the fact that Equation 7-7 does not take the conditional cumulative probability of each combination into consideration. For example, by using Equation 7-7 and a desired confidence level of 60%, the equation gives the duration and cost combination (73, 41). Using the joint cumulative probability

by itself can be deceiving. By examining the joint cumulative probability of the combinations, it is found that there are four combinations that have joint cumulative probability close to 60%. Table 7-2 shows the joint cumulative probabilities, marginal cumulative probabilities, and conditional cumulative probabilities of the four combinations (72, 41), (73, 41), (72, 42), and (73, 42).

Table 7-2 Probability Information of the Four Combinations

Combination	Joint Cumulative Probability (%)	Joint Probability – z (%)	Duration Marginal Cumulative (%)	Cost Marginal Cumulative (%)	Duration Conditional Cumulative (%)	Cost Conditional Cumulative (%)
(72, 41)	58.40	-1.60	62.80	58.60	99.24	72.84
(73, 41)	58.60	-1.40	75.80	58.60	100.00	1.54
(72, 42)	62.80	2.80	62.80	81.80	18.97	100.00
(73, 42)	75.80	15.80	75.80	81.80	74.14	100.00

The selected combination by Equation 7-7 (i.e. (73, 41)) has a cost conditional cumulative probability of 1.54% which is a very low probability. This probability means that given the project duration of 73 days, the likelihood of finishing the project with a cost of \$41,000 is 1.54%. In order to select a most likely schedule, the decision maker should consider the combinations with conditional cumulative probability of at least 50% since it represents the most likely output as shown in Equation 7-13.

$$\arg \min_{d,c} h_z(d, c) = |P(D \leq d_i \cap C \leq c_j) - z| \quad \forall (d, c) \in \mathbb{N}_{D,c} \quad \text{Equation 7-13}$$

$$\text{subject to: } P(C \leq c_j | D = d_i) \geq 50\%$$

$$P(D \leq d_i | C = c_j) \geq 50\%$$

There are two combinations that meet this criterion in Table 7-2 which are (72, 41) and (73, 42). Therefore, the combination that should be selected is (72, 41) since it has the smallest difference between z and the joint cumulative probability.

Figure 7-6 shows the flowchart for finding the best combination that represents the desired confidence level. The process starts by determining the desired confidence level. The desired confidence level is defined by the decision maker and it represents the probability at which the

project will be baselined and budgeted. The combination with the smallest absolute difference between z and the joint cumulative probability and which has conditional cumulative probabilities larger than or equal to 50% is selected. The *Find Best Combination Function* in Figure 7-3 is used for this purpose.

7.5 Analyzing the Selected Solution

7.5.1 Estimating Duration and Cost Joint Contingency

Traditionally, contingencies are estimated for either project cost or project duration without considering the correlation between them, or the impact they have on each other. This is usually done by subtracting the median point from the desired confidence level point (Moselhi, 1997; Fenton et al., 1999). Therefore, there is a need for a method to estimate the joint contingency considering the correlation between the project duration and cost and the impact they have on each other. The correlation can be accounted for by using the joint probability while the impact can be considered in the conditional cumulative probability. Figure 7-7 shows the flowchart for estimating duration and cost joint contingency. Similar to the method explained in *Section 7.4* (Figure 7-6), the process starts by selecting the desired confidence level (z) of the project. Then the best combinations representing 50% joint cumulative probability and z as explained in *Section 7.4* are selected. The joint contingency is estimated by subtracting the project duration and cost corresponding to the desired confidence level from the project duration and cost with 50% joint cumulative probability as shown in Equation 7-14.

$$C(d, c) = h_z(d, c) - h_{0.5}(d, c) \quad \text{Equation 7-14}$$

Where $h_z(d, c)$ and $h_{0.5}(d, c)$ are calculated using Equation 7-14. For example, the best combination that represents 50% is (71, 41) with a joint cumulative probability of 46%. Assuming that the decision maker wants a confidence level of 80% which is best represented by the combination (74, 42) with a joint cumulative probability of 82%. Then the project duration and cost joint contingency is three days and \$1,000, respectively.

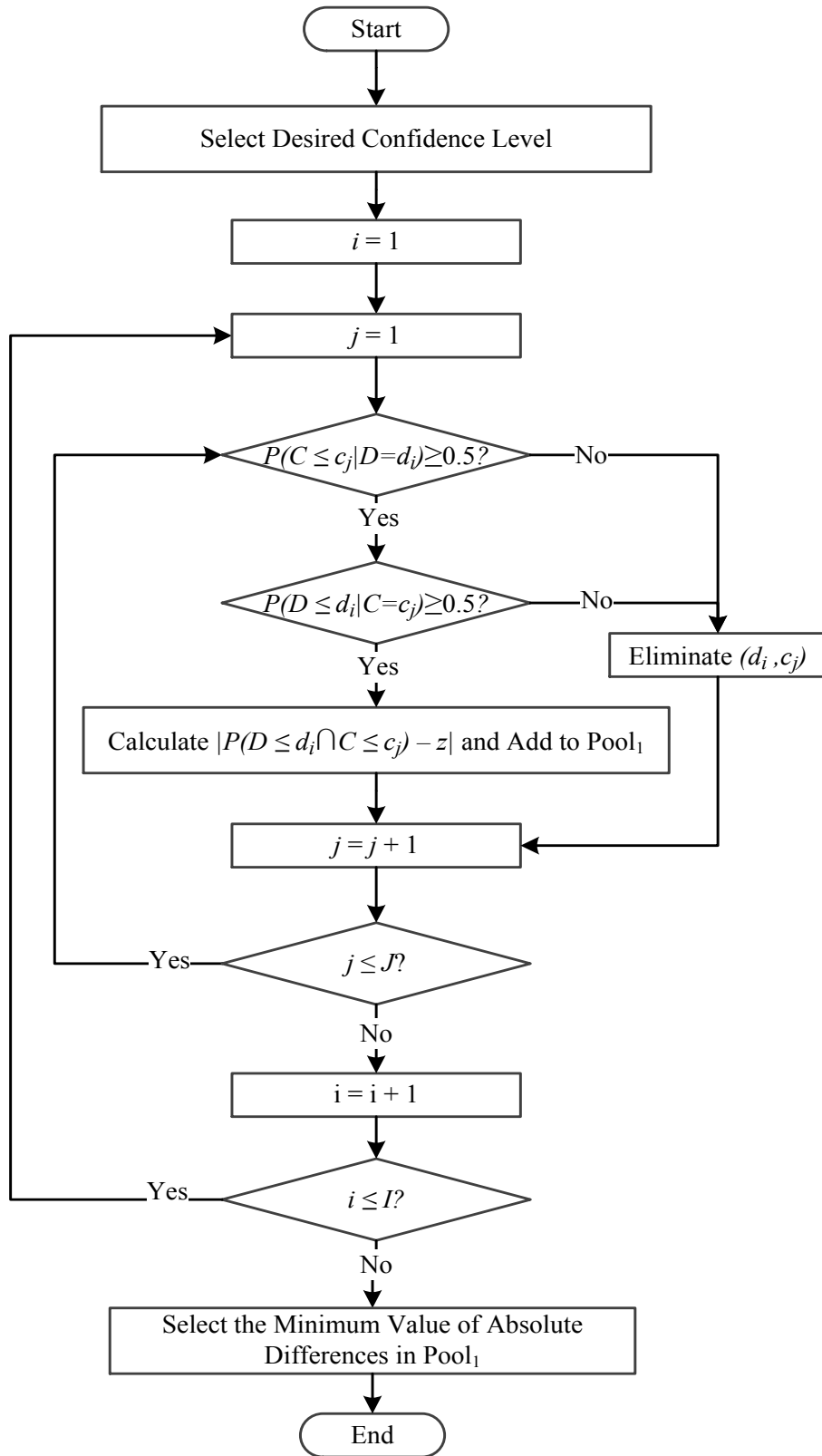


Figure 7-6 Flowchart for Finding the Best Combination

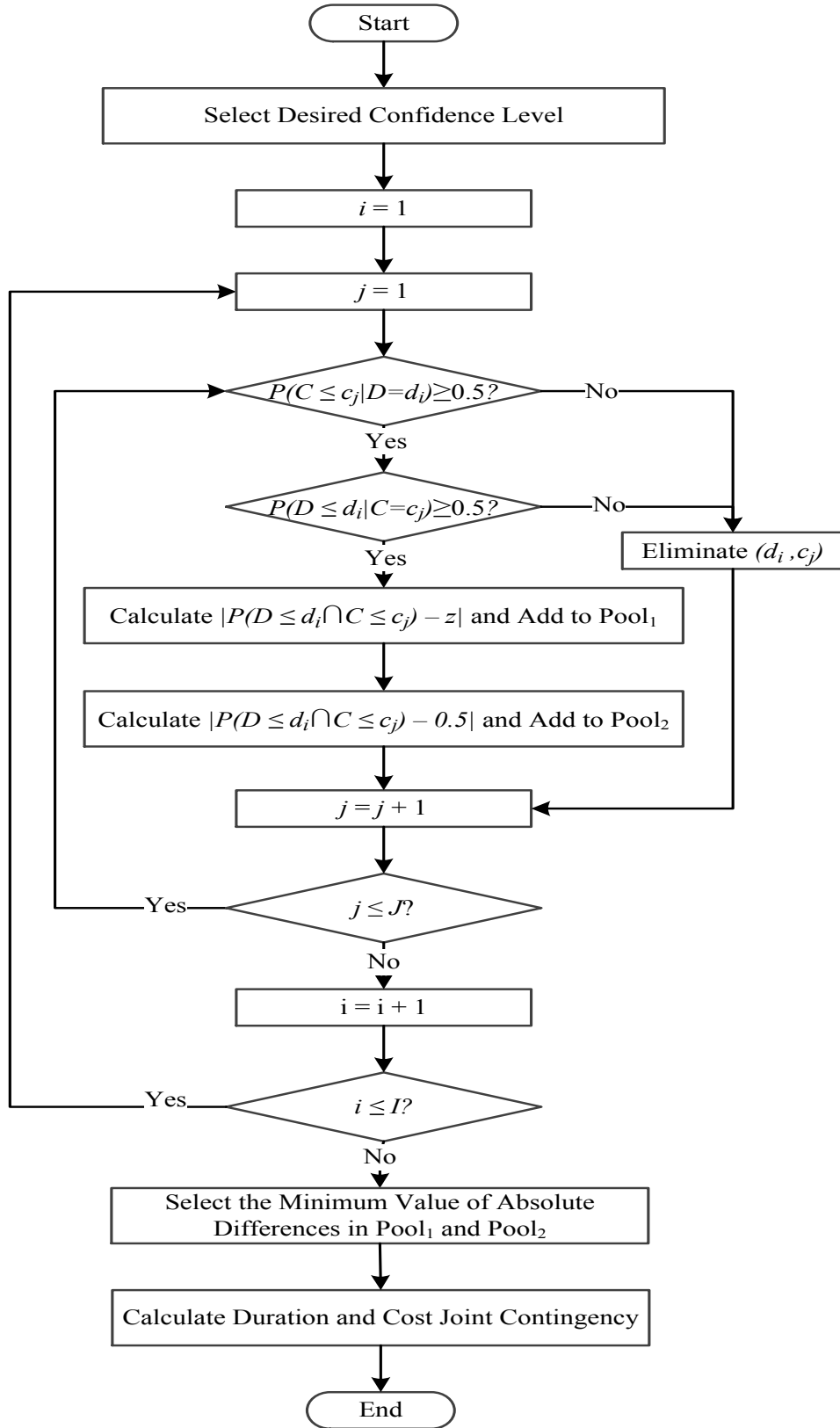


Figure 7-7 Flowchart for Estimating Duration and Cost Joint Contingency

7.5.2 Generating a Schedule to Meet a Specific Probability

The project schedule is essential for resource scheduling, cost estimating, and project control. However, when using discrete event simulation or Monte Carlo simulation, the most common final output is the distributions of total project duration and total project cost. This output does not provide a schedule since it does not assign a duration for each activity or task to meet the mean or any probability of the total project duration or cost. This part of the proposed method describes how a schedule that meets a desired confidence level can be generated as shown in Figure 7-8.

At the start of each simulation replication, a seed number is generated randomly in order to generate independent simulation replications. All the randomly generated seed numbers are saved in order to regenerate the exact simulation replication that resulted in the project duration and cost combination that met the desired confidence level. The simulation is run for a single replication using the seed number and the durations of all the instances of each activity or task are extracted. In some cases, there could be more than one replication that resulted in the same project duration and cost combination, and thus, there could be a number of seed numbers (S) that should be applied. Using the seed number of any of those replications will result in the same project duration and cost combination. However, these seeds will generate different duration and cost for each activity. In order to assist the decision maker in selecting the best seed number for generating the schedule, a method for ranking the seed numbers is proposed. Each activity a of a total of A activities is assigned a value based on the distance between the activity duration and cost generated by the seed number s and the mean activity duration and cost calculated from the N replications. The distance is calculated using Equation 7-15.

$$Distance_a^s = \sqrt{\left(\frac{a_{dur}^s - \overline{a_{dur}}}{\overline{a_{dur}}}\right)^2 + \left(\frac{a_{cost}^s - \overline{a_{cost}}}{\overline{a_{cost}}}\right)^2} \quad \text{Equation 7-15}$$

Where a_{dur}^s is the duration of activity a using seed number s , $\overline{a_{dur}}$ is the mean duration of activity a , a_{cost}^s is the cost of activity a , $\overline{a_{cost}}$ is the mean cost of activity a . In order to obtain a dimensionless distance, the differences of durations and costs are divided by the mean value of each of these variables (i.e., $\overline{a_{dur}}$ and $\overline{a_{cost}}$). The mean of the distances of each seed number s is calculated using Equation 7-16.

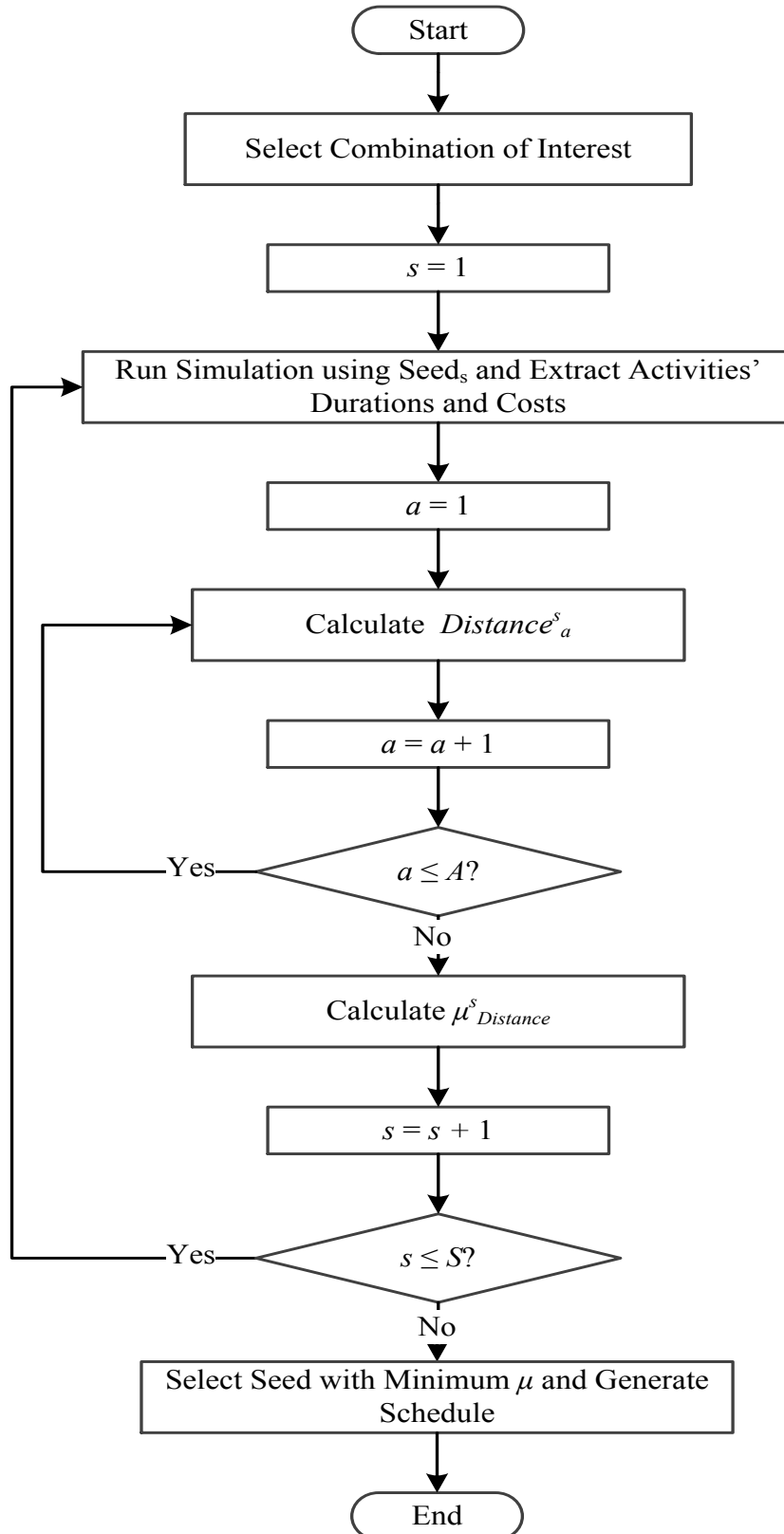


Figure 7-8 Flowchart for Selecting Best Seed Number

$$\mu_{Distance}^S = \sum_{a=1}^A \frac{Distance_a^S}{A}$$

Equation 7-16

7.6 Method Implementation

Two main implementations were developed in order to realize the proposed method as summarized in Figure 7-9. The first implementation is for applying the joint probability to the output of stochastic simulation models, and calculating duration and cost joint contingency. The second implementation is for generating a schedule with a specified probability. These two implementations are described in detail in the following sections.

7.6.1 Applying the Joint Probability

Microsoft Excel is integrated with STROBOSCOPE via VBA in order to obtain the output of the stochastic simulation models of the sub-population Pareto fronts generated by the stochastic simulation-based multi-objective optimization model presented in *Chapter 3* as shown in Figure 7-10.

The process starts by running the simulation N replications for each Pareto solution where each replication represents one potential outcome for the project's duration and cost. The project duration, cost, and seed number are then obtained from each simulation replication. This information is extracted and stored in an array of size $N \times 3$ during the simulation. At the end of the simulation, this array is imported to Microsoft Excel to perform the joint probability calculations. This array is then sorted by duration in an ascending order. If two replications have the same project duration, the information is then sorted by cost in an ascending order. The purpose of this sorting is to reduce the computation time needed to calculate the frequency of each project duration and cost combination.

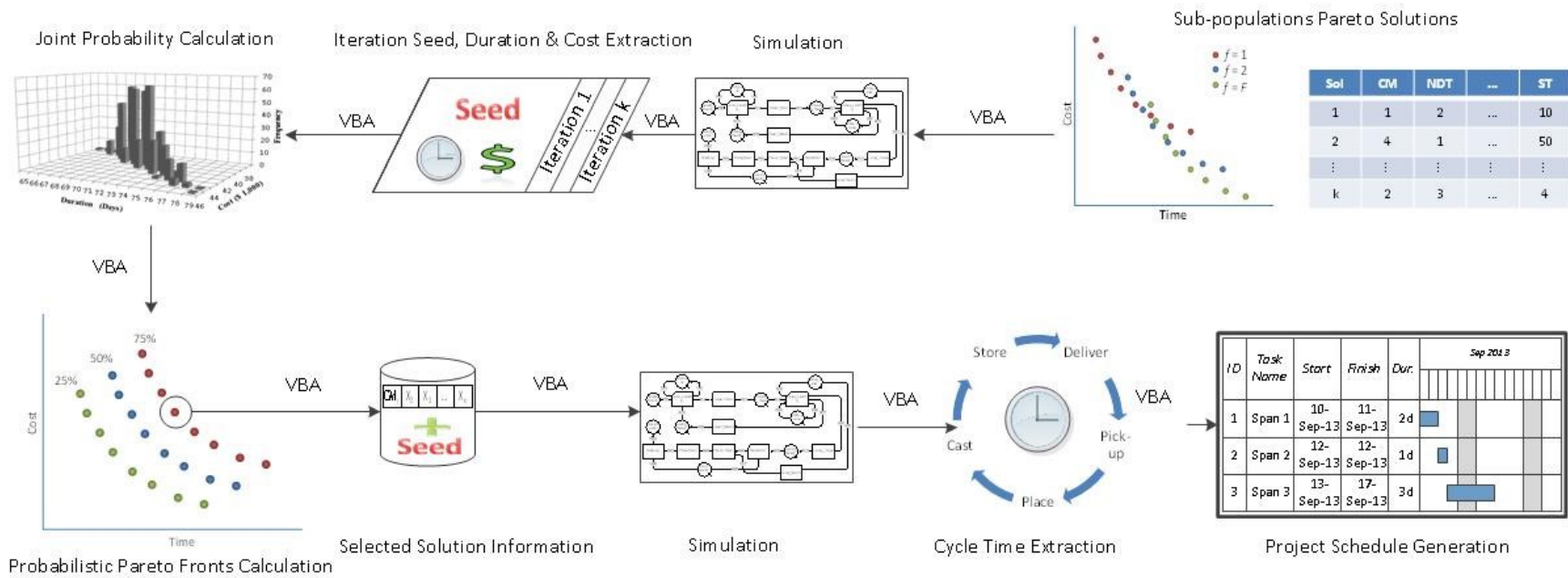


Figure 7-9 Implementation Summary of Proposed Methodology

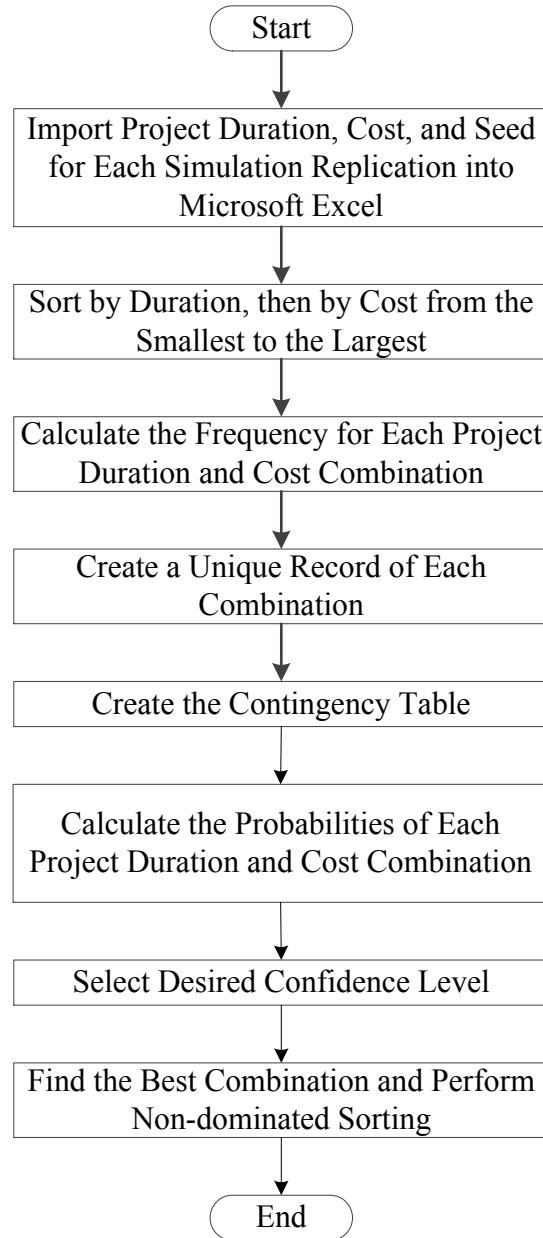


Figure 7-10 Flowchart of Joint Probability Implementation

These frequencies are the basis required to calculate the joint probability of a combination. Afterwards, a unique sorted record of each combination and its frequency's value is created. This is done to eliminate any unnecessary repeated information, to reduce the computation time needed to create the contingency table, and to calculate probabilities of each combination. Finally, the best combination representing a desired confidence level is selected and non-dominated sorting is performed.

7.6.2 Generating a Schedule with a Specified Probability

Generating a schedule representing a specific probability consists of two main steps. The first step is finding the best seed number of the combination representing that probability. The second step is generating the schedule of the best seed number. Figure 7-11 shows the flowchart for schedule generation. The process starts by running the simulation with the seed numbers of the selected combination. The duration and cost of each activity is extracted and imported to Microsoft Excel to find the best seed number. Then, a new project is created in Microsoft Project (Microsoft Corporation 2015d) with a predefined project start date and working calendar. Microsoft Project was integrated with STROBOSCOPE via VBA in order to obtain the duration of each activity using the best seed number. Then, the activities' names and durations are extracted from the simulation and imported to Microsoft Project. Finally, the activities in Microsoft Project are linked together and the schedule is generated.

7.7 Case Studies

Given that construction projects can be categorized under the three main types of cyclic (Halpin and Riggs 1992), repetitive, and non-repetitive projects (El-Rayes, 2001), three case studies are used to evaluate the effectiveness of the proposed method and to quantify the impact of considering the correlation between time and cost in different types of construction projects. A fourth case study is used to demonstrate the concept of joint probabilistic Pareto front.

Evaluation of these simulation models is done in two steps which are: (1) verification and validation (Law and Kelton 1991, Sargent 2010); and (2) uncertainty analysis (Kleijnen, 1996). Verification and validation of the implementations of the VRTs in the simulation models are done by tracing the different entities in the simulation models to assure that the logic of the models are correct and they are running as expected (Sargent 2010). Uncertainty analysis, which is the main focus of this chapter, is done by considering the stochastic durations of the tasks in the simulation models. Two parameters are studied in the case studies: (1) the impact of the level of correlation between time and cost on the effectiveness of the proposed method, and (2) the number of replications required to effectively capture the stochasticity in different project types. Given that time and cost are the most common outputs of construction simulation, these two

performance metrics are used in this case studies as the basis for the comparison of the proposed and traditional methods.

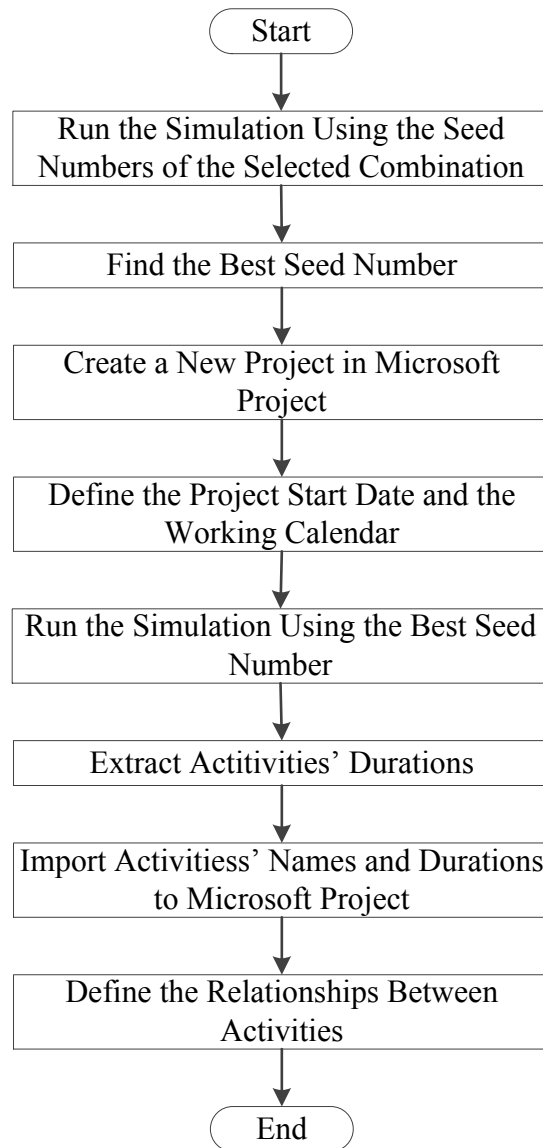


Figure 7-11 Flowchart of Generating Schedule

Case study A is about the construction of a precast full span box girder bridge using launching method which is cyclic in nature. This case study is modeled using discrete event simulation and is used to demonstrate the application of the joint probability and joint contingency methods. Case study B is about a non-repetitive project which is depicted in a schedule network that uses Monte Carlo simulation. This case study is used to demonstrate the application of the joint probability and schedule generating methods. Case study C is about a repetitive project which

can be represented using a repetitive network or Line of Balance combined with Monte Carlo simulation. This case study is used to demonstrate the application of the joint probability method. Table 7-3 summarizes the results of the performance metrics for the three case studies.

Table 7-3 Summary of Performance Metrics for Case studies A, B, and C

Case study	Type of Project	Type of Simulation	Demonstrated Application	Correlation	ΔD (%)	ΔC (%)	N
A	Cyclic	Discrete Event	Joint Probability and Joint Contingency	0.94	(-1, 1)	(-2, 1)	100
B	Non-repetitive	Monte Carlo	Joint Probability and Schedule Generation	0.45	(1, 6)	(2, 8)	5,000
C	Repetitive	Monte Carlo	Joint Probability	0.21	(0, 8)	(0, 5)	5,000

7.7.1 Case study A: Cyclic Project

This case study consists simulates the same case study used in *Section 4.9*. The developed simulation model is shown in Figure 4-2 which shows the cyclic nature of the operation. The selected resolution for the project duration is one day while the selected resolution for the project cost is \$10,000. Figure 7-12 shows the scatter plot of the project duration and cost after 5,000 simulation replications. The correlation between the project duration and project cost is 0.94 which indicates a very strong linear dependency between the project duration and cost. The gaps in Figure 7-12 are because the project duration is calculated in calendar days with five working days per week.

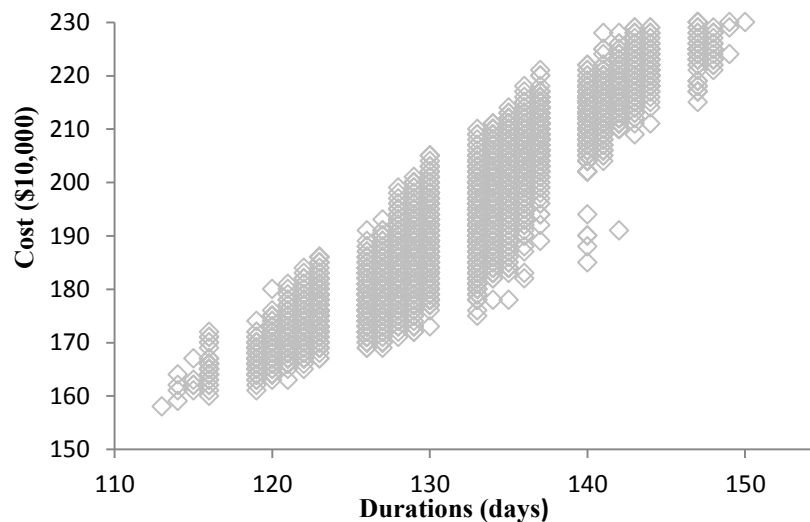


Figure 7-12 Scatter Plot of Project Duration and Cost Combinations for Case Study A

In order to show the shortcomings of using the marginal cumulative probability alone, the project duration and cost corresponding to the cumulative probabilities of 25%, 50%, 75%, 80%, 90% and 95% using the marginal probability and joint probability are calculated and presented in Table 7-4.

Table 7-4 Project Duration and Cost of Different Cumulative Probabilities for Case Study A

Desired Probability (%)	Marginal Duration (days)	Marginal Cost (\$10,000)	Joint Cumulative Probability (%)	Joint Duration (days)	Joint Cost (\$10,000)	Joint Cumulative Probability (%)	ΔD (%)	ΔC (%)
25	127	183	25	127	180	23	0	-2
50	132	194	DNE	133	196	50	1	1
75	136	205	69	136	208	73	0	1
80	138	208	DNE	137	211	79	-1	1
90	141	215	88	141	217	90	0	1
95	143	221	96	142	222	95	-1	0

The marginal project duration and cost are calculated using the mean value, standard deviation, and the desired probability. In addition, the joint probability of the marginal project duration and marginal project cost is calculated. The joint combinations presented in Table 7-4 represent the best possible combination meeting the desired probability and found using Equation 7-13. From the results in Table 7-4, it can be noticed that the project duration and cost combination (132, 194) corresponding to 50% marginal cumulative probability does not exist (DNE). In other words, none of the 5,000 simulation replications resulted in that combination. The difference between the project duration (ΔD) and cost (ΔC) under the two methods is calculated using Equation 7-17 and Equation 7-18, respectively.

$$\Delta D = \frac{\text{Joint Duration} - \text{Marginal Duration}}{\text{Marginal Duration}} \times 100 \quad \text{Equation 7-17}$$

$$\Delta C = \frac{\text{Joint Cost} - \text{Marginal Cost}}{\text{Marginal Cost}} \times 100 \quad \text{Equation 7-18}$$

These equations represent two of the performance metrics of the proposed method. It can be noticed that the difference of the two methods ranges between -1% and 1% in project duration, and between -2% and 1% in project cost. This is due to the fact that the project duration and the project cost have a very strong correlation. However, this is not always the case as can be seen in

the following case studies. The duration and cost joint contingency is estimated, using Equation 7-13 and Equation 7-14, for confidence level of 80%. From Table 7-4, the best combinations to meet 50% and 80% are (133, 196) and (137, 211), respectively. Based on the difference of these two combinations, the joint contingency is 4 days and \$150,000.

To find the minimum number of simulation replications required to obtain sound expected joint value of the project duration and cost, the simulation was run for 100, 200, 500, 1000, 2000 and 5000 replications as shown in Table 7-5. The combinations presented in this table represent the best possible combination meeting 50% joint cumulative probability and found using Equation 7-13. The marginal probability of the project duration is calculated using Equation 7-9. The conditional cumulative probability of the project cost given the project duration is calculated using Equation 7-12. This analysis examines the impact of the number of replications on the improvement of the joint cumulative probability. It can be noticed from Table 7-5 that the difference in the expected joint value between 100 and 5000 replications is insignificant. This can be also as a result of the existence of a strong correlation between the project duration and the project cost.

Table 7-5 Different Number of Simulation Replications for Case Study A

Replications	Duration (days)	Cost (\$10,000)	Joint Cumulative Probability (%)	Duration Marginal Cumulative (%)	Cost Marginal Cumulative (%)	Duration Conditional Cumulative (%)	Cost Conditional Cumulative (%)
100	133	197	50	54	58	100	67
200	133	198	50	54	53	50	63
500	133	195	50	56	56	75	58
1,000	133	196	50	55	55	58	54
2,000	133	195	49	55	53	62	53
5,000	133	196	50	53	55	58	65

7.7.2 Case Study B: Non-repetitive Project

This case study is for a simple project that consists of seven activities (Figure 7-13). The durations, costs, and the logical relationships of the activities are presented in Table 7-6. The durations are modeled using triangular distribution which is defined by the lower limit, the higher limit and the mode. Monte Carlo simulation is used to find the possible outcomes of this project. The selected resolution for the project duration is one day while the selected resolution

for the project cost is \$1,000. Figure 7-14 shows the scatter plot of the project duration and cost after 5,000 simulation replications. The correlation between the project duration and project cost is 0.45 which indicates the existence of a moderate linear dependency between the project duration and the project cost.

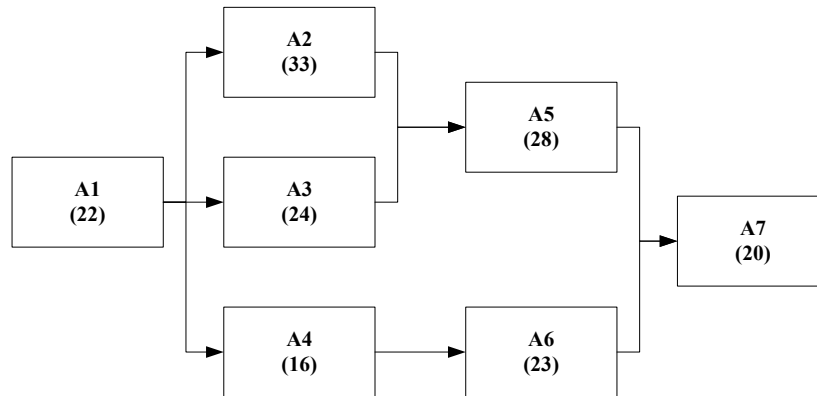


Figure 7-13 Schedule Network for Case Study B

Table 7-6 Project Information for Case Study B

Activity	Predecessor	Duration (Days)			Cost (\$/day)
		Low	Mode	High	
A1	-	12	20	32	1,500
A2	A1	12	30	69	200
A3	A1	10	22	41	300
A4	A1	10	16	25	3,500
A5	A2, A3	16	28	38	1,000
A6	A4	12	18	30	2,000
A7	A5, A6	7	15	23	1,500

The project duration and cost corresponding to several cumulative probabilities are presented in Table 7-7. The difference between the two methods ranges between 1% and 6% in project duration, and between 2% and 8% in project cost. Table 7-8 shows the results of different number of simulation replications. The difference in the expected joint value between 100 and 5000 replications can be significant. This can be also as a result of the existence of a moderate correlation between the project duration and the project cost. Therefore, decision makers should run the simulation for the largest possible number of replications. However, applying a large

number of replications (up to 500,000) resulted in almost the same combination of duration and cost as in the case of 5,000 replications. The small variations in the results for large number of replications (i.e., more than 5,000) can be explained by the interactions between the different variables in the model, and can be neglected.

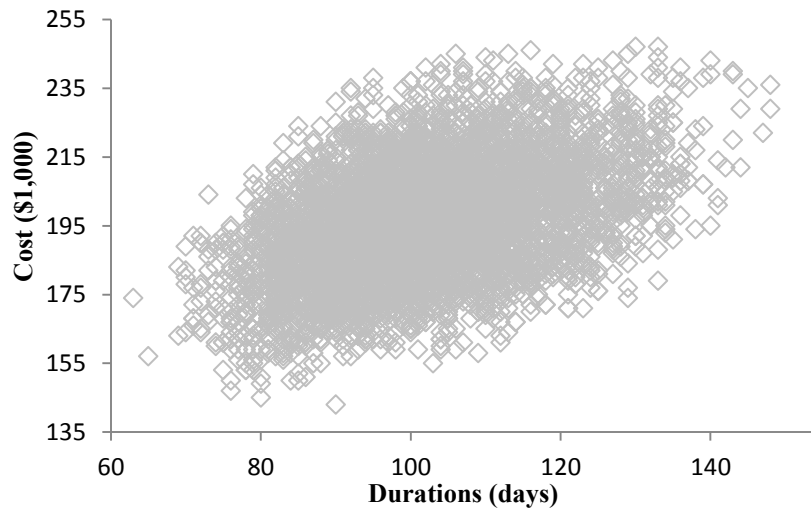


Figure 7-14 Scatter Plot of Project Duration and Cost Combinations for Case Study B

Table 7-7 Project Duration and Cost of Different Cumulative Probabilities of Case Study B

Desired Probability (%)	Marginal Duration (days)	Marginal Cost (\$1,000)	Joint Cumulative Probability (%)	Joint Duration (days)	Joint Cost (\$1,000)	Joint Cumulative Probability (%)	ΔD (%)	ΔC (%)
25	93	185	13	99	194	28	6	5
50	102	196	36	103	207	50	1	6
75	111	207	63	117	211	75	5	2
80	113	210	69	114	223	80	1	6
90	119	217	DNE	121	228	90	2	5
95	124	223	91	125	241	95	1	8

The numbers between parentheses in Figure 7-13 represents the duration of each activity that will result in a project duration and cost combination (103, 207) which represents 50% joint cumulative probability. These durations were found using the method described in *Section 7.5.2*. There are four seed numbers that result in this combination. Table 7-9 shows the durations of the activities resulting from each seed number along with the average duration of each activity. The

distance between each activity and the activity average is calculated using Equation 7-15. Finally, the mean of each seed number is calculated using Equation 7-16.

Table 7-8 Different Number of Simulation Replications for Case Study B

Replications	Duration (days)	Cost (\$1,000)	Joint Cumulative Probability (%)	Duration Marginal Cumulative (%)	Cost Marginal Cumulative (%)	Duration Conditional Cumulative (%)	Cost Conditional Cumulative (%)
100	108	194	48	79	54	50	50
200	119	195	50	93	51	100	50
500	110	201	50	77	62	64	54
1,000	113	199	50	83	58	84	55
2,000	114	197	50	86	55	83	51
5,000	103	207	50	58	76	53	78

7.7.3 Case study C: Repetitive project

This case study is for a project where the network of activities of *Case study B* is repeated five times in a sequence. The durations, costs, and the logical relationships of the activities are the same of *Case study B*. Monte Carlo simulation is used to find the possible outcomes of this project. The selected resolution for the project duration is one day while the selected resolution for the project cost is \$1,000. Figure 7-15 shows the scatter plot of the project duration and cost combinations after 5,000 simulation replications. The correlation between the project duration and project cost is 0.21 which indicates the existence of a weak linear dependency between the project duration and the project cost

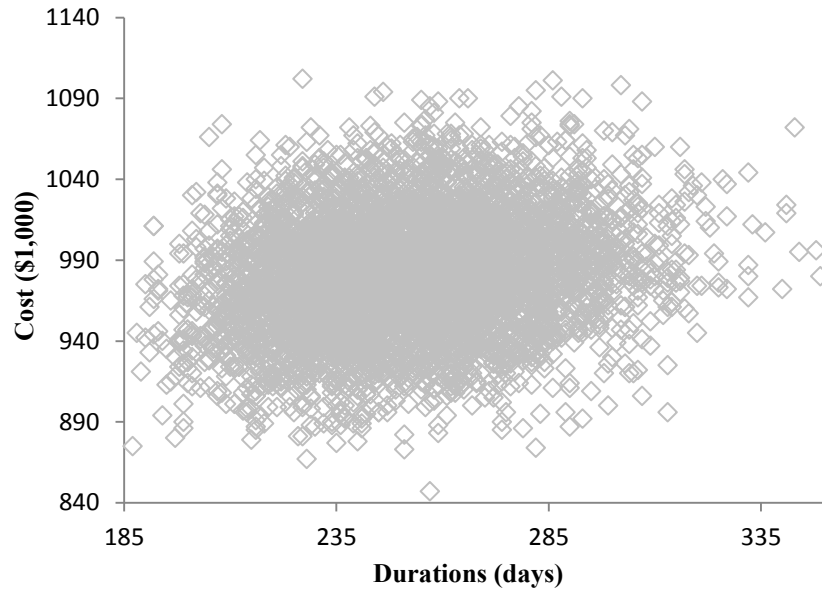


Figure 7-15 Scatter Plot of Project Duration and Cost Combinations for Case Study C

The project duration and cost corresponding to several cumulative probabilities are presented in Table 7-10. The difference between the two methods ranges between 0% and 8% in project duration, and between 0% and 5% in project cost. Table 7-11 shows the results of different number of simulation replications. The difference in the expected joint value between 100 and 5000 replications can be significant. This can be as a result of the existence of a weak correlation between the project duration and the project cost. Therefore, decision makers should run the simulation for the largest possible number of replications.

7.7.4 Cast Study D: Joint Probabilistic Pareto Front

This case study compares the Pareto fronts of two bridge construction methods obtained using the stochastic simulation-based optimization model presented in *Chapter 3*. These methods are precast segmental bridge construction using a launching gantry and using under-slung girder. These two methods are described in *Section 2.2.10* and their simulation models are shown in Figure 4-3 and Figure 4-5, respectively. Table A-2 and Table A-4 show the tasks durations used for launching gantry and using under-slung girder, respectively. The cost data used for both simulation models is presented in *Appendix B*.

Figure 7-16 shows the Pareto fronts generated for the two construction methods and their combined Pareto for 50% cumulative probability. It can be noticed that the under-slung girder

method has only two solutions in the combined Pareto. These Pareto solutions were generated using disjoint probability. To demonstrate the shortcomings of the traditional method, these Pareto solutions were generated using the joint cumulative probability as described in *Section 7.4*. Figure 7-17 shows the three Pareto for 50% joint cumulative probability. It can be noticed that the under-slung girder method has six solutions in the combined Pareto. Figure 7-18 and Figure 7-19 show the same concept for joint cumulative probability of 75% and 95%, respectively. It can be noticed that the combined Pareto fronts for the different joint cumulative probabilities do not contain the same optimum solutions. In other words, the dominance of the optimum solutions changes with the desired joint cumulative probability. Figure 7-20 shows probabilistic Pareto fronts for 50%, 75%, and 95% joint cumulative probability.

7.8 Summary and Conclusions

This chapter presented a new joint probability method that can be used to evaluate the probabilities of the project duration and cost obtained from stochastic simulation models. This method was applied to the sub-populations Pareto fronts obtained from the stochastic simulation-based multi-objective optimization. This chapter: (1) introduced a method to apply joint probability to Pareto solutions; (2) proposed the concept of joint probabilistic Pareto fronts; (3) developed a method to analyze the selected solution; (4) implemented the proposed method; and (5) demonstrated the effectiveness of the proposed method.

Table 7-9 Analysis of Schedule Generation for Case Study B

Activity	Average		Seed Number 1			Seed Number 2			Seed Number 3			Seed Number 4		
	Dur. (days)	Cost (\$1,000)	Dur. (days)	Cost (\$1,000)	Distance	Dur. (days)	Cost (\$1,000)	Distance	Dur. (days)	Cost (\$1,000)	Distance	Dur. (days)	Cost (\$1,000)	Distance
A1	21	31.5	23	34.5	0.135	22	33.0	0.067	22	33.0	0.067	23	34.5	0.135
A2	36	7.2	28	5.6	0.314	32	6.4	0.157	33	6.6	0.118	51	10.2	0.589
A3	24	7.2	11	3.3	0.766	29	8.7	0.295	24	7.2	0.000	31	9.3	0.412
A4	17	59.5	18	63.0	0.083	17	59.5	0.000	16	56.0	0.083	18	63.0	0.083
A5	27	27.0	31	31.0	0.210	32	32.0	0.262	28	28.0	0.052	20	20.0	0.367
A6	20	40.0	19	38.0	0.071	21	42.0	0.071	23	46.0	0.212	28	56.0	0.566
A7	15	22.5	21	31.5	0.566	17	25.5	0.189	20	30.0	0.471	9	13.5	0.566
Mean					0.306			0.149			0.143			0.388

Table 7-10 Project Duration and Cost of Different Cumulative Probabilities of Case Study C

Desired Probability (%)	Marginal Duration (days)	Marginal Cost (\$1,000)	Joint Cumulative Probability (%)	Joint Duration (days)	Joint Cost (\$1,000)	Joint Cumulative Probability (%)	ΔD (%)	ΔC (%)
25	235	956	DNE	244	981	25	4	3
50	252	980	30	260	1,004	50	3	2
75	269	1,005	59	279	1,020	75	4	1
80	273	1,011	66	274	1,057	80	0	5
90	284	1,027	DNE	300	1,033	90	6	1
95	293	1,040	DNE	317	1,043	95	8	0

Table 7-11 Different Number of Simulation Replications for Case Study C

Replications	Duration (days)	Cost (\$1,000)	Joint Cumulative Probability (%)	Duration Marginal Cumulative (%)	Cost Marginal Cumulative (%)	Duration Conditional Cumulative (%)	Cost Conditional Cumulative (%)
100	269	996	50	75	64	100	100
200	250	1,052	50	51	98	100	100
500	253	1,020	50	55	88	80	100
1,000	258	1,003	50	63	73	80	86
2,000	262	998	50	68	70	72	66
5,000	260	1,004	50	64	75	50	64

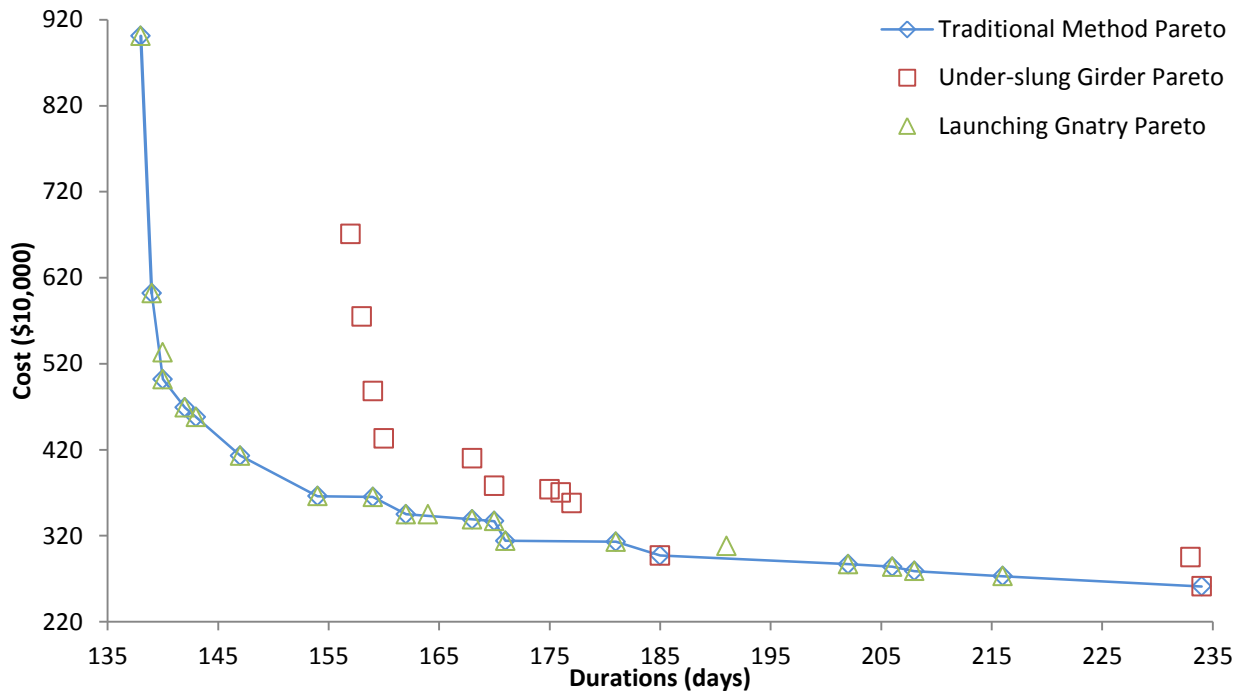


Figure 7-16 Pareto Fronts Generated Using Traditional Method

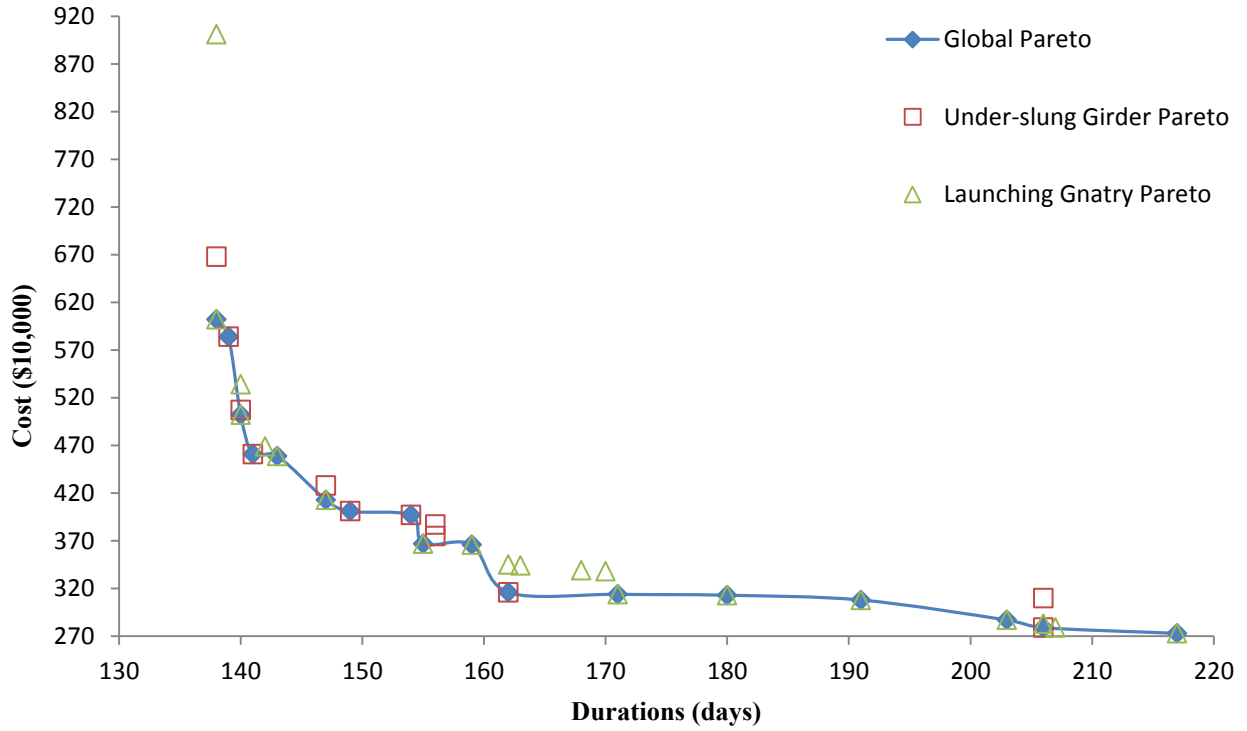


Figure 7-17 Pareto Fronts Generated Using 50% Joint Cumulative Probability

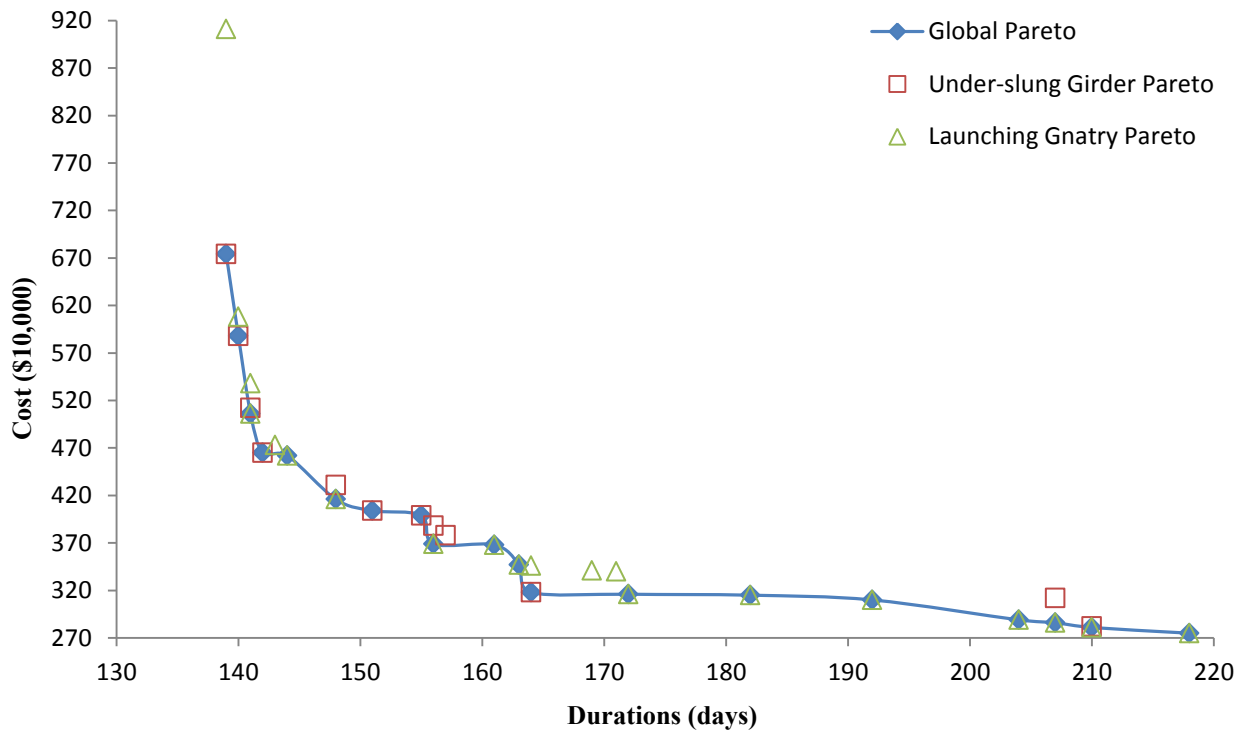


Figure 7-18 Pareto Fronts Generated Using 75% Joint Cumulative Probability

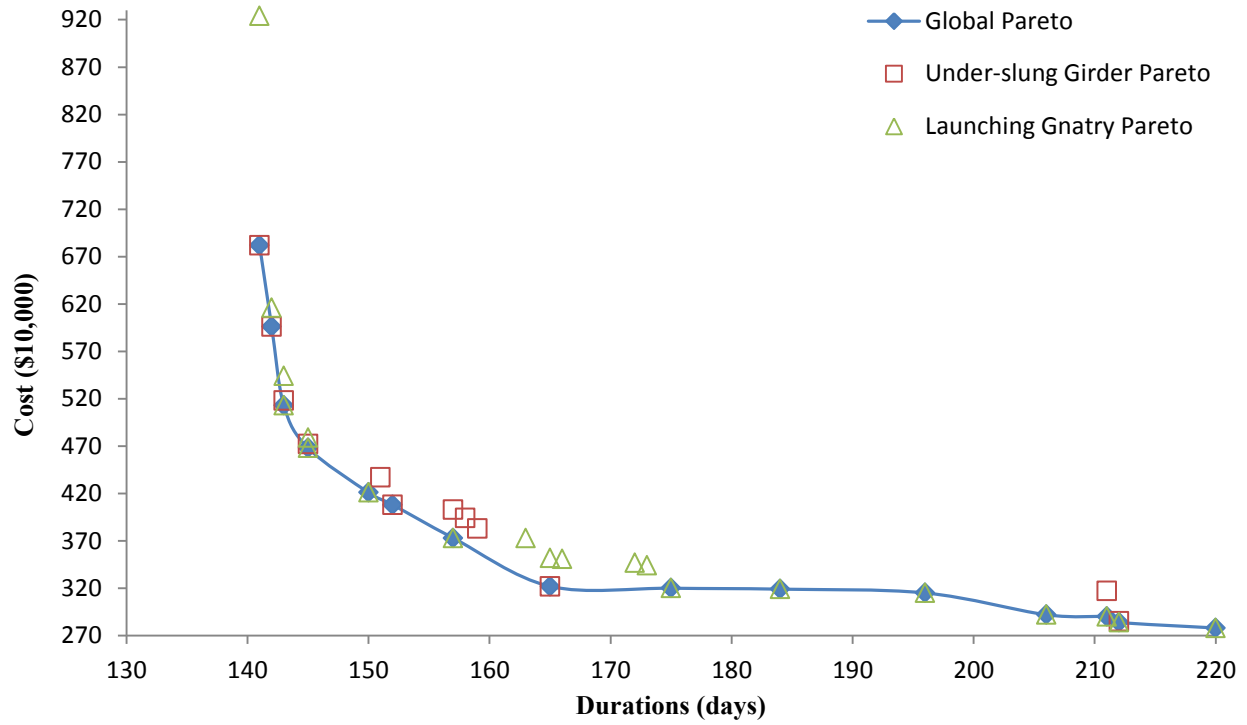


Figure 7-19 Pareto Fronts Generated Using 95% Joint Cumulative Probability

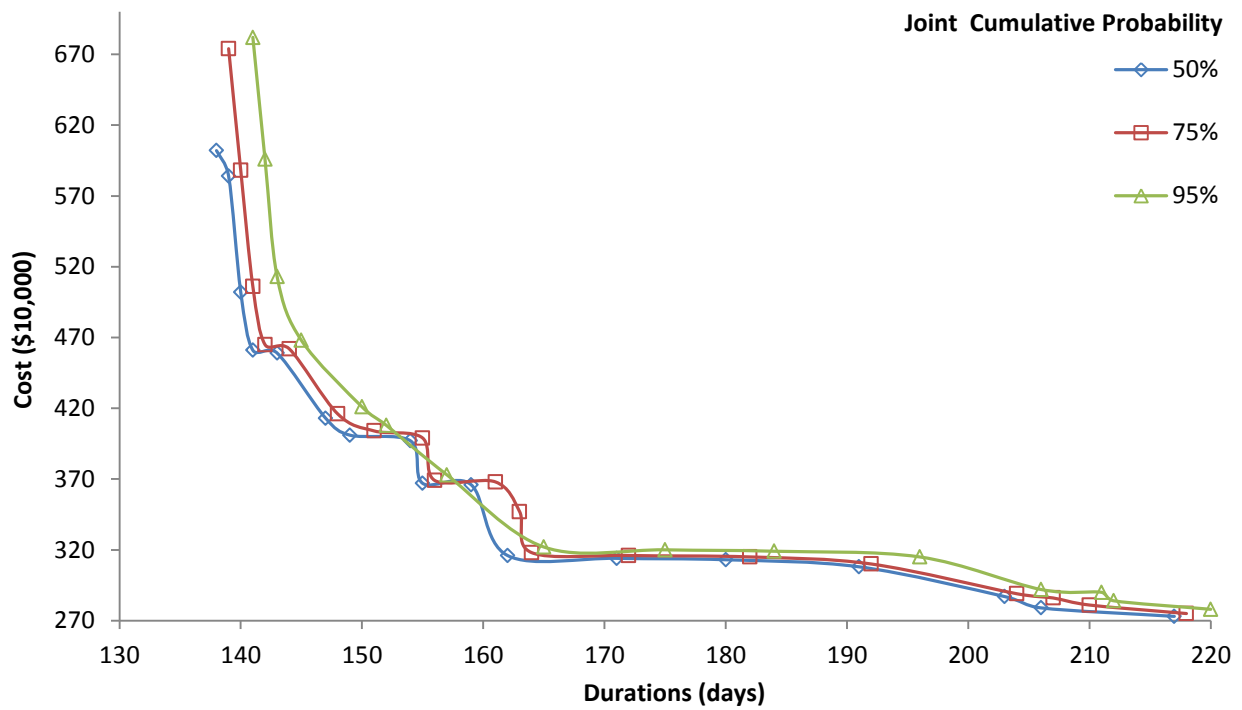


Figure 7-20 Probabilistic Pareto Fronts for 50%, 75%, and 95% Joint Cumulative Probability

The advantages that decision makers can obtain from understanding and analyzing the knowledge considering the joint probability in stochastic simulation models were presented. The limitation of the traditional method of calculating the probability of the performance measure indices of stochastic simulation models and the shortcomings of the traditional method were discussed. To overcome these shortcomings, a new method that uses the joint probability to calculate the probability of occurrence of the outputs of stochastic simulation models was presented. The proposed method considers the simultaneous occurrence of the project duration and cost through the use of joint probability. Moreover, the new concept of joint probabilistic Pareto fronts is described. In addition, a method for calculating the project duration and cost joint contingency is presented. Furthermore, the best schedule representing a specific probability can be generated using the proposed method. The use of the proposed method makes sure that the selected combination has a better chance of occurring, and provides the decision maker with more detailed and accurate information about the project. This is achieved by considering the correlation between the duration and cost, and the impact they have on each other.

Based on the results of the first three case studies, the proposed method shows an improvement over the traditional method as summarized in Table 7-3. For simulation models with high correlation between the outputs, ΔD and ΔC are not as large as in the case of simulation models with moderate or low correlation, which indicates the existence of a negative relationship between correlation and ΔD and ΔC . In addition, the existence of high correlation permits the reduction of the number of simulation replications required to get a sound estimation of a project which also indicates the existence of negative relationship between correlation and the number of replications required. Case Study D showed the shortcomings of the traditional method when generating the Pareto fronts using the disjoint cumulative probability. Using the joint probabilistic front method, a more accurate Pareto fronts can be generated.

CHAPTER 8: CONCLUSIONS AND FUTURE WORK

8.1 Summary and Conclusions of the Research Work

The main aim of this research is to select the best construction scenario of precast box girder bridges in terms of duration and cost. In order to achieve that, the following research developments were made: (1) a stochastic simulation-based multi-objective optimization model; (2) a method for incorporating variance reduction techniques into the proposed model; (3) a method to execute the proposed model in parallel computing environment on a single multi-core processor; and (4) a method to apply joint probability to the outcome of the proposed model.

Chapter 4 presented the proposed the stochastic simulation-based multi-objective optimization model dedicated to bridge construction operations. The aim of the model is to select a near-optimum construction scenario that satisfies predefined objectives. This model is used to select the near-optimum construction scenarios based on quantitative analysis rather than qualitative analysis. The construction scenario in this context consists of two main elements. The first element is the construction method that is used to construct a bridge. The second element is the decision variables related to that construction method. This chapter: (1) identified and modeled the decision variables related for each construction method; (2) formulated the objective functions that are used to estimate construction cost and duration; (3) defined the optimization constraints; (4) developed the simulation models of the selected construction methods; (5) designed the integration between the optimization algorithm and simulation; (6) implemented the model and demonstrated its effectiveness.

Chapter 5 presented a new method that incorporates VRTs into stochastic simulation-based multi-objective optimization. Although VRTs have been used in simulation studies in the past, they are used here in a novel way to improve the performance of the optimization process. The proposed method considered three VRTs, which are CRN, AV and the CM techniques. For each VRT, two approaches for managing the streams were explained, namely, the same streams and the new streams. This chapter: (1) identified and models the required synchronization; (2) formulated a method to compare the performance measure indices of the candidate solutions; (3)

developed a method to compare and select the best VRT; (4) implemented the proposed method and demonstrated its effectiveness.

This method showed an average of 81% reduction in the computation time and an average of 18% improvement in the hypervolume indicator over the traditional method in Case Study A. On the other hand, in Case Study B, the method showed an 87% reduction in the computation time compared with the traditional method while maintaining a high quality of the optimal solutions. In both case studies, the CRN, CRN_{ns}, CM, and CM_{ns} techniques were founded to be effective in reducing the variance of the project duration and cost. Although AV did not show good results in the pilot studies, this should not necessarily be the case for other simulation models. In addition, AV would have similar time savings if it succeeds in inducing negative correlation between the replications in pairs. One limitation of the use of VRTs is that a pilot study is always required since there is no one VRT that is guaranteed to work for all simulation models.

Chapter 6 presented method for implementing the simulation-based optimization model in a parallel computing environment on a single multi-core processor. The behavior of running simulation-based optimization on a single system with multicore architecture is studied. In addition, the impact of multithreading on the performance of simulation-based optimization is examined. The method was implemented using the master/slave paradigm. This chapter: (1) described the proposed method; (2) implemented the method and demonstrated its effectiveness.

As demonstrated by the case studies in this chapter, this method was able to achieve substantial time savings. When the proposed method is used by itself, it was able to save 38% of the time required to solve the optimization problem according to Case Study A. In addition, as demonstrated in Case Study B, combining the proposed method with CRN resulted in a time saving of 90%. Finally, Case Study C showed the benefit of the proposed method when compared with another study that used a server computer and a cluster.

Chapter 7 presented a new joint probability method that can be used to evaluate the probabilities of the project duration and cost obtained from stochastic simulation models. This method was applied to the sub-populations Pareto fronts obtained from the stochastic simulation-based multi-objective optimization. This chapter: (1) introduced a method to apply joint probability to Pareto solutions; (2) proposed the concept of joint probabilistic Pareto fronts; (3) developed a method to

analyze the selected solution; (4) implemented the proposed method and demonstrated its effectiveness.

Based on the results of the first three case studies presented in this chapter, this method shows an improvement over the traditional method. For simulation models with high correlation between the outputs, ΔD and ΔC are not as large as in the case of simulation models with moderate or low correlation, which indicates the existence of a negative relationship between correlation and ΔD and ΔC . In addition, the existence of high correlation permits the reduction of the number of simulation replications required to get a sound estimation of a project, which also indicates the existence of a negative relationship between correlation and the number of replications required. Case Study D showed the shortcomings of the traditional method when generating the Pareto fronts using the disjoint cumulative probability. Using the joint probabilistic front method, a more accurate Pareto fronts can be generated.

8.2 Research Contributions

The contributions of this research include:

- (1) Proposing a stochastic simulation-based multi-objective optimization model (quantitative analysis) for the selection of the construction method for precast concrete box girder bridges that is capable of (a) finding near optimum construction scenarios; and (b) simultaneously minimizing the project's total duration and cost.
- (2) Introducing a method for incorporating variance reduction techniques into the proposed model. The proposed method is capable of: (a) increasing the quality of the optimum solutions; (b) increasing the confidence in the optimality of the optimum solutions; and (c) reducing the computation time required for performing a stochastic simulation-based multi-objective optimization. In addition, the method is able to compare and select the best VRT and to compare the resulting candidate solutions.
- (3) Developing a method to execute the proposed model in parallel computing environment on a single multi-core processor. This method is capable of reducing the computation time required by traditional simulation-based optimization models. The time saving achieved by this method can be used to increase the confidence in the optimality of the optimum

solutions. This increase can be achieved by increasing the number of evaluated candidate solutions, which results in covering a larger portion of the search space of the optimization problem.

- (4) Proposing a method to apply joint probability to the outcomes of the proposed model. This method is capable of: (a) generating joint probability distributions of correlated simulation outputs and calculate their probabilities; (b) generating joint probabilistic Pareto fronts; (c) estimate the duration and cost joint contingency; and (d) generating a construction schedule that meets a specific probability.
- (5) The integration of the above methods within the stochastic simulation-based multi-objective optimization model.

8.3 Limitations and Recommendations for Future Work

A new model and several methods for planning and optimizing the construction of precast box girder bridges were presented in this research. These contributions improve the decision-making process in the planning phase of the project and aid planners in planning the construction operations. However, there some limitations that can be identified which are:

- (1) Sensitivity analysis is required to evaluate the performance of the proposed methods.
- (2) The simulation models presented in this thesis were based on the publically available information which could make these models simplified versions of the real systems.
- (3) The user has to select the applicable construction methods in order to generate the near optimum construction scenarios.
- (4) Only four construction methods are considered in this research, however, in real life more construction methods could be applicable for constructing a specific bridge.
- (5) The developed implementation at this stage is not user friendly.

Several future research areas can be identified in order to enhance the research done in this study and expand it to include other applications. These areas include:

- (1) Evaluating the applicability of the proposed methods in real projects.

- (2) Investigating the impact of using of other metaheuristic algorithms on the computation time of the proposed methods.
- (3) Assessing performance measurement of using VRTs and parallel computing by setting up a proper experiment with benchmarks and appropriate parameters to vary and study.
- (4) Integrating the proposed methodology with a knowledge-based system to select the applicable construction methods to the bridge under study.
- (5) Investigating the time savings that can be achieved using high-level architecture (HLA) (Dahmann, 1997) to evaluate the candidate solutions within the proposed methodology.
- (6) Expanding the optimization problem to generate phasing plans of multiple nearby bridge construction projects that involve multiple contractors. This new optimization problem should consider the spatio-temporal relationship between the projects.
- (7) Visualization using Building Information Modeling (BIM) (Eastman et al., 2011) and Bridge Information Modeling (BrIM) (Bentley Systems Incorporated, 2015) became a very popular approach in the industry as well as in academia in the recent years. There are several areas where contributions to the body of knowledge can be added. 3D/4D Visualization of the construction methods and equipment can be used to: (1) determine the constructability of the construction method and equipment used; (2) study the maneuvering space needed by the used equipment; and (3) analyze and improve safety on construction sites.
- (8) Using BIM/BrIM, the 3D model of the bridge can be integrated with the proposed model to extract the quantities of work to be performed and the type of materials to be used. This information can be used for estimating the cost of the materials used in the project and the durations of the project tasks. Moreover, the number of segments/spans can be extracted from the 3D model to be used as input to the simulation models.
- (9) Integrating the proposed model with the near real-time project progress and resource tracking data to apply the necessary re-planning, re-scheduling and re-allocation of the resources when a deviation from the initial plan is detected.

REFERENCES

- AbouRizk, S., Gonzalez-Quevedo, A., and Halpin, D. (1990). Application of Variance Reduction Techniques in Construction Simulation. *Microcomputers in Civil Engineering*, 5, 299-306
- AbouRizk, S. M., Halpin, D. W., and Lutz, J. D., (1992). State of the Art in Construction Simulation. *Proceedings of the 1992 Winter Simulation Conference*, IEEE, Arlington, 1271-1277.
- Abraham, D. M., and Halpin, D. W., (1998). Simulation of the Construction of Cable-stayed Bridges. *Canadian Journal of Civil Engineering*, 25(3), 490-499.
- Abraham, A., Jain, L., and Goldberg, R., (2005). *Evolutionary Multiobjective Optimization: Theoretical Advances and Applications*. 1st Ed., Springer-Verlag London Limited, London.
- Adeli, h., and Karim, A., (1997). Scheduling/Cost Optimization and Neural Dynamics Model for Construction Projects. *Journal of Construction Engineering and Management*, 123(4), 450-458.
- Al-Bataineh, M., AbouRizk, S., and Parkis, H., (2013). Using Simulation to Plan Tunnel Construction. *Journal of Construction Engineering and Management*, 139(5), 564-571.
- Alanjari, P., Razavialavi, S., & AbouRizk, S. (2014). A Simulation-based Approach for Material Yard Laydown Planning. *Automation in Construction*, 40, 1-8.
- Alberto, L., Azcarate, C., Mallor, F., and Mateo, P., (2002). Optimizaton with Simulation and Multiobjective Analysis in Industrial Decision-making: A Case Study. *European Journal of Operational Research*, 140(2), 373-383.
- Ailland, K., Bargstädt, H. J., and Hollermann, S., (2010). Construction Process Simulation in Bridge Building Based on Significant Day-to-day Data. In *Proceedings of the 2010 Winter Simulation Conference*, Baltimore, MD, 3250-3261.

- Anderson, D. R., Sweeney, D. J., and Williams, T. A., (2012). *Essentials of Modern Business Statistics*. 5th Ed., Cengage Learning, Mason, OH.
- Asmussen, S., and Glynn, P., (2007). *Stochastic Simulation: Algorithms and Analysis*. New York: Springer.
- Barker, J. M., (1980). Construction Techniques for Segmental Concrete Bridges. *PCI Journal*, Volume July-August, 66-86.
- Barney, B., (2013). *Introduction to Parallel Computing*, Lawrence Livermore National Laboratory, Livermore, CA.
- Barton, R. R., and Meckesheimer, M., (2006). Metamodel-Based Simulation Optimization. In: *Handbooks in Operations Research and Management Science*. Amsterdam, Netherlands, 535-574.
- Benaim, R., (2008). *The Design of Prestressed Concrete Bridges*. Taylor & Francis, New York.
- Bentley Systems Incorporated. (2014). About Bridge Information Modeling <http://www.bentley.com/en-US/Solutions/Bridges/brim/>. (15 May 2015).
- Bible, M. J., Bivins, S., and Bivins, S. S., (2011). *Mastering Project Portfolio Management: A Systems Approach to Achieving Strategic Objectives*. Plantation, FL: J. Ross Publishing.
- Bradstreet, L., (2011). *The Hypervolume Indicator for Multi-objective Optimisation: Calculation and Use*. Ph.D. Thesis, The University of Western Australia: Perth.
- Branke, J., Deb, K., Miettinen, K., and Słowiński, R., (2008). *Multiobjective Optimization - Interactive and Evolutionary Approaches*. Springer Berlin Heidelberg, Germany.
- Bratley, P., Fox, B. L., and Schrage, L. E., (1987). *A Guide to Simulation*. New York: Springer.
- Cantú-Paz, E., (1997). *A Survey of Parallel Genetic Algorithms*. Illinois Genetic Algorithms Laboratory. Urbana: University of Illinois at Urbana-Champaign.
- Cantú-Paz, E., and Goldberg, D. E., (2000). Efficient Parallel Genetic Algorithms: Theory and Practice. *Computer Methods in Applied Mechanics and Engineering*, 221-238.

- Cao, M., Lu, M., and Zhang, J., (2004). Concrete Plant Operations Optimization Using Combined Simulation and Genetic Algorithms. *Proceedings of 2004 International Conference on Machine Learning and Cybernetics*, IEEE, Shanghai, China, 4204-4209.
- Carson, Y., and Maria, A., (1997). Simulation Optimization: Methods and Applications. *Proceedings of the 1997 Winter Simulation Conference*, Washington DC, USA, 118-126.
- Chang, D. Y., (1986). *RESQUE: A Resource Based Simulation System for Construction Process Planning*, Ann Arbor, Michigan, PhD Thesis, University of Michigan.
- Chen, C. H., Chen, H. C., and Dai, L., (1996). A Gradient Approach for Smartly Allocating Computing Budget for Discrete Event Simulation. In *Proceedings of the 1996 Winter Simulation Conference*, Piscataway, New Jersey, 398-405.
- Chen H. C., Dai, L., Chen, C. H., and Yücesan, E., (1997). New Development of Optimal Computing Budget Allocation for Discrete Event Simulation. In *Proceedings of the 1997 Winter Simulation Conference*, Piscataway, New Jersey, 334-341.
- Cheng, C.-H., and Lee, L. H., (2011). *Stochastic Simulation Optimization: An Optimal Computing Budget Allocation*. World Scientific Publishing Company, Singapore.
- Cheng, M.-Y., and Wu, Y.-W., (2009). Evolutionary Support Vector Machine Inference System for Construction Management. *Automation in Construction*, 18(5), 597-604.
- Chen, Y., Okudan, G. E., and Riley, D. R., (2010). Decision Support for Construction Method Selection in Concrete Buildings: Prefabrication Adoption and Optimization. *Automation in Construction*, 9(16), 665-675.
- Cohon, J. L., (1978). *Multiobjective Programming and Planning*. Academic Press, New York.
- Colossal Transport Solutions, (2011). Girder Transporter. <<http://www.colossaltransport.com/colossal-equipment-sales/girder-transporter/>> (26 April 2015).

- Continental Engineering Corporation, (2006). Full-span Precast and Launching Method. <http://www.continental-engineering.com/english/page.php?cat_id=171&art_id=168> (22 May 2015).
- Covert, R. P., (2013). *Analytic Method for Probabilistic Cost and Schedule Risk Analysis*. Washington, DC: National Aeronautics and Space Administration (NASA).
- Dahmann, J. S. (1997). High level architecture for simulation. *First International Workshop on Distributed Interactive Simulation and Real Time Applications*, IEEE. 9-14..
- Dawood, N., and Shah, R. K., (2007). An Innovative Approach for Improvement of Communications through Visual Schedule Model in Road Construction. *7th International Conference on Construction Applications of Virtual Reality*, Pennsylvania State University. University Park, Pennsylvania, 216-223.
- Deb, K., (2001). *Multi-objective Optimization Using Evolutionary Algorithms*. 1st Ed., Wiley, Chichester, U.K.
- Deb, K., Pratap, A., Agarwal, S., and Meyarivan, T. A., (2002). A Fast and Elitist Multiobjective Genetic Algorithm: NSGA-II. *Evolutionary Computation*, IEEE Transactions, 6(2), 182-197.
- Degeilh, Y., and Gross, G., (2015). Stochastic Simulation of Power Systems with Integrated Intermittent Renewable Resources, *International Journal of Electrical Power & Energy Systems*, 64, 542-550.
- Dilip, D., Ravi, P., and Babu, G., (2013). System Reliability Analysis of Flexible Pavements. *Journal of Transportation Engineering*, 139(10), 1001-1009.
- Diwekar, U., (2008). *Introduction to Applied Optimization*. 2nd Ed., Springer Science+Business Media, New York.
- Eastman, C., Teicholz, P., Sacks, R., and Liston, K., (2011). *BIM Handbook: A Guide to Building Information Modeling for Owners, Managers, Designers, Engineers and Contractors*. John Wiley & Sons.

- El-Moslmani, K., (2002). *Fleet Selection for Earthmoving Operations Using Queueing Method*, Montreal, Quebec, M.Sc. Thesis, Concordia University.
- El-Rayes, K., (2001). Object-Oriented Model for Repetitive Construction Scheduling. *Journal of Construction Engineering and Management*, 127(3), 199–205
- Emshoff, J. R., and Sisson, R. L., (1970). *Design and Use of Computer Simulation Models*. 1st Ed., Macmillan, New York.
- Evans, M. J., and Rosenthal, J. S., (2010). *Probability and Statistics: The Science of Uncertainty*. 2nd Ed., W. H. Freeman and Company, New York.
- Federal Highway Administration, (2013). Accelerated Bridge Construction. <<http://www.fhwa.dot.gov/bridge/abc/index.cfm>> (22 May 2015).
- Feng, C.-W., Liu, L., and Burns, S. A., (2000). Stochastic Construction Time-Cost Trade-Off Analysis. *Journal of Computing in Civil Engineering*, 14(2), 117-126.
- Feng, C.-W., and Wu, H.-T., (2006). Integrating FmGA and CYCLONE to Optimize the Schedule of Dispatching RMC Trucks. *Automation in Construction*, 15(2), 186-199.
- Fenton, R.E, Cox, R.A., and Carlock, P., (1999). Incorporating Contingency Risk into Project Cost and Benefits Baselines: A Way to Enhance Realism. *INCOSE Conference*, Brighton, England, 9(1), 173-180
- Forbes, C., Evans, M., Hastings, N., and Peacock, B., (2011). *Statistical Distributions*. John Wiley & Sons, Hoboken.
- Fox, G., Johnson, M., Lyzenga, G., Otto, S., Salmon, J., and Walker, D. (1988). *Solving Problems on Concurrent Processors*, Volume 1, Prentice-Hall, Englewood Cliffs, NJ.
- Frantzeskakis, J. M., and Frantzeskakis, M. J., (2006). Athens 2004 Olympic Games: Transportation planning, simulation and traffic management. *ITE Journal*, 76(10), 26-32.
- Fu, M. C., Chen, C.-H., and Shi, L., (2008). Some Topics for Simulation Optimization. *Proceedings of the 2008 Winter Simulation Conference*, IEEE, Austin, TX, 27-38.

- Gerwick, B. C., (1993). *Construction of Prestressed Concrete Structures*. 2 nd Ed., John Wiley & Sons, New York.
- Glover, F., Kelly, J., and Laguna, M., (1996). New Advances and Applications of Combining Simulation and Optimization. *Proceedings of the 1996 Winter Simulation Conference*, IEEE, Piscataway, 144-152.
- Goh, C.-K., and Tan, K. C., (2009). *Evolutionary Multi-objective Optimization in Uncertain Environments*. Springer-Verlag Berlin Heidelberg, Berlin.
- Goldberg, D., Deb, K., Kaegupta, H., and Harik, G., (1993). Rapid, Accurate Optimization of Difficult Problems using Fast Messy Genetic Algorithms. *Proceedings of the Fifth International Conference on Genetic Algorithms*, Morgan Kaufmann Publishers Inc, Urbana-Champaign, 56-64.
- Hajjar, D., and AbouRizk, S., (1999). Symphony: An Environment for Building Special Purpose Construction Simulation Tools. *Proceedings of the 1999 Winter Simulation Conference*, IEEE, Phoenix, Arizona, Volume 2, 998-1006.
- Halpin, D. W., (1977). CYCLONE: Method for Modeling Job Site Processes. *Journal of the Construction Division*, 103(3), 489-499.
- Halpin, D. W., and Riggs, L. S., (1992). *Planning and Analysis of Construction Operations*. John Wiley & Sons, Inc., New York.
- Hannon, J. J., (2007). *Emerging Technologies for Construction Delivery*. Transportation Research Board, National Research Council, Washington, D.C.
- Hassan, M., and Gruber, S., (2008). Simulation of Concrete Paving Operations on Interstate-74. *Journal of Construction Engineering and Management*, 134(1), 2-9.
- Hazok, (2008). Bridging by Segmental Box Girder. <<http://hazok.hubpages.com/hub/Bridging-by-Segmental-Box-Girder>> (02 May 2015).
- He, J., Huang, Y., and Chang, D., (2014). Simulation-based Heuristic Method for Container Supply Chain Network Optimization, *Advanced Engineering Informatics*.

- Hegazy, T., and Kassab, M., (2003). Resource Optimization Using Combined Simulation and Genetic Algorithms. *Journal of Construction Engineering and Management*, 129(6), 698-705.
- Hegazy, T., and Petzold, K., (2003). Genetic Optimization for Dynamic Project Control. *Journal of Construction Engineering and Management*, 129(4), 396-404.
- Heidelberger, P., (1988). Discrete Event Simulation and Parallel Process: Statistical Properties, *SIAM Journal of Statistical Computing*, 9(6), 1114-1132.
- Hewson, N., (2012). *Prestressed Concrete Bridges Design and Construction*. 2nd Ed., ICE Publishing, London.
- Hewson, N. R., (2003). *Prestressed Concrete Bridges: Design and Construction*. Thomas Telford Ltd., London.
- Hillar, G. C., (2010). *Professional Parallel Programming with C#: Master Parallel Extensions with .NET 4*. Wrox Press, Indianapolis.
- Holland, J. H., (1975). *Adaptation in Natural and Artificial Systems*. University of Michigan Press.
- Hong, T., and Hastak, M., (2007). Simulation Study on Construction Process of FRP Bridge Deck Panels. *Automation in Construction*, 16(5), 620-631.
- Huang, R.-Y., Grigoriadis, A. M., and Halpin, D. W., (1994). Simulation of Cable-stayed Bridges using DISCO. *Proceedings of the 1994 Winter simulation Conference*, The Society for Modeling and Simulation International, San Diego, CA, 1130-1136 .
- Hulett, D. T., (2011a). *Integrated Cost and Schedule Risk Analysis Using Monte Carlo Simulation of A CPM Model*. Morgantown, WV: AACE International.
- Hulett, D. T., (2011b). *Integrated Cost-Schedule Risk Analysis*. Surrey, England: Gower Publishing Limited.

- Ioannou, P., and Martinez, J., (1995). Evaluation of Alternative Construction Processes Using Simulation. *Proceedings of Construction Congress 95*, ASCE San Diego, California, 440-447
- James, B. A., (1985). Variance Reduction Techniques. *Journal of the Operational Research Society*, 525-530.
- Jeannotte, K., and Chandra, A., (2005). *Developing and Implementing Transportation Management Plans for Work Zone*, Report 23 CFR 630 Subpart J, FHWA, U.S. Department of Transportation, Washington, DC.
- Jimenez, H. A. T., (2007). *Multi-objective Optimization Algorithms Considering Objective Preferences and Solution Clusters*, PhD Thesis, The State University of New Jersey.
- Kandil, A., and El-Rayes, K., (2006). Parallel Genetic Algorithms for Optimizing Resource Utilization in Large-Scale Construction Projects. *Journal of Construction Engineering and Management*, ASCE, 132(5), 491-498.
- Kandil, A., El-Rayes, K., and El-Anwar, O., (2010). Optimization Research: Enhancing the Robustness of Large-scale Multiobjective Optimization in Construction. *Journal of Construction Engineering and Management*, 136(1), 17-25.
- Kao, S., and Chang, N., (2012). Copula-Based Flood Frequency Analysis at Ungauged Basin Confluences: Nashville, Tennessee. *Journal of Hydrologic Engineering*, 17(7), 790-799.
- Keskin, B. B., Melouk, S. H., and Meyer, I. L., (2010). A Simulation-optimization Approach for Integrated Sourcing and Inventory Decisions. *Computers & Operations Research*, 37(9), 1648-1661.
- Kleijnen, J. P., (1974). *Statistical Techniques in Simulation*. 1st Ed., M. Dekker, New York.
- Kleijnen, J. P., (1975). Antithetic Variates, Common Random Numbers and Optimal Computer Time. *Management Science*, 21(10), 1176-1185.
- Kleijnen, J. P., (1996). Five-stage Procedure for the Evaluation of Simulation Models Through Statistical Techniques. In *Proceedings of the 28th conference on Winter simulation*, John

- M. Charnes, Douglas J. Morrice, Daniel T. Brunner, and James J. Swain (Eds.). IEEE Computer Society, Washington, DC, USA, 248-254.
- L'Ecuyer, P., (1994). Efficiency Improvement and Variance Reduction. *Proceedings of the 26th conference on Winter simulation*, IEEE, San Diego, CA, 122-132.
- Laganá, D., Legato, P., Pisacane, O., and Vocaturo, F., (2006). Solving Simulation Optimization Problems on Grid Computing Systems. *Parallel Computing*, 32(9), 688-700.
- Law, A., (2007). *Simulation modeling and analysis*. Boston: McGraw-Hill.
- Law, A. M., and Kelton, W. D., (1991). *Simulation Modeling and Analysis*. McGraw-Hill, New York.
- Lee, S.-H., (2003). *A Process Model for Controlling Project Productivity of Highway Construction Operations*, Gainesville, Florida, PhD Thesis, University of Florida.
- Lee, D., Yi, C., Lim, T., and Arditi, D., (2010). Integrated Simulation System for Construction Operation and Project Scheduling. *Journal of Computing in Civil Engineering*, 24(6), 557-569.
- Li, H., Cao, J., and Love, P., (1999). Using Machine Learning and Genetic Algorithm to Solve Time-cost Trade-off Problems. *Journal of Construction Engineering and Management*, 125(5), 347-353.
- Li, H., and Love, P., (1997). Using Improved Genetic Algorithms to Facilitate Time-Cost Optimization. *Journal of Construction Engineering and Management*, 123(3), 233-237.
- Liao, T. W., Egbelu, P. J., Sarker, B. R., and Leu, S. S. (2011). Metaheuristics for Project and Construction Management: A State-of-the-art Review. *Automation in Construction*, 20(5), 491-505.
- Liebenberg, A. C., (1992). *Concrete Bridges: Design and Construction*. Longman Scientific & Technical, London.

- Liu, J., Lence, B., and Isaacson, M., (2010). Direct Joint Probability Method for Estimating Extreme Sea Levels. *Journal of Waterway, Port, Coastal, and Ocean Engineering*, 136(1), 66-76.
- Liu, L., Burns, S., and Feng, C., (1995). Construction Time-Cost Trade-Off Analysis Using LP/IP Hybrid Method. *Journal of Construction Engineering and Management*, 121(4), 446-454.
- Liu, L. Y., (1991). *COOPS: Construction Object-oriented Simulation System*, Ann Arbor, Michigan, PhD Thesis, University of Michigan.
- López, R. A. Y., and Halpin, D. W., (2000). A Computer Simulation of the Construction of the Alamillo Bridge in Seville, Spain. In *Proceedings of Construction Congress VI*, 121-130.
- Lu, M., (2003). Simplified Discrete-Event Simulation Approach for Construction Simulation. *Journal of Construction Engineering and Management*, 129(5), 537-546.
- Mahoney, K. M., Porter, R. J., Taylor, D. R., Kulakowski, B. T., and Ullman, G. J., (2007). *Design of Construction Work Zones on High-Speed Highways*, Transportation Research Board, Transportation Research Board of the National Academies, Washington, D.C.
- Martínez, J., (1996). *STROBOSCOPE: State and Resource Based Simulation of Construction Processes*, Ann Arbor, Michigan, PhD Thesis, University of Michigan.
- Marzouk, M., El-Dein, H., Z. and El-Said, M., (2007). Application of Computer Simulation to Construction of Incremental Launching Bridges. *Journal of Civil Engineering and Management*, 13(1), 27-36.
- Marzouk, M., and Moselhi, O., (2003). Object-oriented Simulation Model for Earthmoving Operations. *Journal of Construction Engineering and Management*, 129(2), 173-181.
- Marzouk, M., and Moselhi, O., (2004). Multiobjective optimization of Earthmoving Operations. *Journal of Construction Engineering and Management*, 103(1), 105-113.
- Marzouk, M., Said, H., and El-Said, M., (2008). Special-Purpose Simulation Model for Balanced Cantilever Bridges. *Journal of Bridge Engineering*, 13(2), 122-131.

- Marzouk, M., Said, H., and El-Said, M., (2009). Framework for Multiobjective Optimization of Launching Girder Bridges. *Journal of Construction Engineering and Management*, 135(8), 791-800.
- Marzouk, M., Zein, H., and Elsaid, M., (2006). Bridge-Sim: Framework For Planning And Optimizing Bridge Deck Construction Using Computer Simulation. *Proceedings of the 2006 Winter Simulation Conference*, IEEE. Monterey, CA, 2039-2046
- MathWorks Inc. (2014). *Matlab, User Guide*. The MathWorks Inc.
- MathWorks. (2013). *SimEvents User's Guide*. The MathWorks, Inc.
- Mawlana, M., and Hammad, A., (2013). Simulation-based Optimization of Precast Box Girder Concrete Bridge Construction Using Full Span Launching Gantry. *4th Construction Specialty Conference*, CSCE, Montreal.
- Mawlana, M., and Hammad, A., (2015)(Available online). Joint Probability for Evaluating the Schedule and Cost of Stochastic Simulation Models, *Advanced Engineering Informatics*.
- Mawlana, M., Hammad, A., Doriani, A., and Setayeshgar, S., (2012). Discrete Event Simulation and 4D Modeling for Elevated Highway Reconstruction Projects. *14th International Conference on Computing in Civil and Building Engineering*, Publishing House "ASV". Moscow.
- McCabe, B. (1998). Belief networks in construction simulation. *In Proceedings of the 30th Conference on Winter simulation*. IEEE Computer Society Press, 1279-1286.
- McCahill, D. F., and Bernold, L. E., (1993). Resource-Oriented Modeling and Simulation in Construction. *Journal of Construction Engineering and Management*, September, 119(3), 590-606.
- Microsoft Corporation, (2015). Microsoft Excel. <<http://office.microsoft.com/en-001/excel/>> (10 April 2015).
- Microsoft Corporation, (2015). Microsoft Project. <<http://office.microsoft.com/en-us/project/>> (10 April 2015).

- Microsoft Corporation, (2015). VBA for Office Developers. <<http://msdn.microsoft.com/en-us/office/ff688774.aspx>> (01 April 2015).
- Microsoft Corporation, (2015). Visual C#. <<http://msdn.microsoft.com/en-us/library/vstudio/kx37x362.aspx>> (10 April 2015).
- Mondorf, P. E., (2006). *Concrete Bridges*. Taylor & Francis, New York.
- Moselhi, O., (1997). Risk Assessment and Contingency Estimating, *Transactions of the American Association of Cost Engineers*, Dallas, A.06.1-6.
- Munawar, A., Wahib, M., Munetomo, M., and Akama, K., (2008). A Survey: Genetic algorithms and the Fast Evolving World of Parallel Computing. *10th International Conference in High Performance Computing and Communications*, IEEE, 897-902.
- Murtaza, M. B., Fisher, D. J., and Skibniewski, M. J., (1993). Knowledge-based Approach to Modular Construction Decision Support. *Journal of Construction Engineering and Management*, 119(1), 115-130.
- Nakayama, H., Yun, Y., and Yoon, M., (2009). *Sequential Approximate Multiobjective Optimization Using Computation Intelligence*. Springer-Verlag Berlin Heidelberg, Berlin.
- Nassar, K., El Masry, M., and Sherif, Y., (2011). Multiobjective Optimization of Advanced Shoring Systems Used in Bridge Construction. *International Workshop on Computing in Civil Engineering*, ASCE, Maimi, 94-101.
- Nguyen, L., Phan, D., and Tang, L., (2013). Simulating Construction Duration for Multistory Buildings with Controlling Activities. *Journal of Construction Engineering and Management*, 139(8), 951–959.
- NRS Bridge Construction Equipment, (2008). Full Span Method. <<http://www.nrsas.com/equipments/fullspan.php>> (23 April 2015).

- Odeh, A. M., (1992). *CIPROS: Knowledge-based Construction Integrated Project and Process Planning Simulation System*, PhD dissertation, University of Michigan, Ann Arbor, Michigan.
- Oloufa, A. A., (1993). Modeling Operational Activities in Object-Oriented Simulation. *Journal of Computing in Civil Engineering*, January, 7(1), 94-106.
- Orabi, W., El-Rayes, K., Senouci, A., and Al-Derham, H., (2009). Optimizing Postdisaster Reconstruction Planning for Damaged Transportation Networks. *Journal of Construction Engineering and Management*, 135(10), 1039-1048.
- Pan, N.-F., (2008). Fuzzy AHP Approach for Selecting the Suitable Bridge Construction Method. *Automation in Construction*, 17(8), 958-965.
- Pan, N.-H., Chiu, T.-C., and Chen, K.-Y., (2008). Full-span Pre-cast Launching Method (FPLM) Analysis with Dynamic Simulation - Case studies of Taiwan High-Speed Rail (THSR) Project. *Automation in Construction*, 17(5), 592-607.
- Podolny, W., and Muller, J. m., (1982). *Construction and Design of Prestressed Concrete Segmental Bridges*. John Wiley & Sons, New York.
- Pozo, C., Guillén-Gosálbez, G., Sorribas, A., and Jiménez, L. (2012). Identifying the Preferred Subset of Enzymatic Profiles in Nonlinear Kinetic Metabolic Models via Multiobjective Global Optimization and Pareto Filters. *PLOS ONE*, 7(9), e43487.
- Rajagopalan, N., (2006). *Bridge Superstructure*. Alpha Science International Ltd., Oxford.
- Reddy, P., Ghaboussi, J., and Hawkins, N. M., (1999). Simulation of Construction of Cable-stayed Bridges. *Journal of Bridge Engineering*, 4(4), 249-257.
- Reddy, M., and Kumar, D., (2007). Multiobjective Differential Evolution with Application to Reservoir System Optimization. *Journal of Computing in Civil Engineering*, 21(2), 136-146.
- Rinott, Y., (1978). On Two-stage Selection Procedures and Related Probability-inequalities. *Communications in Statistics*, A7(8), 799-811.

- Rosignoli, M., (2010). Self-launching Erection Machines for Precast Concrete Bridges. *Precast/Prestressed Concrete Institute Journal*, Issue Winter, 36-57.
- RS Means Engineering Department, (2011). *RS Means Heavy Construction Cost Data*. 25th Ed., RS Means, Norwell, MA.
- Saag, J. B., (1999). *Project Development Methodologies for Reconstruction of Urban Freeways and Expressways*, NCHRP Synthesis of Highway Practice 273, Transportation Research Board of the National Academies, Washington, D.C.
- Said, H., Marzouk, M., and El-Said, M., (2009). Application of Computer Simulation to Bridge Deck Construction: Case Study. *Automation in Construction*, 18(4), 377-385.
- Salimi, S., (2014). *Performance Analysis of Simulation-based Multi-objective Optimization of Bridge Construction Processes Using High Performance Computing*, Montreal, Master's Thesis, Concordia University.
- Salimi, S., Mawlana, M., and Hammad, A., (2014). Simulation-based Multiobjective Optimization of Bridge Construction Processes using Parallel Computing. *Proceedings of the 2014 Winter Simulation Conference*, IEEE, Savannah, GA, 3272-3283.
- Salimi, S., Mawlana, M., and Hammad, A., (2015). *Performance Analysis of Simulation-based Multiobjective Optimization Using High Performance Computing*, 2nd International Conference on Civil, Building, Engineering Informatics, Tokyo, Japan.
- Sauvageot, G., (1999). Segmental Concrete Bridges. In: W. Chen and L. Duan, eds. *Bridge Engineering Handbook*. Boca Raton. CRC Press, 11.40-11.41.
- Schruben, L., and Margolin, B., (1978). Pseudorandom Number Assignment in Statistically Designed Simulation and Distribution Sampling Experiments. *Journal of the American Statistical Association*, 73(363), 504-520.
- Senouci, A., and El-Rayes, K., (2009). Time-Profit Trade-Off Analysis for Construction Projects. *Journal of Construction Engineering and Management*, 135(8), 718-725.

- Sivanandam, S. N., and Deepa, S. N., (2008). *Genetic Algorithm Optimization Problems*. Springer Berlin Heidelberg.
- Soetanto, R., Dainty, A. R., Glass, J., and Price, A. D., (2006). A Framework for Objective Structural Frame Selection. *Proceedings of the ICE-Structures and Buildings*, 159(1), 45-52.
- Strukturas DF International, (2011). Precast Full Span Launcher. <http://www.sdi-intl.com/project_5.shtml> (26 April 2015).
- Székely Jr., T., and Burrage, K. (2014). Stochastic Simulation in Systems Biology. *Computation and Structural Biotechnology Journal*, 12(20-21), 14-25.
- Tabai, H., Sasaki, Y., and Yuasa, Y., (1998). Construction Method Selection and Simulation. *Proceedings of the 15th ISARC*, IAARC, Munchen, 79-88.
- Tew, J. D., and Wilson, J. R., (1994). Estimating Simulation Metamodels Using Combined Correlation-based Variance Reduction Techniques. *IIE transactions*, 26(3), 2-16.
- Thomas, H., Maloney, W., Horner, R., Smith, G., Handa, V., and Sanders, S., (1990). Modeling Construction Labor Productivity, *Journal of Construction Engineering and Management*, 116(4), 705-726.
- Touran, A., (1990). Integration of Simulation with Expert Systems. *Journal of Construction Engineering and Management*, 116(3), 480-493.
- Vanegas, J. A., Bravo, E. B., and Halpin, D. W., (1993). Simulation Technologies for Planning Heavy Construction Processes. *Journal of Construction Engineering and Management*, 119(2), 336-354.
- Vernay, D. G., Raphael, B., and Smith, I. F. C., (2014) Augmenting Simulations of Airflow Around Buildings Using Field Measurements, *Advanced Engineering Informatics*, 26(4), 412-424.

- VSL International Ltd., (2013). Bridge Construction Technology. <http://www.vsl.com/index.php?option=com_content&view=article&id=82&Itemid=188> (23 January 2015).
- Wang, W., Rivard, H., and Zmeureanu, R., (2005). An Object-oriented Framework for Simulation-based Green Building Design Optimization with Genetic Algorithms, *Advanced Engineering Informatics*, 19(1), 5-23.
- Wilson, J. R., (1983). Variance Reduction: The Current State. *Mathematics and Computers in Simulation*, 25(1), 55-59.
- Wright, P. H., (1996). *Highway Engineering*. 6th Ed., John Wiley & Sons Inc, New York.
- Wu, Z. Y., Wang, Q., Butala, S., and Mi, T., (2012). *Darwin Optimization Framework User Manual*, , Bentley Systems Incorporated, Watertown, CT.
- Yang, I.-T., (2011). Stochastic Time–cost Tradeoff Analysis: A Distribution-free Approach with Focus on Correlation and Stochastic Dominance. *Automation in Construction*, 20(7), 916-926.
- Yang, I., Hsieh, Y., and Kung, L., (2012). Parallel Computing Platform for Multiobjective Simulation Optimization of Bridge Maintenance Planning. *Journal of Construction Engineering and Management*, 138(2), 215-226.
- Youssef, M. A., Anumba, C. J., and Thorpe, T., (2005). Intelligent Selection of Concrete Bridge Construction Methods in Egypt. *International Conference on Computing in Civil Engineering*, ASCE, Cancun, 1-14.
- Yu, X., and Gen, M., (2010). *Introduction to Evolutionary Algorithms*. 1st Ed., Springer-Verlag London Limited, London.
- Zhang, H., Li, H., and Lu, M., (2008). Modeling Time-Constraints in Construction Operations through Simulation. *Journal of Construction Engineering and Management*, 134(7), 545-554.
- Yucesan, E., and Jacobson, S. H., (1995). On the Simultaneous Construction of Sample Paths,

Proceedings of the 1995 Winter Simulation Conference, Arlington, VA, 357-361.

- Zhang, H., Tam, C., Li, H. and Shi, J. (2006). Particle Swarm Optimization-supported Simulation for Construction Operations. *Journal of Construction Engineering and Management*, 132(12), 1267-1274.
- Zhao, Y., Zhong, W., and Ang, A., (2007). Estimating Joint Failure Probability of Series Structural Systems. *Journal of Engineering Mechanics*, 133(5), 588-596.
- Zheng, D., Ng, S., and Kumaraswamy, M., (2005). Applying Pareto Ranking and Niche Formation to Genetic Algorithm-based Multiobjective Time–cost Optimization. *Journal of Construction Engineering and Management*, 131(1), 81-91.
- Zitzler, E., Brockhoff, D., and Thiele, L., (2007). The Hypervolume Indicator Revisited: On the Design of Pareto-compliant Indicators Via Weighted Integration. *The 4th International Conference on Evolutionary Multi-Criterion Optimization, LNCS 4403*, Springer-Verlag, Matsushima, Japan, 862-876.
- Zitzler, E., Thiele, L., Laumanns, M., Fonseca, C. M., and Da Fonseca, V. G., (2003). Performance Assessment of Multiobjective Optimizers: An Analysis and Review. *IEEE Transactions on Evolutionary Computation*, 7(2), 117-132.

APPENDIX A: TASKS DURATIONS USED IN THE SIMULATION MODELS

Table A-1 Deterministic Tasks Durations for Precast Full Span Erection Using Launching

Gantry

Task	Duration (minutes)	Task	Duration (minutes)
BottomSlab_Web	1673 *	Trailer_Loading	60 **
Inner_Mold	300 *	Trailer_Haul	F (Distance, Speed)
TopSlab	1979 *	Trolley_Loading	60 **
LiftToMold	45	Trailer_Return	F (Distance, Speed)
Cast_Span	1544*	Trolley_Travel	F (Distance, Speed)
Span_Curing	(600 or 1200) *	Reposition	240 **
RemoveInnerMol	255 *	Erection_Span	240 **
Posttension_1st	240 *	Trolley_Return	F (Distance, Speed)
LiftToStorage	60 **	Prepare_Bearing	240 **
Posttension_2nd	240 *	Load_Transfer	60 **
* Adapted from (Marzouk, El-Dein, & El-Said, 2007)			
** Adapted from (VSL International Ltd, 2013)			

Table A-2 Tasks Durations for Precast Segmental Erection Using Launching Gantry

Task	Duration (minutes)	Task	Duration (minutes)
Steel_Cage	Triangular [90, 180, 270] *	Trailer_Haul	F (Distance, Speed)
Insert_Mold	Triangular[15, 30, 45] *	Trailer_Return	F (Distance, Speed)
Cast_Segment	Triangular [90, 180, 270] *	Reposition	Triangular[120, 240, 360]**
Segment_Curing	(600,1200) *	Place_Segment	Triangular[27, 54, 81]**
RemoveMold	Triangular[15, 30, 45] *	Align_Glue	Triangular[240, 480, 720]**
Move_Storage	Triangular[30, 60, 90]	Install_ExtPT	Triangular[240, 480, 720]**
Trailer_Loading	Triangular[30, 60, 90]	Stressing_ExtPT	Triangular[120, 240, 360]**
* Adapted from (Marzouk et al., 2007)			
** Adapted from (VSL International Ltd., 2013)			

Table A-3 Tasks Durations for Precast Segmental Erection Using Falsework Support

Task	Duration (minutes)	Task	Duration (minutes)
Steel_Cage	Triangular [90, 180, 270] *	Trailer_Haul	F (Distance, Speed)
Insert_Mold	Triangular[15, 30, 45] *	Trailer_Return	F (Distance, Speed)
Cast_Segment	Triangular [90, 180, 270] *	Reposition	Triangular[240, 480, 720]**
Segment_Curing	(600,1200) *	Place_Segment	Triangular[27, 54, 81]**
RemoveMold	Triangular[15, 30, 45] *	Align_Glue	Triangular[240, 480, 720]**
Move_Storage	Triangular[30, 60, 90]	Posttension	Triangular[120, 240, 360]**
Trailer_Loading	Triangular[30, 60, 90]	Load_Transfer	Triangular[120, 240, 360]**
* Adapted from (Marzouk et al., 2007)			
** Adapted from (VSL International Ltd., 2013)			

Table A-4 Tasks Durations for Precast Segmental Erection Using Under-slung Girder

Task	Duration (minutes)	Task	Duration (minutes)
Steel_Cage	Triangular [90, 180, 270] *	Trailer_Haul	F (Distance, Speed)
Insert_Mold	Triangular[15, 30, 45] *	Trailer_Return	F (Distance, Speed)
Cast_Segment	Triangular [90, 180, 270] *	Reposition	Triangular[120, 240, 360]**
Segment_Curing	(600,1200) *	Place_Segment	Triangular[27, 54, 81]**
RemoveMold	Triangular[15, 30, 45] *	Align_Glue	Triangular[240, 480, 720]**
Move_Storage	Triangular[30, 60, 90]	Install_ExtPT	Triangular[240, 480, 720]**
Trailer_Loading	Triangular[30, 60, 90]	Stressing_ExtPT	Triangular[120, 240, 360]**
* Adapted from (Marzouk et al., 2007)			
** Adapted from (VSL International Ltd., 2013)			

APPENDIX B: COST DATA USED IN THE SIMULATION MODELS

Resource	Cost	Unit
Indirect cost	500	(\$/day)
Delivery truck	50	(\$/hr)
Truck driver	50	(\$/hr)
Yard crane	50	(\$/hr)
Yard crane driver	100	(\$/hr)
Onsite crane mobilization	900	(\$)
Onsite Crane	150	(\$/hr)
Onsite crane driver	100	(\$/hr)
Gantry mobilization	9,000	(\$)
Gantry	500	(\$/hr)
Gantry driver	200	(\$/hr)
Under-slung girder mobilization	5,000	(\$)
Under-slung girder	100	(\$/hr)
Under-slung girder driver	200	(\$/hr)
Trolley mobilization	900	(\$)
Trolley	150	(\$/hr)
Trolley driver	100	(\$/hr)
Preparation crew mobilization	200	(\$)
Preparation crew	200	(\$/hr)
Stressing crew mobilization	200	(\$)
Stressing crew	200	(\$/hr)
Steel crew mobilization	200	(\$)
Steel crew	200	(\$/hr)
Casting crew mobilization	200	(\$)
Casting crew	200	(\$/hr)
Rebar cage fabrication	500	(\$)
Rebar cage	10	(\$/hr)
Inner mold fabrication	1,000	(\$)
Inner mold	10	(\$/hr)
Outer mold fabrication	1,000	(\$)
Outer mold	10	(\$/hr)
Storage	10	(\$/hr)